An *in vitro* human 3D co-culture model to study endothelial-astrocyte interactions

Thesis

UNRESTRICTED

An *in vitro* human 3D co-culture model to study endothelial-astrocyte interactions

A thesis submitted to The Open University for the degree of Doctor of Philosophy on 12th December 2012

By

Sreekanth Reddy Peddagangannagari, B.Sc., M.Sc.

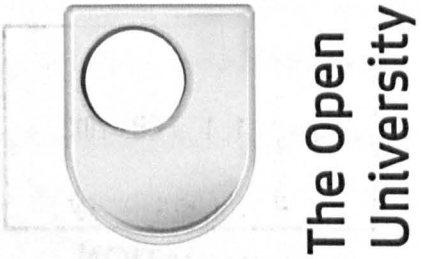

Supervised by **Prof. David K. Male** and co-supervised by **Dr Ignacio A. Romero**

Department of Life, Health and Chemical Sciences,

The Open University, Milton Keynes,

MK7 6AA, United Kingdom.

DATE of SUBMISSION : 20 FEBRUARY 2012

DATE of AWARD : 18 JANUARY 2013

Acknowledgements

My sincere thanks to Prof David Male for this opportunity, for his advice, support, and the freedom from the day of my arrival to the UK and through the course of my PhD.

I am grateful to Dr Ignacio (Nacho) Romero for his kindness, advice, support and especially for his interventions during the critical junctures of my PhD.

It has been a great learning experience working with them, and I am much benefited by David's broader perspective and Nacho's critical view.

My thanks to Dr James Phillips for introducing me to 3D culture and for the suggestions and the consumables. Thanks to Heather Davies for her patient, repeated trials of electron microscopy analysis. Special thanks to Dr Payam Rezaie for helping me with the image analysis, which saved a lot of time for me. Thanks to Dr Emma East for the primary rat astrocyte cultures.

My thanks to Dr Jane Loughlin for the critical comments, the feedback, and the antibodies. I must thank Julia Barkans for being always helpful and making it easy to work in the laboratory. Thanks to Alejandro for his help and the company, and thanks to the fellow PhD students and the members of the department and research school staff for their contribution in this work.

I am thankful to Migraine trust and The Open University for providing the studentship and considerate additional funding.

Although not directly involved with this work, I wish to thank Prof Kumaravel Somasundaram and Prof Paturu Kondaiah of the Indian Institute of Science, Bangalore for their guidance and care.

I would also like to thank the examiners for taking their precious time to appraise this work, and for their constructive criticism, which has improved this thesis.

Declaration

I hereby assert that content of this submitted thesis, is derived entirely from my own work unless specified otherwise. Transmission electron microscopy work was carried out with the help of Heather Davies, Electron Microscopy unit, The Open University, Milton Keynes, UK. Primary rat astrocyte cultures were kindly provided by Dr Emma East/Dr James Phillips, The Open University, Milton Keynes, UK.

I further assert that this thesis does not exceed 100,000 words, including headers and references.

At the time of submission of this thesis, a part of this work has been published in the form of a poster. "13th International Blood-Brain Barrier Symposium, September 2nd -4th 2010, Zurich. *In vitro* interactions between human brain microvascular endothelium and astrocytes. Sreekanthreddy P, Heather A Davies, Ignacio A Romero, David K Male."

-

"Science is a body of knowledge, some of which is nearly certain, some rather uncertain but NONE of it is completely certain." Richard Feynman

-

Abstract

At the gliovascular interface, reciprocal inductive influences between brain microvascular endothelial cells (BMVEC) and astrocytes occur. Most of the knowledge in this area of research is derived from *in vitro* co-culture models in which astrocytes are cultured on a stiff, two-dimensional (2D) surface. Three-dimensional (3D) culture models closely mimic the *in vivo* cellular architecture and they bridge the gap between 2D culture models and animal models.

Hence, an *in vitro* 3D co-culture model was developed and characterised, to study the interactions between BMVEC and astrocytes. In this model, human astrocytes (HA) were seeded inside a collagen type–I gel while human immortalised cerebral microvascular endothelial cells (hCMEC/D3) were cultured on the gel surface. Both cell types were of human origin to improve the translatability of findings to humans *in vivo*. Additional important features of the model are the culture of endothelial cells on a soft matrix, and the simulation of the geometric relationship that exists *in vivo i.e.*, the interaction of astrocytes with BMVEC from their abluminal side.

To determine the effect of the 3D environment on the HA, the proliferation rate and expression of four molecules namely, glial fibrillary acidic protein (GFAP), aquaporin-4 (AQP4), endothelin-1 (Et-1) and endothelin receptor type-B (EDNRB), were compared between 3D and 2D cultured HA. The decreased expression of AQP4 and EDNRB and the much-decreased proliferation rate of 3D HA suggested their reduced reactivity and a similarity to their *in vivo* counterparts. However, 3D HA did not differ from the 2D HA in their ability to release soluble factors that induce barrier properties on BMVEC, as observed by similar levels of three expression markers of barrier phenotype on hCMEC/D3 cells namely, zonula occludens-1, claudin-5, and P-glycoprotein and similar paracellular permeability coefficients to fluorescent-dextrans (70 kDa).

Using the developed model, the effect of endothelial cells on the AQP4 expression in HA was investigated. While the localisation of astrocytic AQP4 did not change, its total, cellular expression levels were decreased as analysed by flow cytometry and fluorescence microscopy. The results could not be explained by physical-contact and therefore may be mediated by soluble factors released by the endothelial cells. Further investigation showed that Et-1, at least by itself, is not the mediator of this effect. The endothelial-astrocyte physical contact points were too few, as revealed by transmission electron microscopy, to study its effect on the localisation of AQP4 in HA.

The developed 3D co-culture model is usable and amenable to various analytical techniques such as fluorescence microscopy, electron microscopy, flow cytometry, and enzyme linked immunosorbent assay. The two-step collagenase digestion method developed in this study further broadens the model's utility to standard molecular and cellular biology techniques. The model has some advantages as well as limitations compared to the existing 2D and 3D co-culture models. The model may be used as an *in vitro* BBB model to study the transcytosis of nanoparticles, leukocytes, and possibly pathogens across the endothelial barrier and their interactions with astrocytes. In addition, the alterations in phenotype of astrocytes and endothelium *in situ*, in response to the soluble factors released by the other cell type can be studied. Further work is needed to validate some of the supposed unique features of the model. With the proposed modifications, it can be made physiologically more relevant, and the usability can be widened.

Table of contents

List of tables

List of figures

Abbreviations

Abbreviation	Description/Full form
2D	Two-dimensional
2D HA	Human astrocytes cultured on two-dimensional surface
3D	Three-dimensional
3D HA	Human astrocytes cultured in three-dimensional collagen hydrogel matrix
8-CPT-cAMP	8-(4-Chlorophenylthio) adenosine-3', 5'- cyclic monophosphate sodium salt
aa	Amino acids/ aminoacid residues
ABC transporters	ATP-binding cassette transporters
ACM	Astrocyte conditioned media
ALP	Alkaline phosphatise
AMT	Absorptive-mediated transcytosis
ANG1	Angiopoietin 1
ANG2	Angiopoietin 2
APC	Astrocyte precursor cells
AQP4	Aquaporin 4
ATP	Adenosine tri-phosphate
AU	Arbitrary units
BAEC	Bovine aortic endothelial cells
BBB	Blood-brain barrier
BCRP	Breast cancer related protein
BEC	Brain endothelial cells
bEnd.3	Immortalised mouse brain endothelial cell line
bFGF	Basic fibroblast growth factor
BL1	Basal lamina, layer 1
BL2	Basal lamina, layer 2
BMVEC	Brain microvascular endothelial cells
BSA	Bovine serum albumin

Abbreviation	Description/Full form
cAMP	Cyclic adenosine mono phosphate
CD13	Cluster of differentiation 13, alanyl aminopeptidase
CLDN5	Claudin-5
CM	Conditioned media
CMFDA	5-chloromethylfluorescein diacetate
CNS	Central nervous system
CNT	Concentrative nucleoside transporter
Conc.	Concentration
CSF	Cerebrospinal fluid
CuZnSOD	Superoxide dismutase-1
CYP1A	Cytochrome P450, family 1, subfamily A, polypeptide 1
CYP2B	Cytochrome P450, family 2, subfamily B
D3M	hCMEC/D3 cell nutrient culture medium
DAPI	4',6-diamidino-2-phenylindole
DMEM	Dulbecco's modified Eagle's medium
DNA	Deoxy ribonucleic acid
DNase I	Deoxyribonuclease I
EAAT	Excitatory amino-acid transporter
EBM®	Endothelial basal medium, from Clonetics™, Lonza.
EC	Endothelial cells
ECL	Enhanced chemiluminescence
ECM	Exta cellular matrix
ECV304	Presumptive human umbilical vein cell line by spontaneous transformation
EDNRA	Endothelin receptor, type A
EDNRB	Endothelin receptor, type B
EDTA	Ethylene diamine tetra acetic acid
EGM-2-MV®	Microvascular endothelial growth medium, from Clonetics™, Lonza.

Abbreviation	Description/Full form
ELISA	Enzyme-linked immunosorbent assay
ENT	Equilibrative nucleoside transporter
Et-1	Endothelin-1
Expt.	Experiment
FBS	Foetal bovine serum
FCS	Foetal calf serum
FITC	Fluorescein isothiocyanate
FSC	Forward scatter
GA-1000	Aqueous solution of Gentamicin Sulfate and Amphotericin-B
GDNF	Glial cell derived neurotrophic growth factor
GFAP	Glial fibrillary acidic protein
GGT	Gamma-Glutamyl transpeptidase
GLUT1	Glucose transporter-1
GPx	Glutathione peroxidase
HA	Human astrocytes
HAM™	Human astrocyte medium ™
HBEC	Human brain endothelial cells
HBMVEC	Human brain microvascular endothelial cells
HBSS	Hank's balanced salt solution
hCMEC/D3	Immortalised human cerebral microvascular endothelial cell line
HRP	Horseradish peroxidase
HUVEC	Human umbilical vein endothelial cells
ICAM2	Intercellular adhesion molecule 2
IgG	Immunoglobulin G
IL-10	Interleukin-10
IL-6	Interleukin-6
IP-10	Interferon-gamma-inducible 10 kDa protein, also known as CXCL10
IP3	Inositol triphosphate

Abbreviation	Description/Full form
JAM	Junctional adhesion molecule
kDa	Kilo dalton
Kir 4.1	Potassium inwardly-rectifying channel, subfamily J, member 10, KCNJ10
LAM	Leukocyte adhesion molecules
LAT	L-type amino acid transporter
LDL	Low density lipoprotein
LIF	Leukaemia inhibitory factor
MCP-1	Monocyte chemo attractant protein-1, CCL2
MCT	Monocarboxylic acid transporter
MDR1	Multidrug resistance protein 1
MEM	Minimum essential medium
MnSOD	Manganese superoxide dismutase
mRNA	Messenger ribonucleic acid
N/A	Not applicable
NADPH	Nicotinamide adenine dinucleotide phosphate, $NADP^+$
NaN_3	Sodium azide
NG2	Neuron-glial antigen 2, Chondroitin sulphate proteoglycan 4 (CSPG4)
NO	Nitric oxide
No.	Number
OAPs	Orthogonal array particles
OAT	Organic anion transporter
OCT	Organic cation transporter
OCL	Occludin
P2Y1	Purinergic receptor P2Y, G-protein coupled, 1 (P2RY1)
P2Y2	Purinergic receptor P2Y, G-protein coupled, 2 (P2RY2)
PBS	Phosphate buffered saline
PDGF	Platelet derived growth factor

Abbreviation	Description/Full form
PDGFR-b	Platelet derived growth factor receptor-beta
PECAM, PECAM1	Platelet endothelial cell adhesion molecule 1
PerCP	Peridinin chlorophyll A
PET	Polyethylene terephthalate
PFA	*p*-formaldehyde
P-gp	P-glycoprotein-1, MDR1, ABCB1
PIC	Protease cocktail inhibitor
PLP	*p*-formaldehyde-lysine-periodate fixative
RO-20-1724	4-(3-butoxy-4-methoxybenzyl)-2-imidazolidinone
RA	Rat astrocytes
RBE4	Rat brain endothelial 4 cell line
RIPA buffer	Radioimmunoprecipitation assay buffer
RMT	Receptor-mediated transcytosis
RT	Room temperature
RT-PCR	Reverse transcriptase-polymerase chain reaction
S100B	S100 calcium binding protein B
SDS	Sodium dodecyl sulfate
SDS-PAGE	Sodium dodecyl sulfate polyacrylamide
SEM	Standard error of mean
SHH	Sonic hedgehog homolog
SGLT1	Sodium dependent glucose transporter 1
SLC	Solute carrier
SMA-α	Alpha-smooth muscle actin
SNAT	Small neutral amino acid transporter
SSC	Side scatter
TEER	Trans endothelial electrical resistance
TEM	Transmission electron microscopy
TGF-β	Transforming growth factor, beta

Abbreviation	Description/Full form
TJP	Tight junctional protein
TLCK hydrochloride	Tosyllysine chloromethyl ketone hydrochloride
Tris	Tris(hydroxymethyl)aminomethane
VEGF	Vascular endothelial growth factor
VEGFA	Vascular endothelial growth factor A, also known as VEGF
ZO-1	Zonula occludens 1, also known as TJP1
ZONAB	zonula occludens 1 (ZO-1)–associated nucleic acid binding protein

Chapter 1:

General introduction

For proper functioning of neurons, the ionic balance has to be maintained within an optimal physiological range. Therefore, neurons and interstitial fluid are separated from the blood by a cellular barrier, so that any fluctuations in the blood composition and any potentially harmful substances in blood will not hinder neuronal function. Along the interface of the central nervous system (**CNS**) and blood, there is a specialised layer of cells that controls the entry of blood borne substances into CNS, which is called the blood-neural barrier. Depending on the anatomical location, this regulatory interface is one of three types. (1) Blood-brain barrier (between blood and brain interstitial fluid), (2) Blood- ventricular cerebrospinal fluid (CSF) barrier (made of choroid plexus epithelium) (3) Arachnoid epithelium between blood and subarachnoid CSF (reviewed in Abbott, 2010).

1.1 Blood-brain barrier (BBB)

A blood-brain barrier (**BBB**) is present in all organisms with a well-developed CNS. The BBB occupies most of the interface between blood and CNS. Among all the blood-neural barriers, the BBB is the tightest barrier; neurons are within 10-20 μm from the BBB and neuronal function is potentially vulnerable to blood borne substances. The BBB is made up of specialised endothelial cells that form the cerebral capillary wall and astrocytic foot processes (reviewed in Abbott, 2010).

Functions of BBB

1. To maintain a stable ionic (K^+, $Ca2^+$, $Mg2^+$) concentration and pH for optimal functioning of neurons.
2. To stop the entry of the neurotransmitter glutamate which fluctuates after food intake (Bernacki, 2008).

3. To stop the entry of unwanted serum proteins and neurotoxic endogenous metabolites or xenobiotics present in the blood.

4. To provide nutrition to the brain (reviewed in Abbott, 2010, Ballabh, 2004).

1.1.1 Cerebral capillary endothelial cells display a unique phenotype

Cerebral capillary endothelial cells have special features that provide the barrier phenotype. In this thesis, henceforth, cerebral capillary endothelial cells will be referred to as brain microvascular endothelial cells (**BMVEC**). BMVEC differ from endothelial cells (**EC**) of the rest of the body in three main aspects (reviewed in Ballabh, 2004).

(1) Extensive tight junctions. The single most important feature of BMVEC is continuous tight junctions. Although peripheral endothelial cells also express tight junctions, BMVEC have a more complex network of tight junctions, which limit the passage of hydrophilic molecules more effectively through the intercellular gaps (Wolburg, 2002). BMVEC tight junctions are tight enough to inhibit the passage of small ions (radius $\geq$3.6 A°) thus; they acquire high transendothelial electrical resistance (**TEER**). The TEER of rat brain *in vivo* is ~1400 $\Omega.cm^2$ (Butt, 1990), whereas in frog brain it has been reported to be ~1870 $\Omega.cm^2$ (Crone, 1982). In non-BMVEC, tight junctional strands are mainly associated with the E-face (extracellular facing lipid leaflet) and almost absent in the P-face (protoplasm facing lipid leaflet); whereas in BMVEC, they are present on both E- and P- faces and sometimes relatively higher in the P-face than in the E-face (Wolburg, 2009a).

(2) Non-fenestrated, continuous endothelium. BMVEC do not have fenestrations and are continuously lined by a basal lamina without intercellular gaps. Therefore, unlike discontinuous (sinusoidal) and fenestrated endothelia the movement of molecules out of the capillary wall is very limited. Fenestrae are small transcellular openings of 60-80 nm in diameter operated by a diaphragm, which increase the permeability of capillaries. Tissues with

high rates of fluid exchange e.g., small intestinal villi, glomeruli of kidney, and endocrine glands have capillaries with fenestrated endothelia. Almost unrestricted transfer of molecules is facilitated by discontinuous endothelium that does not have a basement membrane and has wide intercellular spaces (30-40 μm in diameter). This is found in liver, spleen and bone marrow (Aird, 2007).

(3) Reduced pinocytic activity. In comparison with peripheral endothelium, non-specific, non-receptor mediated, non-adsorptive mediated, fluid phase endocytosis is greatly reduced in BMVEC (Marchesi, 1965).

1.1.2 Additional features of brain capillary endothelial cells

Solute carrier transporters. Because of the three characteristics described above, molecular traffic across the cell layer into the brain is highly reduced. Therefore, the necessary nutrients for the proper functioning of CNS are imported into the brain by specialised transporter proteins present on the capillary wall.

In general, lipid soluble molecules such as oxygen and CO_2 can diffuse through the BBB. However, other nutrients that are polar in nature are transported into brain by several solute carrier (SLC) transporter molecules expressed on BMVEC. For example glucose is transported by GLUT1 and SGLT1; aminoacids by LAT 1-2, SNAT 1-5, EAAT 1-3; nucleosides and nucleotides by ENT 1-2 and CNT 1-3; monocarboxylic acids by MCT 1-2; organic ions by OAT 2-3, OCT 2-3 *etc.* Some of these are predominantly expressed on either the luminal (GLUT1, ENT1-2, OCT 2-3), or abluminal (SGLT1, SNAT2 and -3, EAAT 1-3, CNT 1-3) membrane of the cell (reviewed in Abbott, 2010).

ABC transporters. In addition, to stop the entry of lipid soluble neurotoxins into the brain, ATP-binding cassette (ABC) efflux transporters are expressed on BMVEC. The ABC superfamily consists of at least 48 members and many of them are expressed by BMVEC.

Well studied members include P-glycoprotein (P-gp, MDR, ABCB1), Breast cancer related protein (BCRP, ABCG2) and multidrug resistance proteins, MRP 1-5 (Begley, 2004). While P-gp, BCRP and MRP2 are expressed mainly on the luminal membrane, MRP1 is present on both the luminal and abluminal membranes (reviewed in Abott, 2010).

Transcytosis of macromolecules. The macromolecules required for brain function are transported into the brain by either receptor-mediated transcytosis (RMT; iron, lipoproteins, glycosylated proteins, Leptin, *etc.*) or absorptive-mediated transcytosis (AMT; albumin). BMVEC appears to have a special ability in that endosomes are diverted away from the lysosomal compartment in order to complete transcytosis (Kalimo, 2005, reviewed in Abbott, 2010).

Metabolic barrier/enzymatic barrier/drug metabolising enzymatic barrier: BMVEC express some intracellular enzymes that metabolise potentially toxic lipophilic compounds from both endogenous and exogenous origin into polar metabolites, so that they are unable to cross the abluminal membrane and enter into the brain. The high activity of these enzymes at the circumventricular organs where endothelial tight junctions are absent, suggests a barrier role for these enzymes (el-Bacha, 1999). Some of the intracellular drug-metabolising enzymes namely monoamine oxidase and cytochrome P450 isoforms CYP1A and CYP2B, NADPH-cytochrome P450 reductase, and uridine diphosphate glucuronosyltransferase (UGT) are also found in cultured BMVEC (Chat, 1998). Moreover, extracellular enzymes such as peptidases and nucleotidases may also contribute to the metabolic barrier (Abbott, 2006). Moreover, there may be interplay between ABC efflux transporters and drug metabolising enzymes, which determines the drug penetration and concentration in the CNS (Decleves, 2011).

Mitochondrial content. BMVEC cells have increased mitochondrial content that contributes to 8-11% of their cytoplasmic volume in contrast to 2-5% in peripheral endothelial cells. This

may be to meet the high-energy demand of BMVEC cells to carry out energy-dependent carrier mediated transport activities (Oldendorf, 1977).

1.1.3 Intercellular junctions of BMVEC

Intercellular junctions of BMVEC consist of tight junctions on the apical side and adherens junctions on the basolateral side. A simplified schematic diagram of a junctional complex of BMVEC is illustrated in **Figure 1-1**.

1.1.3.1 Tight junctions

Tight junctions are formed by a group of transmembranous and cytoplasmic proteins linked to the actin cytoskeleton. The transmembranous tight junctional proteins include claudins, occludin, and junctional adhesion molecules (JAMs). They are linked to the actin cytoskeleton and various signalling components, such as protein kinases and GTP binding proteins via multiple adapter proteins (tight junctional associated proteins) belonging to the zonula occludens family (reviewed in Matter, 2003, Huber, 2001). Mainly claudins and occludin are primarily responsible for the selective paracellular permeability of brain endothelial cells. The function of JAMs is less well understood and probably involved in leukocyte adhesion and intercellular localisation of occludin (**Figure 1-1**).

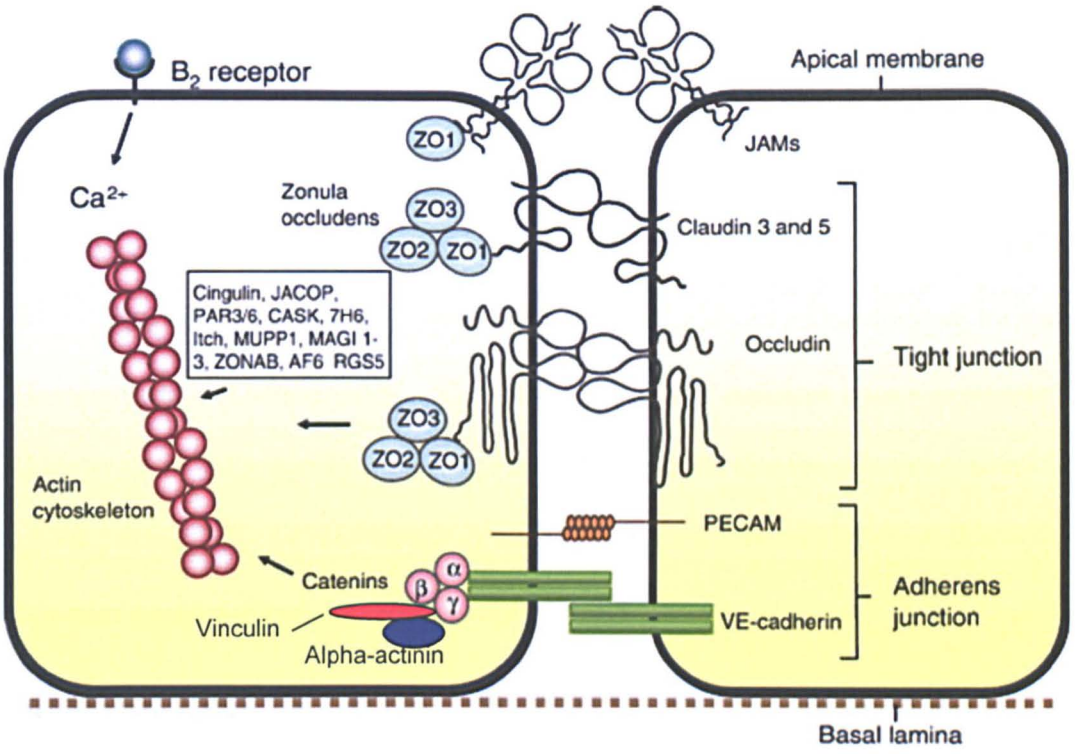

Figure 1-1 Junctions of BBB endothelial cells

Tight junctions consist of transmembrane proteins occludin, claudin -3, -5 and junction adhesion molecules (JAMs). Claudins and occludin have four transmembrane domains. These are attached to first level adapter proteins ZO-1, ZO-2, and ZO-3, which are connected to the actin cytoskeleton through secondary adapter proteins like cingulin, cingulin-like-1, and ZONAB *etc.* JAMs are IgG superfamily members. Adherens junctions are mainly formed by vascular endothelial cadherin (VE-cadherin) and platelet endothelial adhesion molecule (PECAM). VE-cadherin is a transmembrane protein, whose cytoplasmic domain is linked to α, β, δ catenins that are in turn liked to the actin cytoskeleton. Catenins are also attached to focal adhesion molecules like vinculin and α-catenin, which are required for cell-matrix interaction. Activation of B2 bradykinin receptor leads to a rise in intracellular calcium, resulting in centripetal pulling of the actin cytoskeleton, which in turn regulates the transmembrane protein configuration. The image is adapted from Abbott *et al.* (2010).

1.1.3.1.1 Claudins

Claudins (~23 kDa) are the most important tight junctional molecules that confer selective barrier properties to BMVEC. Among at least 20 known members of the claudin family, claudin-3, -5 and -12 are generally expressed in BMVEC. Activation of Wnt/B-catenin signalling, which is known to be involved in BBB development and maturation, increases claudin-3 expression (Liebner, 2008). The BBB in claudin-5 deficient mice was selectively permeable to <800 Da molecules indicating a role of claudins in the size-selective permeability of the BBB (Nitta, 2003). Loss of claudin-3, and -5 in glioblastoma multiforme indicates their role in barrier integrity (Wolburg, 2003, Liebner, 2000).

1.1.3.1.2 Occludin

Occludin is a 65-kDa protein that exists in several isoforms, and was the first discovered transmembrane tight junctional molecule (Furuse, 1993). Occludin does not seem to contribute directly to barrier tightness but may be involved in intracellular signalling that modulates tight junctions (Saitou, 2000). Occludin function is modulated by phosphorylation but it is not yet certain whether its phosphorylation increases or decreases BBB integrity (Sakakibara, 1997, Antonetti, 1999).

1.1.3.1.3 Zonula occludens

Transmembrane junctional proteins are connected to the actin cytoskeleton via cytoplasmic adapter proteins called zonula occludens -1, -2, and -3 (ZO-1, ZO-2, ZO-3), which are again linked to the actin cytoskeleton via secondary adapter proteins like cingulin, Cingulin-like 1 *etc.* They are localised to the cytoplasmic face of tight junctions. ZO-1 (220kDa) was the first identified and most studied tight junctional associated protein (Stevenson, 1986).

ZO proteins belong to a family of membrane-associated guanylate kinase-like (MAGUK) proteins. The presence of PDZ, an SRC homology-3, and a guanylate kinase-like domain,

enables these proteins to serve both structural and signalling functions. Nuclear localisation and nuclear export signals on these proteins suggest that they regulate gene expression. Nuclear localisation of ZO-2, which resulted in increased proliferation, has been reported (Traweger, 2008).

1.1.3.2 Adherens junctions

Adherens junctions are mainly formed by cadherins (calcium dependent adhesion molecules), which are transmembrane glycoproteins. VE-cadherin (vascular endothelial cadherin) is a well-studied cadherin present on all endothelial cells. BMVEC transiently express N-cadherin during early angiogenesis stages before VE-cadherin begins to appear. Pericytes may directly interact with N-cadherin on BMVEC (Gerhardt, 1999, Gerhardt, 2000). Cadherin-10 was reported to be a BBB specific form as it is expressed only in tight microvasculature such as the BBB, retinal endothelium, and ventricular epithelium, but not in the brain circumventricular organs (CVO), glioblastoma tumours, and non-CNS tissues. Interestingly, there seems to be an inverse relation between the expression of cadherin-10 and VE-cadherin (Williams, 2005).

Adherens junctions are essential for lateral cohesion of cells. Adherens junctions themselves cannot act as a paracellular barrier; but indirectly contribute to tightness of the barrier by helping in the formation, organisation, and regulation of tight junctions. VE-cadherin is linked to the actin cytoskeleton via scaffolding proteins called α-, β-, δ– Catenins. Beta-catenin emerged as a key mediator between adherens and tight junctions. VE -cadherin promotes claudin-5 transcription by preventing the nuclear accumulation of transcriptional regulators, FoxO1 and β-catenin, which repress the claudin-5 promoter (Taddei, 2008). Stabilisation of β-catenin enhances barrier maturation *in vivo* and claudin-3 upregulation and tight junction formation and regulation of BBB specific genes *in vitro* (Liebner, 2008).

1.2 Gliovascular interface

1.2.1 Cellular constituents of BBB

Although BBB functions are primarily performed by BMVEC, these cells are closely associated structurally and functionally with other cell types. The BMVEC lining the capillary wall are surrounded by basal lamina and pericytes, which are in turn surrounded by perivascular endfeet of astrocytes, microglia, and neuronal processes (**Figure 1-2**). Sometimes, perivascular macrophages are also found between BMVEC and astrocytes. The capillary wall is often made of single endothelial cell, which is surrounded by a first (inner) layer of basal lamina in which pericytes are embedded. A second layer of basal lamina, which is present abluminal to the pericytes, is completely covered with astrocytic endfeet thus separating astrocytes from endothelial cells by two layers of basal lamina. Therefore, BMVEC, pericytes, and astrocytes are separated from each other by a basal lamina without direct cell-cell contact (Simard, 2003). *In vivo* BMVEC are very thin with a thickness of ~0.5 μm (Abbott, 2010). The interactions between different cellular components of BBB are essential for induction and maintenance of the BBB phenotype of BMVEC.

1.2.1.1 Basal lamina

The bilayered basal lamina present between BMVEC and astrocytes usually has a thickness of 20-200 nm (Brightman, 1969, Cornford, 2005). The layer beneath the BMVEC, known as endothelial basement membrane, is deposited by the BMVEC itself. Pericytes also may secrete or induce endothelial cells to secrete some of the matrix components (Stratman, 2009). The layer adjacent to the endfeet, known as the parenchymal or glial basement membrane is deposited by astrocytes and leptomeningeal cells. The main components of basal lamina are collagen type IV, laminins, heparan sulfate proteoglycans, nidogens, and fibronectin. The composition of each layer is not the same and some components are specific to each layer. At the level of capillaries, both layers are fused and appear as a single layer. Collagen type-IV,

perlecan, a heparan sulfate proteoglycan, and Laminins -411 and -511 are specific to endothelial basal lamina whereas Laminin-211 is specific for the glial basal lamina (Engelhardt, 2009). Agrin, a heparan sulfate proteoglycan secreted by endothelium (Stone, 1995, Noell, 2009) is also located in the basal lamina between the endfeet of astrocytes and endothelium, but there is ambiguity about its location on which layer of the basal lamina.(Wolburg-Buchholz, 2009).

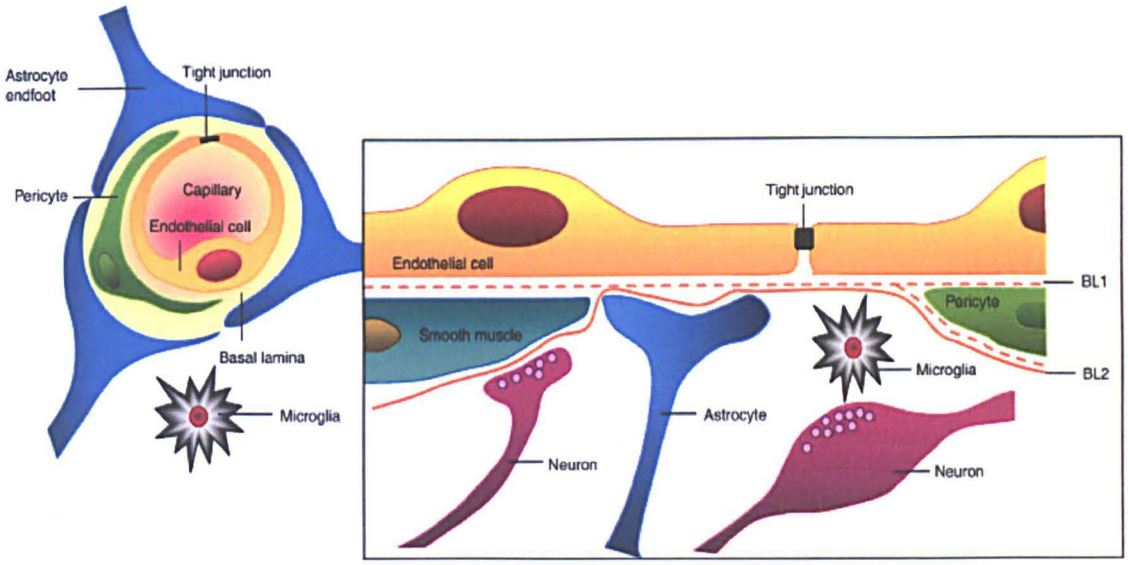

Figure 1-2 Cellular constituents of blood-brain barrier

The capillary wall is made of endothelial cells, with tight junctions sealing the intercellular gaps. Abluminal to the endothelial cells is a basal lamina (BL1) in which pericytes are embedded. Pericytes and the basal lamina (BL2) are ensheathed by astrocytic endfeet. BL2 is different from BL1 in its composition. Pericytes do not fully cover endothelial cells while astrocytes fully cover the capillary wall. At larger vessels, pericytes are replaced by smooth muscle cells. Microglial cells are immunocompetent cells of the brain. Perivascular macrophages are not shown in the image. Axonal projections from the neurons release vasoactive mediators thus regulating the arteriolar contraction. Generally, astrocytes act as a bridge between neurons and the arteriole wall. Image source: (Abbott, 2010)

1.2.2 The capillary wall is ensheathed by astrocytic endfeet

The endothelial cells are ensheathed by astrocytic endfeet. Studies reported varying coverage of astrocytic endfeet, ranging from 2/3 rd of the capillary surface to complete (reviewed in Mathiisen, 2010). A recent study (Mathiisen, 2010) using electron microscopic 3D reconstruction techniques on rat hippocampus reports that endfeet almost completely cover the capillary wall. Two thirds (~63%) of the capillary surface is in direct contact with endfeet, ~37% of capillary surface is in direct contact with pericytes and probably ≤ 1% capillary surface i.e., basal lamina is in contact with apparent microglial processes. Almost all the abluminal surface of pericytes is covered with astrocytic endfeet except ≤1 %, which is open for direct interaction with neuropil elements. So, effectively, 2/3 rd of the capillary surface is in direct contact with endfeet and 1/3 rd is covered with pericytes, which is covered abluminally by astrocytic endfeet. In another study using rat brain cortex and hippocampal slices, it was confirmed that astrocytic endfeet cover the entire surface of micro and macro vessels as evidenced by AQP4 staining (Simard, 2003).

1.2.3 Astrocytes themselves can play a barrier role

Although the capillary tube is completely ensheathed by astrocytes, the barrier provided by astrocytes is not as tight as the endothelial barrier as they do not have tight junctions (Simard, 2003). However, endfeet of astrocytes regulate water flux between blood and brain and are responsible for water content in the brain (Haj-Yasein, 2011). The early vertebrates, elasmobranch fish have a BBB made by perivascular glial end-feet. Some of the higher invertebrates (insects, crustaceans, and cephalopods) also have a barrier made of glial cells. Therefore, it appears that during evolution, a glial barrier is replaced by a more sophisticated endothelial barrier. Traces of the glial barrier may still be observed in some regions of mammalian brain such as the choroid plexus, circumventricular organs and retinal pigment epithelium (Abbott, 2005).

1.2.4 The barrier phenotype of capillary endothelium is not intrinsic but induced by the surrounding neural micro environment

If the barrier phenotype of capillary endothelial cells is the consequence of having developed from specialised mesoderm, as Bevan *et al.* (Bevan, 1979) suggested, then it is unclear why a barrier is absent in some areas of the brain, and why the capillaries in the peripheral nerves display a barrier phenotype. Therefore, it seems more likely that the special properties of capillary endothelial cells are not intrinsic but induced by their immediate tissue neural microenvironment. For the first time, Stewart *et al.* provided convincing evidence for this hypothesis through a quail-chick transplantation study (Stewart, 1981).

1.3 Astrocytes are main inducers of BBB phenotype in capillary endothelial cells

Although, it was proven that the neural microenvironment could induce the BBB phenotype in capillary endothelial cells, it was not known which cell type was responsible for this. Because, astrocytes most closely interact with capillary endothelial cells, they were thought to be responsible for the BBB phenotype induction in the endothelial cells, if not playing an active role in barrier function (Davson, 1967).

The initial evidence for BBB induction potential of astrocytes came from *in vitro* cell culture studies. Cultured BEC, either primary or immortalised cells, do not retain all features of the *in vivo* BBB phenotype. However, when co-cultured with astrocytes, at least some features of the BBB were partly restored. Gamma-glutamyl transpeptidase (GGT), a marker for *in vivo* BMVEC is generally lost in *in vitro* cultured cells. When, GGT negative mouse BMVEC cultures were co-cultured with C6 glioma cells, GGT expression increased (DeBault, 1980). Similarly, rat astrocytes induced an increase in length, width and complexity of tight junctions of bovine BMVEC in co-cultures (Tao-Cheng, 1987). C6 glioma cells were able to re-establish the polarised, Na^+ dependent neutral amino acid transport on cultured BEC cell membranes in co-culture (Beck, 1984).

Direct evidence for the BBB induction potential of astrocytes was provided by Janzer *et al.* (1987). When rat astrocytes were transplanted into the anterior eye chamber of the rat, the non-neural endothelial cells invaded astrocyte aggregates and formed capillaries that displayed barrier properties, indicating that astrocytes have BBB induction potential.

Subsequently, several *in vitro* co-culture studies have demonstrated the role of astrocytes on the induction of several BBB features of BEC (Abbott, 2002, Haseloff, 2005, Abbott, 2006, Bauer, 2000).

1.3.1 Physical barrier markers/Tight junctional proteins

Upregulation of tight junctional proteins or an increase in their complexity and organisation or increase in TEER resistance or decrease in paracellular permeability has been demonstrated by several studies (Dehouck, 1990, Sobue, 1999b, Rist, 1997).

1.3.2 Transport barrier markers

GLUT-1: Glucose transporter 1 (GLUT1, SLCC2A1) facilitates the transport of glucose across the plasma membrane of BMVEC from the blood to brain side. GLUT1 activity as measured by glucose uptake was enhanced in BMVEC when co-cultured with astrocytes or astrocytoma cells in a time dependent manner and the constant presence of astrocytes was necessary for induction (Maxwell, 1989).

P-glycoprotein: P-gp levels and activity were increased by C6 glioma factors on a rat brain endothelial cell line, RBE4 (El Hafny, 1997). Similarly, rat primary astrocytes also induced expression of P-gp protein on primary bovine BMVEC in co-culture (Gaillard, 2000). Increased cell surface expression of P-gp and its mRNA was also observed in a human co-culture model (Megard, 2002).

In another study, Na^+ K^+ ATPase activity of BMVEC was induced after co-culturing with astrocytes (Bauer, 1990).

Induction of polarity: *In vivo* BMVEC express many molecules in a polarised manner, either on the luminal or abluminal membrane. *In vitro* BMVEC lose their polarity. For example, P-gp is predominantly localised to the luminal membrane of BMVEC *in vivo.* Re-induction of the polarity *i.e.,* luminal localisation and increased activity of P-gp were observed when rat BMVEC were co-cultured with rat astrocytes in a 3D co-culture model (Al Ahmad, 2010). Similarly, C6 glioma cells were able to re-establish the polarised, Na^+ dependent neutral amino acid transporter on BMVEC cell membranes in co-culture (Beck, 1984).

Low Density Lipoprotein (LDL) receptors: In general, circulating LDL keeps the LDL receptors at a low level in vascular endothelial cells. However, *in vivo* BMVEC express LDL receptors unlike macro-vascular endothelial cells. Using an *in vitro* co-culture system, it has been shown that a soluble factor released by astrocytes increases the LDL receptor expression on BMVEC and it has been proposed that the lipid requirement of astrocytes modulates the LDL receptor expression of BMVEC (Dehouck, 1994).

Gamma-glutamyl transpeptidase (GGT): GGT plays a key role in the gamma-glutamyl cycle. This pathway is involved in synthesis and degradation of glutathione, and has been shown to influence amino acid transport in various tissues. The presence and high activity of GGT is considered a marker for a functional barrier phenotype of BMVEC (Hawkins, 2006). *In vitro* cultured BMVEC generally lose their GGT activity. Apart from early studies by DeBault *et al.* (1980) later studies also have shown that GGT activity can be reinduced in BMVEC by co-culturing with astrocytes or by exposing to astrocytic conditioned media (Hayashi, 1997, Dehouck, 1990).

1.3.3 Other markers

Alkaline phosphatase (ALP): A high specific activity of ALP is correlated with a mature differentiated BBB (Vorbrodt, 1986, Dermietzel, 1991) and is used as a marker for the BBB phenotype of BMVEC (Betz, 1980). Astrocytes in co-culture increased the ALP activity in bovine BMVEC (Sobue, 1999b). Similarly, immortalised rat BMVEC showed increased ALP activity in co-culture with astrocytes (Blasig, 2001, Beck, 1986). Synergistic stimulation of GGT and ALP activities by retinoic acid and astroglial factors in immortalised rat BMVEC has also been shown (El Hafny, 1997).

1.3.4 The BBB in astrocytoma

In astrocytomas, loss of tight junctional proteins namely, occludin (Papadopoulos, 2001), claduin-3 (Wolburg, 2003), and claudin -5 (Liebner, 2000) has been observed. This suggests

that the barrier phenotype of BMVEC depends on the microenvironment, especially astrocytes. A leaky vasculature in astrocytoma tissue might be the result of either discontinued secretion of the inductive signals or secretion of factors that increase the vascular permeability. Indeed astrocytoma cells secrete vascular growth factor (VEGF) which promotes angiogenesis while simultaneously increasing vascular permeability (Connolly, 1991, Machein, 1999). Taken together, evidence of BBB compromise in astrocytoma supports the theory that normal astrocytes are important, if not necessary, for BBB maintenance.

1.3.5 Contrary evidence for an astrocytic role in BBB induction

BBB formation during development: The primary source of signals for induction of the BBB phenotype in BMVEC remains a matter of debate since astrocytes, pericytes (section 1.6.1), neurons (section 1.6.2), and neuronal progenitor cells (Weidenfeller, 2007) were all shown to have barrier enhancing properties. In the brain, *de novo* vasculogenesis is followed by angiogenesis, which is followed by barriergenesis. Differentiation of nascent capillary endothelial cells into BBB forming mature BMVEC is termed barriergenesis (Engelhardt, 2003). During the time of barriergenesis, mature astrocytes are absent or scarce but become the predominant population only during postnatal stages. Therefore, barriergenesis or BBB formation begins much earlier than gliogenesis (reviewed in Lu, 2012, reviewed in Saunders, 2000, Holash, 1993). During embryogenesis, as the endothelial cells invade the CNS, pericytes are recruited to the growing vessels, and this event correlates in time with the development of BBB properties on endothelial cells, which occurs before gliogenesis (Daneman, 2010). Therefore, it is unlikely that astrocytes are the primary inducers of the BBB phenotype in endothelial cells. Since the BBB phenotype arises even in the absence of pericytes, other cell types such as neural progenitor cells may be the primary source of BBB inductive signals. In agreement with this, differentiating neural progenitors were shown to enhance barrier properties (TEER) of BMVEC *in vitro* to similar levels as astrocytes, but their effect was earlier

and shorter than that of astrocytes (Weidenfeller, 2007). Therefore, Daneman *et al.* (2010) hypothesised that neural progenitor cells induce early BBB specific genes on endothelial cells, then pericytes regulate BBB development until maturation and astrocytes regulate BBB maintenance during adulthood (**Figure 1-3**). Even in adult life, soluble factors released by stem cells present in the subventricular zone and subgranular zone of the hippocampus, may still be responsible for the maintenance of the BBB phenotype (Lu, 2012).

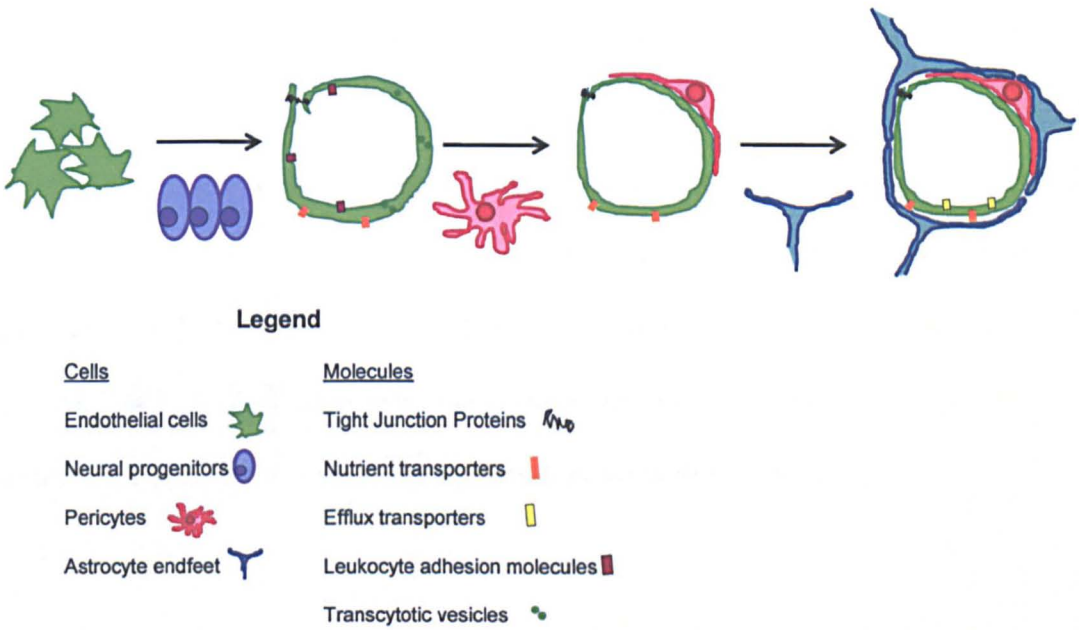

Figure 1-3 Multiphase regulation of BBB phenotype of BMVEC by multiple cell types

The model proposed by Daneman *et al.* (2010) suggests that during embryonic development neural progenitors induce endothelial cells to express a few BBB specific proteins, including tight junction molecules and nutrient transporters. Later pericytes are recruited to vessels and then strengthen the BBB properties by inducing proper organisation of the tight junctions, and by reducing the transcytosis, and leukocyte adhesion molecules. Astrocytes, which come into the scene later, encircle the capillary wall and regulate BBB maintenance during health and disease through adulthood. The image is reproduced from Daneman, 2010.

A few more observations suggest that astrocytes may not be the primary inducers of the BBB phenotype in endothelial cells. Pial vessels in frog and rat display all the characteristics of the BBB, despite not being covered by astrocytic endfeet (Crone, 1982, Butt,

1990). Similarly, iris capillaries even in the absence of astrocytes, maintain barrier properties (Small, 1993). In circumventricular organs, despite the presence of astrocytes, vessels are leaky. However, it is argued that astrocytes do not ensheath the vessels in this region; therefore, it is not directly comparable to other regions of the brain (Bouchaud, 1989). It was reported that although selective removal of astrocytes caused BBB leakage, the BBB could self-repair even in the absence of direct astrocyte contact (Willis, 2004), raising a doubt on the necessity of astrocytes for BBB maintenance. More importantly, the results of Janzer *et al.* (1987), which provided the first *in vivo* evidence for an astrocyte role in BBB induction through graft experiments, could not be reproduced by Stewart and colleagues (Holash, 1993). They argued that limitations in the experimental methodology of Janzer *et al.* does not justify the conclusion that matured astrocytes have a primary inductive role but may have a role in the maintenance of the BBB phenotype in already differentiated or BBB committed endothelial cells. Altogether, it appears that the role of astrocytes in the maintenance of the BBB is not doubted, but their role in *de novo* BBB induction remains to be determined.

1.4 Modes of inductive signalling at the BBB

In vivo, astrocytes are in physical contact with the capillary wall. Therefore, it seems obvious that astrocytes may induce the BBB phenotype on BMVEC through physical contact. However, in some regions of the brain, pial microvessels, despite not being ensheathed by astrocytes, show at least some BBB features. This gives rise to the idea that soluble factors released by the glia limitans might also show BBB-inducing properties (Allt, 1997).

1.4.1 Induction through soluble factors

Several *in vitro* studies have demonstrated, using non-contact co-culture systems or astrocyte conditioned media (ACM), that BBB induction can occur through soluble factor signalling. Some of the BBB features induced by astrocyte released factors were decreased paracellular permeability to various paracellular tracers (Sobue, 1999b, Cecchelli, 1999, Siddharthan, 2007), increased TEER resistance (Hurst, 1996, Siddharthan, 2007) and modulation of system L transporters (Omidi, 2008), and increased ALP activity (Sobue, 1999b).

1.4.1.1 Identification of soluble factors

Some of the astrocyte-released factors that are responsible for their BBB induction potential have been identified namely, transforming growth factor, beta (TGF-β) (Tran, 1999), basic fibroblast growth factor (bFGF) (Sobue, 1999b), glial derived neurotrophic growth factor (GDNF) (Igarashi, 1999, Utsumi, 2000) and angiopoietin 1 (ANG1) (Lee, 2003), and recently sonic hedgehog (SHH) (Alvarez, 2011).

1.4.2 Induction through direct physical contact

Although, BBB induction is carried out by soluble factors released by astrocytes, several studies have shown, by comparing the effects of contact co-culture with non-contact co-culture, that the physical contact further enhances induction of the BBB phenotype. For the list of studies, see **Table 1.**

Table 1 List of *in vitro* studies that demonstrated that physical contact between BMVEC and astrocytes causes enhanced induction of BBB phenotype on BMVEC

Examined BBB phenotype	Endothelial cell source	Astrocyte cell source	Co-culture system	Reference
GGT	Mouse immortalised BMVEC (ME-2)	C6 glioma cells	Coverslip EC cultures facing astrocyte bed	(DeBault, 1980, DeBault, 1981)
Increase in the TJP complexity	Bovine BEC	Rat astrocytes	EC culture directly grown on astrocyte bed	(Tao-Cheng, 1987)
Increased activity of GGT and ALP	Porcine BMVEC	C6 glioma cells	Contact-transwell	(Meyer, 1991)
Reduced paracellular permeability to L-glucose, formation of TJP like structures	Bovine BEC, Bovine AEC	Rat astrocytes	Contact-transwell	(Isobe, 1996)
Increased GGT activity, transferrin receptor expression, P-gp expression, mitochondria no., and decreased permeability to inulin	HUVEC	Rat foetal astrocytes	Contact-transwell	(Hayashi, 1997)
Increased occludin, and CLDN5 and increased TEER	Porcine BMVEC	Rat astrocytes	Contact-transwell	(Malina, 2009)
Increased TEER	Human BMVEC	Human astrocytes	Contact-transwell	(Kuo, 2011)

Interestingly, physical contact seems to be necessary for the induction of Gamma-glutamyl transpeptidase (GGT). It has been shown in an *in vitro* co-culture study that only those BMVEC in physical contact with astrocytic end feet had increased activity of the enzyme GGT (DeBault, 1980, DeBault, 1981). In another study that co-cultured HUVEC cells with rat foetal astrocytes, only a contact co-culture system induced GGT activity while in a non-contact co-culture system, enzyme levels were not induced (Hayashi, 1997). Importantly, a non-contact co-culture system was able to induce other BBB features such as increased GLUT1 and transferrin expression and decreased permeability to inulin, although less effectively than in a contact co-culture system.

1.4.3 Basal lamina/Extra cellular matrix (ECM) mediated induction

Tao-Cheng *et al.* (1987) proposed that since they have observed no direct intercellular junctional communication between these two cell types either *in vivo* or *in vitro*, the tight junctional induction in their co-culture experiments could be occurring through extracellular matrix associated non-soluble factor mediated signalling.

In another study, based on the experiments using BMVEC grown in the presence of ACM, with or without endothelial-derived-ECM coated substrate, it was clear that tight junction formation was dependent not only on astrocyte derived factors but also on a 'competent extracellular matrix' (Arthur, 1987).

The importance of ECM was also realised when Miziguchi *et al.* (1994) reported that GGT activity in BMVEC is regulated by astrocyte derived ECM, and that the component of ECM that regulates GGT activity in BMVEC originates from the BMVEC-astrocyte interaction.

In vivo, the basal lamina between BMVEC and astrocytes contains ECM proteins such as fibronectin, collagen type IV, laminin-1 *etc.* Even *in vitro* cultured BMVEC also secrete these molecules (Tilling, 2002). When porcine BMVEC were grown on a substrate coated with

these ECM molecules, BBB induction was evident by increased TEER (Tilling, 1998). More-convincing evidence came when porcine BMVEC, grown on astrocyte deposited ECM, displayed higher TEER compared to BMVEC grown on their own-ECM. Furthermore, TEER of BMVEC grown on ECM deposited by non-brain endothelial cells was decreased (Hartmann, 2007).

Taken together, in most cases induction occurs through soluble factor mediated signalling. However, a co-culture system that provides physical contact between the two cell types seems to induce the BBB phenotype more efficiently. The reasons for this can be as follows.

1. Direct endothelial-astrocyte physical contact is necessary for the induction.
2. Extracellular matrix associated signalling: the BBB induction that depends on physical contact could occur through extracellular matrix associated non-soluble factor mediated signalling. Since there is no direct intercellular junction/communication between these two cell types either *in vivo* or *in vitro*, the inducing factor could be deposited onto the basal lamina present between astrocytes and BMVEC (Tao-Cheng, 1987).
3. ECM molecules secreted by astrocytes onto basal lamina/ablumen of BMVEC may signal the maturation of the BBB phenotype.
4. A high local concentration of astrocyte-released factor is acting on the endothelial membrane. ECM may play an additional role in increasing the local concentration.
5. Induction depends on the exclusive activation of abluminal membrane (Abbott, 2002).
6. Because of proximity, short-lived (labile) factors have more possibility of acting upon endothelium.

1.5 Calcium signalling between astrocytes and endothelium

Inter-endothelial communication and inter-astrocyte communication occurs by spreading of calcium waves. However, communication between these two cell types was not proposed until a study with primary rat cortical astrocytes and ECV304 cells (Braet, 2001).

However, the cell line ECV304 was demonstrated to be a human bladder cancer derived epithelial cell line T24/83 (Brown, 2000) and not endothelium as originally thought.

A study by Simard *et al.* (2003) on freshly prepared rat brain slices did not find cx43 gap junctions in endothelial cells. In addition, purinergic receptors P2Y (1), P2Y (2), and P2Y (4) were not detected in endothelial cells and these cells responded poorly to purinergic receptor stimulation. Since astrocytes, endothelial cells, and pericytes are separated from each other by a basal lamina, it also needs to be explained how a (labile) messenger molecule can cross the intact basal lamina under normal physiological conditions (Simard, 2003). So, further work is needed to determine the mechanism underlying the bidirectional calcium signalling between astrocytes and endothelial cells.

1.5.1 Astrocytes are mediators of neurovascular coupling

Astrocytes act as a connection between endothelial cells and neurons. When a neuronal signal activates astrocytes, calcium releases from internal stores and an intracellular calcium wave propagates. Among the astrocytes, signalling is transmitted thorough gap junctions. At the gliovascular interface, activated astrocytes transduce the signal by releasing vasomodulatory substances thus regulating vasodilation and probably vasoconstriction (Zonta, 2003, Metea, 2006, reviewed in Fiacco, 2006). This process of regulation of local blood flow by neuronal signalling mediated by astrocytes, referred to as neurovascular coupling, was first demonstrated by Zonta *et al.* (2003) in rat cortical slices.

1.5.2 Astrocytes modulate BBB through calcium signalling

Astrocytes that interact with the arteriole wall regulate blood flow. Similarly, astrocytic endfeet that are in contact with the capillary wall are hypothesised to modulate BBB characteristics through calcium signalling.

1. A change of intracellular calcium levels has been observed during disruption of tight junctions (Brown, 2002, Tiruppathi, 2002). Therefore, it is possible that under pathological conditions, astrocytic factors that increase intracellular calcium levels will increase BBB permeability.
2. Leybaert *et al.* (2004) coined the word neuro-barrier coupling to propose that astrocytes regulate the carrier-mediated transport across the BBB, especially glucose uptake, depending on the local metabolic demand of neurons and astrocytes.

1.6 The BBB inductive effect of other cell types

Though astrocytes are the main inducers of the BBB phenotype, other cell types surrounding the BBB were also shown to play a role in BBB induction.

1.6.1 Pericytes

Pericytes (section 1.2.1), generally found abluminal to capillary endothelial cells embedded within the basal lamina are contractile in nature and mesenchymal in origin. However, each of these characteristics is disputable and hence there is still ambiguity about their identity, ontogeny, and progeny (Armulik, 2011, Krueger, 2010).

BMVEC and pericytes are separated from each other by a basal lamina. But there may be some direct contact points (reviewed in Gerhardt, 2003). Though several molecular expression markers such as PDGFR-b (platelet derived growth factor receptor-beta), α-SMA (alpha-smooth muscle actin), Desmin, NG2 (chondroitin sulphate proteoglycan 4), CD13 (alanyl aminopeptidase) were used to identify pericytes, there is no specific marker that does not change with developmental or physiological state (Armulik, 2011).

Several *in vitro* studies have shown that pericytes are important for induction of optimal barrier properties (Dohgu, 2005, Hori, 2004) and especially play a key protective role during hypoxia (Hayashi, 2004, Al Ahmad, 2009, Al Ahmad, 2010). However, pericytes have also been reported to decrease barrier properties (Zozulya, 2008, Thanabalasundaram, 2010). The seemingly opposing roles of pericytes were found to be dependent on their differentiation stage; while bFGF induced alpha-SMA negative pericytes protect the barrier integrity, TGF-β-differentiated, α-SMA positive pericytes do the opposite (Thanabalasundaram, 2011).

The role of pericytes in BBB induction and maintenance has been confirmed from the recent studies on pericyte-deficient mice (Armulik, 2010, Daneman, 2010). These studies have shown that during embryonic development pericytes rather than astrocytes take part in the initiation

of barrier formation. There seems to be a positive correlation between pericyte-coverage and permeability of the capillary. Pericytes inhibit the expression of vascular permeability factors such as VEGFA (vascular endothelial growth factor A, VEGF) and ANG2 (angiopoietin 2) in endothelial cells and thus bring about the decrease in vascular permeability. Decrease in vascular permeability mainly results from reduced transcytosis and by maintenance of polarised features of astrocytic endfeet (AQP4) and additionally by proper organisation of the tight junctions without increasing their expression levels. Pericytes also inhibit the immune cell infiltration by decreasing the expression of leukocyte adhesion molecules.

1.6.2 Neurons

Induction of GGT and Na^+ K^+ ATPase was observed when endothelium was co-cultured with cortical brain slices or with an isolated neuronal membrane fractions (Tontsch, 1991). More interestingly, it has been shown that whilst astrocytes seem to induce the overexpression of occludin, neurons induce its peripheral localisation. Hence, co-culture of BMVEC with neurons and astrocytes has a synergistic effect (Savettieri, 2000, Schiera, 2003).

1.6.3 Microglia and perivascular macrophages

Microglia are brain parenchyma resident immunocompetent cells that are sparsely in contact with the capillary wall whereas perivascular macrophages are in close contact with BMVEC as they lie between BMVEC and astrocytic endfeet. However, their origin, function and expression markers are not well characterised (Guillemin, 2004). In general, they are considered blood-derived, differentiated monocytes. As these cells interact with BMVEC at the BBB, they may have a role in its induction and/or maintenance. Indeed, the TEER of bovine BMVEC and human BMVEC cultures was increased when co-cultured with macrophages isolated from peripheral blood. Interestingly, the induction produced by macrophages was similar to that of C6 glioma cells, whose BBB induction potential has been demonstrated in several *in vitro* BBB models (Zenker, 2003).

1.7 Endothelial cells have a reciprocal inductive influence on the astrocyte phenotype

Endothelial cells (EC) themselves can release signalling molecules that act in a paracrine manner inducing various functions in surrounding nonvascular cells (Crivellato, 2007). Eight out of eleven morphological subtypes of astrocytes interact directly with blood vessels (Reichenbach, 2004 as cited in Abbott, 2006). The total capillary surface area in the human brain is 12 to 18 m^2 (Nag, 2005). Because of the dense microvasculature, all astrocytes will be within 25 μm from the capillary wall (Abbott, 2010). Therefore, it is conceivable that astrocytes would be influenced by their physical proximity to BMVEC. Indeed, some of the previous studies have shown that endothelium does affect some of the properties of astrocytes.

Induction of astrocyte polarity

Astrocytes are also polarised cells in terms of both structure and function. The cell membrane of the perivascular endfeet of astrocytes apposed to the capillary wall has a much higher density of orthogonal arrays of intramembranous particles (OAPs) in comparison with the membrane facing the neuropil. The OAPs comprise of systematically arranged aquaporin-4 (AQP4), a water channel protein and Kir 4.1, a potassium channel protein (reviewed in Wolburg, 2009b). This heterogeneity of astrocytic cell membrane domains is often termed 'astrocyte polarity'. In cultured astrocytes, the polarity of OAPs/AQP4 is not maintained (Nicchia, 2000). Therefore, it is apparent that astrocyte polarity may be induced by their close physical interaction with the capillary wall.

Indeed, it was observed that astrocytes that were co-cultured in contact with BMVEC had an increased number of OAPs compared to solo-cultured astrocytes (Tao-Cheng, 1990). Similarly, when mouse cortical astrocytes were grown in contact with bEnd3 cells (immortalised mouse brain capillary derived endothelial cells), polarisation of AQP4 was

restored only in those astrocytes that were in contact with endothelial cells (Nicchia, 2004). In another study that co-cultured a rat brain endothelial cell line (RBE4) with rat astrocytes in a collagen gel, the AQP4 expression was increased in astrocytic processes that were in contact with endothelial cells compared to those not in contact (Al Ahmad, 2010).

Later, it was shown that the polarisation of OAPs/AQP4 is partially dependent on the presence of agrin, a heparin sulphate proteoglycan, on the sub-endothelial basal lamina (Noell, 2009). There are two isoforms of agrin; A0B0 (endothelial isoform) and A4B8 (neuronal isoform). Recent *in vitro* culture studies have shown that astrocytes derived from agrin-null mice grown on agrin A0B0/A4B8 coated surface have increased OAP density (Fallier-Becker, 2011). Altogether, these data suggest a role for physical contact between astrocytes and BMVEC or its basal lamina in the induction of polarity of astrocytes.

LIF released by endothelium induces astrocyte differentiation

Leukaemia inhibitory factor (LIF) released by endothelial cells of rat optic nerve has been shown to differentiate the rat astrocyte precursor cells (APC) into GFAP positive mature astrocytes (Mi, 1999, Mi, 2001). Earlier, Richards *et al.* (1996) had shown that LIF could induce differentiation of astrocyte precursors into astrocytes.

Astrocyte morphology and calcium signalling

When neonatal mouse cortical astrocytes were co-cultured with bEnd.3 cells, immortalised mouse brain endothelial cells (BEC) , the confluent monolayer of astrocytes changed to a network of columnar multicellular aggregates (Yoder, 2002). These morphological changes appeared to be specific to astrocyte-BEC interactions as neither cell type behaved similarly, when co-cultured with other cell types. In addition, these co-cultured astrocytes have increased Ca^{2+} responses to glutamate and bradykinin compared with solo-cultured astrocytes. The increased response to bradykinin was specific since astrocytes co-cultured with neurons showed only an increased response to glutamate but not bradykinin.

Glutamine synthetase activity

Spoerri *et al.* (1997) demonstrated that soluble factors present in the conditioned media obtained from human retinal endothelial cells were able to induce glutamine synthetase activity in rat C6 glioma cells, thus suggesting a role in preventing extracellular glutamate toxicity in the CNS.

Growth stimulation

Estrada *et al.* (1990) have shown that a soluble peptide factor released by brain endothelial cells induced DNA synthesis and cell proliferation in astrocytes and pericytes.

Laminin-5 production by astrocytes

Wagner *et al.* (2000) have shown that laminin-5 production by rat cell lines (2222CRL and 12X2H) was increased when contact-co-cultured with rat non-brain endothelial cells. This effect was dependent on either physical contact between both cell types or on an insoluble matrix compound secreted by endothelial cells, recognised by astrocytes. Laminin-5 and its ligand $\alpha 6\beta 4$ integrin are components of hemi-desmosome like structures that provide support to the cell membrane of perivascular endfeet (Nakano, 1992, Wagner, 1997, Baker, 1996). Increased laminin-5 production by astrocytes in turn may help in maintenance of the BBB integrity.

Mutual induction of antioxidant enzymes in co-culture

Schroeter *et al.* (1999) have shown that the activity of antioxidant enzymes such as manganese superoxide dismutase (MnSOD), glutathione peroxidase (GPx), and superoxide dismutase-1 (CuZnSOD) were elevated in co-culture of rat astrocytes and BEC compared to solo-cultures of either cell type. The increased antioxidative potential could help in maintenance of BBB integrity and the CNS during oxidative stress.

1.8 *In vitro* co-culture models to study endothelial-astrocyte interactions

The selective barrier function of the BBB is essential for proper function of the CNS, at the same time; it hinders drug delivery. To circumvent this problem, a thorough understanding of BBB formation, function, and maintenance is necessary. *In vivo* studies are undoubtedly of great use but they are relatively difficult to carry out, and difficult to interpret because of the complex environment and pertaining ethical issues. Alternatively, *in vitro* models are convenient because of their relative simplicity. They are easy to set up with different experimental parameters, and are easy to interpret due to fewer experimental variables. *In vitro* models are highly preferred, compared to *in vivo* models, to study the role of a single parameter such as cell type or a molecule. Therefore, much of the invaluable data about cell signalling and mechanisms, and the roles of a specific cell types are derived from *in vitro* models.

An ideal *in vitro* BBB model should mimic functionally as closely as possible the *in vivo* situation. Therefore, functionally a BMVEC of the BBB model should: (Naik, 2012)

1. be able to form a paracellular barrier by expressing tight junctions
2. have polarised expression of transporters on the luminal versus abluminal membrane
3. express functional efflux proteins
4. be able to discriminate permeability of substances according to their oil/water partition coefficient.

Initial models consisted of solo-cultures of primary BMVEC. Later studies have shown that BMVEC lose their *in vivo* barrier phenotype soon after they are cultured *in vitro* (reviewed in Engelhardt, 2003, Lyck, 2009). Therefore, to restore their barrier phenotype to the original state, it seemed necessary that the model should reproduce the anatomy of the *in vivo* BBB to some extent, at least in two aspects.

1. Interactions of BMVEC with other cellular partners of the gliovascular unit in a way that represents their geometrical relationship *in vivo*.
2. BMVEC should experience a shear stress.

Astrocytes are considered as predominant maintainers of the BBB phenotype. Therefore, most models consist of co-cultures of BMVEC with astrocytes. In recent times, as the role of pericytes on BBB development has been elucidated, tri-culture models that include pericytes along with astrocytes and BMVEC are being used. A few models have simulated the flow conditions to create a shear stress on BMVEC, and as expected shear stress was shown to be an important regulator of BBB phenotype. As the three-dimensional (3D) cell culture technique is gaining popularity, a few 3D co-culture models have been constructed aiming to reproduce the architecture of the BBB more closely. In the past three decades, several configurations of co-culture have been tried by researchers. These can be broadly divided into three categories.

1. Two-dimensional (**2D**) static models (section 1.8.1)
2. Dynamic, flow based models (section 1.8.2)
3. Three-dimensional (**3D**) models (section 1.9.2)

The configuration of the model determines its amenability to various analytical techniques, and so each model has some technical advantages and limitations. Since no single *in vitro* models is suitable for all purposes, it is a researcher's choice to decide on the model based on the question to be investigated. Depending on the research question and the required analytical technique, a particular model may be more suitable than others. Static models have been introduced first, later flow based models have been introduced, and more recently 3D models are under development, including the present study. An *in vitro* BBB model has two purposes: (1) to understand the basic biology of BBB, which will help to treat vascular causes of CNS disorders such as Alzheimer's disease and migraine (2) to screen potential therapeutic drugs for

CNS pathologies. Although a main purpose of these models is to investigate the BBB, the same models have been used to study the effect of endothelium on astrocytes.

1.8.1 2D static models

Static models do not provide shear flow. Cells are cultured on a 2D substrate so, cell-cell and cell-matrix interactions occur in only two dimensions. Hence, in terms of 3D interactions and shear stress, they do not mimic the BBB situation *in vivo*. Despite these limitations, these models were widely used and were enormously helpful to the advancement of the research field. These configurations may however limit translatable findings of the 2D static models. These models are mainly of five types based on the configuration, and they are described below.

1.8.1.1 Transwell insert, non-contact model

In this set up, astrocytes are cultured on the base of a tissue culture well while EC are cultured on the base of an upper chamber insert on a porous membrane (Cecchelli, 1999, Boveri, 2005, Siddharthan, 2007, Omidi, 2008, Sobue, 1999b).

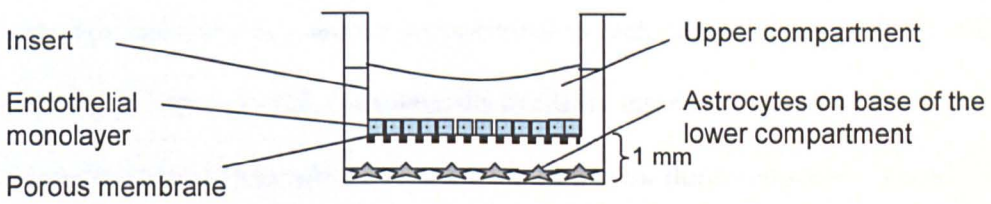

Figure 1-4 Non-contact co-culture configuration using a transwell

1.8.1.2 Transwell insert, contact model

EC are cultured on the upper surface insert membrane while astrocytes are cultured on the lower surface of the membrane. Theoretically, astrocytes can extend their endfeet through the pores and can make physical contact with EC present on the upper side. This configuration mimics the *in vivo* geometry whereas astrocytes contact the abluminal side of BMVEC. Several

studies have used this model to study the effect of physical contact on BBB phenotype induction in EC (Dehouck, 1990, Gaillard, 2001, Ma, 2005, Malina, 2009, Hayashi, 1997, Isobe, 1996, Kuo, 2011).

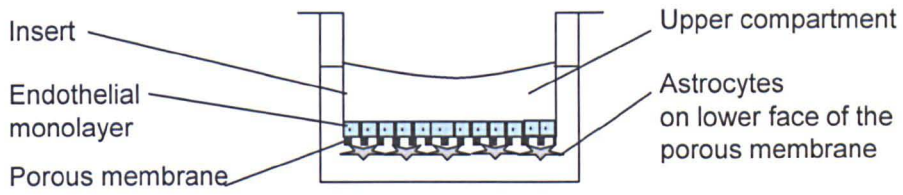

Figure 1-5 Contact co-culture configuration using a transwell

Three main factors that determine the physical contact between EC and astrocytes in this setting are pore-size, pore density, and thickness of the membrane. It has been reported that 1.0 μm pore size is optimal since smaller pores do not facilitate extension of cell processes and larger pores allow transmigration of the cells (Demeuse, 2002). However, Hayashi *et al.* used membranes with a pore size of 3.0 μm while Isobe *et al.* used a pore size of 0.45 μm in their study. The study of Hayashi *et al.* also indicates that pore density, physical contact, and BBB phenotype induction are directly proportional to each other (Hayashi, 1997). Depending on the nature of the material, commercially available insert membranes have a thickness from 10 μm (Polyester/ Polycarbonate) to 30 μm (Poly-tetra-fluoro-ethylene). Therefore, the length of the cell process should be 10-30 μm to be able to make contact with EC on the upper surface. In addition, the percentage of porosity is limited to ~15-20%. Because of these reasons, the actual physical contact between EC and astrocytes would be less. To overcome these limitations, an insert membrane with thickness of 1 μm and ~50% porosity to increase the physical contact was synthesised (Ma, 2005). Further standardisation is required with regard to pore size, pore density, and thickness of the membrane to optimise the physical contact. Hence, when comparing the results of different laboratories, it is essential to take into account pore size and porosity. Whether this configuration provides adequate physical contact

is questionable but it certainly keeps both cell types in close physical proximity. This is advantageous in two contexts.

1. Secreted factors that have a short half-life can reach the target EC in less time as they are within 10-30 μm distance unlike non-contact cultures where the typical distance is ~1000 μm.
2. This configuration also provides a local high concentration of astrocyte released factors.

Advantages and limitations of transwell models

Advantages: Both contact and non-contact models are the most widely used *in vitro* configurations. These models are easy to set up, do not demand great technical expertise, and are amenable to various analytical methods. The main advantage of the transwell model over any other model is the facility to assess the functional barrier phenotype of endothelium through assays such as paracellular permeability, drug transport, TEER measurement. Cells can be analysed *in situ* by microscopy or cells of each cell type can be harvested separately and can be analysed by standard molecular biology techniques. Transwell systems in multiwell plates are convenient for high throughput drug permeability screening studies. Even tri-cultures along with pericytes can be set up using this system.

Disadvantages: In the non-contact model, there is no physical contact between astrocytes and EC and the distance between the insert membrane and the base of dish is generally $\geq$ 1 mm. Therefore, non-contact models are useful only to study the role of astrocytic released soluble factors. Even in the contact models, the physical contact between the cell types is minimal. In addition, there will be a non-uniform pattern of expression of cell adhesion and tight junctional molecules from the centre of the insert compared to the edges of the insert membrane (edge effect).

1.8.1.3 Astrocyte conditioned media

Nutrient culture media supernatant collected from confluent astrocyte cultures is termed 'astrocytic conditioned media' (**ACM**), which presumably contains relevant secreted factors. EC cultures are grown in the presence of astrocytic conditioned media either neat or at times diluted with fresh nutrient media, generally at 1:2 ratio. In laboratories where primary cell culture sources are limiting, conditioned media is stored frozen until required. Several groups have studied the effect of astrocytic soluble factors using this methodology (Rubin, 1991a, Gaillard, 2000, Prat, 2001, Culot, 2008, Omidi, 2008, Gardner, 1997, El Hafny, 1997).

The main advantage of this method is its simplicity. There is no need to maintain the EC and astrocytes cultures simultaneously, which reduces the work burden. If EC are cultured on a transwell insert, then all the technical advantages of transwell models are applicable to this methodology too. However, this model has a few limitations, namely,

1. Only the effect of soluble factors can be studied.
2. The concentration of astrocytic factors would be diluted in the cases where less than 100% ACM is used.
3. Short-lived, labile factors may have been destroyed if fresh conditioned media was not used.

1.8.1.4 EC grown on coverslips facing the confluent astrocyte bed

This is an early co-culture system, which was used to study the importance of physical contact between the two cell types. Astrocytes are cultured to confluence on the bottom of the dish. On these feeder layers, EC cultured on coverslips are laid facing down so that close cell-cell contact is maintained (DeBault, 1980).

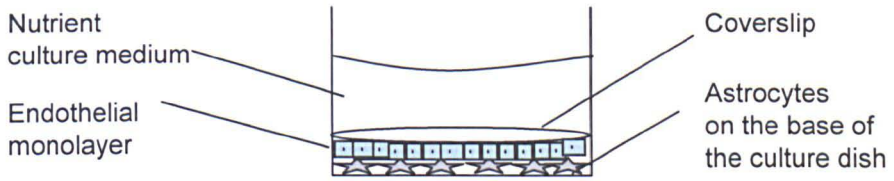

Figure 1-6 A co-culture configuration in which BMVEC are grown underside of a coverslip facing astrocyte bed

Advantages: The striking advantage of this model is extensive physical contact between EC and astrocytes. In addition, it is easy to set up, and there is no need for special apparatus.

Limitations: *In vivo* endothelium has a liquid phase at its apical/luminal side, a solid phase at its basal/abluminal side and interacts with astrocytes from their basal side. The main problem with this model is that the apical surface of endothelium interacts with the astrocytes. Moreover, endothelium is not situated at a true liquid-solid-interface. The current configuration does not allow paracellular permeability, TEER resistance, and drug transport studies. In addition, a few technical problems are associated with this set up (Tao-Cheng, 1987).

1. The EC culture may detach from the coverslip and start to grow into the astrocytic bed. Therefore, it may not be possible to harvest the cell types into pure fractions for downstream analyses such as cell lysate preparation.
2. Contact between the two cell types will be uneven because of natural variability in the thickness of both monolayers.
3. Coverslips are not static but are easily displaced by even a little movement of the culture dish. Therefore, continuous contact between the cell types is not maintained and moreover it may cause damage to cells or this mechanical shock may give rise to more variability from one region to other.

1.8.1.5 EC grown directly on a confluent astrocyte bed

In this model, EC are seeded directly on a confluent astrocyte layer. This set up was used to study the effect of primary rat astrocytes on tight junction formation in bovine EC using freeze fracture electron microscopy (Tao-Cheng, 1987).

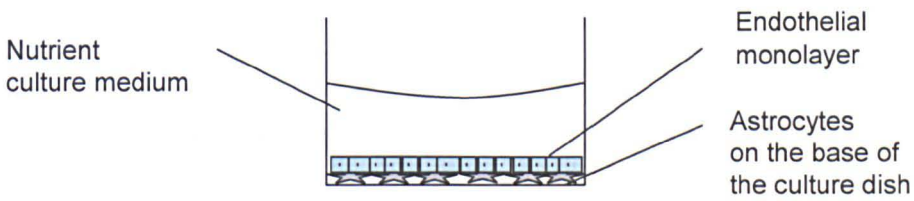

Figure 1-7 A co-culture configuration in which BMVEC are grown directly on an astrocyte bed

A similar set-up was used to co-culture bEnd3 cells, immortalised mouse brain capillary derived endothelial cells, on a confluent layer of mouse cortical astrocytes to study the endothelial influence on astrocytes using fluorescent light microscopic methods (Yoder, 2002). This same co-culture setup, and procedure were used later to study the endothelial co-culture (bEnd3) effect on rat astrocytic AQP4 localisation and redistribution (Nicchia, 2004).

Advantages: This model provides physical contact between endothelial cells and astrocytes and is convenient to study physical contact dependent properties of either cell type.

Limitations: EC and astrocytes do not remain as two separate layers. This set-up is not suitable to study endothelial monolayer dependent properties and especially functional assays. Altogether, the usefulness of this model is even more restricted than the previous model.

1.8.2 Dynamic, flow based models

To improve upon 2D static models, dynamic, flow based models have been introduced. These models provide shear stress to EC hence mimicking the *in vivo* BBB closer than 2D static models. *In vivo* capillary endothelial cells experience continuous shear stress because of intra capillary blood flow, which may induce or modulate their specialised phenotype. Indeed, EC grown *in vitro* under shear stress change their orientation towards the direction of flow, have a reorganised cytoskeleton, undergo mitotic arrest, have a low turn over, grow large, and are more differentiated. EC grown under shear stress acquire an enhanced BBB phenotype, with increased expression of tight junctions, multidrug transporters, carrier-mediated transporters, polarised expression molecules on apical vs. basal membranes, and produce vasoactive substances (Ziegler, 1994, Ballermann, 1995, Ando, 1996, Akimoto, 2000, Cucullo, 2011, reviewed in Naik, 2012). Therefore, it is well established that shear stress is an important contributor for the BBB phenotype of BMVEC.

Few researchers have included a shear stress component in their models. The very first *in vitro* shear stress model used a cone-plate apparatus (Bussolari, 1982, Dewey, 1981) (**Figure 1-8**). Later parallel-plate flow chambers were developed and mainly used for leukocyte adhesion and migration studies (Gerszten, 1996). All these studies were performed on solo-cultures of EC.

A hollow fibre model that mimics capillaries *in vivo* was first developed by the pioneering work of Ballermann's group (Ott, 1995, Ballermann, 1995). This model was further developed into the so called dynamic *in vitro* BBB model (DIV-BBB) by Janigro's group in which EC are cultured in the lumen of hollow fibres and are exposed to flow while the astrocytes are seeded in the abluminal compartment (**Figure 1-9**). The hollow fibre mimics the capillary shape and its wall is porous such that it allows nutrient exchange but not the migration of cells (Stanness, 1996, Stanness, 1997, Cucullo, 2002). Since a hollow fibre with luminal flow resembles the three-dimensional (3D) structure of a capillary, it is sometimes referred to as a 3D model, but

it should be differentiated from 3D matrix based models (section 1.9.2) in which cells are surrounded by 3D matrix.

Few side-by-side comparison studies have shown that induction of a barrier phenotype in the dynamic flow based co-culture model is superior to static 2D transwell co-cultures. In the dynamic model when co-cultured with C6 glioma cells, bovine aortic endothelial cells became much tighter compared to static transwell co-cultures, as assessed by TEER, and selective permeability to [^{14}C] phenytoin and [^{3}H] sucrose (Santaguida, 2006). Similarly, when bovine aortic endothelial cells were co-cultured with foetal rat astrocytes, only the dynamic model could induce the polarisation of GLUT-1 (luminal) and hexokinase (abluminal), but not a static transwell system (McAllister, 2001). In another study, the TEER of hCMEC/D3 cells was increased by 15 to 20 times, from a static transwell model to a DIV-BBB model (~1200 $\Omega.cm^2$) (Cucullo, 2008).

Advantages: EC grown in dynamic models regain many properties such as cell morphology and turn over, that are reminiscent of *in vivo* BMVEC. EC grown in the dynamic model become much tighter compared to 2D static models, as evidenced by high TEER (>1100 $\Omega.cm^2$), which was rarely achieved using 2D static models, except in a few studies (**Table 2**). The model is automated, and allows real-time measurement of TEER, and study of varying levels of shear stress. Both cell types can be easily separated and can be subjected to further down stream analyses. Cultures can be maintained for as long as a few months. Recent modifications in the model permit the study of leukocyte trafficking too (Santaguida, 2006).

Limitations: It is not possible to do microscopic analysis of the luminal compartment, and to examine the morphological changes of EC *in situ*. Compared to the transwell system, this system is not convenient for high throughput studies. Generally, a higher number of cells (> 1 million) are required, which is limiting when working with the primary cells. Greater technical expertise, time and expense is needed to establish and standardise the model in a laboratory.

Therefore, this model has not been widely used across different laboratories (Naik, 2012, Ogunshola, 2011). Although these models are closer to the situation *in vivo* by simulating blood flow and generating shear stress on EC, they are deficient in two main aspects, namely, astrocytes are not cultured in a 3D matrix and there is insufficient physical contact between luminally cultured EC and abluminally cultured astrocytes.

A relatively simple flow-based model was developed by Siddharthan *et al.* (2007), in which cells are cultured on a snap well insert, which is kept in a transparent plastic flow chamber. Using this model, they have demonstrated that human astrocytes and shear stress have additive effects on the BBB phenotype of HBMVEC as measured by paracellular permeability to FITC-dextrans. Since cells are cultured on inserts, unlike the capillary flow model, this model is convenient for microscopic analysis. This model is much easier to adapt to other laboratories.

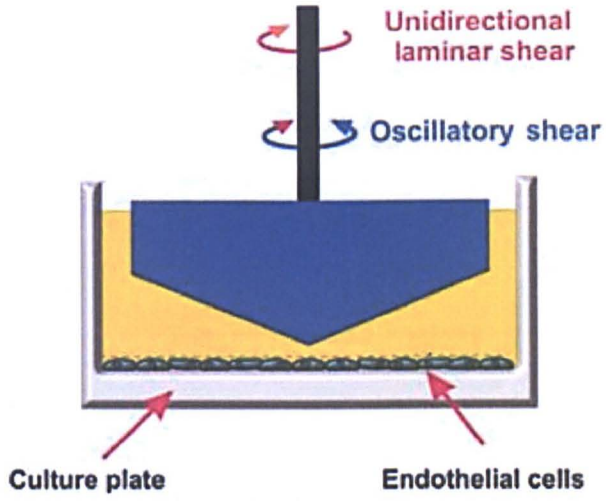

Figure 1-8 Schematic representation of a cone and plate shear apparatus

In this rudimentary model developed by Gimbrone and colleagues (Bussolari, 1982), the endothelial monolayer is cultured at the base of culture dish and shear stress is generated by a cone and plate viscometer. The level of shear stress is determined by the angular velocity and the cone angle. The model does not precisely create the *in vivo* flow conditions, and does not include co-culture of astrocytes. However, the model was successfully employed to culture cells under controlled levels of fluid shear stress *in vitro* for ≥ 7 days. The image is adapted from Naik *et al.*, 2012.

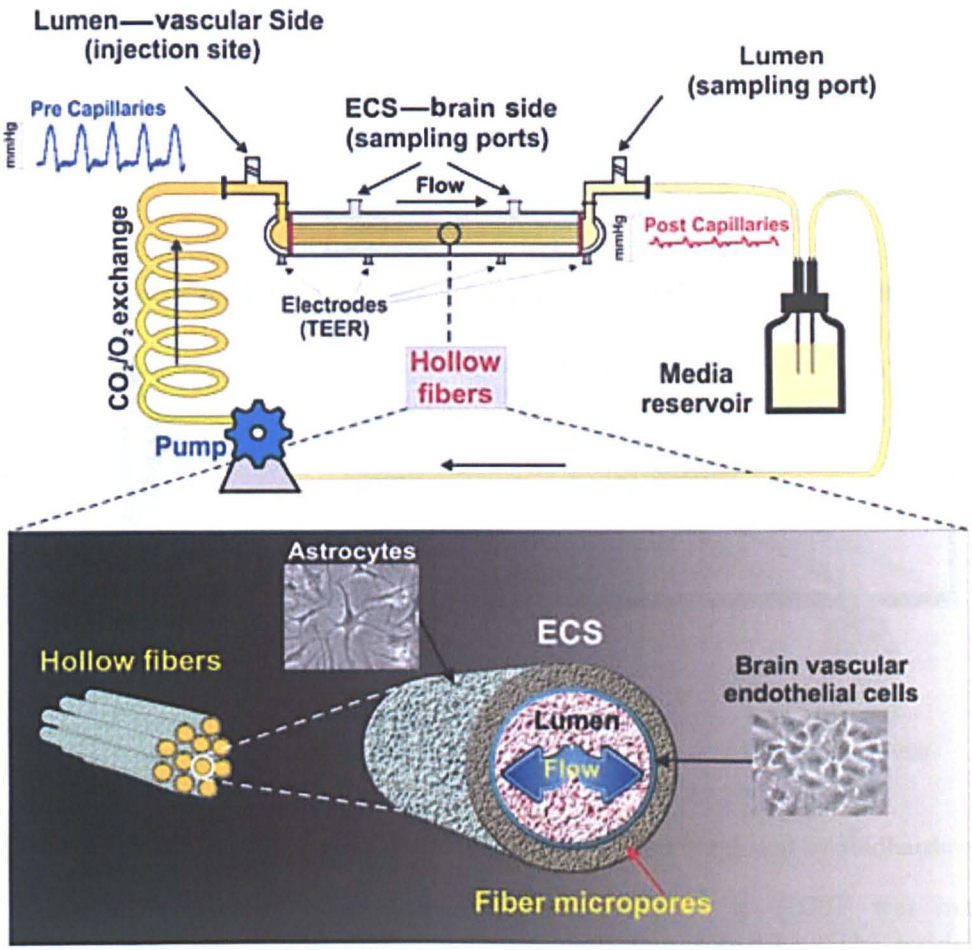

Figure 1-9 Schematic representation of a dynamic *in vitro* BBB model (DIV-BBB) by Cucullo *et al.* (2002)

The top panel shows a schematic representation of a dynamic *in vitro* BBB model developed by Cucullo *et al.* (2002). The bottom panel shows an enlarged view of hollow fibres. In this model, the EC are cultured in the lumen of polypropylene micro porous hollow fibres, while astrocytes are cultured on the outer surface of the fibre. The bundle of hollow fibres is suspended inside a sealed chamber. The lumina of hollow fibres are in continuity with a flow path consisting of gas-permeable silicon tubing, which is connected to a nutrient culture medium source. The luminal and abluminal compartments can be accessed through separate ports. The cells seeded on the lumina of fibres are exposed to controlled pulsatile flow generated by a pump. The waveform of the shear pressure changes from the pre- to post-capillary region mimicking the observed *in vivo* rheological changes. Image source: Naik, 2012.

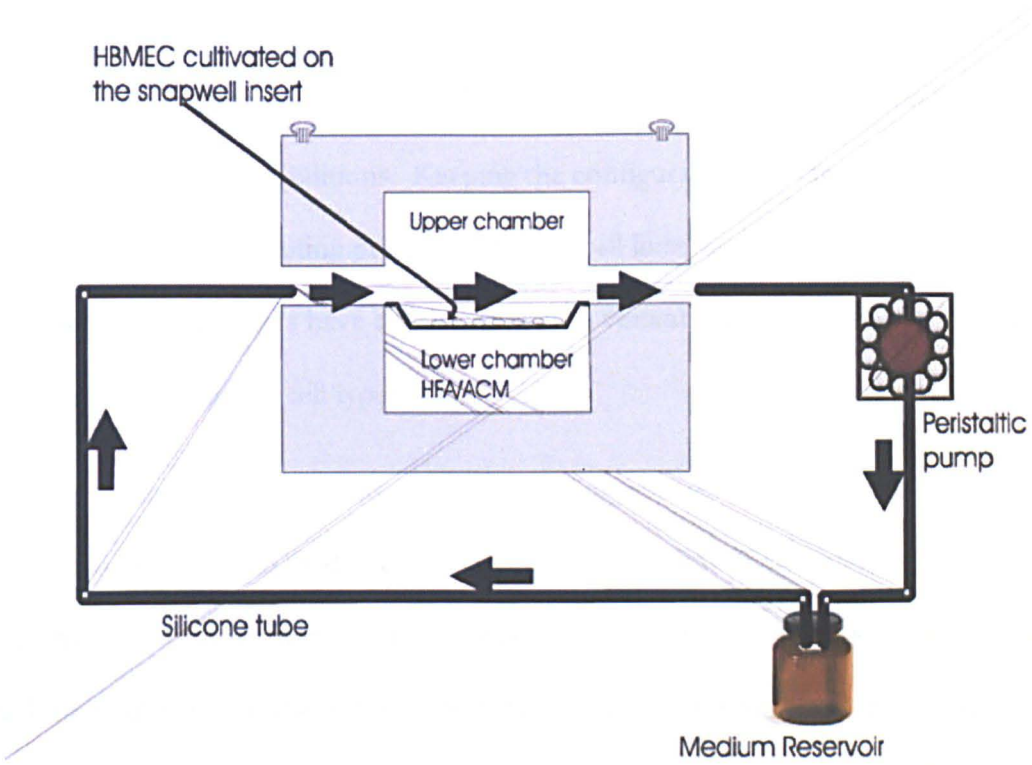

Figure 1-10 Schematic representation of a shear flow model developed by Siddharthan et al. (2007)

The *in vitro* flow model developed by Siddharthan *et al.* (2007) was manufactured in collaboration with World Precision Instruments (Sarasota FL). The model consists of a transparent plastic chamber, having hollow space, in which a snapwell™ insert (12 mm) is lodged, that separates the upper from the lower chamber. The upper and the lower chambers are tightly sealed with an O-ring and stainless steel screws. The flow chamber, peristaltic pump, and nutrient culture media reservoir are connected by the silicon tube. The arrow indicates the direction of the flow. The entire setup is kept inside a CO_2 incubator. The nutrient culture medium passing through the upper chamber applies the shear stress on the EC cultured on the snapwell™ membrane. Astrocytes are grown on an 8 mm coverslip, which fits in the lower chamber. Cell seeding is carried out outside the system. Soon after the cells are adhered, the snapwell™ insert, and coverslip are transferred into the chamber and grown under flow. Image was taken from Siddharthan, 2007.

1.8.3 Further commentary on existing BBB models

The advantages of BBB models depend not only on the configuration, but also on the cells, their species, and culture conditions. Keeping the configuration the same, but using cells of different species, or substituting primary cells with cell lines, and sometimes with non brain endothelial cells, researchers have developed several variants of BBB to suit their purposes, based on the availability of cell types.

BMVEC and astrocytes of various sources including mouse, rat, porcine, and bovine and sometimes human are used (**Table 2**). Isolation of primary BMVEC is laborious and the yield is generally low except for bovine and porcine cells. In addition, contamination with other cell types during isolation, instability of the phenotype with increasing passage, and batch-to-batch variation, which all affect the reproducibility of the results, discourage the usage of primary cells. Therefore, immortalised cell lines (**Table 3**) are also widely used because of their convenience, despite their deficiencies compared to primary cells in some of their properties (Gumbleton, 2001, Roux, 2005). Especially for industrial purposes, or applications that involve high throughput, immortalised cells are extremely convenient.

Using both BMVEC and astrocytes from a human source should increase the accuracy of drug permeability values and specificity, which in turn increases the translatability of the findings to humans *in vivo*. For example, for some of the antiepileptic drugs such as phenytoin, the affinity of P-glycoprotein differs between mouse and human (Baltes, 2007). However, obtaining primary human cells is an even greater problem because of the scarcity of human brain tissue and ethical concerns. Therefore, studies that use human primary BMVEC or astrocytes are relatively few. A few human immortalised BMVEC lines have been developed (Table 3), but none of them are well characterised or retain the BBB phenotype, except the hCMEC/D3 cell line which is therefore widely in use (section 1.10.1).

A new strategy to circumvent the human tissue problem is the use of human embryonic neural progenitor cells (NPC), which have a self-renewal capacity and can be maintained in the culture for a long time. These can be readily differentiated into astrocytes or neurons and used for BBB modelling studies. These NPC derived cells are able to enhance BBB properties just like primary cells derived from the human brain tissue (Lippmann, 2011). If human embryonic tissue is scarce, it is possible to produce astrocytes and neurons from neural stem cells, which can be generated from induced pluripotent stem cells that are derived from adult somatic cells. This strategy is especially useful for the generation of pericytes since they are a rarer cell type (Keep, 2011). Non-brain endothelial cells such as human umbilical vein endothelial cells (HUVEC) and bovine aortic endothelial cells are also used by researchers.

Both cross-species (heterologous, non-syngeneic) and single-species (homologous, syngeneic) models have been used, and until recently there was no clear evidence to say that BBB induction is better when BMVEC and astrocytes are of same species and/or age-matched since single-species models did not induce barrier phenotype more than cross-species models (**Table 2**). Wuest *et al.* (2012) reported for the first time the advantage of a single-species model after a systematic study, in which they have observed that the paracellular tightness of mouse BMVEC was ~2 fold more in co-culture with mouse astrocytes compared to co-culture with rat astrocytes, as assessed by a paracellular permeability assay. Therefore, it appears that some of the inductive signals released by astrocytes are not conserved across the species and it is preferable to use a single-species model, especially to study immune related inflammatory events (Descamps, 2003, Coisne, 2005).

Optimisation of the culture conditions can greatly improve the performance of the model. Few groups have experimented with barrier enhancing biochemical agents. For example, addition of hydrocortisone, 8-CPT-cAMP, and RO-20-1724 to nutrient culture media was shown to enhance the BBB phenotype on BMVEC when cultured alone or co-cultured with

astrocytes (Hoheisel, 1998, Gaillard, 2001, Perriere, 2007, Weidenfeller, 2005). A membrane permeable cAMP analogue, 8-CPT-cAMP, activates intercellular membrane channels and the effect is prolonged by adding an inhibitor of cAMP phosphodiesterase, RO-20-1724, leading to enhanced junctional coupling. Removing the serum from the nutrient culture media also improved the paracellular tightness (Franke, 2000, Nitz, 2003). A recent study has shown that through standardisation of nutrient media, feeding strategy, cell density, cell seeding time, and culture growth it was possible to increase the TEER by 200% compared to the routine methodology (Wuest, 2012). Therefore, dedicating time for optimisation of culture conditions is equally important to other aspects of the model development.

An ideal *in vitro* model should restore the BBB phenotype of BMVEC to its *in vivo* status. The most distinctive feature of *in vivo* BMVEC is paracellular tightness, which is manifested in high TEER values ($\geq$1500 $\Omega.cm^2$). Therefore, TEER is one of the parameters used to judge the effectiveness of the model. In general, TEER achieved by static *in vitro* models is considerably less than that *in vivo*, and the maximum achieved so far is 800 $\Omega.cm^2$ (**Table 2**). Usually, co-culture with astrocytes is required to increase TEER, but it has been reported that porcine BMVEC cultures alone achieved TEER values as high as ~700 $\Omega.cm^2$ (Franke, 1999). It was not studied if TEER can be further increased by co-culture with astrocytes in this model.

The dynamic model (DIV-BBB) routinely achieves high TEER compared to the static transwell models (**Table 2**). The improvement of the dynamic model using either primary human BMVEC or immortalised human BMVEC cells (hCMEC/D3), is a significant milestone in the development of *in vitro* BBB models, as the TEER achieved in these models is $\geq$1100 $\Omega.cm^2$, which is approaching the *in vivo* values (Cucullo, 2007, Cucullo, 2008). Notably, this was accomplished using an immortalised cell line, which mostly obviates human brain tissue procurement for primary BMVEC isolation.

Table 2 Comparison of *in vitro* model configurations, cell type and species, and transendothelial resistance (TEER) achieved by the model (adapted from Ribeiro, 2010)

Model configuration	Cell type and Species	TEER ($\Omega.cm^2$)	Reference
Dynamic, flow based model	Bovine aortic EC with C6 rat glioma cell line	736 ± 38	(Stanness, 1997)
	Bovine aortic EC with C6 rat glioma cell line	650 ± 26	(Santaguida, 2006)
	Human BMVEC and human astrocytes; species-consistent	>1100	Cucullo, 2007
	hCMEC/D3 with and without human astrocytes; species-consistent	~1200	Cucullo, 2008
Static, non-contact transwell	Bovine BMVEC and rat astrocytes	800	(Cecchelli, 1999)
	Mouse BMVEC and mouse astrocytes; species-consistent	777 ± 15	(Coisne, 2005)
	Human BMVEC and human astrocytes; species-consistent	~500	(Siddharthan, 2007)
	Rat BMVEC and rat astrocytes in a differentiation medium; species-consistent	270 ± 12	(Perriere, 2007)
Static, contact transwell	Bovine BMVEC and rat astrocytes in a differentiation medium	670 ± 47	(Gaillard, 2001)
	Human BMVEC and human astrocytes; species-consistent	225 ± 13	(Megard, 2002)
	Porcine BMVEC and porcine astrocytes; species-consistent	116 ± 3	(Jeliazkova-Mecheva, 2003)
	Rat BMVEC, rat astrocytes, and rat pericytes; species-consistent	354 ± 15	(Nakagawa, 2009)
Static, transwell, solo-culture	Porcine BMVEC solo-culture	700 ± 100	(Franke, 1999)

Table 3 Immortalised BMVEC lines reported in the literature (adapted from Gumbleton, 2001).

Species	Cell line identifier and the first cited reference
Rat	RCE-T1 (Mooradian, 1991), CR3 (Lechardeur, 1995), GP8.3(Greenwood, 1996), GPNT (Regina, 1999), RBEC1 (Kido, 2000), rBCEC4 (Blasig, 2001),. RBE4 (Couraud, 2003).
Mouse	MBEC (Tatsuta, 1992), S5C (Wijsman, 1998), TMBB4 (Asaba, 2000).
Porcine	PBMEC (Teifel, 1996)
Bovine	SV-BEC (Durieu-Trautmann, 1991), t-BBEC-117 (Sobue, 1999b), BBEC-SV (Stins, 1997).
Human	HBEC-51 (Xiao, 1996), BB19 (Prudhomme, 1996), SV-HCEC (Muruganandam, 1997), hCMEC/D3 (Weksler, 2005), TY08 (Sano, 2010)

1.9 Three-dimensional (3D) cell culture

In vivo, cells are in a 3D matrix and therefore receive physical support, biochemical signals, and nutrients from all directions. Therefore, to mimic the 3D environment *in vivo*, 3D cultures have been developed. In 3D culture, cell behaviour is different from 2D cultures and models resembling the *in vivo* situation better. Therefore, using 3D culture models can quicken the understanding of basic biology, and development of therapeutic and pharmacological products (Lee, 2008, Sun, 2006, Neuwelt, 2008). 3D cultures differ from 2D cultures not only in dimensionality but also in rigidity. These two fundamental differences lead to four major differences in cellular properties between 3D and 2D cultures.

1. In 2D cultures, cells are often supported on the ventral side, nutrients are supplied from the dorsal side, and so the cell surface is unnaturally polarised. In 3D cultures, physical support and nutrient supply occurs from all directions.
2. In 2D cultures, the cells are cultured on a hard substrate, whereas in 3D cultures, the matrix is generally soft and pliable.
3. In 2D cultures, the cell-matrix interactions occur only on the ventral side, whereas in 3D cultures these occur throughout the surface of the cells. Equally importantly, because of the difference in the stiffness of the matrix, the nature of cell-matrix interactions also differ.
4. In 2D cultures, the cell-cell interactions generally occur through the lateral sides, whereas in 3D cultures, these may occur from any side of the cells, and cells can move in the 3D matrix and form cellular assemblies.

Many studies have shown that cellular properties in 3D cultures differ from that of 2D cultures. For example, the gene expression profile was altered when the culture environment was changed from 2D to 3D, as was observed in several cell types including, neuroblastoma

cells (Li, 2007), fibroblasts (Chiquet, 2009) and smooth muscle cells (Stegemann, 2005). In general, in 3D matrices, physical and mechanical stimuli are different from 2D cultures. Because of this, many cellular properties such as adhesion, proliferation, migration, differentiation, and morphology are modulated (Lee, 2008). Integrin-signalling, which is sensitive to mechanosensation, is also generally altered in 3D cultures (Larsen, 2006, Yamada, 2003).

1.9.1 Behaviour of cells in 3D cultures is closer to that *in vivo*

Although, there is increasing evidence that cell behaviour in 3D culture differs from that of 2D cultures, it is not always established whether these changes are physiologically relevant. However, some data illustrate that changes that occur in 3D culture do reflect conditions *in vivo*.

1. Morphology: In 2D cultures, cells are compelled to adapt to a 2D rigid substratum, which necessitates an unnatural flattened morphology (Maltman, 2010). The effect of 3D culture conditions on fibroblast morphology is well studied. The absence of dorsal anchorage in 2D cultures makes the cells spread out in an extreme fashion and induces the formation of lamellipodia, stress fibres, and focal adhesions. In 3D cultures, the presence of both dorsal and ventral anchorage balances the spreading with retraction therefore cells have a more elongated, spindle-shaped morphology typical of fibroblasts *in vivo* (Green, 2007). Similarly, when rat astrocytes were transferred from a 2D to 3D matrix, stress fibres were decreased, and became less reactive and similar to their *in vivo* counterparts (East, 2009, Georges, 2006).

2. Cellular reorganisation and morphogenesis: In a 3D matrix, cells can migrate and reorganise themselves in a manner similar to their native anatomical architecture. Epithelial cells behave very similarly to fibroblasts in 2D culture; but when cultured in 3D collagen gels, they undergo morphogenesis, forming polarised, growth-arrested acini (a spherical monolayer of cells enclosing a lumen) or tubules. Loss of polarisation in breast carcinoma derived

epithelial cells cannot be discerned in 2D cultures, but in 3D culture, it can be distinguished by the formation of disorganised cellular masses (Petersen et al., 1992). 3D culture has proven to be indispensable, to study the process of epithelial polarisation, and to identify the molecular signals that determine the epithelial architecture (O'Brien, 2002). Similarly, endothelial cell morphogenesis, which does not occur in a 2D culture system, can only be observed and analysed in a 3D culture system. Much of the understanding about endothelial tubulogenesis during vasculogenesis and angiogenesis is derived from 3D culture systems (Davis, 2012).

3. Cell-matrix interactions: Studies on fibroblasts and smooth muscle cells suggest that cell-matrix interactions in 3D matrices differ from that on 2D substrates but are similar to that *in vivo*, by restricted usage of integrins, reduced phosphorylation of focal adhesion kinase, and overall reduced focal adhesions. Not only the composition but also the dimensionality and pliability of the 3D culture matrix can generate *in vivo* like cell-matrix interactions (Li, 2003, Cukierman, 2001).

4. Resistance to cytotoxic drugs: Often cells *in vivo* exhibit more resistance to cytotoxic drugs, compared to 2D cultured cells. Cells grown in 3D culture are also more resistant to cytotoxic drugs, as evidenced by increased LD50 value for various cell types (Sun, 2006, Horning, 2008). Like *in vivo*, cells in 3D culture secrete more ECM and are surrounded by cells in all directions. Because of these reasons, drug accessibility decreases. Since p21 protein was observed to be overexpressed in 3D cultured cells (Li, 2003), its anti-apoptotic function (Janicke, 2007) may also be responsible for the increased drug resistance in these cells. Hence, it is not unreasonable to think that 3D cultured cells behave similarly to *in vivo* cells, in terms of cytotoxic resistance. Therefore, 3D culture models are increasingly preferred over 2D models to evaluate *in vitro* drug toxicity (Mitra, 2012).

1.9.2 3D models to study endothelial-astrocyte interactions

At the BBB, BMVEC are situated at a liquid-solid interface and astrocytes are in a 3D matrix. In both 2D static models and flow-based models, EC are cultured in a solid-liquid interface, but astrocytes are cultured on a 2D substrate. The need to improve upon this limitation and the understanding that cell behaviour in 3D culture has more physiological relevance resulted in the development of 3D co-culture models, to study endothelial-astrocyte interactions.

Some previous studies have used 3D gel cultures of endothelial cells alone to study angiogenesis and tubule formation (Koh, 2008, Davis, 2007). Madri and colleagues developed a mixed co-culture model in which rat astrocytes were co-cultured with either beagle BMVEC or a rat brain endothelial cell line (RBE4) cultured in a gel made of calf dermis collagen type-I (Ment, 1997, Chow, 2001). This model was used to study the role of astrocytes in microvascular angiogenesis in normal and hypoxic conditions. In this pioneering work, they reported that beagle BMVEC in 3D gel matrix behaved like *in vivo* BMVEC, by proliferating less, and organising into tubules, and depositing ECM proteins (fibronectin and laminin). In addition, the astrocytes enveloped these tubules and established a bidirectional signalling, imitating an *in vivo* brain capillary.

This model was adapted recently by Al Ahmad *et al.* (2010) who developed a 3D collagen gel tri-culture model in which a rat brain endothelial cell line (RBE4), rat primary astrocytes, and rat primary pericytes were co-cultured in a gel made of rat tail collagen type I. They studied the BBB induction and maintenance potential of pericytes and astrocytes during tubulogenesis and during hypoxic insult. In this model, cells are surrounded by a 3D collagen matrix, which facilitates physical interaction between the cells and allows the reorganisation of cells to form tubular structures with a lumen that mimics capillary formation *in vivo*. The key findings of the study are as follows.

Pericytes are pro-angiogenic (increased number of tubules) while astrocytes are anti-angiogenic (decreased number of tubules), but co-culturing both cell types together with endothelial cells *i.e.*, tri-culture favours the anti-angiogenic phenotype and thus contributes to induction/-maturation of the BBB phenotype of endothelial cells. Induction of the BBB phenotype was assessed by formation of adherens junctions (β-catenin), localisation of tight junctional proteins (ZO-1 and claudin-5) at cell-cell junctions, polarised expression of P-gp and multidrug resistance protein-2 (MRP2) on the luminal membrane, and polarised functional activity of P-gp. A major finding was the importance of pericytes during prolonged hypoxia. In normal circumstances, astrocytes alone appear to be sufficient to induce the BBB phenotype, but during hypoxia, both pericytes and astrocytes are required to maintain the BBB integrity, as evaluated by the localisation of claudin-5 and ZO-1 and preservation of tubule integrity. Altogether, they demonstrated the model's suitability to study BBB formation and development.

In the present study, the 3D co-culture model has a different configuration from Al Ahmad *et al.*'s mixed co-culture model and therefore can serve different purposes.

1.10 Aims of the present study

The main drawback of conventional *in vitro* 2D co-culture models is that astrocytes are cultured on a stiff, two-dimensional (2D) matrix, which is unnatural and different from their native environment. In addition, the *in vivo* geometric relationship between BMVEC and astrocytes is not always maintained and in some models, physical contact is inadequate or absent. Therefore, to improve upon these limitations, we aimed to develop an *in vitro* 3D co-culture model to study interactions between human BMVEC and astrocytes. The main aims of this study were as follows.

1. To establish an *in vitro* human 3D co-culture model to study interactions between BMVEC and astrocytes
2. To investigate whether 3D cultured astrocytes have improved BBB induction potential than 2D cultured astrocytes
3. To investigate the inductive effect of BMVEC on astrocytes using this 3D culture model

1.10.1 Cells used in the study

Species-matched, human co-culture model

One advantage of the present model is that human cells are used so the findings can be more readily translated to humans *in vivo*. In this study, primary human astrocytes and immortalised human BMVEC (hCMEC/D3) were used.

The source of primary human astrocyte cultures can be brain tissue of either adult or foetus. Adult brain tissue is obtained either from epilepsy patients who undergo temporal lobectomy or from post-mortem cases. Foetal brain is generally from pregnancy abortion cases. The source of tissue may be relevant since maturity and heterogeneity of astrocytes may differ between embryonic and adult stages (Bushong, 2004, reviewed in Wang, 2008). Although,

both foetal (Hurwitz, 1993, Siddharthan, 2007) and adult (Megard, 2002) astrocytes were shown to have barrier-enhancing capacities, so far, no systematic study has compared their barrier enhancing potentials. Because of the limited availability of human tissue, researchers' choice of adult versus foetal appears to be mainly based on the logistics. In the present study, human foetal astrocytes were used.

hCMEC/D3 cells

hCMEC/D3, a human cerebral microvascular endothelial cell line, is the only well characterised human cell line that is suitable for BBB studies. hCMEC/D3 cells were immortalised by transfecting with the human telomerase catalytic subunit and Simian virus 40 Large T antigen (Weksler, 2005). These cells retain the characteristics of primary brain endothelial cells and express specific brain microvascular endothelial markers, cell surface adhesion molecules, tight junctional proteins, ABC transporter proteins and chemokine receptors over the course of 35 passages.

Although paracellular permeability of confluent monolayer of these cells to larger hydrophilic molecules is comparable to other widely used *in vitro* BBB models, their permeability to much smaller sized ions is relatively high, which is indicated by low TEER (<40 $\Omega.cm^2$). However, these cells attain high TEER values (1200 $\Omega.cm^2$) under shear stress, even in the absence of astrocytic factors (Cucullo, 2008). This suggests that these cells did not lose their native BBB phenotype but require optimal culture environment to display these characteristics. These cells are very similar to primary human BMVEC in immune barrier properties, and so desirable for *in vitro* immune migration studies (Daniels, 2013).

These cells have been proven to be a useful substitute for primary human BMVEC and many research groups have used these cells since their introduction in 2005, and published more than 75 research articles to date.

Chapter 2:

Establishment of an *in vitro* human 3D co-culture model to study endothelial-astrocyte interactions

2.1 INTRODUCTION

A major drawback in the current models to study interactions between BMVEC and astrocytes is that astrocytes are cultured on a 2D surface. Cells in 3D culture often display different properties than 2D cultured cells (See section 1.9) and may be more similar to their *in vivo* counter parts (Lee, 2008, East, 2009). Moreover, 3D cell culture models facilitate the analysis of cell behaviour in a more physiologically realistic state and thus bridge the gap between 2D cell culture models and *in vivo* animal models (Neuwelt, 2008, Maltman, 2010). Therefore, the chief aim of this study was to develop an *in vitro* co-culture model that mimics the *in vivo* situation. In this model, astrocytes are cultured in a 3D collagen gel while endothelium is grown on the surface of the gel. The main features of the model are:

1. **HA are cultured in 3D environment:** In this model, human astrocytes (HA) are grown in the 3D collagen matrix and so, may display different properties compared to those cultured on a 2D surface and may be more similar to their *in vivo* counterparts (East, 2009).
2. **Endothelial-astrocyte interaction:** Astrocytes cultured inside the gel can interact with the abluminal side of endothelium through soluble factor mediated interaction and/or physical contact. This would mimic the *in vivo* geometric relationship between the two cell types.
3. **Endothelial cells are cultured on a pliable matrix:** Endothelial cells are cultured on the surface of a pliable, soft hydrogel gel surface, which is different from a

collagen-coated hard substrate of conventional 2D models. The phenotype of cells depends on the rigidity of the matrix on/in which they are cultured (Janmey, 2009). It has been shown that bovine aortic endothelial cells (BAEC) cultured on the gel surface of collagen type-I, acquire a more differentiated phenotype, and become more similar to quiescent *in vivo* endothelium, than those cultured on the plastic surface (Beck, 2004). This was evidenced by decreased expression of platelet-derived growth factor-B, fibronectin, fibronectin isoform ED-B, a decreased mitotic index, and increased expression of connexin-40 in BAEC cultured on a gel surface compared to those cultured on a plastic surface. In addition, it has been shown that matrix rigidity that is reflective of the situation *in vivo* will induce stem cells to differentiate into specific cell types (Engler, 2006). Therefore, it is conceivable that endothelium cultured on the pliable, soft matrix of collagen gel may assume a more differentiated phenotype than that grown on a rigid matrix. It may also be noted that BAEC cultured on a collagen gel surface had a decreased proliferation rate, decreased thrombospondin expression, but increased laminin B2 expression, compared to those grown on a collagen coated plastic surface, which again suggests the role of substrate rigidity on endothelial properties (Canfield, 1990).

The present model differs from previous published 3D co-culture models (Ment, 1997, Al Ahmad 2010) in two aspects.

1. In their models, both astrocytes and BMVEC were cultured in a 3D matrix, whereas in the present model, only astrocytes are cultured within a 3D environment, while BMVEC are cultured on the surface of the gel.
2. In the present model, endothelial cells are cultured on the surface of the gel containing astrocytes have two faces. One, apical surface facing the nutrient culture media and the other, basal surface, facing the HA seeded in the gel. This configuration simulates

blood side/liquid interface (luminal) and brain parenchyma side/solid interface (abluminal) of the *in vivo* HBMVEC, which may be essential for the induction of its polarised membrane characteristics and barrier phenotype.

2.1.1 Reactive astrocytes

Astrocytes are highly differentiated, slowly dividing, multifunctional cells present in the CNS (Ransom, 2012, Colodner, 2005). During CNS injury and disease or any kind of insult, astrocytes respond by a process generally known as gliosis or reactive gliosis, and those responding astrocytes are known as reactive astrocytes. Reactive astrogliosis is a complex, graded phenomenon in which astrocytes undergo several phenotypic changes (reviewed in Sofroniew, 2009). Often these changes occur in a progressive graded manner as the severity of the insult increases. Generally, changes in the molecular expression precede hypertrophy, which is followed by proliferation and eventually by a scar formation. Molecular expression changes include but are not limited to the upregulation of intermediate filament proteins (e.g., glial fibrillary acidic protein (GFAP), Vimentin, Nestin), transcriptional regulators (e.g., nuclear factor kappa-light-chain-enhancer of activated B cells (NF-kB), signal transducer and activator of transcription-3 (STAT3)), extra cellular matrix molecules (e.g., laminins, integrins), and the release of inflammatory cytokines. Molecules such as transforming growth factor β (TGF-β), glutamate, and nitric oxide released by neighbouring cell types such as microglia, neurons, and endothelial cells are directly responsible for triggering the reactivity in astrocytes. During gliosis, astrocytes gain or lose some new functions, and of them may be either beneficial or detrimental on surrounding cells depending on the context.

When astrocytes are cultured *in vitro* on a 2D surface, they spontaneously acquire a reactive phenotype as manifested by increased GFAP expression and proliferation rate compared to their *in vivo* counterparts (reviewed in Wu, 1998, Holley, 2005). It has been shown that when 2D cultured rat astrocytes are transferred to a 3D collagen matrix, they become less reactive as

observed by reduced expression of reactive markers such as GFAP, aquaporin-4, and chondroitin sulphate proteoglycan (East, 2009). It is not known whether HA also become less reactive in a 3D culture environment. Therefore, another aim of this study was to investigate the effect of 3D culture conditions on the reactive state of human astrocytes.

In this study, a 3D co-culture model was established, and then 3D culture conditions were optimised. The purity of primary human foetal astrocyte cultures was also determined. Finally, the effect of a 3D culture environment on the reactive state of human astrocytes was studied by analysing their proliferation rate and GFAP expression.

2.2 METHODS

The reagents and antibodies used in this study are listed in **appendices A** and **B** respectively.

2.2.1 Human astrocytes (HA) and their culture conditions

Human foetal astrocytes, (**HA**, ScienCell research laboratories) isolated from the cerebral cortex, at passage 3 to 5 were used in this study. For routine maintenance, the cells were grown on collagen type I-coated culture dishes in the presence of human astrocyte medium (HAM; ScienCell research laboratories). This consists of basal medium, 2% FBS and astrocytic growth supplement, whose composition is undisclosed by the manufacturer. However, for all experiments, to keep the culture conditions identical, both HA solo and co-cultures were grown using D3M media (see **2.2.2.1**).

2.2.2 hCMEC/D3 2D culture: maintenance and passaging

2.2.2.1 Nutrient culture medium for hCMEC/D3 cells

In this study, hCMEC/D3 cells between passage 23 and 33 were used (Weksler, 2005). The hCMEC/D3 cells were cultured in EGM-2 MV medium (EGM-2 MV, Clonetics® Endothelial Cell Systems, Lonza Inc.). The culture medium has two components, basal medium, and growth supplements. Composition of the basal medium and the concentrations of the growth supplements are optimised by the manufacturer for the microvascular endothelial cell growth and are not disclosed. The culture medium, included full volumes of ascorbic acid and hydrocortisone , half the volume of foetal bovine serum (FBS; final concentration of 2.5%) and quarter volumes of the human basic fibroblastic growth factor, human epidermal growth factor, insulin-like growth factor-1 and vascular endothelial growth factor and 0.5 ml of GA-1000 (Gentamicin sulphate and amphotericin-B) in basal medium (EBM-2). Here after, this nutrient culture medium will be referred as **D3M**.

2.2.2.2 Growth surface preparation for hCMEC/D3 cultures

Plastic flasks were coated with collagen type-1 from calfskin. Coating was done by layering the collagen, at 100 μg/ml in Hank's balanced salts solution (HBSS), on to the culture surface, for 1 h at RT then it was rinsed once with HBSS.

Transwell polyester membrane inserts were first coated with collagen as described above, and then the collagen solution was removed and coated with fibronectin at 10 μg/ml in HBSS, for 1 h at RT. The fibronectin solution was removed, before plating the cells.

2.2.2.3 hCMEC/D3 culture maintenance

The hCMEC/D3 cells were grown until confluent at 37°C in 5 % CO2, 95% air, in a humid atmosphere, with fresh medium every 2-3 days. To split cell cultures, cells were washed twice with HBSS without Ca^{2+} and Mg^{2+} then incubated with trypsin (0.25%)-EDTA (20 mM) at 37°C until cells detached. EGM-2 MV culture medium was then added to neutralise trypsin activity and the cells were split at a ratio of 1:3 onto collagen-coated tissue culture flasks.

2.2.3 3D collagen gel culture

In this model, three-dimensional scaffolding was provided by a gel prepared from rat collagen type-I. The basic principle of collagen gel preparation is that collagen is soluble in acidic pH but becomes a gel at neutral/alkaline pH. The gel mixture was composed of

1. 10% (v/v) 10× minimum essential medium (MEM) with Phenol Red
2. 80% (v/v) type-I rat tail collagen (2.15 mg/ml; First Link, UK),
3. 10% (v/v) cell suspension in D3M.

All the reagents were maintained at 4°C. The MEM and collagen were mixed together and neutralised using sodium hydroxide. Neutralisation was assessed by the colour change of phenol red from yellow (acidic) to red (neutral). After neutralisation, the collagen–MEM mixture was gently mixed with the cell suspension and transferred to culture plates (0.40

ml/well in a 24 well plate, resulting in a gel thickness of ~1.3 mm,). Then, the culture plate was incubated in 5% CO_2 at 37 °C for 10 min to allow the gelation. Immediately, the 2.5 ml of nutrient culture media was added gently drop wise onto gels. The procedure is illustrated in **Figure 2-1.**

2.2.3.1 HA 3D solo-culture setup

To setup HA 3D solo-culture, HA cell suspension in 100 µl was mixed with 900 µl of collagen gel mixture, then 400 µl was plated onto the culture dish as explained in section 2.2.3.

2.2.3.2 hCMEC/D3 solo-culture setup

To setup an hCMEC/D3 solo-culture, first an empty collagen gel (400 µL) without cells but with 100 µl of sterile deionised water was cast. hCMEC/D3 cell suspension was gently added drop wise on to the gel surface. Generally, 40 x 10^3 cells were plated per square centimetre area of the gel surface.

2.2.3.3 Co-culture of HA and hCMEC/D3

To setup a co-culture, HA were embedded into collagen gel as explained in section 2.2.3.1. On the gel surface, hCMEC/D3 cell suspension was gently added drop wise. The cell density of both HA and hCMEC/D3 were the same in solo- and co- cultures.

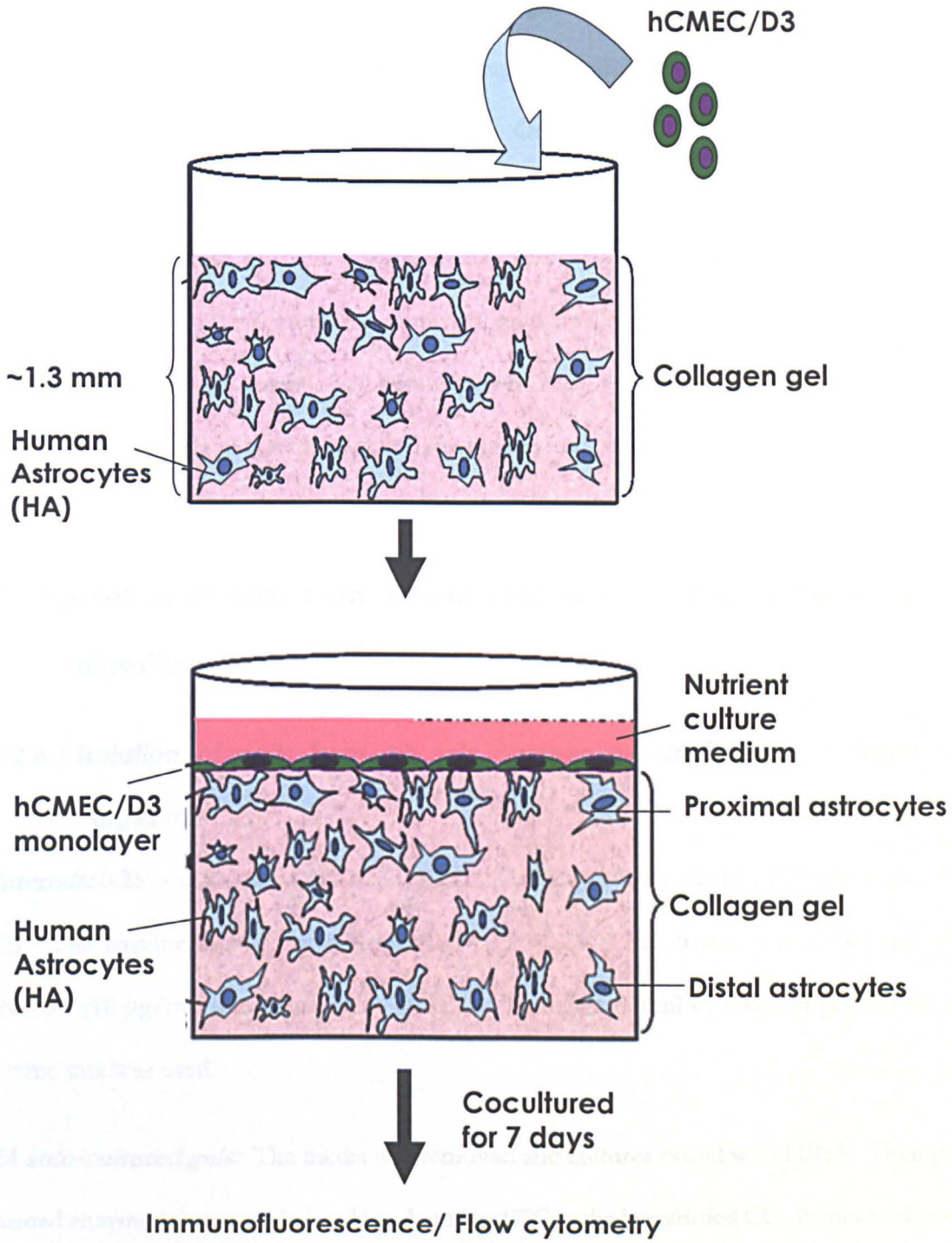

Figure 2-1 Preparation of 3D collagen gel co-culture

In this model, first, HA were seeded inside the 3D matrix of collagen gel then, hCMEC/D3 cells were plated on the surface of the gel to grow as a monolayer. This setup simulates the *in vivo* geometric spatial configuration. Cells were co-cultured for 7 days before they were analysed by immunofluorescence microscopy or flow cytometry.

2.2.3.4 Nutrient culture medium for co-cultures

In the experiments where co-cultures were compared with solo-cultures, all cultures were grown in the same nutrient media, which is D3M. Other wise, for routine sub-culturing, and for initial experiments, human astrocyte medium (HAM) was used. In all cases, culture media was replaced with fresh nutrient culture media every two days until analysis on day 7 by immunofluorescence, flow cytometry or immunogold labelling and electron microscopy. The seven-day culture period was selected because the hCMEC/D3 cell confluent monolayer can be maintained without overgrowth while allowing the study of influence of one cell type on the other.

2.2.4 Isolation of cells from 3D collagen gel cultures by collagenase digestion

2.2.4.1 Isolation of cells from 3D solo-cultures by single-step collagenase digestion

Materials: 0.25% collagenase, DNase I, EDTA, 0.25% Trypsin-EDTA, DMEM with 10% FCS. The enzyme mixture of collagenase (0.25%), TLCK hydrochloride (0.147 ng/ml), DNase-1 (10 μg/ml) was prepared in DMEM. To digest 0.5 ml of collagen gel, 0.5 ml of enzyme mix was used.

HA solo-cultured gels: The media was removed and cultures rinsed with HBSS. Then pre warmed enzyme mix was added and incubated at 37°C in the humidified CO_2 incubator for 45 min. Digestion was terminated by adding EDTA (final concentration, 20 mM). Cells were pelleted by centrifuging at 320 g, for 5 min at 4°C.

hCMEC/D3 solo-cultured gels: Culture media was removed, pre warmed enzyme mix was added then incubated at 37°C in the humidified CO2 incubator. After 15 min, the top hCMEC/D3 monolayer was detached from the gel intact (**Figure 2-2**). By gentle aspiration

using a white tip, the detached cell layer was put into a 0.25% trypsin-EDTA solution, treated for one min, to make into a single cell suspension. The reaction was stopped by adding an equal volume of DMEM/10% FCS.

2.2.4.2 Isolation of cells from 3D co-cultures by two-step collagenase digestion

HA and hCMEC/D3 co-cultured gels: First, the hCMEC/D3 cells were removed as explained above. This fraction was transferred into a tube. The remaining lower portion of the gel was incubated for a further 30 min to complete the digestion before terminating the reaction by adding EDTA.

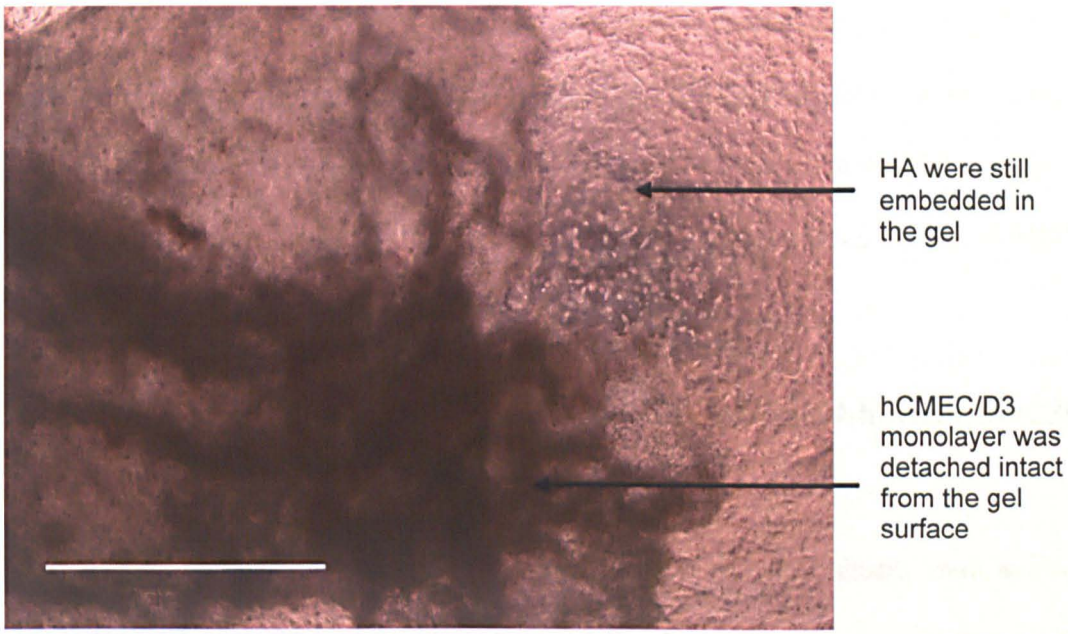

Figure 2-2 Two-step collagenase digestion method

To isolate the HA and hCMEC/D3 from a 3D gel co-culture into two separate cell populations, a two-step collagenase digestion method was developed. After 15 min of exposure to collagenase, the hCMEC/D3 monolayer was detached from the gel surface and transferred into a fresh container. The gel was treated with collagenase for a further 30 min. The separated hCMEC/D3 monolayer was subsequently trypsinised. Scale bar represents 1 mm.

2.2.5 Estimation of purity of HA co-culture fraction isolated from co-cultured gel

Three types of collagen gel cultures were set up:

1. hCMEC/D3 solo-culture, in which Cell tracker™ Green CMFDA loaded hCMEC/D3 cells were layered on top of the collagen gel,
2. HA solo-culture, in which unloaded human astrocytes are embedded in the gel and
3. Co-culture, in which unloaded HA were embedded in the gel and Cell tracker™ Green CMFDA loaded hCMEC/D3 cells were layered on the top of the gel.

These cells were co-cultured for seven days before undergoing collagenase digestion as explained in section 2.2.4. After collagenase digestion of these three gels, four cell fractions *viz.*, HA solo, HA co, hCMEC/D3 solo and hCMEC/D3 co were obtained and analysed by flow cytometry. Cell tracker™ Green CMFDA dye can be detected in the FL1 channel of the FACSCalibur™ flow cytometer. In the HA co fraction, the contaminating hCMEC/D3 populations were detected by their CMFDA fluorescence.

2.2.6 PECAM-1 as a selection marker to differentiate HA from hCMEC/D3 in a mixed population by flow cytometry

3D HA solo, 3D HA-hCMEC/D3 co and hCMEC/D3 solo cultures were isolated by collagenase digestion after 7 days (section 2.2.4). Isolated cells were washed and then incubated with monoclonal PECAM1 antibodies conjugated PerCP-eFluor® 710, for 30 min at 4°C. After two washes, the cells were suspended in PBS and fluorescence was measured by flow cytometry. This antibody works only on unfixed cells. Antibody diluent was 0.1% NaN_3, 0.1% BSA in PBS. Washes and general steps were performed as explained previously (section 2.2.9).

2.2.7 Immunofluorescence microscopy analysis of 2D cultures

2D cultures were set up on the collagen, type I, coated coverslips. After reaching confluence, cells were rinsed with HBSS, before fixing with 4% *p*-formaldehyde (PFA) in PBS for 20 min. Cells were washed thrice before incubating with saponin (0.05% w/v in PBS) and normal goat serum (5% v/v in PBS) for 30 min. Saponin was used as a mild cell permeabilising agent and normal goat serum was used to block non-specific binding of antibodies. Then, cells were washed once before incubating with primary antibody solution for 1 h at RT. Simultaneous staining with isotype-matched antibodies or diluent alone were used as negative controls. Again, cover slips were washed thrice before they were incubated with secondary antibodies for 1 h. Cover slips were washed and mounted with Dapi-Fluoromount-G™ and stored in the dark at 4 °C until they were imaged. Antibody solutions were prepared in phosphate buffered saline (PBS) containing 2.5% normal goat serum, 0.05% saponin. To wash, coverslips were incubated with 5 ml of PBS containing 0.05% saponin on a shaker for 5 min. Images were captured with an Olympus BX61 microscope using Cell^P imaging software.

2.2.8 Immunofluorescence microscopy analysis of 3D cultures

The immunofluorescence protocol for 3D collagen gel cultures was similar to conventional processing of coverslip cultures, except that incubation times were increased to allow the adequate diffusion of antibodies through the gel.

Gels were briefly rinsed with HBSS w/o Ca^{2+} and Mg^{2+} before they were fixed by 4% PFA for 45 min. Then, the gels were washed for 30 min, with three changes of PBS for every 10 min. Then the edges (the interface of gel and culture dish) of each gel were removed before incubating with saponin (0.05% w/v in PBS) and normal goat serum (5% v/v in PBS) for 1 h. Gels were again washed for 15 min, with three changes of PBS before incubating with primary antibody solution over night at 4°C. Gels were washed for 1 h, with four changes of PBS for every 15 min before incubating with secondary antibodies and Hoechst 33258 (1 μg/ml) for

1 h and 30 min. Then gels were washed for 6 h, with fresh changes of PBS for every 30 min. Incubations were carried out in the absence of shaking, in 24 or 48 well plates depending on gel size, while washes were carried out in a six-well plate on a shaker. Gels were placed in CoverWell™ imaging chambers and imaged using a Leica TCS SP5 confocal microscope and LAS AF software. From the z-stack of images, a maximal intensity projection image was generated, which was used for analysis.

2.2.9 General flow cytometry procedure

Cultures were subjected to enzymatic treatment (Trypsin-EDTA or collagenase) to obtain a single cell suspension. The cell pellet was collected by centrifuging. After two washes, cells were fixed in 4% PFA for 20 min. After two washes, cells were incubated with primary antibodies for 1 h at RT. Control staining was carried out simultaneously with a corresponding matched isotype IgG for mouse primary antibodies, or antibody diluent for rabbit antibodies. Cells were washed twice, then incubated with 10 μg/ml of Alexa Fluor® 488 conjugated secondary antibodies for 45 min. Cells were washed twice, suspended in PBS, then analysed by FACSCalibur™ using Cell Quest software. For each sample, data from 10,000 cells were collected. Antibody diluent contains 0.1% BSA, 2.5% normal goat serum in PBS. Each wash was done in 4 ml of PBS; cells were collected by centrifuging at 320 g for 5 min. If cell-permeabilisation was needed, saponin (0.05%, final concentration) was added to the antibody diluent and washing buffer.

2.2.10 Effect of 3D collagen matrix on proliferation of HA

0.2 x 10^6 cells were seeded onto 2D collagen-coated plastic culture dish and into 3D collagen gel (section 2.2.3.1) and cultured for 7 days before they were harvested and total cell number were counted using Neubauer haemocytometer. 2D HA cultures were harvested by trypsinisation whereas 3D HA cultures were harvested by collagenase digestion (section

2.2.4.1.) Data were collected from quadruplicate experiments with single sample in each experiment. Data were analysed using the formulas as given below.

Fold increase in cell number = Harvested cell number /Seeded cell number

Number of cell divisions = Log 2 (fold increase in cell number)

Cell doubling time = Culture duration/number of cell divisions

2.2.11 Analysis of purity of HA culture

On day-1, HA cultures (passaged 3-5), were trypsinised, and plated on to collagen coated coverslips and 3D gel cultures. 3D HA culture (0.5 x 10^6 cells/ml) was setup as described in section 2.2.3.1. After 8 h, some coverslips were fixed with 4% PFA for 20 min, then washed and labelled as day-1 and stored at 4 °C. The remaining coverslips (2D day-8) and 3D HA cultures (3D day-8) were cultured for 7 more days, then fixed in 4 % PFA, and stored at 4 °C. Fixed coverslips and gels were analysed by immunofluorescence microscopy. A general procedure for 2D cultures/coverslips is described in section 2.2.7, and for 3D cultures is described in section 2.2.8. For double immunofluorescence of GFAP and TE7, first mouse TE7 antibodies, then Goat anti-mouse Alexa 488 antibodies, then rabbit GFAP antibodies, then Goat anti-rabbit DyLight A459 antibodies were applied. Similar steps were carried out for double staining of GFAP and S100 calcium binding protein B (S100B), using mouse GFAP antibodies and rabbit S100B antibodies.

Sampling, imaging, and analysis

Three independent experiments were performed, and within experiment, triplicate samples for 2D cultures and duplicate samples for 3D cultures were analysed. For each sample, images were captured of 8 random fields, and at least 500 cells were counted per sample. In a given field, the total number of cells was determined by counting DAPI/Hoechst stained nuclei, and the number of positive cells was determined by counting characteristically stained cells. Cell

count was carried out using touch count feature of Cell^F software. 2D day-1 culture is a control for both 2D day-8 and 3D day-8 cultures.

2.2.12 GFAP expression analysis of 3D HA vs. 2D HA cultures by flow cytometry

Culture setup

On day-1, non-confluent HA 2D cultures were trypsinised and a portion of this cell population was fixed with 4% PFA for 20 min, then washed and labelled as day-1 and stored at 4 °C. The remaining cells were used to setup three types of cultures, namely, 3D HA, 2D HA non-confluent, and 2D HA confluent cultures. HA 3D culture (0.5 x 10^6 cells/ml) was setup as described in section 2.2.3.1. 2D HA confluent culture were set up by plating 2 x 10^5 cells into a culture dish of area 4 cm^2 (12-well plate) while 2D HA non-confluent cultures were set up by plating 2 x 10^5 cells into a 25 cm^2 flask. 2D culture dishes were coated with collagen, type-I before the cells were plated.

Flow cytometry procedure

After 7 days, cells from 3D culture were isolated from the gels as described in the section 2.2.4.1 and cells from 2D cultures were isolated by trypsinisation. Then, cells were collected by centrifuging and subjected to two washes before fixing the cells with 4% PFA for 20 min. Subsequently these along with day-1 cells were analysed by flow cytometry as described in section 2.2.9. GFAP G-A-5 monoclonal antibodies, isotype control IgG1, and Alexa Fluor® 488-conjugated goat anti-mouse IgGs (H+L) were used. Simultaneously hCMEC/D3 cells were analysed for GFAP expression as additional negative control for staining.

Data analysis

The effect of culture conditions was measured using two parameters namely, the percentage of GFAP positive cells and GFAP expression per cell. The fluorescence level of GFAP staining

in hCMEC/D3 cells was considered as non-specific background and was used to set the threshold for GFAP specific staining. HA that had fluorescence value above the threshold were considered GFAP positive. Thus, for each sample, the percentage of GFAP positive cells was determined. GFAP expression per cell, for each sample, was determined from the geometric mean of fluorescence intensities of GFAP positive population. [Geometric mean was used because when the data follows log normal distribution (long tail); geometric mean is the better measure of its central tendency.]

Results are expressed in relation to the day-1 value (either 1.0 or 100%). Thus, normalised data from quadruplicate experiments are shown but statistical analysis was performed on the raw data.

2.2.13 Statistical analysis

Graph plotting and statistical analysis was carried out using GraphPad PRISM v 4.0. Statistical significance of data was assessed by Paired *t*-test. $P \leq 0.05$ was considered as significant. * indicates $P \leq 0.05$, ** indicates $P \leq 0.01$, *** indicates $P \leq 0.001$.

2.3 RESULTS

2.3.1 Seeding cell density of HA was optimised to prevent gel contraction

Preliminary experiments using conditions optimised for rat astrocytes in 3D gel cultures (East, 2009) showed that HA seeded at 2.0 x 10^6 cells/ml decreased the size of 3D gels. To determine the highest seeding cell density that did not lead to gel contraction, gels were seeded with three different cell densities namely, 0.25 x 10^6, 0.5 x 10^6 and 1.0 x 10^6 per ml as described in section 2.2.3.1, and examined for gel contraction visually (by naked eye) for the next seven days. Gel contraction was imaged using a digital camera. Gels seeded with 1.0 x 10^6 cells/ml were contracted by day 5, while gels with 0.5 x 10^6 cells/ml and 0.25 x 10^6 cells/ml were not contracted by the end of day 7 (**Figure 2-3**). The cell density, 0.5 x 10^6 cells/ml was considered as optimal as it was the highest cell density that did not contract the gel before seven days.

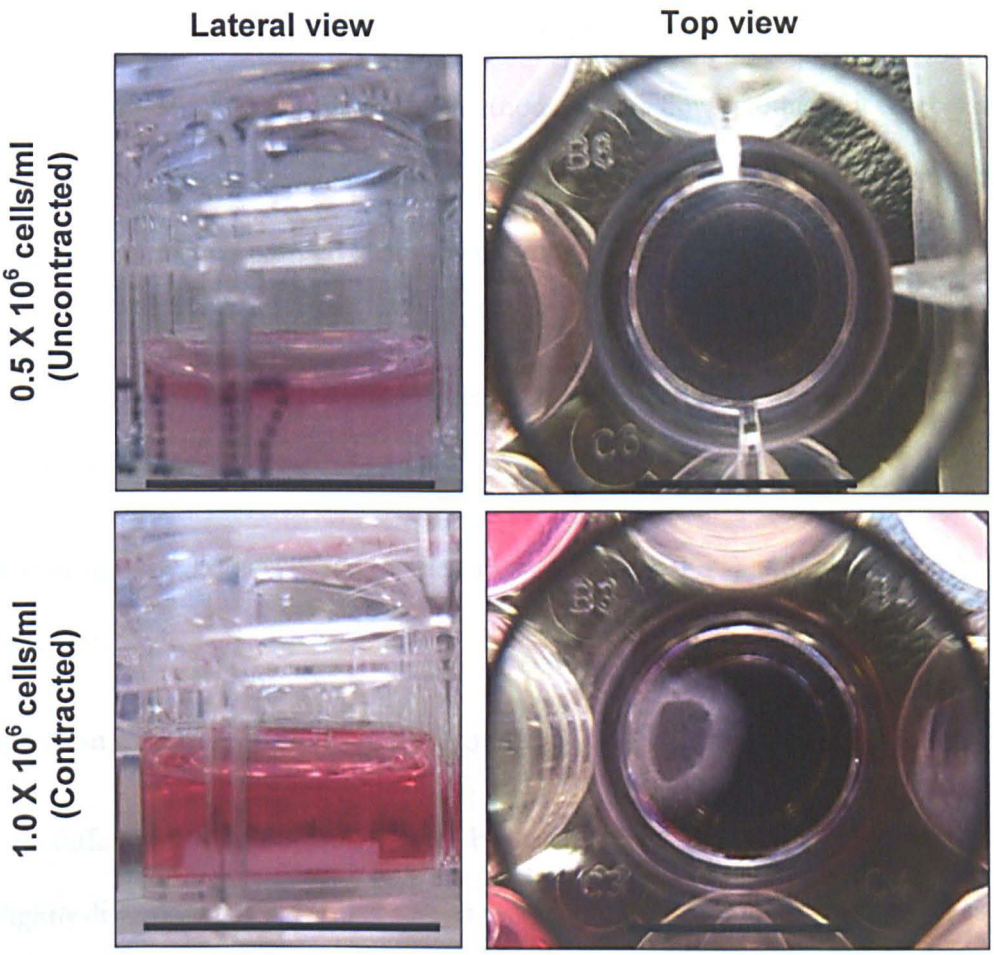

Figure 2-3 Gel contraction was directly proportional to HA cell density

Optimal HA cell density required to maintain the 3D gel cultures without contraction was determined. Gels seeded with 1.0 x 10^6 cells/ml were contracted by the 5th day, while gels with 0.5 x 10^6 cells/ml were uncontracted at 7days. The cell density, 0.5 x 10^6 cells/ml was considered as optimal as it was the highest possible cell density at which gel cultures did not contract for at least seven days. Images are representative of a single experiment while the experiment was performed at least three times. Scale bar indicates 1.55 cm, which is the width of the culture well.

2.3.2 Two-step collagenase digestion method was used to isolate HA and hCMEC/D3 from collagen gel into two separate cell fractions

To analyse HA cultured in the collagen gels, by methods such as flow cytometry, it is necessary to isolate them from the gel. Isolation of cells from 3D HA solo-cultures and 3D hCMEC/D3 solo-cultures was carried out by a single-step collagenase digestion as described in 2.2.4.1. In the case of 3D co-cultures, cells not only need to be isolated from the gel but also HA and hCMEC/D3 need to be separated from each other. To this purpose, two simpler methods were considered:

- Identification of cell type based on their forward scatter (FSC) and side scatter (SSC) properties.
- Separation of cell types using a percoll gradient.

There was no difference in the FSC property of HA vs. hCMEC/D3 cells, although each cell type was slightly different in their SSC properties, this difference was not sufficient to separate the two cell populations. Nor did a 50% percoll gradient separate the cell types from each other. Therefore, a two-step collagenase digestion method was developed as described in 2.2.4.2. Using this method, cells can be isolated from the gel matrix and both cell types, HA and hCMEC/D3 can be separated into two separate fractions.

During the two-step collagenase digestion of co-cultured gels, it is possible that a few hCMEC/D3 cells will come into the HA fraction of the digest. The percentage of contaminating hCMEC/D3 cells in the HA fraction was estimated as described in 2.2.5.

The percentage of contaminating CMFDA-loaded hCMEC/D3 cells in the HA co fraction was found to be ~7-8% (N=3; **Figure 2-4.C**). However, this level of purity of the HA fraction (~92-93%) did not interfere with flow cytometry analysis since the median fluorescence value of HA co fraction was close to that of a HA solo cell population (**Figure**

2-4.A&C). Therefore, it was concluded that the HA fraction obtained from co-culture by the two-step collagenase method was sufficiently pure to analyse by flow cytometry.

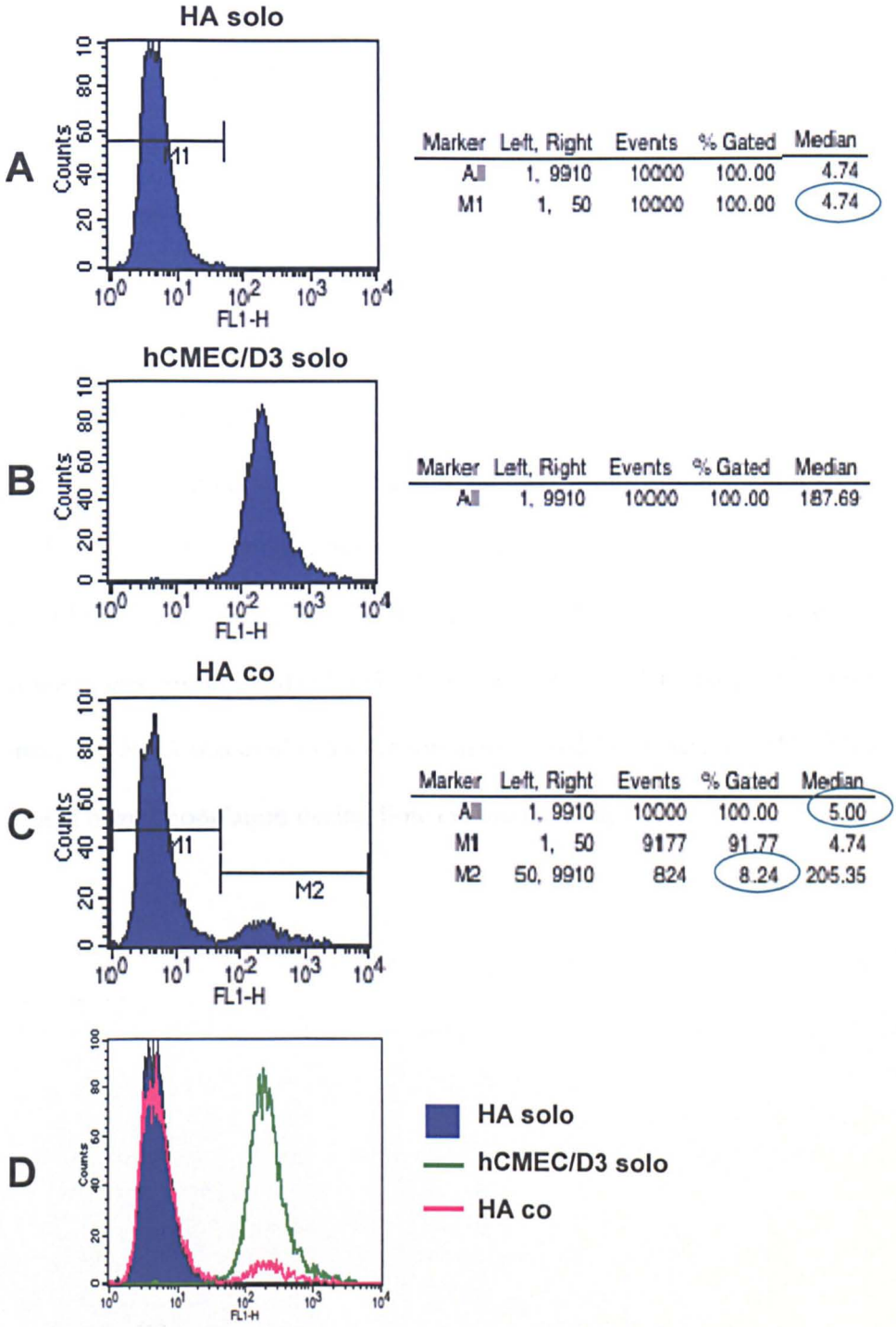

Figure 2-4 Flow cytometry analysis of purity of HA co fraction isolated from 3D co culture

3D HA solo- and 3D co- cultures were set up using CMFDA labelled hCMEC/D3 and unlabeled HA. By two-step collagenase digestion method, HA co cell fraction was isolated and its purity was assessed by flow cytometry. Results of a representative experiment are shown here. Percentage of contaminating hCMEC/D3 was found to be ~8 % (**C, M2 population**). This level of contamination did not affect the median fluorescence of HA co (**C**) compared to HA solo (**A**) as evidenced by similar median fluorescence value of HA co population (5.00) compared to that of HA solo (4.74). Similar results were obtained in two further experiments. N=3.

2.3.3 PECAM1 expression was exclusive to hCMEC/D3 cells

Although the two-step collagenase digestion method yields ~92% pure population of HA, it was considered that using a cell type-selective expression marker would improve the identification of the two cell populations during flow cytometry analysis. For this purpose, two endothelial specific cell-surface expression markers, platelet endothelial cell adhesion molecule-1 (PECAM1) and intercellular adhesion molecule-2 (ICAM2) were screened. Expression of these molecules on confluent hCMEC/D3 cells and HA was analysed by flow cytometry as described in section 2.2.9, using mouse anti-PECAM1 and ICAM2 antibodies. ICAM2 was found to be expressed in both HA and hCMEC/D3 cells (N = 2, data not shown) while PECAM1 was exclusively expressed on hCMEC/D3 cells (**Figure 2-5**). PECAM1 staining intensities on hCMEC/D3 cells were 11.8 ± 1.1 fold higher than those of HA cells. Hence, PECAM1 was used as a selection marker to differentiate hCMEC/D3 cells from HA cells in a mixed population during flow cytometry analysis.

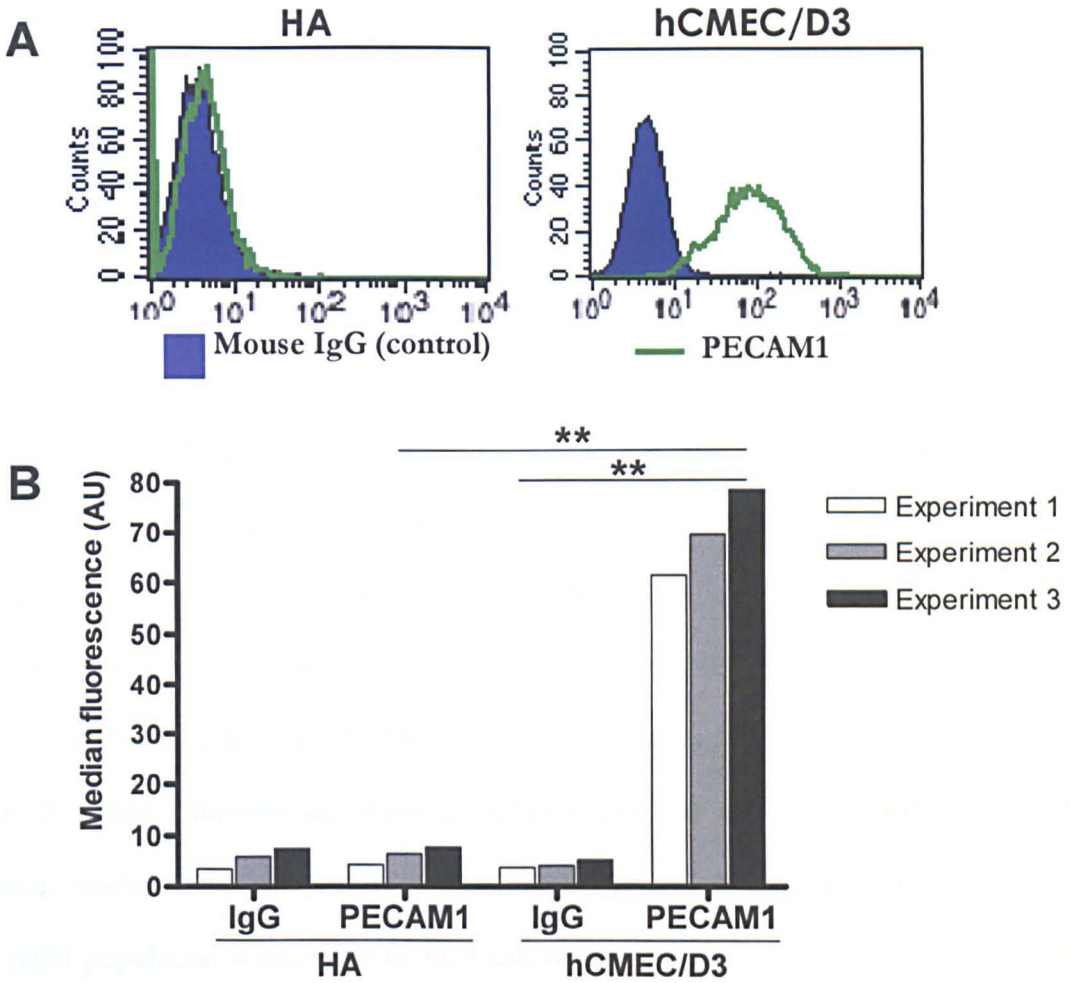

Figure 2-5 PECAM-1 was exclusively expressed on hCMEC/D3 cells

Expression of PECAM-1 was analysed by flow cytometry in hCMEC/D3 cells and HA. **A:** On HA, PECAM1 staining levels were not different from control staining levels as seen by overlapping histograms. In contrast, hCMEC/D3 cells stained for PECAM1 intensely, as seen by clearly separated histograms. **B:** Bars represent the median fluorescence values in arbitrary units (AU). PECAM1 staining intensities of hCMEC/D3 cells were statistically different from intensities of IgG control and PECAM1 intensities of HA. ** indicates $P \leq 0.01$ using Paired *t*--test, N = 3.

2.3.4 A combination of PECAM-1 expression and SSC gating was used to separate the cell types in a mixed population

PECAM-1 was found to be exclusively expressed on hCMEC/D3 cells but not HA cells. Therefore, whether PECAM-1 could be used as a selection marker during flow cytometry was tested. 3D HA solo, 3D HA-hCMEC/D3 co and hCMEC/D3 solo cultures were established and cell populations were isolated by collagenase digestion after 7 days, then analysed by flow cytometry as described in 2.2.6. SSC properties of HA and hCMEC/D3 were slightly different. So, the differences in both the properties, SSC and PECAM-1 expression, were exploited to differentiate the cell types. When PECAM-1 fluorescence (along the *X*-axis) and SSC (along the *Y*-axis) of cells were plotted, HA and hCMEC/D3 formed two distinct populations (**Figure 2-6 A** and **B**). Two gates were drawn, exclusive for each cell type. The median PECAM-1 fluorescence value of solo-cultures was almost the same as that of co-cultures for both HA and hCMEC/D3 cell types (**Figure 2-6 C**). These data confirm that each gated population is exclusive to each cell type. Therefore, the two-step collagenase digestion procedure and subsequent gating based on PECAM1 expression and SSC properties was sufficient to differentiate hCMEC/D3 cells from HA during flow cytometry.

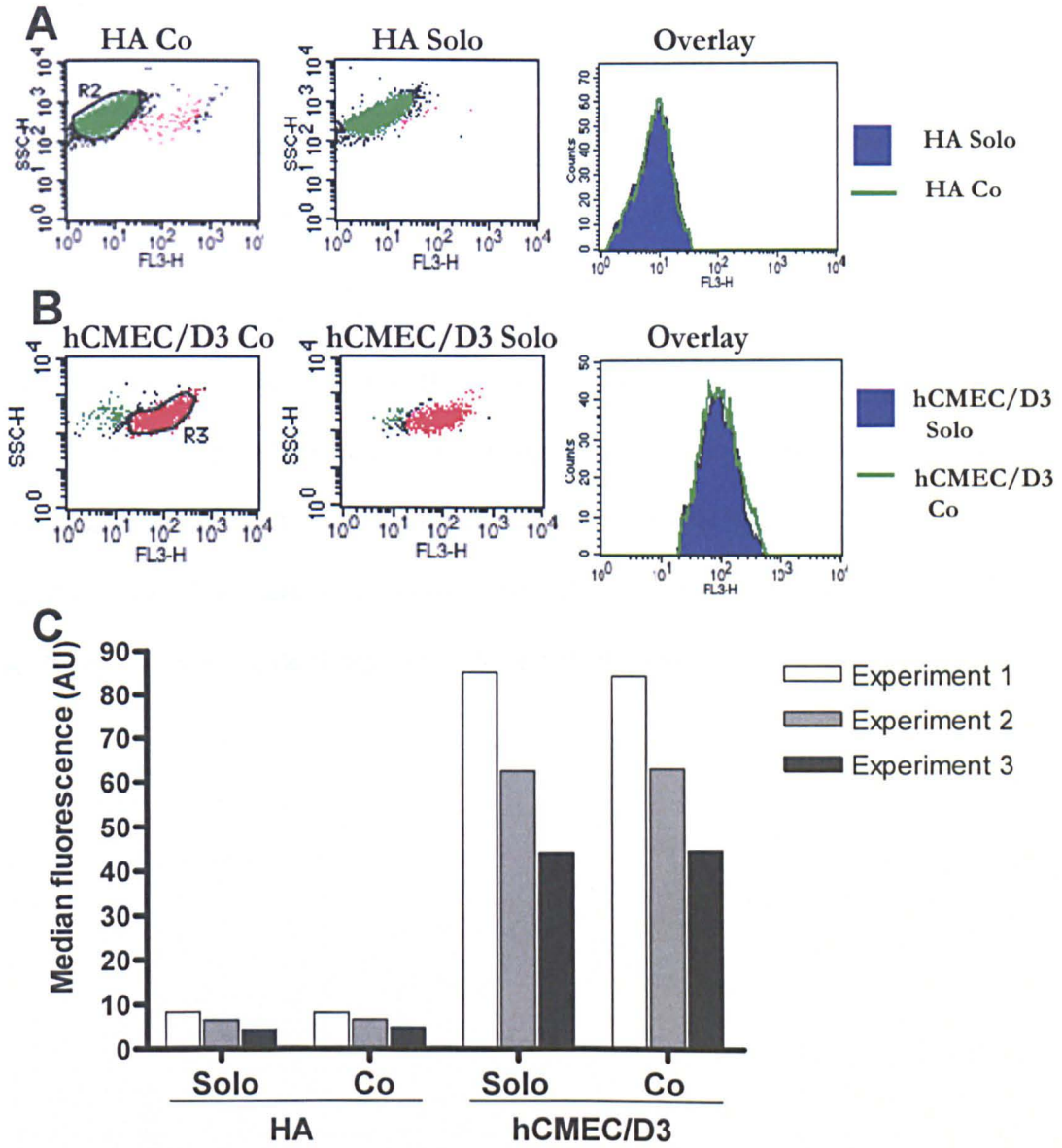

Figure 2-6 Gating based on a combination of PECAM-1 expression (FL3) and SSC was used to separate the HA from the hCMEC/D3 cells.

HA and hCMEC/D3 formed two distinct cell populations when their PECAM-1 fluorescence (X-axis) and SSC (Y-axis) were plotted. A gate was drawn for each cell type. Median PECAM-1 fluorescence value of solo-culture was similar as that of co-culture for both HA and hCMEC/D3 cell types. **A and B:** FL3-SSC plots from a single experiment are shown. **C**: Bars represent the median PECAM1 (FL3) fluorescence values. For both HA and hCMEC/D3 cell types, co-culture values were not statistically different from that of solo-culture, and values were very similar. These data confirm that each gated population is exclusive to each cell type. Paired *t*-test, N = 3.

2.3.5 Effect of 3D collagen matrix on the proliferation of HA

To determine the effect of 3D culture on the proliferation of HA, 2D HA and 3D HA cultures were seeded with same number of cells (0.2×10^6). After 7 days, cells were harvested, counted, and total cell number was related to seeding cell number (**Figure 2-7**).

2D HA total cell number increased 7.5 ± 0.4 times over seeding cell number indicating that they divided 2.9 ± 0.08 times during the 7-day culture duration. In contrast, 3D HA cell number ($0.211 \pm 0.016 \times 10^6$) did not change significantly from the seeding cell number. It appears that unlike 2D HA, whose cell doubling time is ~2.41 days, 3D HA did not divide during the 7-day culture period. It is possible that 3D HA, either do not divide or divide much more slowly *i.e.*, their cell doubling time is longer than 7 days.

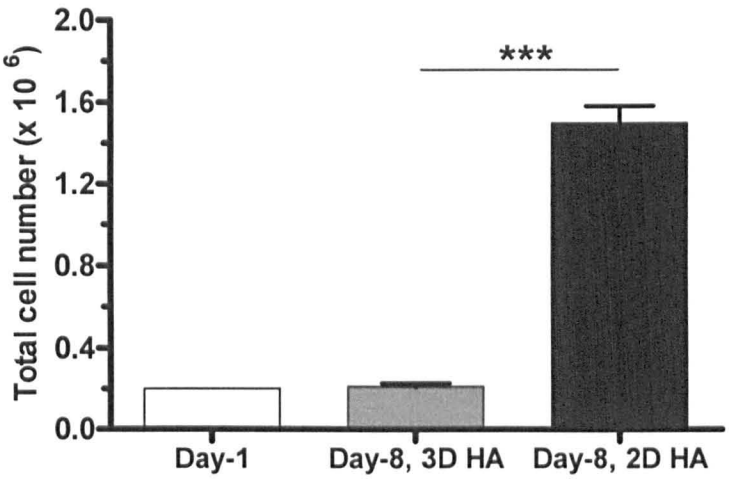

Figure 2-7 3D collagen matrix reduces proliferation of HA

2D HA and 3D HA cultures were set up with same seeding cell number, 0.2 x 10^6, and cultured for 7 days, before cells were harvested and counted using a Neubauer haemocytometer . Bars show the recovered cell number. 3D HA total cell number did not change statistically from the seeding cell number *i.e.*, Day-1. In contrast to 3D HA, 2D HA divided 2.9 ± 0.08 times during the 7-day culture period. *** indicates $P \leq 0.001$ using Paired *t*-test. N = 4.

2.3.6 Determination of purity of HA culture by immunofluorescence microscopy

Primary astrocyte cultures are often contaminated with other cell types such as fibroblasts, microglia, and oligodendrocytes although contamination with oligodendrocytes or microglia is unlikely to be high. Therefore, the main objective of this experiment was to determine the percentage of fibroblasts in our culture. To determine the extent of contamination of other cell types in HA cultures used in this study, four expression markers namely GFAP, to identify astrocytes, TE7, to identify fibroblasts, O1, to identify oligodendrocytes, and CD68, to identify microglia, were analysed by immunofluorescence microscopy.

GFAP staining was heterogeneous across the cell population. Non-nuclear, fibrillary staining was considered as true positivity of GFAP expression. Cells that showed other patterns of staining were considered as GFAP negative. In contrast, TE7 staining was punctate (**Figure 2-8**). To determine the specificity of anti-TE7 antibody, HA cultures were double stained with anti-GFAP and anti-TE7 antibodies. Results show that TE7 expression is exclusive to non-GFAP expressing cells, which confirms the specificity of the antibody for fibroblasts (**Figure 2-8**).

To examine the effect of subculturing/passaging on the purity of the HA cultures, the expression of GFAP and TE7 was studied on day-1 and day-8. The culture setup is described in section 2.2.11. In addition, expression changes were compared between 2D and 3D cultures.

On day-1, 29.2- 46.9% of cells were GFAP positive and 1.7 - 2.8% of cells were TE7 positive (**Figure 2-9** to **Figure 2-11**).

O1 staining on HOGs, a human oligodendroglioma derived cell line (Post, 1992), indicated the functionality of the antibody, while absence of O1 staining in HA cultures indicated the

absence of oligodendroglial cells (**Figure 2-12**). CD68 (KP1) staining on CHME3, a human foetal microglial cell line, indicated the functionality of the antibody (Flynn, 2003); while its absence in HA cultures indicated the absence of microglial cells in the culture (**Figure 2-12**).

In 2D cultures, on day-8, the percentage of GFAP positive cells was decreased by ~1.9 times whereas the percentage of TE7 positive cells was increased by ~2.7 times. In 3D cultures, on day-8, the percentage of GFAP positive cells was marginally decreased by ~1.048 fold (~5%), which is statistically not significant, whereas the percentage of TE7 positive cells was increased by ~3.2 fold.

O1 marker and CD68 expression in Day-8 cultures were not analysed as these markers were not detected on Day-1 cultures.

In 2D cultures, on day-1, S100B staining was detected in the cytoplasm as well as in the nucleus. S100B expression was found in ~90% of the cells (**Figure 2-13**). Double immunostaining has shown that almost all the GFAP positive cells also expressed S100B. There were ~5% of cells that did not express either GFAP or S100B.

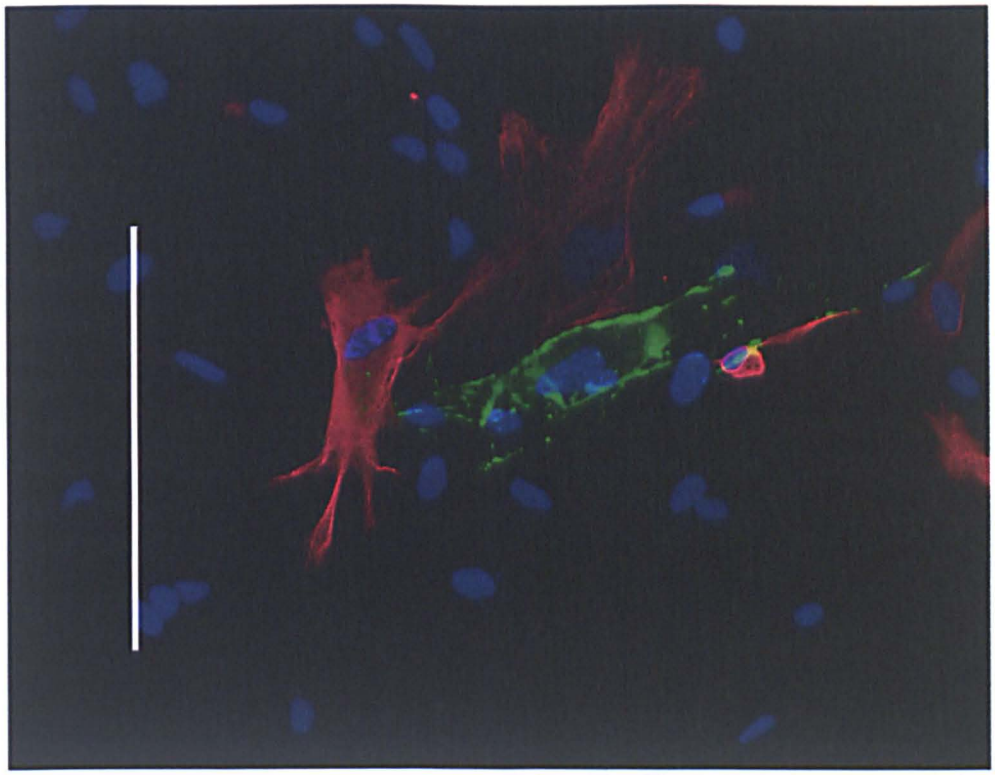

Figure 2-8 Anti-TE7 antibody does not bind to GFAP expressing cells

To determine the exclusivity of TE7 staining, double immunofluorescence analysis was carried out on HA cultures (passage 8) using TE7 and GFAP antibodies. TE7 staining is seen in green while GFAP staining is seen as red. Blue is nucleic acid stained with DAPI localised to nucleus. Expression of GFAP and TE7 are mutually exclusive. Scale bar represents 200 μm.

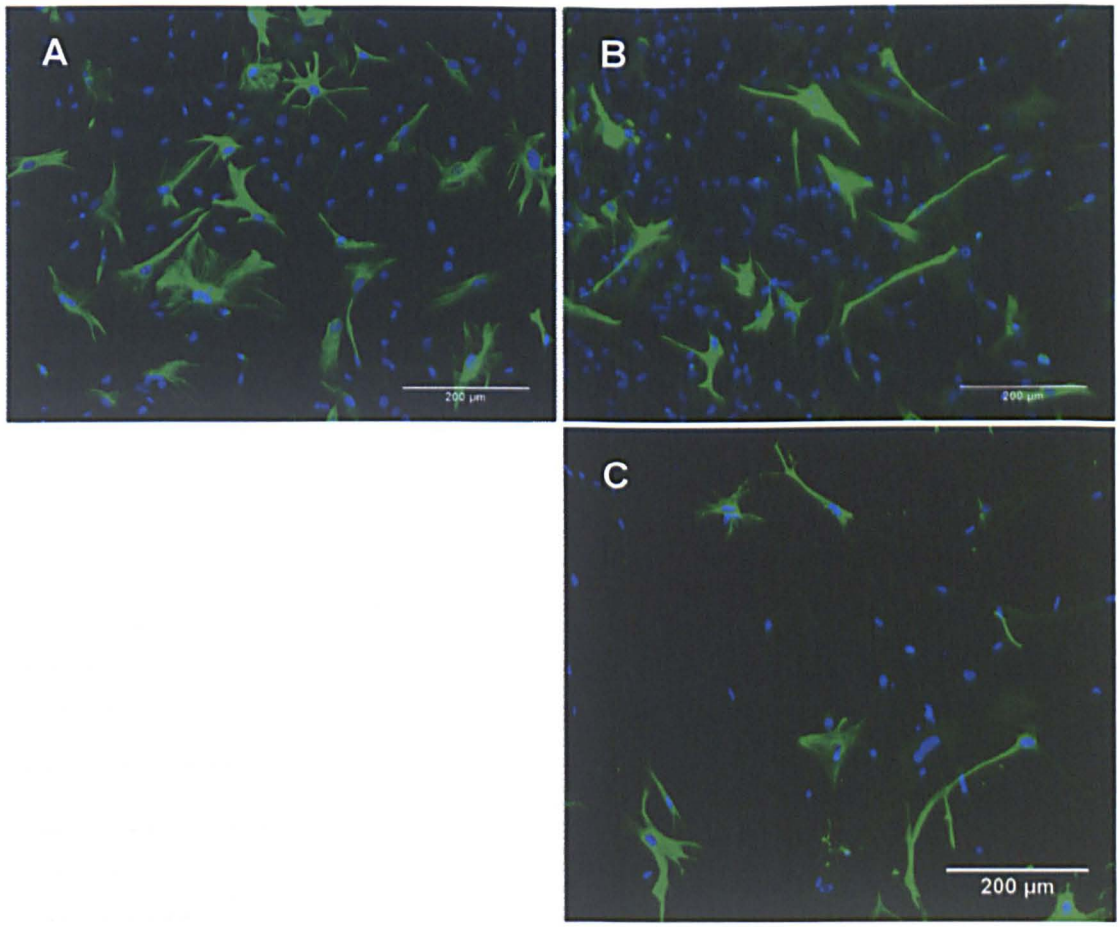

Figure 2-9 GFAP expressing cells in day-1 and day-8 of HA cultures

To determine the percentage of GFAP expressing cells and its change over the 7-day culture period, day-1, and day-8 cultures of HA (passages 3 to 5) were analysed by immunofluorescence microscopy. Expression changes of GFAP were also compared between 2D and 3D cultures. Images were captured and the percentage of positive cells was calculated. Green fibrillary, cytoplasmic staining indicates GFAP expression. Blue staining by DAPI indicates the nucleus of the cell. Representative images of each culture condition are shown here. **A**: Day-1 2D culture. **B**: Day-8 2D culture **C:** Day-8 3D culture. Day-1 2D culture is the control for both 2D and 3D, day-8 cultures. Scale bar represents 200 µm.

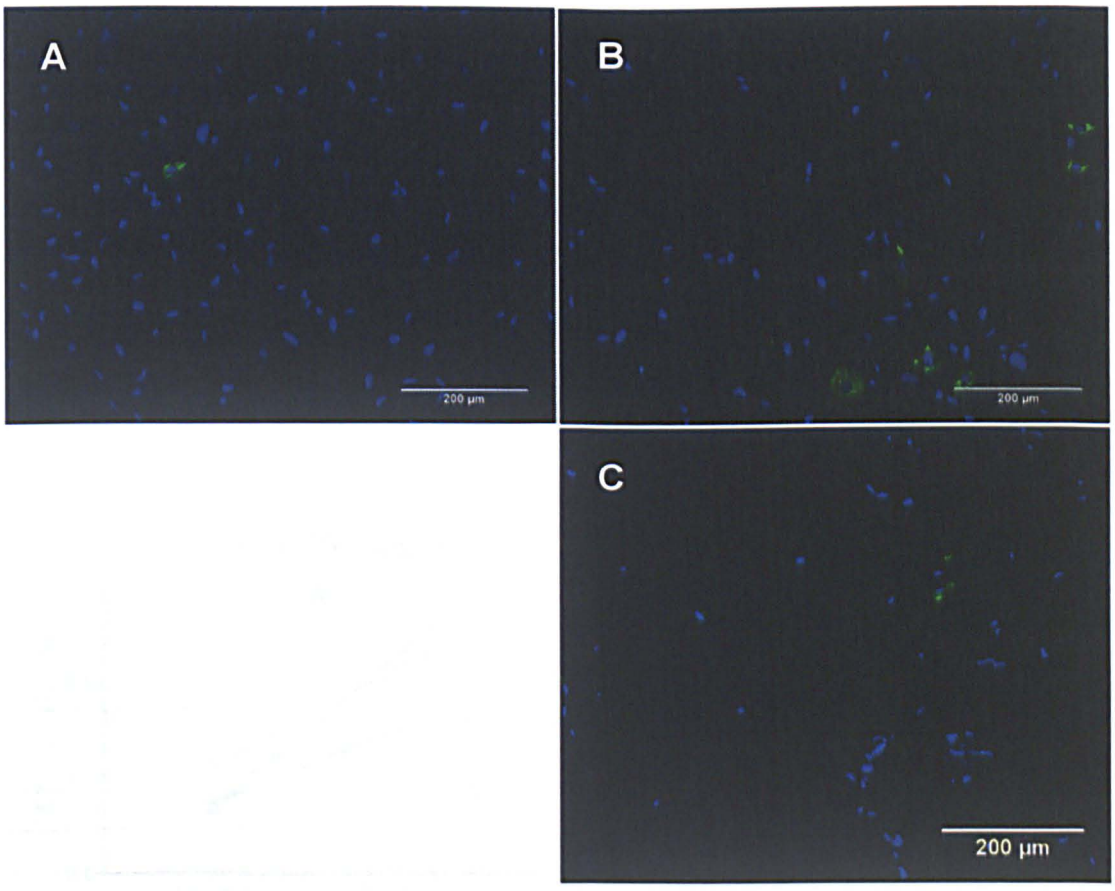

Figure 2-10 Fibroblasts in day-1 and day-8 of cultures of HA

To determine the percentage fibroblasts and its change during the 7-day culture period, day-1, and day-8 cultures of HA (passage 3 to 5) were analysed by immunofluorescence microscopy using TE7 antibodies. Expression changes of TE7 were also compared between 2D and 3D cultures. Images were captured and the percentage of positive cells was calculated. Green staining indicates TE7 expression. Blue staining by DAPI indicates the nucleus of the cell. Representative images of each culture condition are shown here. **A**: Day-1 2D culture. **B**: Day-8 2D culture **C:** Day-8 3D culture. Day-1 2D culture is the control for both 2D and 3D day-8 cultures. Scale bar represents 200 µm.

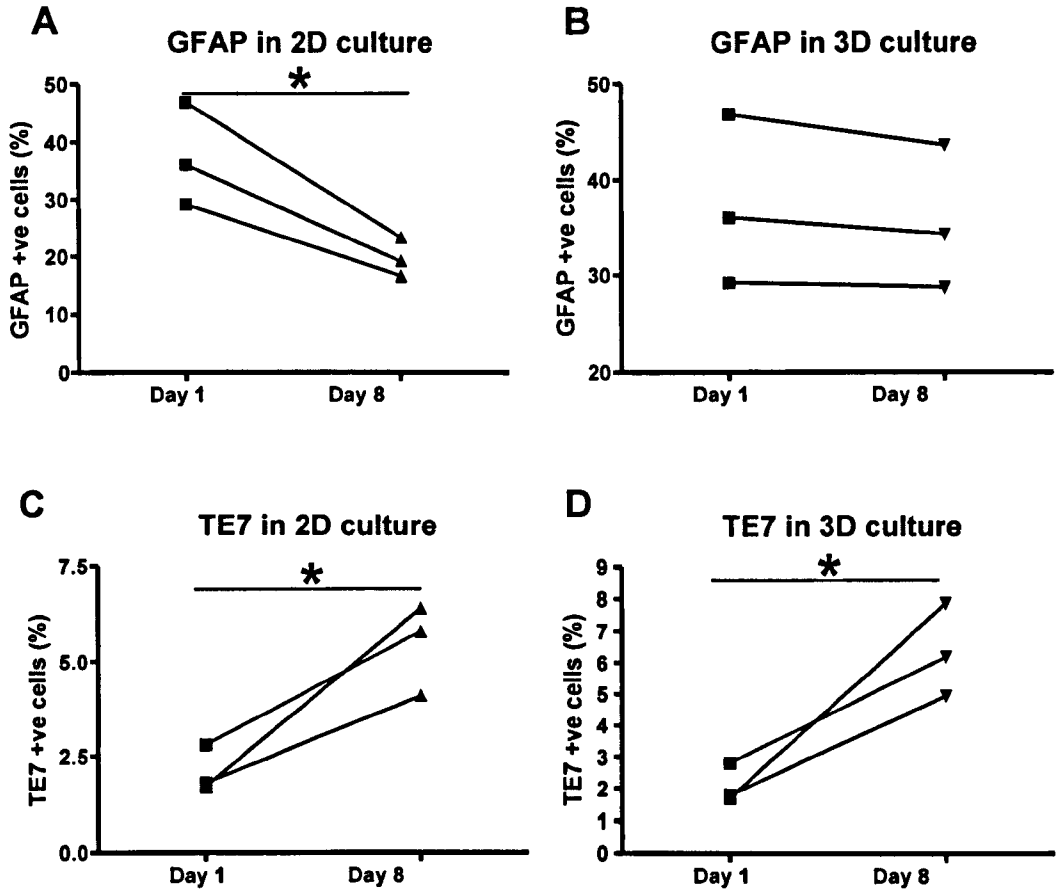

Figure 2-11 Percentage of GFAP expressing astrocytes and fibroblasts in HA cultures on day 1 and day 8 of culture

To determine the percentage of GFAP expressing cells and fibroblasts, HA cultures (passage 3 to 5) were analysed by immunofluorescence microscopy using anti-GFAP and anti-TE7 antibodies. Three independent experiments, within each experiment, triplicate samples for 2D cultures and duplicate samples for 3D cultures were analysed. Images were captured at eight different fields, at least 500 cells were analysed per sample, and percentages of positive cells were plotted. Over the 7-day culture period, in 2D cultures, the percentage of GFAP positive cells decreased while the percentage of TE7 expressing cells increased. In 3D cultures, the percentage of TE7 positive cells also increased over 7-days. In contrast, the percentage of GFAP expressing cells did not change statistically, in 3D cultures. * indicates $P \leq 0.05$ using Paired *t*-test, N = 3.

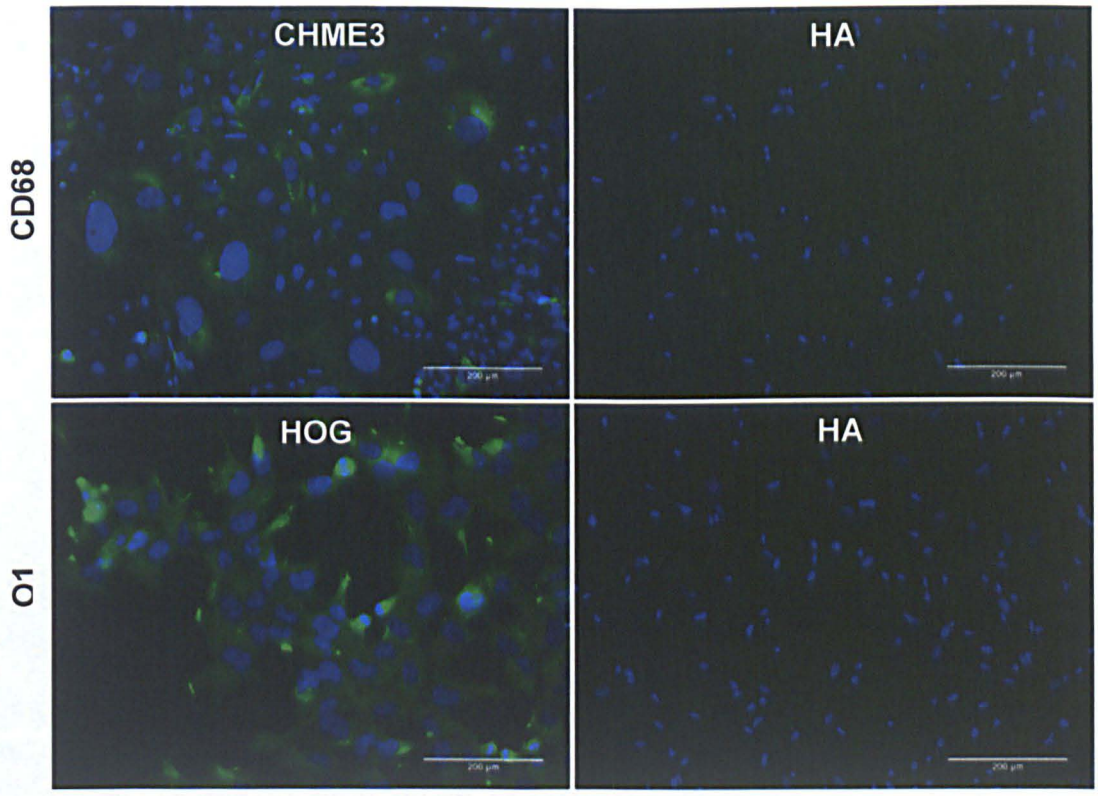

Figure 2-12 Absence of microglia and oligodendrocytes in HA cultures

To identify microglia and oligodendrocytes in HA culture, expression of CD68 and O1 were analysed by immunofluorescence microscopy. As a positive control, for CD68, CHME3, a human foetal microglial cell line, and for O1, HOG, an oligodendroglioma derived cell line, were used. Representative images are shown here. Green staining indicates the expression of tested marker while blue indicates the nuclear staining by DAPI. While CHME3 were stained for anti-CD68 (KP1) HA did not stain, indicating the absence of microglia in the HA culture. Similarly, while HOG were positive for O1, HA were negative for O1 indicating the absence of oligodendrocytes in the culture. Representative images are shown here. N = 3. Scale bar represents 200 μm.

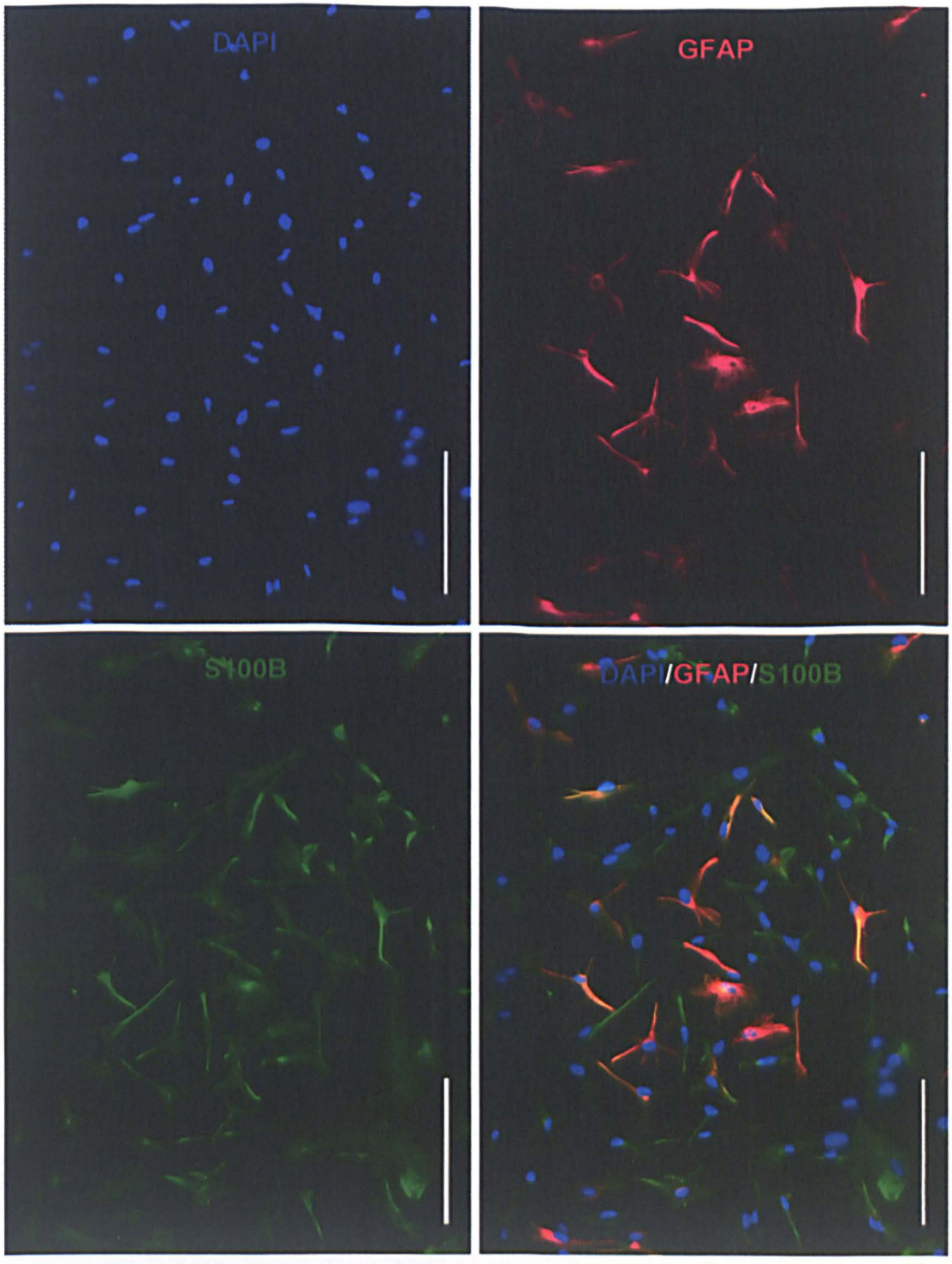

Figure 2-13 S100B expression in HA cultures as analysed by immunofluorescence microscopy

To determine the S100B expression, double immunofluorescence analysis using S100B and GFAP antibodies was carried out on HA, passage 3, cultures. A representative image is shown here. S100B staining was seen in the cytoplasm and nucleus whereas GFAP staining was exclusively cytoplasmic and fibrillary. In the overlaid image, the golden colour indicates co-expression of S100B and GFAP. S100B is expressed in ~90% of the cells. Almost all GFAP expressing cells express S100B. Approximately 5% cells express neither GFAP nor S100B. Scale bar represents 200 μm. N = 3.

2.3.7 GFAP expression analysis in 3D HA solo compared to 2D HA solo by flow cytometry

To examine the effect of the 3D environment on GFAP expression, 3D HA and confluent and non-confluent 2D HA cultures were set up and cultured for 7 days and the percentage of GFAP positive cells and GFAP expression per cell of these cultures were compared with original cultures (day-1 2D HA non-confluent) using flow cytometry (**Figure 2-14.A**).

Percentage of GFAP positive cells

At day-1, the percentage of GFAP expressing cells in 2D cultures was in the range 25-50%. Among the 2D cultures, there was a decrease of ~44% in the percentage of positive cells from day-1 to day-8 in both confluent and non-confluent cultures. However, in 3D cultures, there was no significant decline in the percentage of GFAP expressing cells during the 7 days (**Figure 2-14 B**).

GFAP expression per cell

Analysing just the GFAP-positive subset of cells (**Figure 2-15**), it was noted that GFAP expression per cell from day-1 to day-8 in 2D non-confluent culture was not changed. Comparing with in day-8 cultures, GFAP expression was higher in day-8 2D confluent cultures (~50%) and day-8 3D cultures (~65%) in comparison to day-8 2D non-confluent cultures. In 3D cultures, GFAP expression per cell was higher than that of non-confluent 2D cultures, but statistically not different from that of confluent 2D HA cultures.

Taken together, in 2D cultures, the percentage of GFAP positive cells was decreased without losing the GFAP expression over the 7 days of culture. In contrast, in 3D cultures, the percentage of positive cells remained the same and the GFAP expression per cell remained at higher levels, equivalent to that of confluent 2D cultures. In 2D cultures, GFAP expression per cell increased with confluence but the percentage of GFAP positive cells did not change.

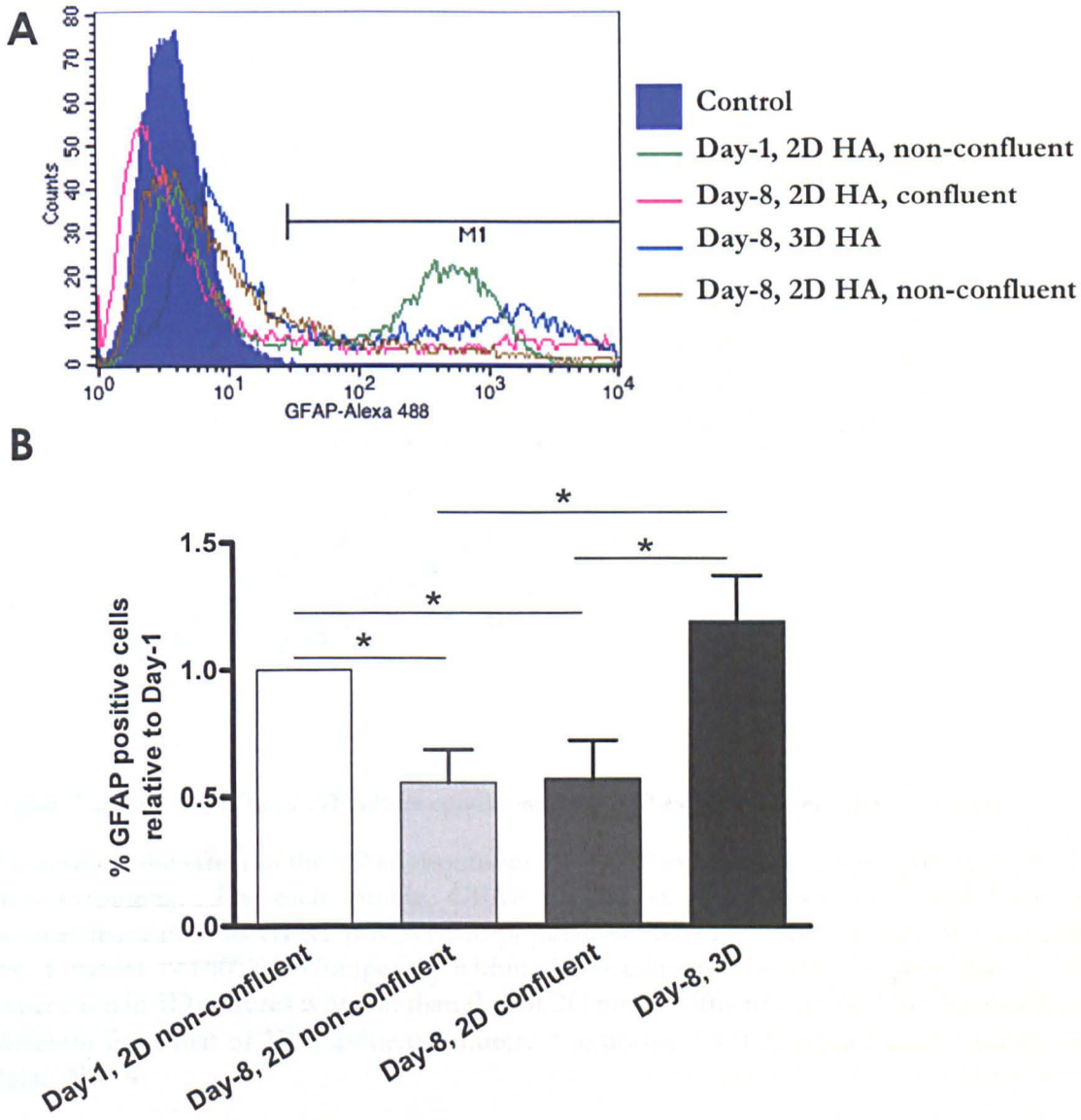

Figure 2-14 Effect of 2D and 3D culture conditions on percentage of GFAP positive cells in HA cultures

To examine the effect of the 3D environment on GFAP expression, 3D HA and 2D HA confluent and 2D HA non-confluent cultures were set up and maintained for 7 days before analysis by flow cytometry. **A:** Representative histogram of GFAP. Only those cells with the intensity values in the range of M1 were considered as GFAP positive. **B:** Each bar represents the data normalised to corresponding day-1 data value. Data indicate that over the 7-day culture the percentage of GFAP positive cells decreases in 2D culture but not in 3D culture. * indicates $P \leq 0.05$ using Paired *t*-test on raw data. N = 4.

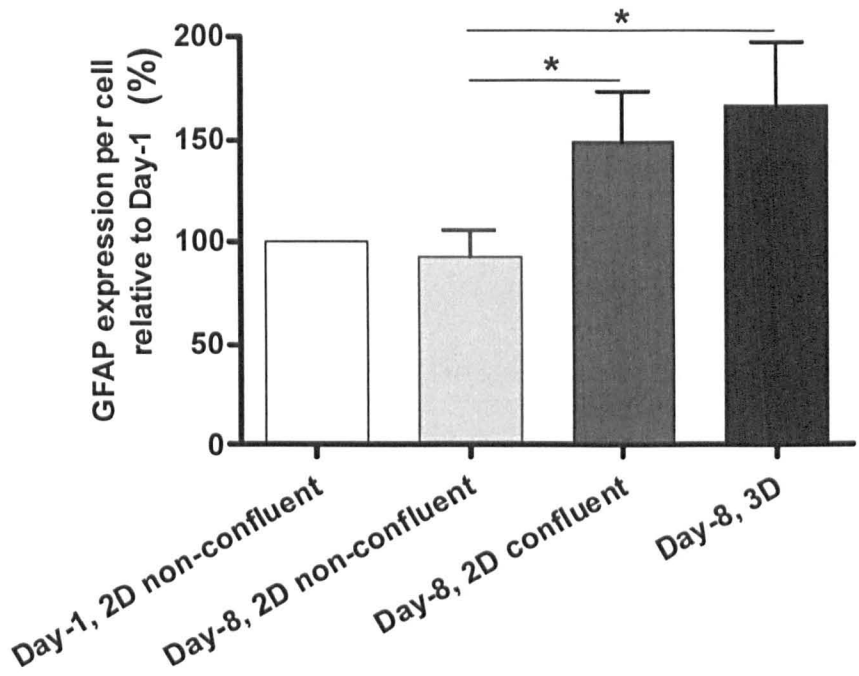

Figure 2-15 Effect of 2D and 3D culture conditions on GFAP expression per cell in HA cultures

To examine the effect of the 3D environment on GFAP expression, cultures were analyzed by flow cytometry. For each sample, GFAP expression per cell was calculated from the geometric mean of its GFAP positive sub-population. Bars represent the data normalised to day-1 values (=100%). Comparing within day-8 cultures, the data suggest that GFAP expression in 3D cultures is higher than that of 2D non-confluent cultures but statistically not different from that of 2D confluent cultures. * indicates $P \leq 0.05$ using Paired *t*-test on raw data. N = 4.

.

.

2.4 DISCUSSION

The general aim of this study was to develop an *in vitro* 3D model in which astrocytes are maintained in a 3D environment in co-culture with brain endothelial cells. To this purpose, we developed a model in which primary human foetal astrocytes were cultured in a collagen gel matrix, while human immortalised brain microvascular endothelial cells (hCMEC/D3) were cultured on the surface of the gel. First, 3D culture conditions were standardised, then the purity of primary HA cultures was analysed, and the effect of 3D culture conditions on proliferation and GFAP expression was studied.

2.4.1 Standardisation of 3D culture conditions

2.4.1.1 Scaffold/Matrix

For 3D cultures, different matrices have been in use such as collagen type-I, collagen type-IV, fibrin, human platelet-poor plasma, and alginate (Girandon, 2011, Frampton, 2011). In this study, collagen type-I was used. It is easily available and cost effective compared to collagen type-IV, and other ECM based gels. In addition, unlike ECM based gels, not having a complex composition of extra cellular matrix and growth factors allows more control over the experiment and better interpretation of results. Collagen gels are transparent so, they are easy to monitor and analyse by various microscopic methods. More importantly, many 2D endothelial cultures and 3D cultures of astrocytes developed by others have used collagen type-I as a substratum and therefore to make the findings of this study comparable with other studies collagen type-I was chosen as substrate.

2.4.1.2 Cell density optimisation in 3D HA culture

In the brain parenchyma, astrocyte cell density is ~ 20 million per ml (Appaix, 2012, McCaslin, 2011). In 3D cultures, cells seeded at such high density are not viable because of limited diffusion. A cell culture media perfusion system would be necessary in order to achieve in 3D

cultures the high density that is comparable to *in vivo* (Cullen, 2007). Similar previous 3D culture studies using primary rat astrocytes such as those of East *et al.* (2009) and Ahmad *et al.* (2010) have used 2.0-2.5 million cells per ml. HA used in this study could not be cultured at that density because the gels were contracting before 7 days. This time was selected since it allows time for the cultures to establish and then perform experimental treatments (*e.g.*, cytokine stimulation and cell functional assays). Since gel contraction would make further experimental analyses difficult, and may influence the astrocyte phenotype, the highest cell density that did not cause gel contraction was determined. The gel contraction is directly proportional to the cell density as was observed in 3D cultures of human fibroblasts and porcine retinal astrocytes or porcine retinal pigment epithelial cells (Redden, 2003, Guidry, 1992b). Therefore, by seeding the gel with three different cell densities, it was determined that 0.5×10^6 cells/ml was the highest cell density that did not cause gel contraction for at least 7 days. All the experiments in this study were carried out at this cell density.

Gel contraction is dependent on cell type and its species of origin. Among astrocytes, while rat astrocytes do not appear to cause gel contraction (East, 2009, Al Ahmad, 2010), porcine astrocytes do (Guidry, 1992b). In addition, the purity of the astrocyte cultures may be a critical factor in gel contraction. Indeed, fibroblasts are widely reported to cause gel contraction (Nishiyama, 1988, Guidry, 1992a, Taliana, 2000, Guidry, 1992b). The purity of primary rat astrocyte cultures in 3D model of East *et al.* (2009) has been reported to be 95% although the nature of contaminating cell types was not described. The HA culture used in this study shows, apart from GFAP +ve S100B+ astrocytes and GFAP –ve S100B +ve astrocytes, a small percentage of fibroblasts which may account for the gel contraction observed at higher cell densities. However, it is not known whether human astrocytes, whether they are GFAP +ve or GFAP –ve, can also cause gel contraction or whether the developmental stage of the isolated cells (foetal vs. post-natal or adult astrocytes) play a role in the observed effect.

2.4.1.3 Two-step collagenase digestion method

A two-step collagenase digestion method was developed to isolate both cell types *viz.*, HA and hCMEC/D3 from collagen gel co-cultures into two separate fractions. This isolation method in conjunction with PECAM-1 as a selection marker was adequate for further flow cytometry analysis. Once the cells are isolated from the gel by the two-step collagenase digestion method, they can be analysed by various standard molecular biology analytical techniques such as immunoblotting and RT-PCR which is an advantage over previous 3D culture models such as that developed by Al Ahmad *et al.* (2010). Altogether, the present 3D gel culture model using collagen type-I in conjunction with the two-step collagenase method is easy to set up, monitor, and analyse by various analytical techniques.

2.4.2 Purity and contamination of other cell types in HA culture

In this study, primary human foetal astrocyte cultures were used between passages 3 and 5. These cultures showed 29.2 - 46.9 % GFAP positive astrocytes, 1.7 - 2.8 % of fibroblasts, and no oligodendrocytes and microglial cells were detected. The percentage of fibroblasts was always < 8% whether in 2D or 3D cultures which is close to the 95% purity previously published for rat astrocytes (East, 2009).

A single expression marker that selectively identifies all different subpopulations of astrocytes in primary cultures of foetal origin could not be identified. While the majority of cells were positive for S100B, it has been previously shown thatS100B is expressed not only by astrocytes but also by oligodendrocytes in the rat CNS. In astrocytes, it is co-localised to intermediate filaments such as GFAP, and in oligodendrocytes, it is co-localised to microtubules (Richter-Landsberg, 1995). In the present study, all GFAP positive cells and ~90% of GFAP negative cells were S100B positive. The absence of O2 marker expressing cells indicated the absence of oligodendrocytes in the culture. Therefore, it is reasonable to suggest that O2 negative, S100B positive cells are likely to be astrocytic in origin.

Few markers have been previously used to identify fibroblasts. These are anti-fibroblast surface protein antibody (1B10), anti-fibroblast antibody (5B5), and anti-fibroblast specific protein-1 (FST1). All these antibodies have limitations. Anti-FST1 antibodies have been shown to bind astrocytes (Takenaga, 2006) whereas5B5 antibodies recognise only proliferating fibroblasts (Janin, 1990). The 5B5 and 1B10 antibodies also show little specificity as they recognise other cell types such as tissue macrophages, myoepithelialcells, and follicular dendritic cells. In contrast, the TE-7 antibody used in the present study, raised against thymic stroma of human origin, appears specific for fibroblasts and recognises both proliferating and quiescent fibroblasts in culture (Goodpaster, 2008). The TE7 antibody recognises a marker of mesodermally derived (mesenchymal) human connective tissue (Haynes, 1984). The leptomeningeal (mesenchymal) cell type is also a potential contaminating cell type in human brain derived cultures (Rutka, 1987). Since TE7 antibody recognises mesenchymal cells, GFAP negative and TE7 negative cells in the HA cultures in the present study are unlikely to be leptomeningeal cells.

In addition, no oligodendrocytes or microglia were detected in the HA cultures. CD68 is a widely used marker for microglia (Pulford, 1989) and was able to identify most cells from an immortalised human foetal microglial cell line indicating its suitability for detecting the absence of microglia in this study. It is worth noting, however, that the O1 marker selected to identify oligodendrocytes is expressed mainly by differentiated cells unlike the O4 marker, which is expressed in early stages of development in undifferentiated oligodendrocytes (Itoh, 2002, Sommer, 1982). It is thus possible that the contaminating cells in the primary foetal HA cultures will constitute an O4 positive oligodendrocyte/type-2 astrocyte (O-2A) progenitor cell population (Rivkin, 1995, Armstrong, 1990).

2.4.3 GFAP expression in 2D HA culture

The primary HA used in this study were purchased from a commercial provider. GFAP expression analysis by microscopy and flow cytometry analyses revealed the occurrence of GFAP expression only in a subset of the whole population of HA, which is not unexpected. Though GFAP is a widely used marker for rodent astrocytes *in vivo* and *in vitro*, its status as a marker for human astrocytes is not resolved. It has been reported that GFAP positive astrocytes are uncommon in primary human astrocyte cultures established from adult human brain tissue (Rezaie, 2003, Macikova, 2009). In addition, GFAP expression appears to vary depending on the region and developmental stage of the brain.

The percentage of GFAP positive cells was decreased over the 7-day culture period in 2D cultures but not in 3D cultures as shown by flow cytometry and further corroborated by microscopy analysis. During the 7-day culture period, in 2D cultures, the overall cell population increased by ~7.5 times while the percentage of GFAP positive cells decreased. The decrease in the percentage of GFAP positive cells may be due to either a higher proliferation rate of GFAP negative cells or a loss of GFAP expression for every cell division. Flow cytometry analysis also suggested that over the 7-day culture period, GFAP expression per cell does not decrease. Therefore, the higher proliferation rate of GFAP negative cells compared to GFAP positive astrocytes is the most plausible explanation for this decline. The percentage of fibroblasts in culture were always less than 10%, and so, the proliferation of fibroblasts during 7-day culture period could not fully account for the decreased percentage of GFAP positive cells during that period. It could be inferred that these more proliferative, GFAP negative, TE7 negative cells are astrocytes that do not express GFAP. A subgroup of cell that do not express GFAP, but which show a higher proliferation rate than GFAP expressing astrocytes has been previously reported in primary astrocyte cultures of human (Macikova, 2009) and rat (Sergent-Tanguy, 2006).

2.4.4 3D collagen matrix reduces proliferation of HA

While 2D HA divided every ~2.4 days, 3D HA did not proliferate during the 7-day culture period. 3D HA either stopped dividing completely or divided slowly *i.e.*, their cell doubling time is longer than 7 days. This result is congruent with Al Ahmad *et al.* (2010) who reported that rat primary astrocytes did not proliferate in 3D collagen cultures over 6-days of culture in collagen type I gels. The 3D environment did not reduce the proliferation rate of fibroblasts, as their proliferation rate in 3D collagen matrix is similar to that for cells grown on 2D surface. It is then likely that the 3D matrix effect on proliferation is specific to astrocytes.

Interestingly, collagen type -I and -IV both were shown to decrease the proliferation of neonatal rat astrocyte 2D cultures compared to those cultured on a fibronectin coated substrate (Goetschy, 1987). However, in the present study, since 2D culture surfaces were also coated with collagen, the effect cannot be attributed to differences in the composition of the extracellular matrix. The difference in the collagen matrix of 2D and 3D cultures is in dimensions and rigidity; while the 3D culture matrix is soft and flexible, HA on a 2D culture grow on a stiff substrate. It has been previously shown that on hard substrates proliferation of astrocytes increases whereas on the softer substrates proliferation decreases (Georges, 2006). Therefore, it could be inferred that reduced proliferation of HA in the 3D collagen matrix is because of the softness of the matrix compared to 2D substrates.

In vivo normal astrocytes are quiescent, slowly dividing cells with very low turnover, which undergo rapid cell division following CNS injury leading to severe gliosis (reviewed in Sofroniew, 2010, Colodner, 2005). An increased proliferation rate, also known as hyperplasia, is a characteristic feature of reactive astrocytes. *In vitro* 2D cultured astrocytes acquire a reactive phenotype spontaneously as manifested by an increased proliferation rate (reviewed in Wu, 1998, Holley, 2005). In the present study, when 2D HA were transferred to 3D matrix

their proliferation was reduced. Therefore, it appears that HA in 3D collagen matrix revert to a less reactive state, resembling their *in vivo* counterparts.

2.4.5 Effect of 3D environment on GFAP expression

Over expression of GFAP is considered a marker for *in vivo* reactive astrocytes. *In vitro*, decreased expression of GFAP was used as a maker for a less reactive state of astrocytes (reviewed in Wu, 1998, East, 2009, reviewed in Kang, 2011). To assess the reactive state of HA in 3D culture, the percentage of GFAP expressing cells and GFAP expression per cell were analysed and compared with those of 2D HA cultures,. 3D culture conditions decreased neither GFAP expression per cell nor the percentage of GFAP expressing cells. Therefore, it can be inferred that reactive state of 3D cultured HA appears to be not different from that of 2D cultured HA. These results are not congruent with East *et al.* (2009) in which rat astrocytes in 3D culture expressed less GFAP compared to their counterparts in 2D culture. The discrepancy could be attributed to a difference in the species of cell origin as this study used human astrocytes (HA). No published study has addressed this question on human astrocytes.

In 3D cultures, over the 7-day culture period, in contrast to 2D cultures, the percentage of GFAP expressing cells did not decrease. This could be due to the low proliferation rate of HA in 3D culture unlike HA in 2D cultures. GFAP expression per cell in 3D cultures is higher than that of non-confluent 2D cultures but no different from that of confluent 2D cultures. This could be because of the greater amount of cell-matrix interactions furnished in 3D cultures. Indeed, cell-matrix interactions in 3D cultures modulate several properties of cells including differentiation of various cell types (Adelow, 2007, Ozeki, 2011). It is known that differentiated astrocytes express higher levels of GFAP than undifferentiated cells (Mi, 1999). Therefore, it can be speculated that higher cell-matrix interactions provided in the 3D gel cultures induced further differentiation of astrocytes, thereby maintaining their GFAP

expression. Further work is necessary to determine whether the effect is generic to a 3D matrix or specific to a collagen type I matrix.

2.4.6 3D HA differ from 2D HA

Whereas no decrease in GFAP expression in 3D culture would suggest no change in the reactive state of HA, the absence or much reduced proliferation of HA in 3D culture would indicate a less reactive state. These results are not contradictory since not all phenotypical changes need to occur simultaneously when a reactive cell reverts to quiescence. Especially *in vivo*, GFAP overexpression occurs early in gliosis, prior to hypertrophy and to increased proliferation in later severe stages of gliosis (reviewed in Sofroniew, 2010). It is possible that restoration of quiescence occurs in the reverse order *i.e.*, first proliferation rate decreases, then cell size decreases and finally GFAP expression decreases. It will be interesting to determine whether more prolonged culture (>7 days) would cause any of those effects. In addition, investigation of more expression markers would be necessary to affirm the effect of 3D culture on the reactive state of HA.

An important feature of 3D *in vitro* models is their ability to simulate *in vivo* conditions. Our results show that 3D cultured astrocytes have different properties compared to 2D astrocytes. Indeed, 3D culture conditions certainly influenced two properties of HA; a major effect on proliferation, and a minor effect on GFAP expression. Moreover, the observed reduced proliferation in 3D conditions also suggests a higher resemblance to *in vivo* HA than 2D HA. Expression analysis of more molecules (section 2.1.1) and comparison of various functional properties such as synthesis of glutamine, uptake of K^+ and glutamate is required to determine whether 3D HA are more similar to quiescent astrocytes *in vivo* than 2D HA.

2.5 CONCLUSIONS

1. To study the interactions between hCMEC/D3 cells and HA an *in vitro* 3D co-culture model using collagen type-1 was developed.
2. 3D HA are less proliferative in comparison to 2D HA and therefore less reactive and more similar to *in vivo* HA.
3. GFAP expression levels of 3D HA are higher than those of non-confluent 2D HA but similar to confluent 2D HA.
4. The two-step collagenase digestion method was developed to isolate endothelial cells and astrocytes from the gel and from each other so that they could be analysed by flow cytometry and other analytical methods.

Chapter 3:

Astrocyte induction of BBB phenotype: comparison of 2D cultured HA vs. 3D cultured HA

3.1 INTRODUCTION

Several *in vivo* and *in vitro* studies have demonstrated the ability of astrocytes to induce or enhance the barrier phenotype of the BMVEC (DeBault, 1980, Janzer, 1987, reviewed in Abbott, 2006). In these *in vitro* studies, the astrocytes were generally cultured on 2D surfaces. It has been shown that cells cultured in 3D matrices display different properties than those in 2D cultures (Lee, 2008, Li, 2007, Kofron, 2009, Larsen, 2006, Abbott, 2003). Astrocytes in 3D cultures have been shown to be in a less reactive state, and express fewer stress fibres and have a different cell morphology compared to 2D astrocytes (Georges, 2006, East, 2009).

Reactive astrocytes secrete angiogenic factors and pro-inflammatory factors that are known to damage the BBB integrity, and therefore reactive astrocytes may have a negative influence on BBB maintenance. Accordingly, it has been reported that the new vessels that grow into glial scars may not develop a proper BBB phenotype (reviewed in Pardridge, 1998). In contrast, there is also some evidence for an enhanced BBB induction potential of reactive astrocytes. Hypertrophic reactive astrocytes seem to activate Sonic Hedge Hog signalling on BMVEC more vigorously than normal astrocytes and are thus better inducers/maintainers of BBB (Alvarez, 2011). Reactive astrocytes were shown to have a protective role in brain ischemia (Li, 2008). Taken together, it is possible that reactive astrocytes have a pronounced BBB induction potential as a protective response during CNS pathological conditions. To resolve this issue, further work is needed. Therefore, it is relevant to characterise the reactive state of HA in 3D culture, and correlate it to their BBB induction potential.

Results presented in the previous chapter suggest that 3D HA differ from 2D HA in their proliferation capacity, are therefore less reactive, and closer to their counterparts *in vivo*. We therefore hypothesised that 3D HA induced a BBB phenotype in BMVEC to a larger extent than 2D HA. Hence, we compared the BBB phenotype inducing/enhancing properties of the 3D HA with 2D HA on hCMEC/D3 2D monolayer cultures.

3.1.1 Markers to assess barrier phenotype

BBB can be functionally categorised into three elements. (1) The physical tight junction barrier made up of transmembrane components and cytoplasmic associated proteins such as ZO-1, claudin-5, and occludin. (2) The transport barrier controlled by transporter proteins e.g., the ABC family of efflux transporters and GLUT1. (3) The metabolic barrier comprising, amongst others, peptidases, nucleotidases, monoamine oxidase and cytochrome P450 (Abbott, 2006). In this study, two tight junctional barrier markers namely, claudin-5 (CLDN5), and zonula Occludens (ZO-1) and a marker for the transport barrier, P-glycoprotein (P-gp) were studied. To assess functional tight junctional barrier phenotype, measurement of paracellular permeability to hydrophilic tracers is a widely used assay.

3.1.2 Specific aim

- To determine whether soluble factors released from 3D HA are able to induce or enhance the BBB phenotype on hCMEC/D3 monolayer cultures to a larger extent than 2D HA.

To compare the effect of 2D vs. 3D cultured astrocytes on the induction of the barrier phenotype in hCMEC/D3 cells; human astrocytes were cultured on either the top (2D HA culture) or inside (3D HA culture) collagen gels. Conditioned media obtained from these astrocyte cultures was added to hCMEC/D3 cultures grown on coverslips or transwell inserts and their BBB phenotype was analysed.

3.2 METHODS

The reagents and antibodies used in this study are listed in **appendices A** and **B** respectively.

3.2.1 Astrocyte conditioned media (ACM) preparation and setup of coverslip cultures

On day zero, four collagen gel cultures were set up.

1. 3D HA solo-culture: HA (4 X 10^5) were plated in collagen gels in 12-well plates as described in section 2.2.3.1.
2. hCMEC/D3 solo-culture: hCMEC/D3 cells (1.6 X 10^5) were plated on the surface collagen gels in 12-well plates as described in section 2.2.3.2.
3. Co-culture: As described in section 2.2.3.3, HA (4 X 10^5) were plated in collagen gels while hCMEC/D3 cells (1.6 X 10^5) were plated on the surface of the same gel in 12-well plates.
4. 2D HA solo-culture: HA (4 X 10^5) were plated on the surface of collagen gels in 6-well plates as described in section 2.2.3.2. 2D cultures were set up in larger surface areas i.e., 6-well plates to accommodate the same number of cells that were plated in 3D cultures (12-well plate).

On the same day, 2D cultures of hCMEC/D3 cells were set up on collagen-coated coverslips or collagen and fibronectin coated transwell inserts (section 2.2.2.2). Both collagen gel cultures and coverslip cultures were grown in the D3M. On the coverslips or transwell inserts, cells were plated at a density of 4 X $10^4/cm^2$. Every two days, for the next four days, astrocyte-conditioned media of gel cultures was mixed with fresh nutrient culture media at a 1:1 ratio, and transferred onto hCMEC/D3 cultures. After six days, hCMEC/D3 coverslip cultures were analysed by immunofluorescence microscopy or flow cytometry, whereas the transwell insert cultures were analysed by a paracellular permeability assay. Cell lysates were prepared

from the same transwell inserts, and analysed by immunoblotting after overnight incubation in the respective conditioned media.

3.2.2 Immunoblotting analysis of tight junctional proteins

Transwell insert hCMEC/D3 cultures exposed to conditioned media (section 3.2.1) were lysed with RIPA buffer mixed with protease inhibitor cocktail, and stored at -70°C until used for immunoblot analysis.

Cell lysates were mixed with an equal volume of 2X Laemmli's buffer then boiled at 85°C for 5 min. Polyacrylamide gels were cast with a 12 % resolving gel and 5 % stacking gel. Running buffer was standard Tris-glycine buffer (25 mM Tris, 192 mM glycine, 0.1% SDS, pH 8.3). Electrophoresis was carried out at 100-150 V until the dye front reached the end of the gel. Then proteins were transferred onto nitrocellulose membranes using a wet blotting system (BioRad), run at 0.15 Amp, overnight at 4°C. Transfer buffer was deionised water having 25 mM Tris, 192 mM glycine, and 20 % v/v ethanol. After the completion of transfer, blocking (5% skimmed milk, 0.1 % v/v tween 20 in PBS) of the membrane to decrease the non-specific signal, was performed for 1 h at RT and blots were then incubated with anti-ZO-1, anti-CLDN5 or anti-actin β (ACTB) antibodies over-night at 4°C. ACTB was used as loading control. Membranes were then subjected to four 15 min washes in washing solution (0.1 % v/v tween 20 in PBS) and then incubated with horseradish peroxidase (HRP)-conjugated species-specific secondary antibodies for 1 h at room temperature. The membranes were then washed four times each for 15 min, followed by a 15 min wash in PBS alone. Nitrocellulose membranes were then incubated with chemiluminescence western blotting detection reagent and then exposed to film.

Films were developed and scanned and the images were analysed by ImageJ software to obtain background-subtracted total pixel intensities of the bands. For each sample, ZO-1 and CLDN5 data are normalised with ACTB (loading control) then ratios were calculated with

reference to a control sample (hCMEC/D3 conditioned media treatment). Log2 converted ratios were used for plotting and statistical analysis. The data is from triplicate experiments with three replicates within each experiment.

3.2.3 Immunofluorescence microscopy analysis of tight junctional proteins

Immunofluorescence microscopy was carried out as described in section 2.2.7 with the following changes. Cells were fixed with methanol at -20 °C for 10 min then rehydrated in PBS for 20 min. Cells were then blocked with 5% normal goat serum for 30 min before incubating with primary antibody solution for ZO-1 and CLDN5 for 3 h at RT.

Image capturing and quantitative analysis

Images were captured using an Olympus BX61 microscope with Cell^{P} imaging software. For each coverslip, ten images were captured at randomly selected fields with the same exposure time. Fluorescent staining intensity was analysed by using ImagePro™ software. For each image, the percentage area of staining was measured. The percentage area of staining is the percentage of pixels whose values are above a threshold value. The threshold value was chosen based on background intensity levels and this value is kept constant across the images in a given experiment. For ZO-1, the staining at tight junctions was selectively quantitated by excluding nuclear and perinuclear staining. In the case of claudin-5, the staining intensity at cell-cell junctions was not always above the intracellular staining intensity hence the intensity of the whole cell was measured. The percentage area of staining for each tight junction marker was compared across different conditioned media treatments. Cells exposed to conditioned media obtained from hCMEC/D3 solo cultures were used as control and compared with the remaining conditioned media treatments.

To eliminate inter-experimental variability between control cultures, raw data was normalised to reference treatments (conditioned media by hCMEC/D3 solo-cultures). For each experiment, the percentage area value of each image was divided by the mean percentage area

value of the reference samples. Thus normalised data retains the distribution and the relative variance of the raw data (Valcu, 2011). All values were given as the mean ± standard error of the mean (SEM).

3.2.4 Effect of conditioned media on P-gp expression by flow cytometry

Cultures were established and conditioned media was collected as explained in section 3.2.1 except that hCMEC/D3 cells were plated directly onto collagen-coated 12 well plates instead of cover slips. After six days, hCMEC/D3 cultures were trypsinised and analysed by flow cytometry as described in section 2.2.9. Cell surface expression was analysed using fixed cells in the absence of permeabilisation while total cellular expression was analysed using permeabilised cells. P-gp monoclonal (MRK16) antibodies were used for this purpose.

Graphs were plotted with normalised data. Within each experiment, the median fluorescence value of each sample was normalised to median fluorescence value of reference treatments (conditioned media by hCMEC/D3 solo cultures). However, the paired *t*-test was performed on the raw data. All values were given as the mean ± SEM.

3.2.5 ACM effect on paracellular permeability of hCMEC/D3 monolayers

Transwell insert cultures of hCMEC/D3 cells were exposed to conditioned media as described in section 3.2.1. The paracellular permeability assay was performed and permeability coefficients of the hCMEC/D3 monolayers were calculated as per Dehouck *et al.* (1992).

Briefly, at the time of assay, 0.5 ml of 2 mg/ml fluorescein isothiocyanate (FITC)-dextran solution (FD-70), was added into the upper chamber/insert. The inserts were then transferred sequentially at 5 min intervals from a well into another well in a 12-well tissue culture plate containing 1.5 ml of transport buffer for 30 min. Transport buffer was DMEM containing 2% foetal calf serum. The concentration of FITC-dextran concentration in the bottom chamber was measured at an excitation wavelength of 485 nm and emission wavelength of 520 nm with

a fluorescence plate reader (BMG Optima™). Concentration of FITC-dextran in the bottom chamber was estimated by interpolation onto a standard curve of FITC-dextran solutions.

The volume of FITC-dextran, which had crossed the monolayer and reached the bottom chamber (Cleared volume), was measured by this formula.

$$\text{Cleared volume } (\mu L) = [C]_B \times V_B / [C]_U$$

Where $[C]_U$ is the concentration in the upper chamber, $[C]_B$ is the concentration in the bottom chamber, and V_B is the volume in the bottom chamber (=1.5 ml).

Cumulative cleared volume for every 5 min interval, during 30 min experiment, was plotted against time and the slope was calculated by linear regression analysis. Permeability coefficient (P_e) is calculated as follows:

$$1/PS_e = 1/PS_{ef} - 1/PS_f$$

$$P_e = PS_e / S$$

Where, PS_{ef} is the slope of endothelial cells grown on insert filters (µl per min), PS_f is slope of the insert filter without cells (µl per min), PS_e is the product of permeability and the surface area of endothelial cells (µl per min), S is the surface area of the filter (cm2), and P_e is the permeability coefficient of the endothelial cells (cm per minute).

The higher the P_e value the more permeable the hCMEC/D3 cells are to the FITC-dextran. The data was collected from triplicate experiments with three replicates within each experiment. Exposure to hCMEC/D3 conditioned media was the control. P_e values were compared and statistical significance was determined.

3.2.6 Statistical analysis

Graph plotting and statistical analysis was carried out using GraphPad PRISM v 4.0. Statistical significance of the data was assessed by Paired *t*-test. $P \leq 0.05$ was considered as significant.

3.3 RESULTS

3.3.1 Neither 2D HA ACM nor 3D HA ACM had an effect on total cellular expression of ZO-1 or CLDN5 as analysed by immunoblotting

To determine the effect of conditioned media on total cellular expression of tight junction proteins, ZO-1 and CLDN5 were analysed by immunoblotting (**Figure 3-1.A**).

In comparison to hCMEC/D3 conditioned media treatment, neither 2D nor 3D HA ACM altered total cellular ZO-1 expression in hCMEC/D3 cells. In addition, the effect of 3D HA ACM was not different from that of 2D HA ACM (**Figure 3-1.B**).

Similar results were observed for CLDN5. Neither 2D nor 3D HA ACM induced total cellular CLDN5 expression in hCMEC/D3 cells. In addition, the effect of 3D HA ACM was not statistically different from that of 2D HA ACM (**Figure 3-1.C**).

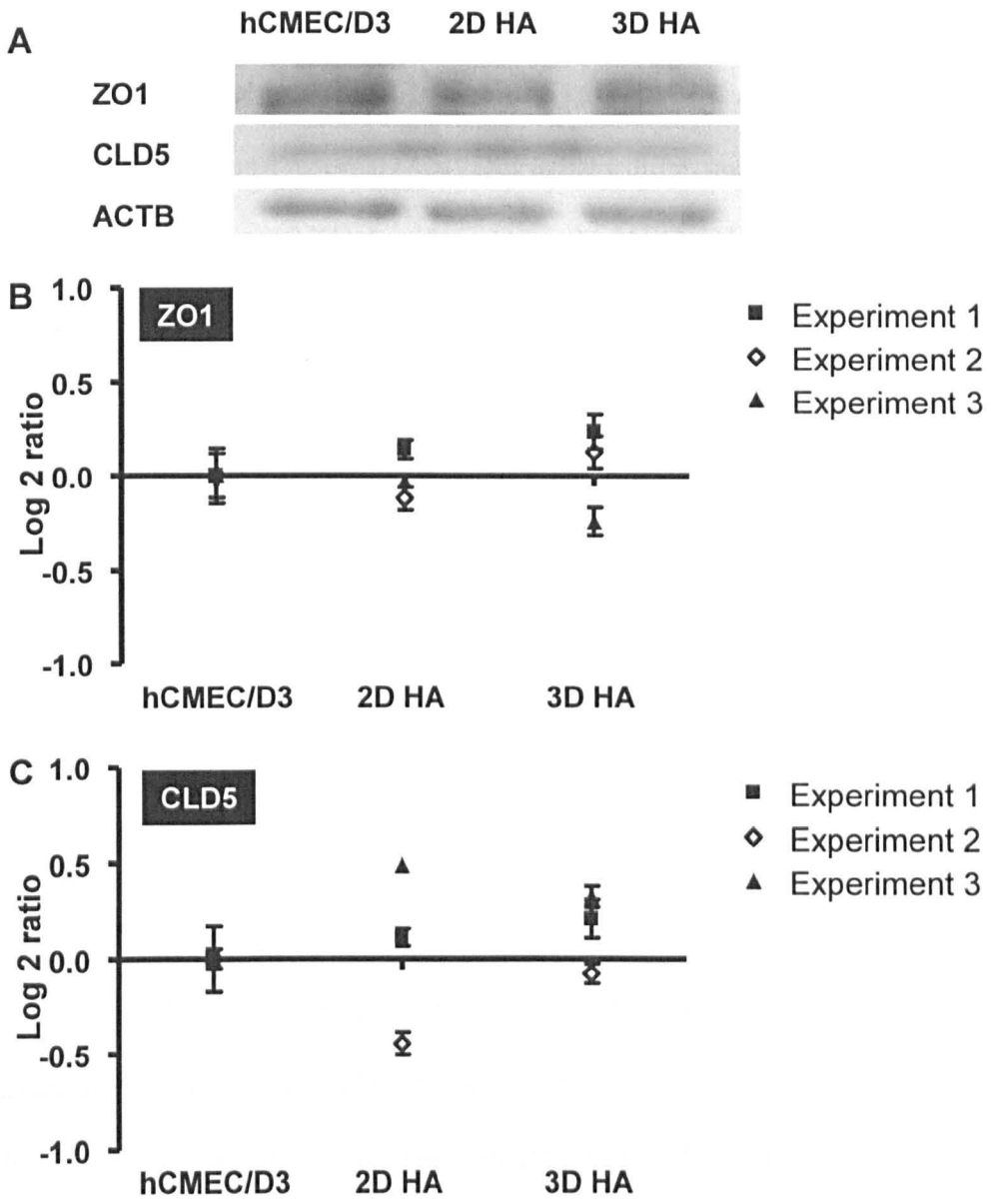

Figure 3-1 Effect of astrocyte conditioned media on total cellular expression of ZO-1 and CLDN5 by hCMEC/D3 cells as analysed by immunoblotting

Transwell insert cultures of hCMEC/D3 cells were exposed to conditioned media before cell lysates were prepared and analysed by immunoblotting for total cellular expression of ZO-1 and CLDN5 proteins. Exposure to conditioned media from hCMEC/D3 solo culture is the control. **A:** A sample immunoblot is shown. **B:** Neither 2D HA ACM nor 3D HA ACM consistently induced total cellular ZO-1 expression in hCMEC/D3 cells. In addition, the effect of 3D HA ACM was not different from that of 2D HA ACM. **C:** Similarly, neither 2D HA ACM nor 3D HA ACM induced total cellular CLDN5 expression consistently in hCMEC/D3 cells. In addition, the effect of 3D HA ACM was not different from that of 2D HA ACM. Data represent mean ± SEM of triplicate samples. $P \geq 0.05$ was considered significant using Paired *t*-test. N = 3.

3.3.2 Both 3D and 2D HA ACM increased ZO-1 levels at cell junctions as analysed by immunofluorescence microscopy

To determine whether 3D HA, compared to 2D HA, has a differential effect on the expression and subcellular localisation of ZO-1 and CLDN5, hCMEC/D3 coverslip cultures were exposed to conditioned media obtained from respective culture conditions and analysed by immunofluorescence microscopy.

ZO-1 staining was mainly detected along the cell-cell borders although a relatively fainter expression was observed in the nucleus. Visually, there was no obvious difference in the staining pattern or intensity levels across different treatments (**Figure 3-2**). To identify quantitatively subtle differences in protein expression along the cell-cell borders, which is in principle associated with tight junctions, the normalised percentage area of staining along the cell membrane was calculated and compared across different conditioned media treatments (**Figure 3-3**).

Both 2D HA ACM (1.37±0.16) and 3D HA ACM (1.42±0.16) induced slightly higher levels of ZO-1 at cell junctions in hCMEC/D3 cells compared to control medium (1.0±0.10). Induced higher levels of ZO-1 by 3D HA ACM was statistically not different from that of 2D HA ACM. Hence, in this aspect, 3D HA did not appear to be different from 2D HA. The expression of ZO-1 in cells incubated with conditioned media from co-cultures (1.33 ± 0.12) was statistically not different compared to any other treatments.

PAGE NUMBERING AS ORIGINAL

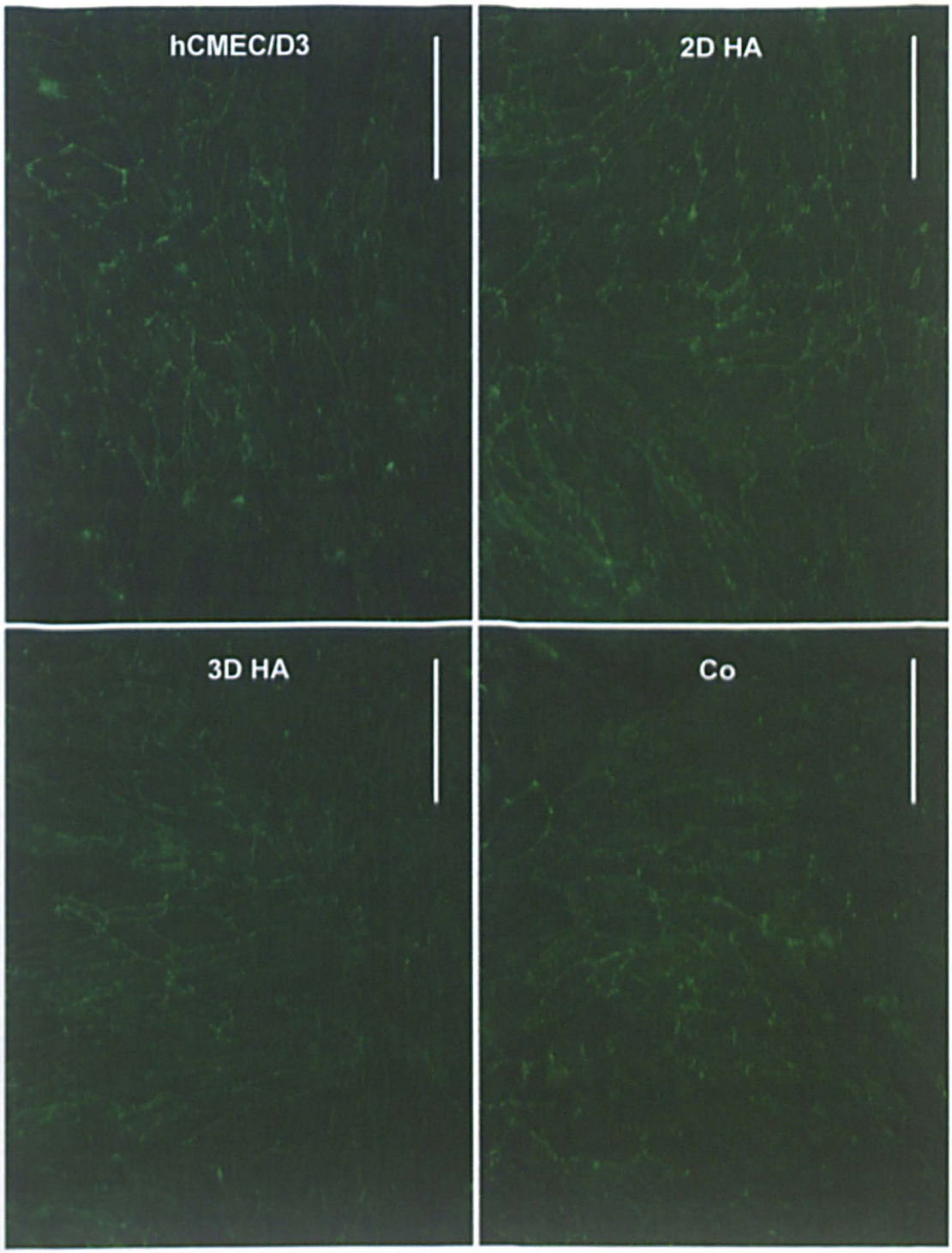

Figure 3-2 Effect of astrocyte conditioned media on ZO-1 subcellular distribution as analysed by immunofluorescence microscopy

hCMEC/D3 cultures grown on coverslips were fixed with methanol and analysed by immunofluorescence microscopy for the expression and localisation of ZO-1. A representative image of immunostaining from each conditioned media treatment is shown. ZO-1 was detected predominantly at cell-cell junctions but also in the nucleus and perinuclear regions to a lesser extent. Scale bar represents 100 μm. .

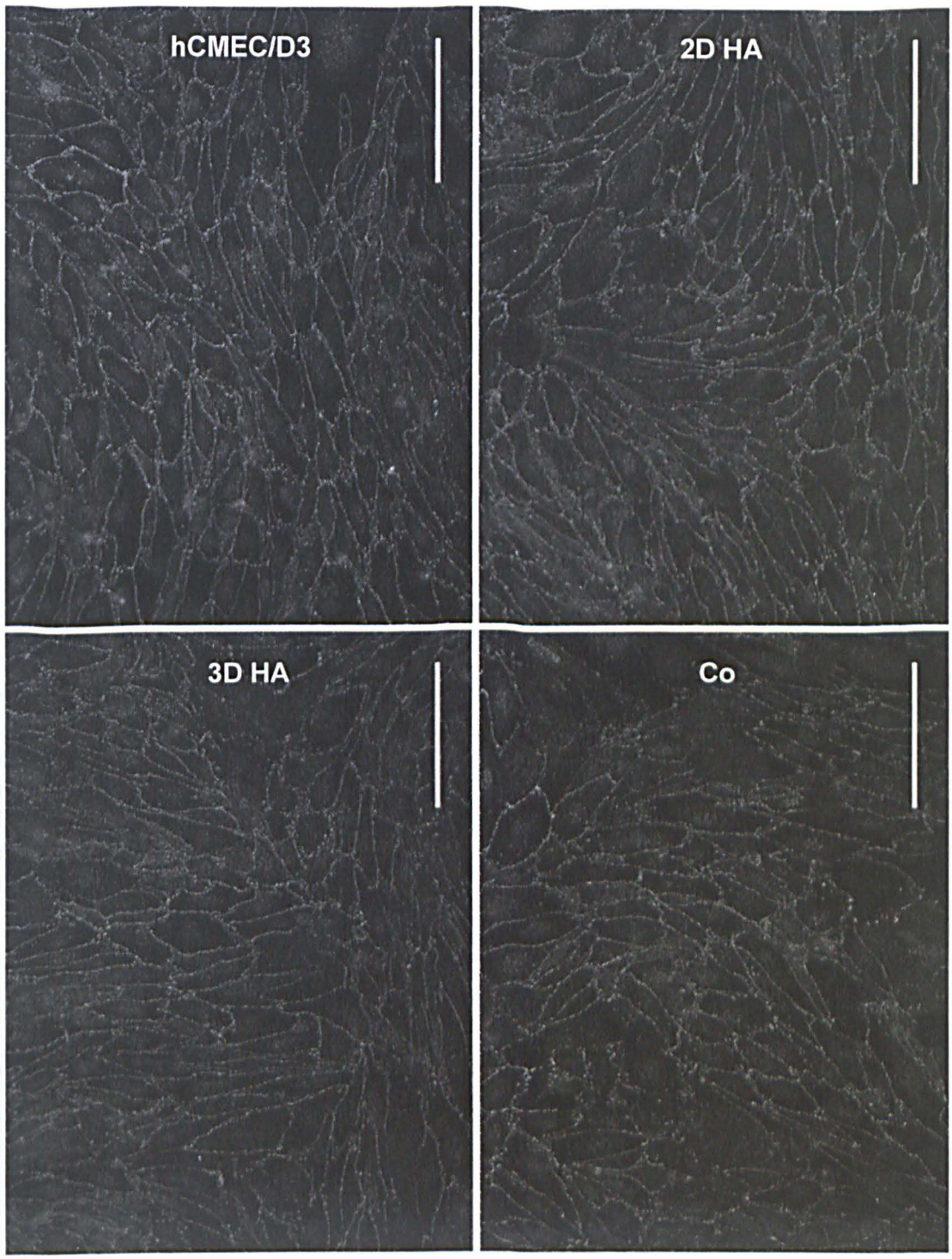

Figure 3-2 Effect of astrocyte conditioned media on ZO-1 subcellular distribution as analysed by immunofluorescence microscopy

hCMEC/D3 cultures grown on coverslips were fixed with methanol and analysed by immunofluorescence microscopy for the expression and localisation of ZO-1. A representative image of immunostaining from each conditioned media treatment is shown. ZO-1 was detected predominantly at cell-cell junctions but also in the nucleus and perinuclear regions to a lesser extent. Scale bar represents 100 μm. .

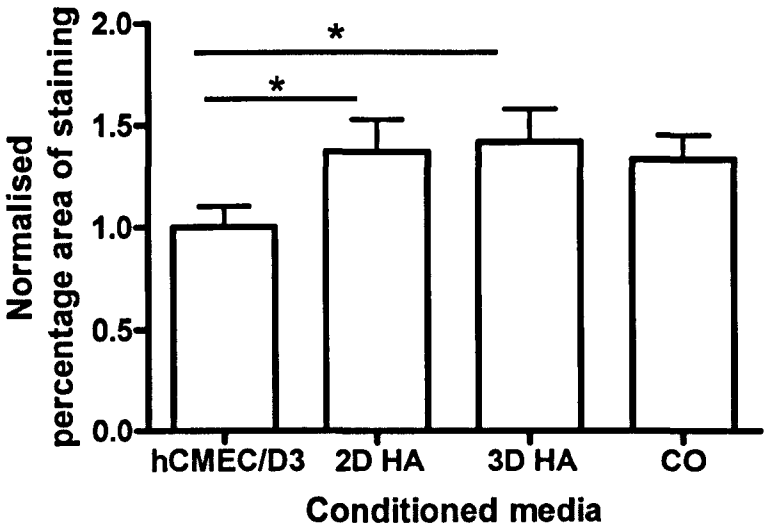

Figure 3-3 Effect of astrocyte conditioned media on ZO-1 levels at cell-cell junctions by hCMEC/D3 cells as analysed by immunofluorescence microscopy

hCMEC/D3 cultures grown on coverslips were exposed to the conditioned media obtained from cultures as stated in the X-axis. The bars show the normalised percentage area of anti-ZO-1 staining localised to cell-cell junctions. Treatment with conditioned media obtained from hCMEC/D3 solo cultures was used as a control. Both 2D HA ACM and 3D HA ACM induced a higher junctional localisation of ZO-1 protein. However, there was no difference between the induced effects of 3D HA ACM and 2D HA ACM. Co-culture conditioned media did not induce any changes in ZO-1 expression compared to any other treatment. All data are mean ± SEM, $*P \leq 0.05$ using Paired *t*-test, N = 3.

3.3.3 Claudin-5 expression was increased by 2D HA

Claudin-5 staining was variable from cell to cell, with fainter staining throughout the cytoplasm but relatively more intense staining at cell-cell borders. Qualitatively, there was no detectable difference in the staining pattern or intensity levels across different treatments (**Figure 3-4**). Hence, to analyse quantitatively subtle differences in the total amount of protein expression, the total percentage area of staining was calculated and compared across the treatments (**Figure 3-5**).

In comparison to hCMEC/D3 conditioned medium (1.0±0.06), 2D HA ACM (1.33±0.11) induced higher expression of claudin-5, but 3D HA ACM did not (1.25±0.07). However, the difference between the effects of 3D and 2D ACM was not statistically significant. Therefore, it was inferred that 3D HA were not different from 2D HA, in their induction potential through released factors, on claudin-5 expression in hCMEC/D3 cells. The effect of conditioned media from co-culture (1.12±0.08) was not different compared to any other treatment.

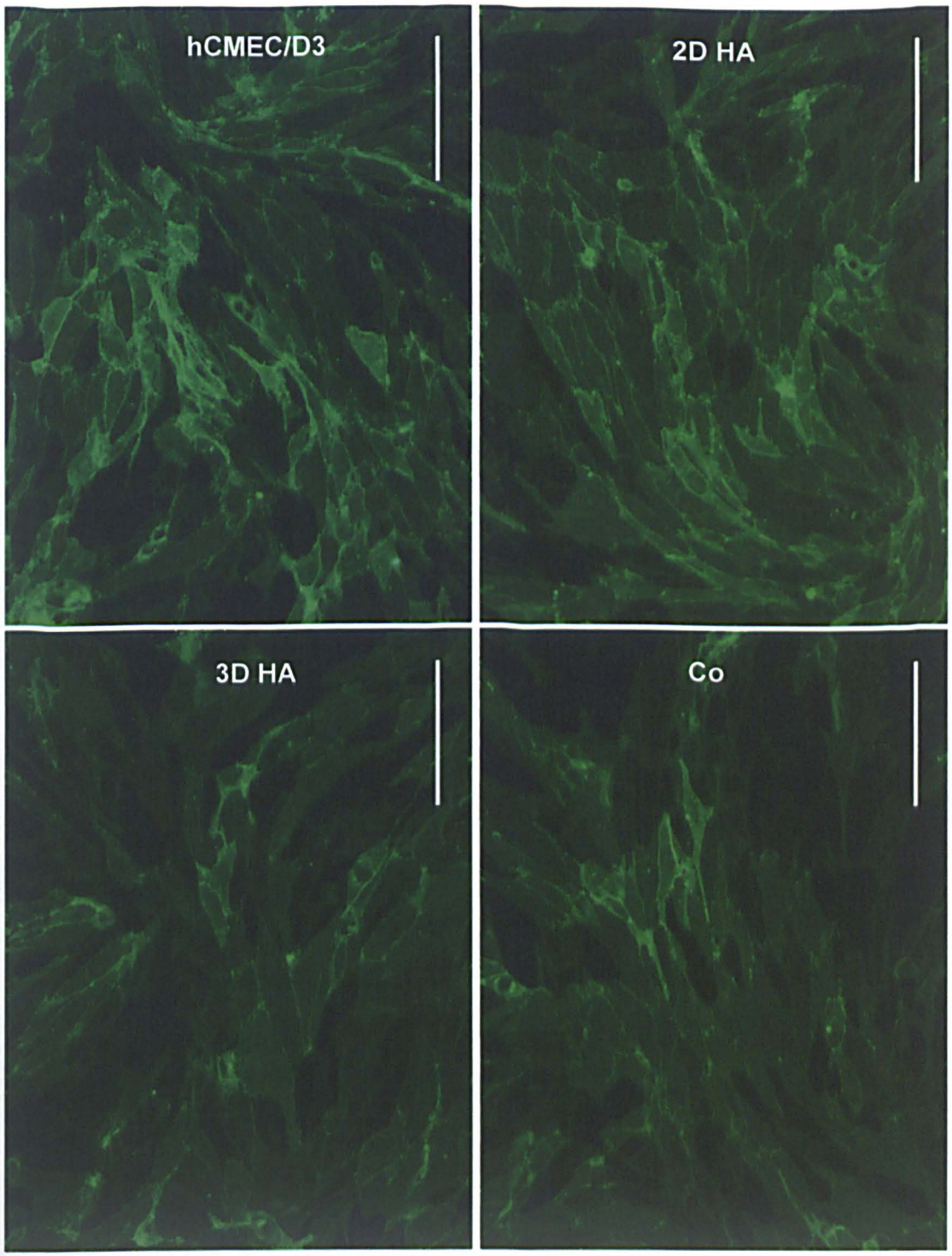

Figure 3-4 Effect of astrocyte conditioned media on CLDN5 subcellular distribution as analysed by immunofluorescence microscopy

hCMEC/D3 cultures grown on coverslips were fixed with methanol and analysed by immunofluorescence microscopy for the expression and localisation of CLDN5. A representative image of immunostaining from each conditioned media treatment is shown. CLDN5 staining was detected at cell-cell junctions and faintly throughout the cytoplasm. Scale bar represents 100 μm.

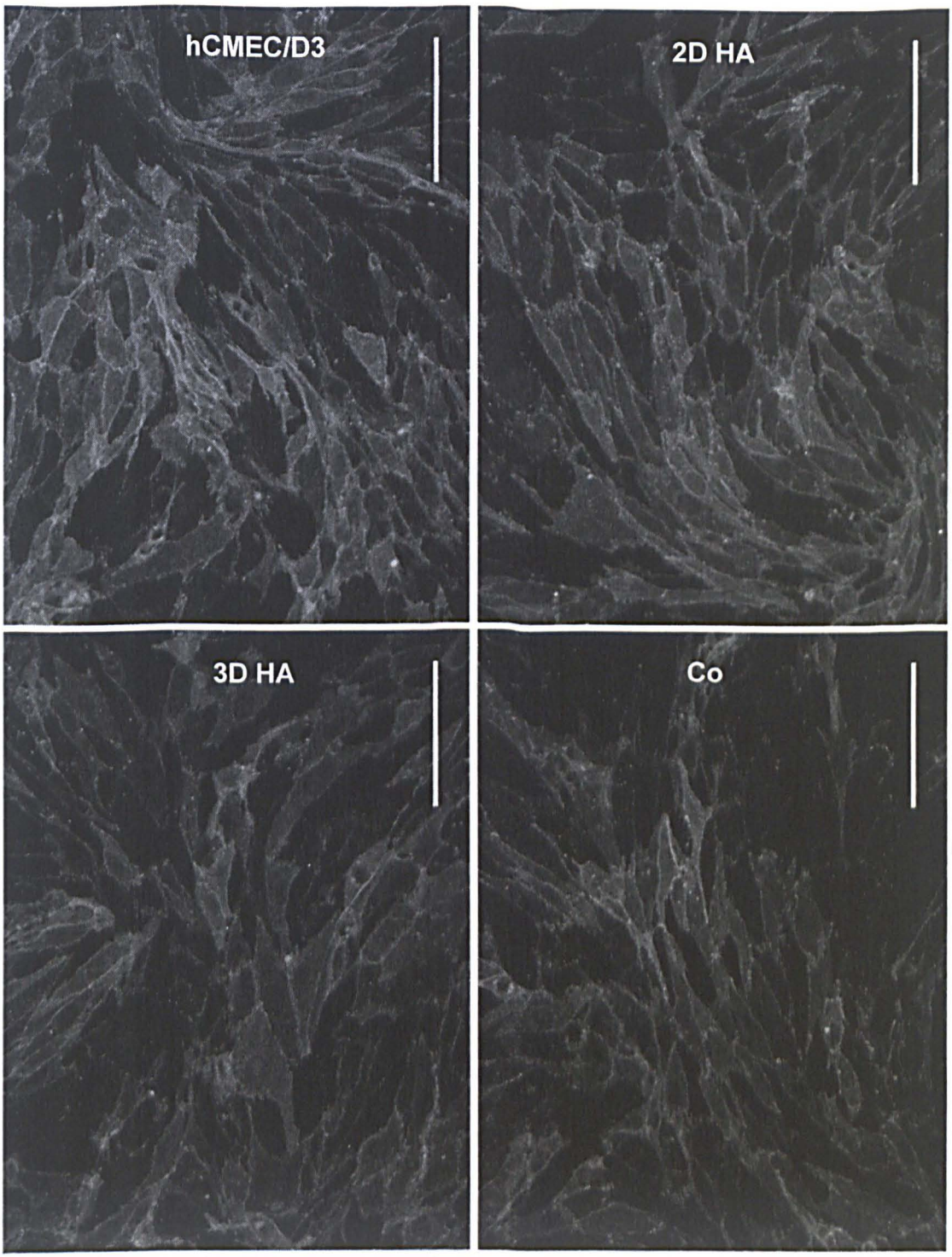

Figure 3-4 Effect of astrocyte conditioned media on CLDN5 subcellular distribution as analysed by immunofluorescence microscopy

hCMEC/D3 cultures grown on coverslips were fixed with methanol and analysed by immunofluorescence microscopy for the expression and localisation of CLDN5. A representative image of immunostaining from each conditioned media treatment is shown. CLDN5 staining was detected at cell-cell junctions and faintly throughout the cytoplasm. Scale bar represents 100 μm.

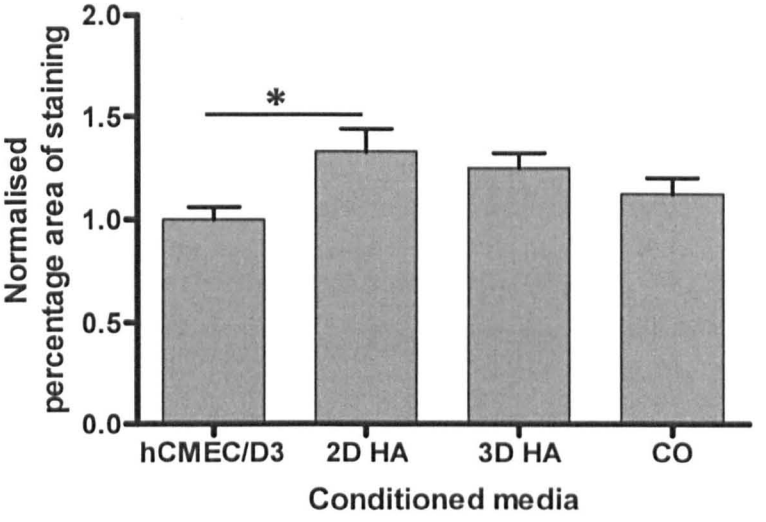

Figure 3-5 Effect of astrocyte conditioned media on CLDN5 expression on hCMEC/D3 cells as analysed by immunofluorescence microscopy

hCMEC/D3 cultures grown on coverslips were exposed to the conditioned media obtained from cultures as stated in the X-axis. The bars show the normalised percentage area of anti-CLDN5 staining. Treatment with conditioned media obtained from hCMEC/D3 solo culture was used as control. ACM from 2D HA but not 3D HA induced the higher expression of CLDN5 protein. However, there was no difference between the induced effects of 3D HA compared to 2D HA. Co-culture conditioned media did not induce CLDN5 overexpression compared to any other treatment. All data are mean ± SEM, $*P \leq 0.05$ using Paired *t*-test, N=3.

3.3.4 P-glycoprotein expression was not affected by either 2D HA ACM or 3D HA ACM

hCMEC/D3 cells were grown in the presence of conditioned media obtained from either 2D HA or 3D HA and their P-gp expression was analysed by flow cytometry. Specific cell-surface expression was analysed on non-permeabilised cells (**Figure 3-6**), while total cellular expression was analysed in permeabilised cells (**Figure 3-7**).

In comparison to hCMEC/D3 conditioned medium, neither 2D ACM nor 3D ACM induced statistically significant changes in the cell-surface expression of P-gp. In addition, there was no statistically significant difference between the effects of 3D and 2D ACM. Similarly, total cellular expression of P-gp was not affected by either 2D ACM or 3D ACM and there was no difference between the effects of 3D and 2D ACM. Therefore, it was inferred that 3D HA were not different from 2D HA in their inducible effect through released factors on P-gp expression in hCMEC/D3 cells.

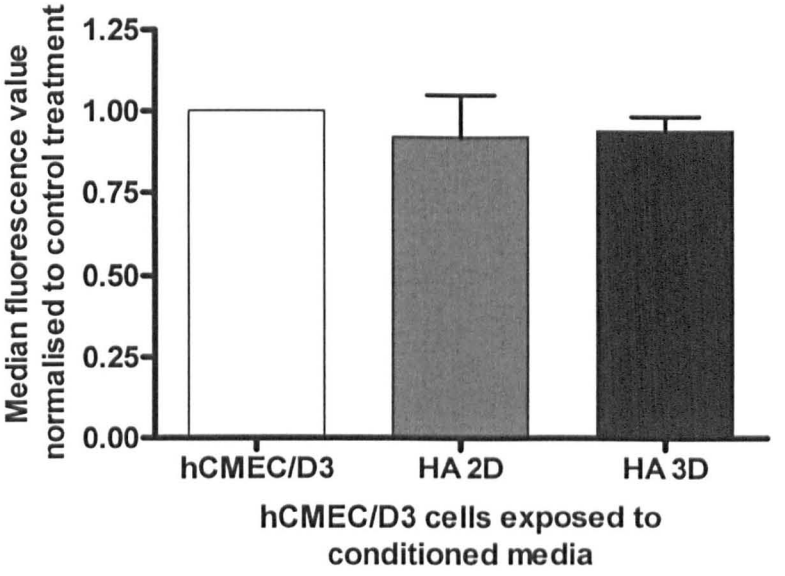

Figure 3-6 Cell-surface expression of P-gp was not affected by conditioned media of either 2D or 3D HA

hCMEC/D3 cultures were exposed to the conditioned media before analysis by flow cytometry. Median fluorescence value of each treatment normalised to that of hCMEC/D3 CM treatment was plotted on theY-axis. In comparison to hCMEC/D3 conditioned medium, neither 2D ACM nor 3D ACM induced statistically significant changes in the cell-surface expression of P-gp. In addition, there was no statistically significant difference between the effects of 3D and 2D HA ACM. All data are mean ± SEM. $P \leq 0.05$ was considered significant using Paired *t*-test. N = 3.

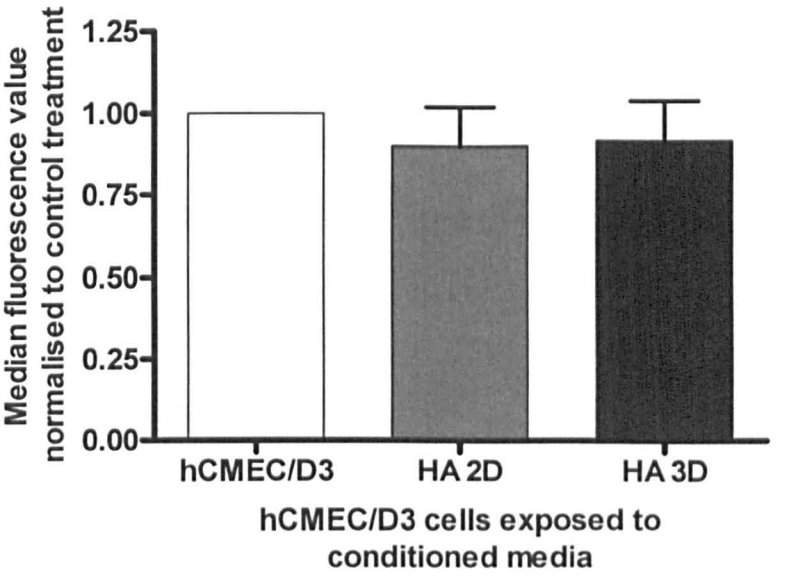

Figure 3-7 Total cellular expression of P-gp was not affected by conditioned media of either 2D or 3D HA

hCMEC/D3 cultures were exposed to the conditioned media before analysed by flow cytometry. Median fluorescence value of each treatment normalised to that of hCMEC/D3 CM treatment was plotted on the Y-axis. All data are mean ± SEM of triplicate experiments. In comparison to hCMEC/D3 conditioned medium, neither 2D nor 3D HA ACM induced statistically significant changes in the total cellular expression of P-gp. In addition, there was no statistically significant difference between the effects of 3D and 2D HA ACM. All data are mean ± SEM. $P \leq 0.05$ was considered significant using Paired *t*-test. N = 3.

3.3.5 Neither 2D HA nor 3D HA ACM had an effect on paracellular permeability of hCMEC/D3 cells

To determine whether 3D HA ACM induce the paracellular tightness to a larger extent than 2D HA ACM, hCMEC/D3 transwell insert cultures were exposed to conditioned media obtained from respective culture conditions and their permeability to the paracellular tracer, fluorescent dextran, 70 kDa, was measured (**Figure 3-8**).

In comparison to control medium, neither 2D HA ACM nor 3D HA ACM induced statistically significant changes in the paracellular permeability coefficient of hCMEC/D3 cells. In addition, there was no statistically significant difference between the ACM effects of 3D HA and 2D HA.

Therefore, these results show that 3D astrocytes were not different from 2D cultured astrocytes in terms of their inducible effect on hCMEC/D3 cells to paracellular permeability of FITC dextran, 70 kDa.

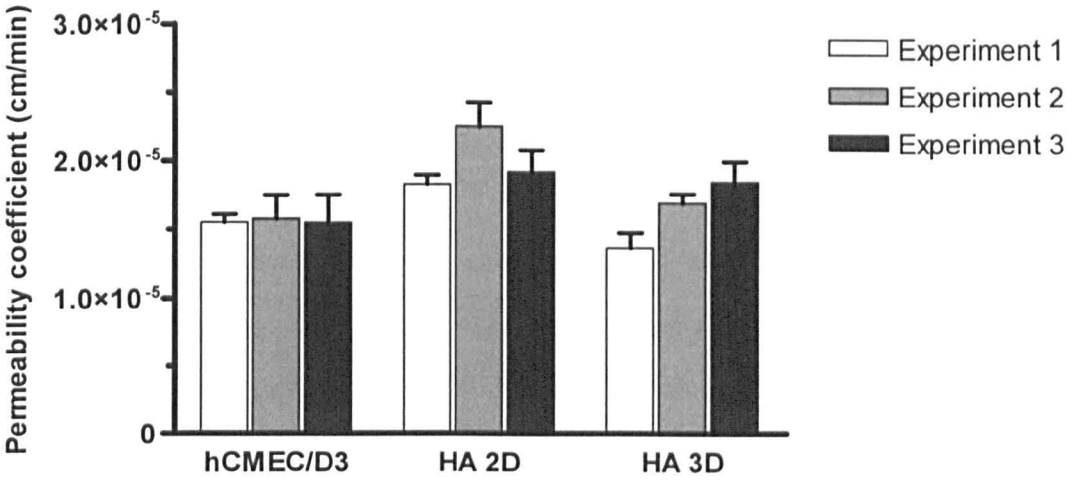

Figure 3-8 Effect of astrocyte conditioned media on the paracellular permeability of hCMEC/D3 cells

Transwell insert cultures of hCMEC/D3 cells were exposed to conditioned media obtained from the cultures for 4 days. The paracellular permeability of the cells to FITC dextran, 70 kDa, was measured. Exposure to conditioned media obtained from hCMEC/D3 solo culture was used as reference. Neither 2D HA nor 3D HA induced significant effect on paracellular permeability of hCMEC/D3 cells. In addition, the effect of 3D HA was not different from that of HA 2D. Data represent mean ± SEM of triplicate samples. $P \leq 0.05$ was considered significant using Paired *t*-test. N = 3.

3.4 DISCUSSION

3.4.1 The barrier inducing effect of 3D HA is not different from that of 2D HA

In the present chapter, we investigated the effect of 3D culture on the barrier inducing or enhancing properties of human astrocytes on hCMEC/D3 cells. Barrier induction capacity of astrocytes depends partly on physical contact and partly on soluble factors (section 1.4).

Few studies have demonstrated the secretion of these factors by astrocytes or astrocyte-derived tumour cells in 3D environments. In this context, GDNF was shown to be released by human astrocytes in compressed polyethylene terephthalate (PET) 3D fabrics at concentrations sufficient to elicit an effect (Basu, 2005). By contrast, bFGF was shown to be secreted by hypoxic human astrocytoma cells in monolayers at a higher rate than in 3D culture conditions, but this effect was also associated with increased VEGF production, a known inducer of BBB breakdown (Kim, 2011). The contribution of each of these astrocyte-secreted factors to the induction of the barrier phenotype in BMVEC and a systematic comparison in their levels between astrocytes in 2D and 3D environments remains to be determined.

In this study, we investigated only the effect of soluble factors, by comparing the effect of conditioned media collected from 3D HA culture with that of 3D HA culture. The results indicate that 3D HA were not different from 2D HA in their capacity to induce the changes in expression pattern or levels of tight junctional proteins ZO-1 or CLDN5 or in their capacity to enhance the tight junctional barrier as measured by paracellular permeability to the hydrophilic tracer, FITC dextran, 70 kDa. This may indicate that glial factors (see section 1.4.1.1) released by 3D cultured astrocytes may be similar in quality and quantity to those released by 2D cultured astrocytes.

More importantly and surprisingly, hCMEC/D3 cells responded poorly to factors released by either 2D HA or 3D HA. This was unexpected because astrocytes are known to be inducers and/or enhancers of barrier phenotype *in vivo* and *in vitro* as well (see section 1.3).

3.4.2 Response of hCMEC/D3 cells to astrocyte-released factors

In vitro cultures of primary BMVEC of various species (rat, mouse, and bovine) respond to astrocytic factors by displaying an enhanced BBB phenotype. Few studies have used primary, human BMVEC (HBMVEC) in their *in vitro* co-culture BBB model (Cucullo, 2007) and shown an improved barrier phenotype in response to astrocyte-secreted factors (Rubin, 1991b, Megard, 2002, Siddharthan, 2007, Kuo, 2011).

Being immortalised, hCMEC/D3 cells may differ from primary cells in some of their properties. Initially, when the hCMEC/D3 cell line was generated and characterised, the authors reported that hCMEC/D3 cells may be able to respond to astrocyte-released factors as manifested by an increased expression of claudin-5 and occludin and a decreased paracellular permeability but without increase in transendothelial electrical resistance (TEER) (Weksler, 2005). Recently, hCMEC/D3 cells were shown to respond to rat C6 glioma cells, when co-cultured in transwell inserts, as their permeability to paracellular tracers was decreased (Hsuchou, 2010). In addition, when hCMEC/D3 cells were co-cultured with primary human astrocytes their TEER resistance was increased (Hatherell, 2011). In contrast, in a flow-based model, the basal BBB phenotype of hCMEC/D3 cells was enhanced as determined by TEER measurements (~1000 $\Omega \cdot cm^2$), but there was no further increase in TEER when co-cultured with HA (Cucullo, 2008). Similarly, when hCMEC/D3 cells were co-cultured with HA in a non-contact transwell co-culture system, the barrier phenotype was largely unaffected as evidenced by unchanged mRNA levels of tight junctional proteins including ZO-1 and CLDN5 (Urich, 2012).

3.4.2.1 Tight junctional protein expression

The present study investigated the effect of astrocyte-released factors on the expression pattern and the expression levels of ZO-1 and CLDN5 proteins in hCMEC/D3 cells. 2D HA released factors did not have an effect on total cellular expression of ZO-1 as shown by immunoblotting analysis. However, ZO-1 localisation appeared to be influenced by astrocytic factors. ZO-1 is generally present partly in the nucleus where it interacts with the transcription factor ZONAB (Balda, 2000) and partly at cell-cell junctions. In the presence of 2D HA ACM, as shown by immunofluorescence microscopy analysis, a higher amount of ZO-1 is present at the cell-cell junctions. This presence of a higher amount of ZO-1 at cell-cell junctions cannot be due to because of increased expression but could be because of re-localisation of ZO-1 from the nucleus to cell-cell junctions. Total cellular expression analysis of CLDN5 by immunoblotting showed no increase whereas by immunofluorescence microscopy analysis showed a modest increase. To resolve the conflicting results of CLDN5 and to corroborate the ZO-1 findings, further work needs to be carried out using an alternative analytical method. ACM treated hCMEC/D3 cell lysates can be separated into nuclear, cytosolic, and membranous fractions by differential detergent fractionation, and levels of ZO-1 and CLDN5 could be analysed in each fraction by immunoblotting (Tai, 2009). Such analysis would reveal the effect of culture conditions on the subcellular redistribution of the protein along with changes in total cellular protein levels.

3.4.2.2 Paracellular permeability

Although the effect of ACM on the expression of CLDN5 is questionable and the effect on apparent ZO-1 relocalisation is very modest, the effect of ACM on paracellular permeability of hCMEC/D3 monolayers was analysed, as the paracellular barrier property does not entirely depend on these two proteins. Results have shown that neither 2D HA nor 3D HA increased the paracellular tightness as evidenced by no significant change in the permeability coefficient

of hCMEC/D3 cells to FITC-dextran, 70 kDa. Although, Hsuchou et al. (2010) have shown that paracellular permeability of hCMEC/D3 cells was decreased when co-cultured with astrocytes, their source of astrocytes was C6 glioma cells and the paracellular tracer they have used was FITC-dextran, 20 kDa, 33 Å, which is ~2 times smaller than the tracer used in this study, which is FITC-dextran, 70 kDa, 60 Å. These results would suggest that the inductive effect of astrocytes on BMVEC paracellular permeability might be size-dependent. Indeed, it has been previously shown that claudin-5 knock-out mice show restricted paracellular permeability to tracers larger than 800 Da similar to wild-type mice but an increased permeability to smaller molecules (Nitta, 2003). In addition, it may be dependent on the source of astrocytes used for these assays, with differing abilities according to developmental stage, species, and/or whether they are tumourigenic. To date, no study has shown the effect of human foetal astrocytes on the paracellular permeability of hCMEC/D3 cells.

3.4.2.3 HA does not influence the BMVEC P-gp expression

We have investigated the effect of primary human ACM on P-gp expression in hCMEC/D3 cells. Neither cell surface nor total cellular expression of P-gp was affected by ACM treatment. Previous studies have shown that astrocytic factors are able to induce the expression of P-gp on non-human primary brain endothelial cells. El Hafny *et al.* found that P-gp levels and activity were increased by C6 glioma factors on the rat brain endothelial cell line, RBE4 (El Hafny, 1997). Similarly, rat primary astrocytes also induced expression of P-gp protein on primary bovine capillary endothelial cells in co-culture (Gaillard, 2000).

In the context of human brain endothelium, a recent study by Kuo *et al.* (2011), demonstrated, decreased calcein-AM uptake in HBMVEC co-cultured with HA suggesting an increased efflux transporter activity. However, they did not study whether the effect was due to increased P-gp expression and/or increased functional activity. Increased P-gp functional activity without changing the P-gp expression has been demonstrated in cultured brain

endothelial cells, in response to dexamethasone (Regina, 1999). This effect may occur by increased membrane localisation, by increased luminal polarisation of P-gp and/or, as demonstrated by Regina *et al.* (1999), by activation of intracellular signalling pathways (e.g. PKC) that affect the activity of this efflux pump.

Nevertheless, there is a single study that demonstrated an increased cell-surface as well as mRNA expression of P-gp in HBMVEC when co-cultured with HA (Megard, 2002). The apparent discrepancy between the results in that study and our results may be attributed to the immortalised nature of hCMEC/D3 cells. This inference is supported by the Urich *et al.* (2012), in which they have shown that P-gp mRNA expression in hCMEC/D3 cells was not increased by astrocytic released factors.

3.4.3 Modest induction of barrier phenotype

The poor or limited effect of HA released factors on induction of barrier phenotype of hCMEC/D3 cells that is observed in this study could be explained as follows.

Co-culture methodology

Contact-co-culture system furnishes physical contact and higher local concentration of factors whereas non-contact co-culture systems and astrocyte conditioned media methodology do not (section 1.4). hCMEC/D3 were shown to respond better to astrocytes and become tighter in contact co-cultures, compared to non-contact co-cultures, as evidenced by much reduced paracellular permeability (Hsuchou, 2010) and much increased TEER (Hatherell, 2011). In another study that used non-contact co-culture system, human foetal astrocytes were not able to induce tight junctional proteins on hCMEC/D3 cells (Urich, 2012). Taken together, it appears that hCMEC/D3 cells, unlike primary BMVEC, may require higher concentrations of astrocyte released factors and/or physical contact with astrocytes for their barrier phenotype induction.

The present study is comparable to Hatherell *et al.* (2011), since both have used hCMEC/D3 cells and human foetal astrocytes. Hence, the discrepancy in the results could be attributed to the conditioned media methodology used in this study. Moreover, the present study used 50% astrocyte conditioned media, which would further dilute the inductive factors. In the present study, ACM methodology was selected because all other experimental parameters could be kept constant, while comparing the effect of 2D HA vs. 3D HA.

In addition, the present study used 2.5% foetal calf serum while Hatherell *et al.* have used 2% human serum. It is possible that certain serum factors may have a complementary role in BBB induction and these may not be conserved across species and so may require human serum as supplementation in the nutrient media instead of routinely used foetal calf serum.

GFAP positivity of astrocytes

As presented in Chapter 2, human astrocyte cultures used in this study had ~29.2 - 46.9% GFAP positive cells, < 10 % fibroblasts, and the remaining are presumed to be GFAP negative, S100B positive astrocytes. Few previous studies have demonstrated a positive correlation between GFAP expression of astrocytes and their BBB induction potential (Pekny, 1998, Kakinuma, 1998, Liedtke, 1996).

A positive role of GFAP in the BBB-inducing capacity of astrocytes was demonstrated in an *in vitro* study using GFAP-negative astrocytes isolated from GFAP deficient mice. GFAP negative astrocytes had reduced capacity compared to GFAP positive astrocytes, to induce BBB phenotype on bovine aortic endothelial cells (BAEC) in a flow-based co-culture system. BAEC grown in the presence of GFAP-ve astrocytes were able to exclude Evans blue similarly to controls, but showed a reduced restriction to the passage of K^+ and sucrose, and lower TEER values compared to controls (Pekny, 1998).

Astrocytes produce angiotensinogen. Knockout mice studies revealed the positive role of angiotensinogen in BBB formation and repair. Angiotensinogen increases the expression of laminin and GFAP expression. So, a positive correlation between GFAP expression and BBB inducing potential has been indicated (Kakinuma, 1998).

Liedtke *et al.* (1996) have shown that GFAP expression by astrocytes may be necessary for their ability to induce proper vascularisation and BBB integrity especially in the spinal cord of the mouse (Liedtke W 1996). However, there has been no evidence for a role of GFAP in BBB formation in the brain of mice (Pekny, 1995, Gomi, 1995).

Taken together, it can be speculated that the poor barrier phenotype induction potential of HA observed in this study may be due to the low number of GFAP positive cells in the HA cultures used in this study.

3.4.4 Limitations and future work

In this study, we have investigated the expression level and pattern of only two tight junctional proteins namely ZO-1 and CLDN5. However, it is possible that astrocytes induce the barrier phenotype by over expression and/or modulation of other tight junctional molecules such as occludin, claudin-1 and -3, JAMs and other ZO family members. Therefore, studying the effect of ACM on these molecules also would be useful to compare the ACM effects of 3D HA vs. 2D HA.

In this study, to determine ACM effect on functional BBB phenotype, the paracellular permeability of BMVEC was assessed using 70 kDa FITC-Dextran. A permeability analysis to different sized molecules (smaller as well as larger than 70 kDa) could be also useful in determining whether the astrocyte inductive influence is size-dependent. In addition, drug permeability assays also could be investigated.

We did not investigate the effect of ACM on TEER of hCMEC/D3 cells, although TEER is a reliable indicator of barrier phenotype in endothelial monolayers. TEER depends on sealing of intercellular clefts with tight junctional proteins in such a manner that even passage of ions of radius ≥3.6 Å is restricted. Since TEER depends on passage of ions, even few small gaps in the monolayer may cause very low TEER values (Madara, 1998). Therefore, a suitable TEER assay demands an endothelial monolayer with high barrier integrity. But, TEER of hCMEC/D3 monolayer during basal conditions is very low (20-40 $\Omega.cm^2$). For these reasons, it was not our priority to do TEER comparisons. However, Hatherell *et al.* (2011) have used TEER as an indicator of barrier integrity in their studies, and found that TEER of hCMEC/D3 cells increased when co-cultured with astrocytes. Therefore, it may be useful to do TEER measurement to compare ACM effects of 3D HA vs. 2D HA.

Urich *et al.* (2012) reported that even in a non-contact co-culture system, the immune surveillance phenotype of brain endothelial cells is readily influenced by astrocytic released factors whereas the barrier phenotype is not. These authors have shown that molecules responsible for cell adhesion, migration, and extravasation (e.g., VCAM1, E-selectin) on hCMEC/D3 cells were down regulated by astrocytic factors, which could be related to restoration of immune surveillance function of BMVEC. Therefore, it would be interesting to study in future the effect of 2D HA vs. 3D HA on the immune phenotype of hCMEC/D3 cells.

To reach definitive conclusions, about the role of 3D HA compared to 2D HA on BBB phenotype of endothelial cells, further experiments such as whole genome expression analysis and functional assays would be necessary.

3.5 CONCLUSIONS

1. hCMEC/D3 cells respond to human astrocyte-released factors by re-localisation of ZO-1 to cell-cell junctions without overexpression.

2. The tight junctional barrier-inducing potential of soluble factors released by 3D HA appears not to be different from those released by 2D HA.

Chapter 4:

Endothelial influence on astrocytic AQP4 expression

4.1 INTRODUCTION

In the CNS, because of their physical proximity, the properties of astrocytes may be influenced by BMVEC. Indeed, CNS endothelial cells have been shown to modulate the morphology, growth, differentiation, and polarity of astrocytes (section 1.7). *In vivo*, the expression of proteins such as AQP4 and Kir 4.1, a K^+ channel, are predominantly localised to the perivascular end feet of astrocytes (Wolburg, 2009b, Rash, 1998, Fallier-Becker, 2011), suggesting that the astrocytes are polarised by their physical interaction with endothelium. However, polarised expression of AQP4 is lost in cultured astrocytes (Nicchia, 2000). Some *in vitro* studies have shown that co-culturing astrocytes in contact with BMVEC could restore the polarity of AQP4, whereas non-contacting astrocytes did not (Tao-Cheng 1990, Nicchia, 2004, Al Ahmad, 2010).

The underlying mechanisms causing the polarisation of AQP4 in astrocytes are beginning to be unravelled. Polarisation of AQP4 has been shown to be partially dependent on the presence of agrin, a heparan sulphate proteoglycan on the sub-endothelial basal lamina (Noell, 2009). However, the underlying mechanisms and relative contributions of cell-contact versus soluble endothelial factors remain to be elucidated. The objective of the study was to investigate whether endothelium influences astrocytic AQP4 expression through physical contact, or through released soluble factors or both. Another objective was to determine whether the 3D model facilitates the contact between astrocytes and the abluminal face of the endothelial monolayer.

4.1.1 Aquaporin 4 (AQP4)

The aquaporin family of proteins consists of at least 13 members that function as fluid-selective channels in the plasma membrane of many cells. Aquaporin-4 (AQP4) is abundantly expressed in the CNS (Jung, 1994), but also expressed in kidney, lung, stomach, and skeletal muscle. This gene has two alternatively spliced transcript variants encoding two distinct isoforms, M1 and M23. These isoforms organise into supramolecular structures called orthogonal arrays of particles (OAPs) in the plasma membrane (Jin, 2011). AQP4 is generally highly expressed in osmosensory areas, predominantly on astrocytes and subpopulations of ependymal cell membranes. On astrocytes, AQP4 is mainly localised to the membrane that is in direct contact with capillaries (Nielsen, 1997).

4.1.2 Aims

1. **Role of soluble factors**: Do endothelium-released factors have any role on the expression levels or localisation of astrocytic AQP4?
2. **Role of physical contact**: Does astrocytic AQP4 relocate to the part of the cell membrane that is in contact with endothelium in a co-culture of astrocytes and endothelium?

4.2 METHODS

The reagents and antibodies used in this study are listed in **appendices A** and **B** respectively.

4.2.1 Immunofluorescence microscopy analysis of AQP4 in 2D cultures

HA and hCMEC/D3 cells were plated on ethanol-sterilised, collagen-coated cover slips as described in section 2.2.2.2. After the cultures reached confluence, cells were fixed and analysed as described in section 2.2.7. AQP4 (H-80) antibodies (Santa Cruz Biotechnology, Inc) were used for this purpose. AQP4 (H-80) is a rabbit polyclonal antibody raised against amino acids 244-323 mapping at the cytoplasmic C-terminus of AQP4 of human origin.

4.2.2 Flow cytometry analysis of AQP4 in 2D cultures

HA and hCMEC/D3 cells were plated (4 X 10^4 per cm^2) onto six-well plates and grown until confluence. Confluent cultures were trypsinised and analysed by flow cytometry as described in section 2.2.9. Permeabilisation was performed by addition of 0.05% saponin to antibody diluent and wash buffer. AQP4 (H-80) antibodies (Santa Cruz Biotechnology, Inc.) were used for this purpose.

4.2.3 Immunoblotting of AQP4 in cell lysate of 2D cultures

HA and hCMEC/D3 cells were plated (4 X 10^4 per cm^2) onto 6-well plates. After reaching confluence, cell lysates was prepared using RIPA buffer as per the manufacturer's protocol. A protease inhibitor cocktail was added to lysates and stored at -70°C until use. The protein concentrations of the cell lysates were calculated using the BioRad detergent compatible protein assay, using bovine serum albumin as a standard. For each lane of the SDS-PAGE gel, a cell lysate equivalent to 20 μg of total protein was loaded. Immunoblotting was performed as described in section 3.2.2 using rabbit, anti-AQP4 polyclonal antibodies (1 μg/ml; #AB2218, Millipore (U.K.) Ltd.).

4.2.4 Immunofluorescence microscopy of astrocytic AQP4 in 2D HA solo-, 3D HA solo-, and 3D HA co- cultures

3D HA solo- and co- cultures (2 x 10^5 cells/400 μL) were set up in a 24-well plate as described in section 2.2.3. Cultures were maintained for 7 days before the cells were fixed and analysed by immunofluorescence microscopy as described in section 2.2.8. 2D HA culture (2 x 10^5 cells) was set up on a 70% ethanol-sterilised, collagen-coated, coverslips. Coverslips were subjected to same procedure as gels.

Image capturing

3D Gels were placed in CoverWell™ imaging chambers and imaged using a Leica TCS SP5 confocal microscope and LAS AF software. Three random fields were imaged per gel. The measurements of each field were 775 μm X 775 μm X 100 μm in x, y and z dimensions respectively. The thickness of each slice was 1 micron. From the z-stack of images, a maximal intensity projection image was generated. This image was analyzed by Image Pro™ software. 2D coverslips were also imaged at the same voltage/gain settings.

Image analysis

The percentage area of pixels stained above threshold pixel intensity was calculated. Threshold pixel intensity was determined based on background fluorescence and was kept constant across images. The percentage area staining of each image was normalised with the total number of cells present in the image. Cell number was obtained from counting the number of Hoechst stained nuclei using Cell^{F}software (touch count feature). Thus, mean percentage area of staining per cell was calculated and compared between the culture conditions.

4.2.5 Flowcytometry of astrocytic AQP4 in 2D HA solo-, 3D HA solo-, and 3D HA co- cultures

3D HA solo- and co-cultures were set up as described in section 2.2.3. HA were plated at 2 x 10^5 cells/400 µl and hCMEC/D3 cells were plated at 4 x 10^4 cells/cm^2. 2D HA cultures (2 X 10^5 cells) were set up on the surface of collagen gels (400 µL) in 12-well plates. Cultures were maintained for 7 days before the cells were isolated from the gels by collagenase digestion as described in section 2.2.4.

Isolated cells were washed and then incubated with monoclonal PECAM1 antibodies conjugated PerCP-eFluor® 710 for 30 min at 4°C. Since this antibody works only on unfixed cells, cells were not fixed before they were incubated with PECAM1 antibodies. Antibody diluent was 0.1% NaN_3, 0.1% BSA in PBS. Then the cells were washed, fixed, and analysed using AQP4 (H-80) antibodies as described in 2.2.9. The two-step collagenase digestion procedure and subsequent cell gating based on PECAM1 expression and SSC properties were used to identify astrocytes separately from hCMEC/D3 cells in a co-cultured cell population as described in section 2.3.4.

Median fluorescence values obtained after flow cytometry analysis were compared across the culture conditions. Due to inter experimental variability between controls, graphs were plotted with normalised data obtained from triplicate experiments. Within each experiment, the median fluorescence value of the test sample was normalised to the median fluorescence value of the reference/control condition. All values were given as the mean ± SEM.

4.2.6 Immuno gold transmission electron microscopy of AQP4 in 3D Rat astrocyte solo-culture

Primary rat astrocytes (RA), kindly provided by Dr Emma East/Dr James Phillips, were established from cortices of post-natal two-day old pups (East, 2009). 3D rat astrocyte (RA) solo-cultures were set up as described in section 2.2.3, except that instead of HA, Rat astrocytes were used. RA were plated at 5 x 10^5 cells/ml and hCMEC/D3 cells were plated at 4 x 10^4 cells/cm^2. Cultures were maintained for 7 days before the cells were fixed and analysed by immunogold transmission electron microscopy (**TEM**) as described in section 4.2.7.

4.2.7 General procedure of immunogold transmission electron microscopy (TEM)

Fixation and sample preparation for TEM

Paraformaldehyde-lysine-periodate fixative (PLP): Fixative solution consisted of 2 % (w/v) PFA, 0.075 M lysine monohydrochloride, 0.01 M sodium metaperiodate dissolved in 0.1 M phosphate buffer.

Incubation buffer: 0.01 M PBS comprising 1% NGS, 0.8% BSA, and 0.1% cold water fish gelatin.

Blocking buffer: 0.01 M PBS comprising 5% NGS, 5% BSA, and 0.1% cold-water fish gelatin.

3D collagen gel cultures were fixed by incubating with PLP fixative solution for 4 h at RT then over night at 4°C. Then gels were washed twice with phosphate buffer (PB) before being cut into 2 mm strips and processed with a Leica AFS2 automatic freeze substitution system. Gel pieces were embedded in the acrylic resin Lowicryl HM20 and polymerised at -30°C under ultra violet light. Then the gel embedded resin was cut into ultrathin sections (~70 nm) using an ultra-microtome (Leica Inc.) and the sections were mounted onto formvar (Agar Scientific) coated nickel slot grids.

Immuno reaction steps

All immunoreactions were performed at RT in 20-40 µl droplets on a parafilm lined box lid that was covered during the incubation. Grids were incubated with 0.05 M glycine, aldehyde quencher, for 20 min before incubating in blocking buffer for 15 min to inhibit non-specific binding. Grids were incubated in drops of anti-AQP4 antibodies diluted in incubation buffer (20 µg/ml, Millipore) or in incubation buffer alone (as a negative control) in a humid chamber overnight. The grids were then washed with incubation buffer, 3 x 5 min, by transferring from one drop to another. Then grids were incubated with a goat anti-rabbit IgG conjugated to 10 nm gold particles for 2 h (British Biocell International). Grids were again washed with incubation buffer, 3 x 5 min before fixing with 2.0 % w/v glutaraldehyde in PBS. Then grids were washed with deionised water, 3 x 5 min, allowed to air dry and counter stained with 4 % (w/v) aqueous uranyl acetate for 25 min. After a final wash in deionised water the immunogold labelled gel sections were examined using a JEOL JEM 1400 transmission electron microscope (JEOL Ltd.). Images were captured by AMT XR60 11 mega pixel digital camera using AmtV600 software

4.2.8 Statistical analysis

Graph plotting and statistical analysis was carried out using GraphPad PRISM v 4.0. Statistical significance of the data was assessed by Paired *t*-test. $P \leq 0.05$ was considered as significant.

4.3 RESULTS

4.3.1 2D cultured HA expressed AQP4

By immunofluorescence microscopy: 2D coverslip cultures of HA were analyzed for AQP4 expression by immunofluorescence microscopy. AQP4 was detected in all the cells. Protein staining was punctate suggesting that AQP4 could be in both the plasma membrane and/or cytoplasmic vesicles (**Figure 4-1.A**).

By flow cytometry analysis: Further, 2D coverslip cultures of HA were analysed by flow cytometry. The histogram plot clearly shows a higher fluorescence intensity of anti-AQP4 antibody stained cells than that of control (**Figure 4-1.C**).

By immunoblotting analysis: To further confirm the expression of AQP4 in 2D cultured HA, cell lysates were prepared from the confluent cultures and analysed by SDS-PAGE and immunoblotting. A band of approximately 35 kDa was detected (**Figure 4-1.E**). This corresponds to AQP4 isoform_1 whose mol. wt. is 34.83 kDa (Human protein reference database (HPRD) ID: 02631). Hence, it was concluded that AQP4 was expressed in 2D cultured HA.

4.3.1.1 2D cultured hCMEC/D3 cells also expressed AQP4

2D cultures of hCMEC/D3 cells were also analysed for AQP4 expression by the same three methods and AQP4 was expressed in these cells too. Immunofluorescence microscopy showed faint cytoplasmic staining, and relatively intense punctate peri-nuclear staining (**Figure 4-1.B**). Flow cytometry demonstrated fluorescence of anti-AQP4 stained cells compared to the negative control (**Figure 4-1.D**) and the presence of ~35 kDa band on the immunoblot (**Figure 4-1.E**) indicated the expression of AQP4 in 2D cultured hCMEC/D3 cells.

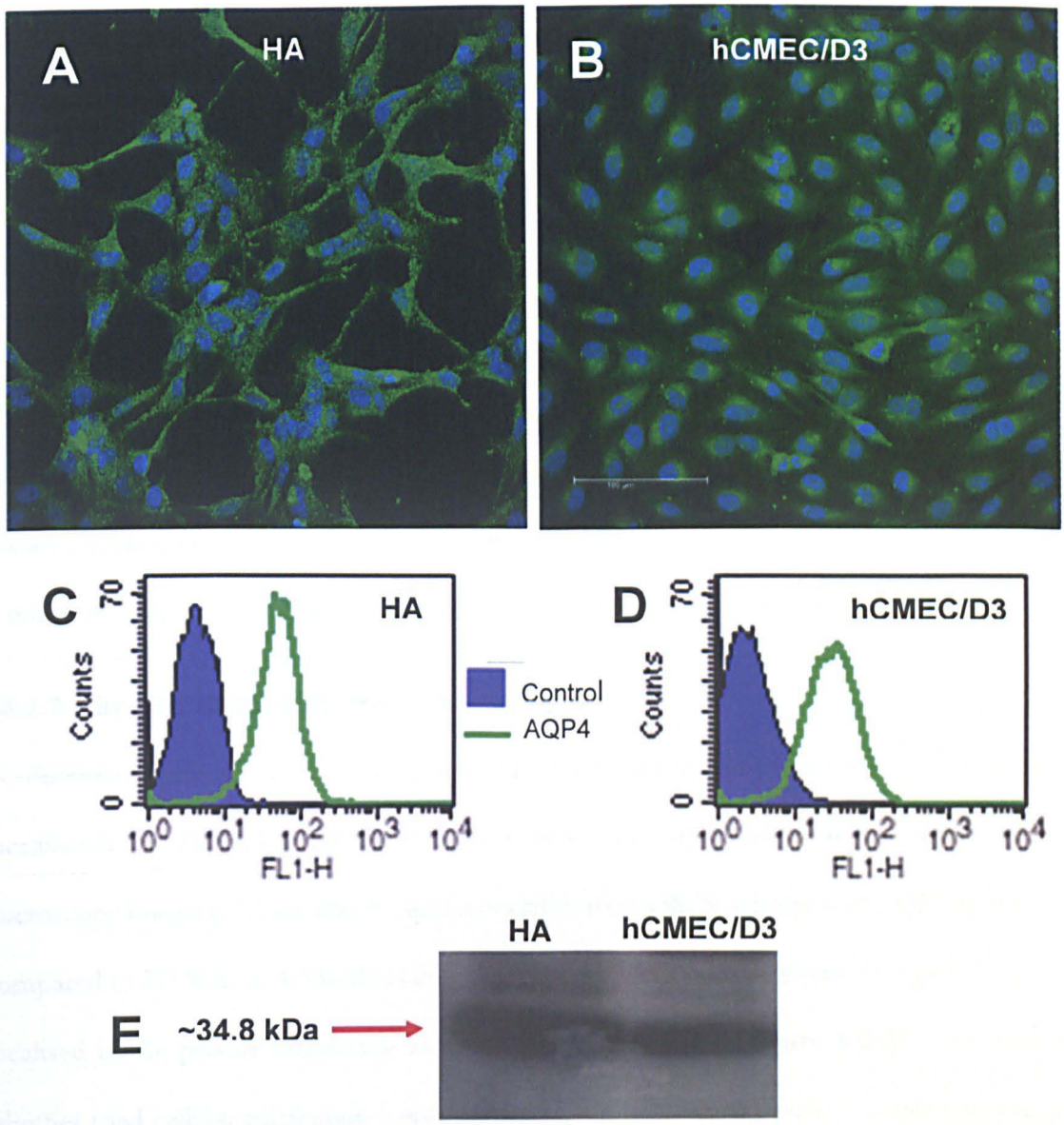

Figure 4-1 AQP4 was expressed in 2D cultures of HA and hCMEC/D3 cells

Expression of AQP4 was investigated in 2D solo-cultures of HA and hCMEC/D3 cells by three different techniques. By immunofluorescence microscopy analysis AQP4 expression was detected in HA (**A**) and hCMEC/D3 cell (**B**). Green stain indicates the presence of AQP4 and blue/violet staining indicates nuclear DNA. In HA, AQP4 appears to be located partly in the plasma membrane, partly in cytoplasmic vesicles, and partly in the cytosol. In hCMEC/D3, faint cytoplasmic staining, and a relatively intense punctuate peri-nuclear staining was seen. Flow cytometry analysis also demonstrated the expression of AQP4 in HA (**C**) and hCMEC/D3 cells (**D**). The presence of ~34.8 kDa band in SDS-PAGE/immunoblotting also indicated the expression of AQP4 in HA and hCMEC/D3 cells (**E**). N = 3. Scale bar represents 100 μm, and is applicable to both the images.

4.3.2 Astrocytic AQP4 expression was decreased in 3D solo-culture compared to 2D solo-culture

4.3.2.1 By flow cytometry

To determine whether the 3D collagen matrix environment alters astrocytic AQP4 expression, 3D HA solo- and 2D HA solo-cultures were set up and total, cellular, AQP4 expression levels were analysed by flow cytometry. In comparison to 2D HA solo-culture, 3D HA solo-culture reduced the expression of AQP4 by ~20% (**Figure 4-2.C**). Histograms of both 2D and 3D cultures showed unimodal distributions (**Figure 4-2.A**). This suggests that AQP4 expression is uniform (homogeneous) across the 2D and 3D cultured cell population.

4.3.2.2 By immunofluorescence microscopy

To determine whether the 3D collagen matrix environment alters astrocytic AQP4 cellular localisation, 3D HA solo- and 2D HA solo-cultures were analysed by immunofluorescence microscopy imaging. There was no apparent difference in the localisation of AQP4 in 3D HA compared to 2D HA. In both 2D and 3D cultures, AQP4 expression remained punctate and localised in the plasma membrane and cytoplasmic vesicles. (**Figure 4-3.A**). To analyse whether total cellular expression levels were changed between the culture conditions image quantitation was carried out. In comparison to 2D HA solo-culture, AQP4 expression was decreased by ~32% in 3D HA solo-culture (**Figure 4-3.B**).

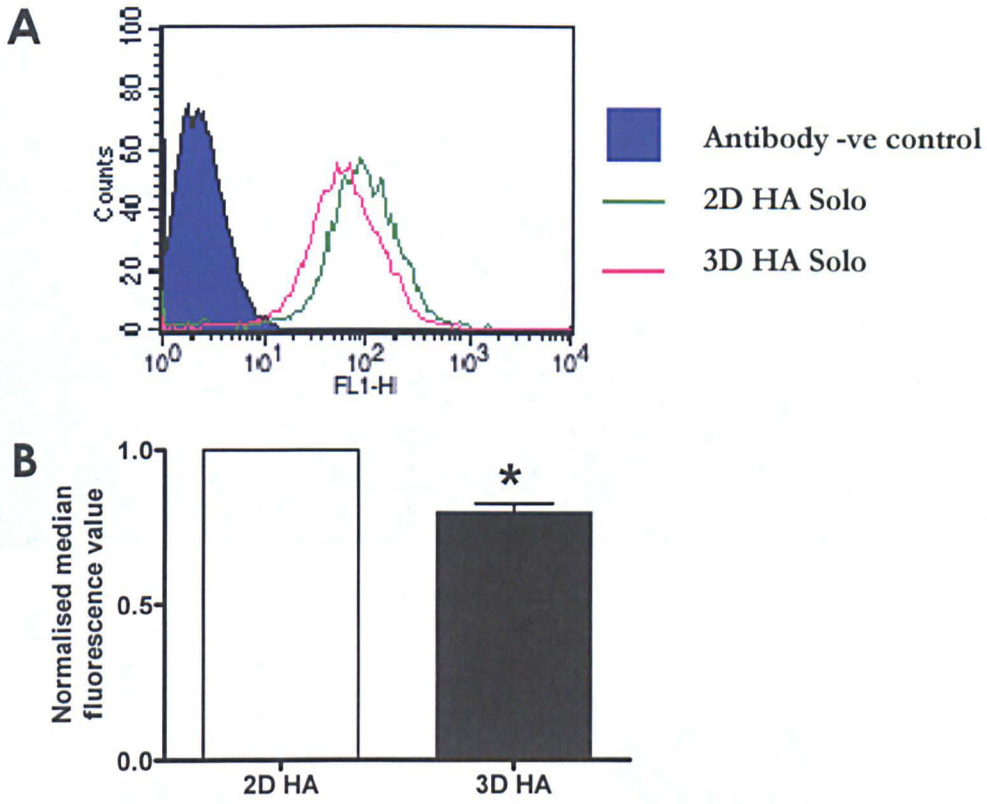

Figure 4-2 AQP4 expression was decreased in 3D HA solo-culture compared to 2D HA solo-culture as analysed by flow cytometry

HA were cultured either on the surface (2D HA solo) or inside the collagen gel (3D HA solo) for seven days. Cells were isolated by collagenase digestion and analysed for AQP4 expression by flow cytometry. Median fluorescence values were compared between the samples. **A:** A representative histogram of flow cytometry is shown. **B:** Bar diagram showing the statistically significantly decreased expression of AQP4 in 3D HA solo-culture compared to 2D HA solo-culture. For ease of comprehension mean ± SEM of normalised data were plotted. However, Paired *t*-test was performed on raw data. * indicates $P \leq 0.05$. N = 3.

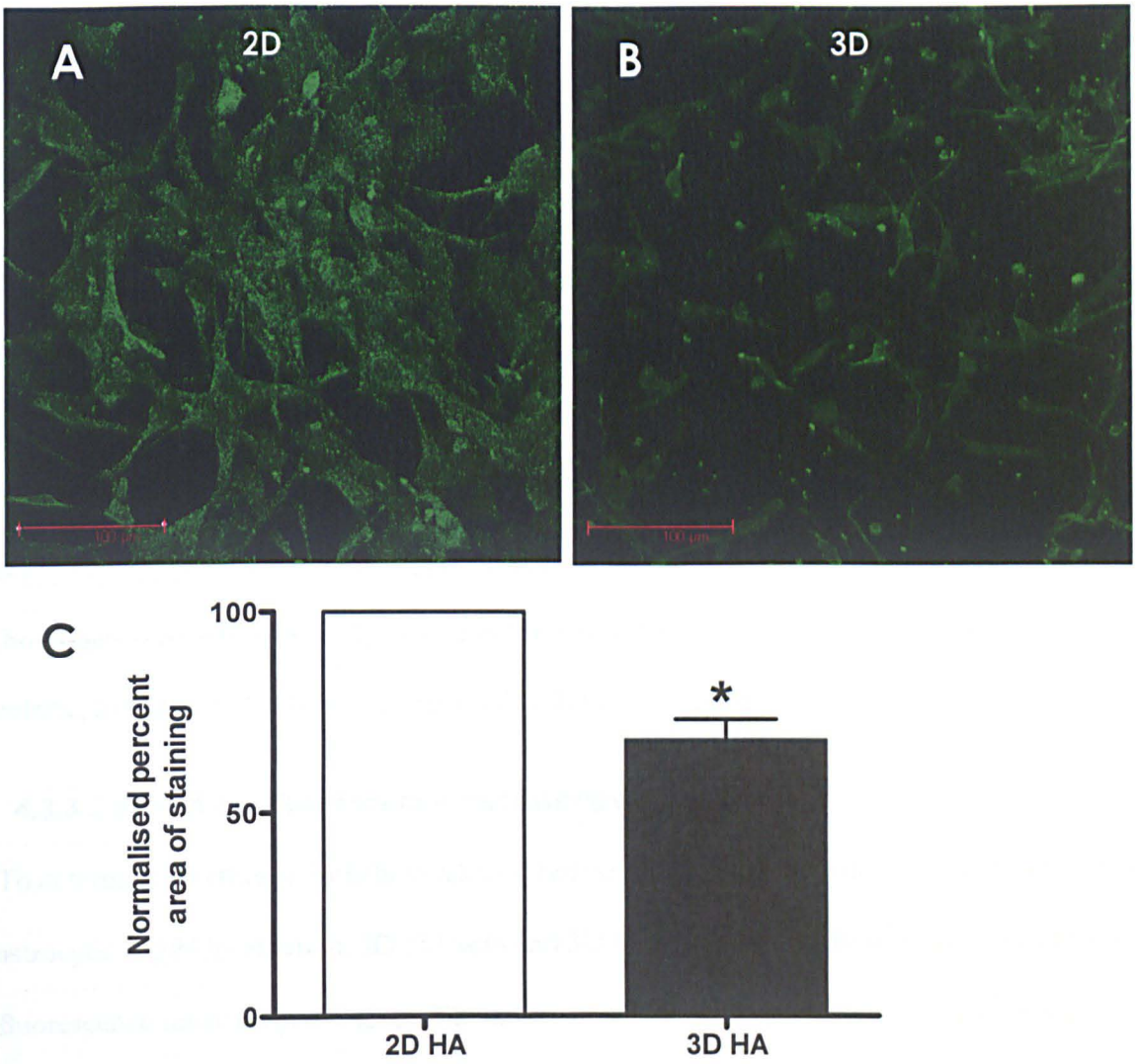

Figure 4-3 AQP4 expression was decreased in 3D HA solo-culture compared to 2D HA solo-culture as analysed by immunofluorescence microscopy

HA were cultured either on the coverslip (2D HA solo) or inside the collagen gel (3D HA solo) for seven days. Then cells were fixed and analysed for AQP4 expression by immunofluorescence confocal microscopy imaging. Three random fields per sample were captured; the percentage area of staining per cell was measured and compared between samples. AQP4 expression was less in 3D HA solo-culture compared to 2D HA solo-culture. **A:** A representative image showing AQP4 expression in 2D HA solo culture. **B:** A representative image showing decreased AQP4 expression in 3D HA solo culture. **C:** Bar diagram showing the statistically significant decreased expression of AQP4 in 3D HA solo-culture compared to 2D HA solo-culture. * indicates $P \leq 0.05$, using Paired *t*-test. N=3. Scale bar represents 100 μm.

4.3.3 Astrocytic AQP4 expression was further decreased in 3D HA co-culture in comparison to 3D HA solo-culture

4.3.3.1 By flow cytometry

To investigate whether endothelium released factors have an effect on the expression levels of astrocytic AQP4, 3D HA solo and 3D HA co-cultures were analysed by flow cytometry (**Figure 4-4 A**). Compared to 3D HA solo-culture, the total cellular expression of AQP4 in 3D HA co-culture was decreased by ~17 % (**Figure 4-4 B**). The unimodal distribution of cells in both culture conditions suggested that the decrease of AQP4 expression is uniform (homogeneous) across the cell population (**Figure 4-4 A**). However, in comparison to 2D HA culture, a decrease of ~34% was observed in 3D HA co-culture.

4.3.3.2 By immunofluorescence microscopy

To determine whether endothelium released factors have an effect on the expression levels of astrocytic AQP4 localisation, 3D HA solo and 3D HA co-culture were analysed by immuno-fluorescence microscopy imaging. There was no obvious difference in the localisation and expression pattern of AQP4 in 3D HA co-culture compared to 3D HA solo-culture (**Figure 4-5 A**). Then, total cellular AQP4 was measured by image quantitation. In comparison to 3D HA solo-culture, 3D HA co-culture expressed ~26% less total, cellular AQP4 (**Figure 4-5 B**), and in comparison to 2D HA culture, ~49% decrease was observed in 3D HA co-culture.

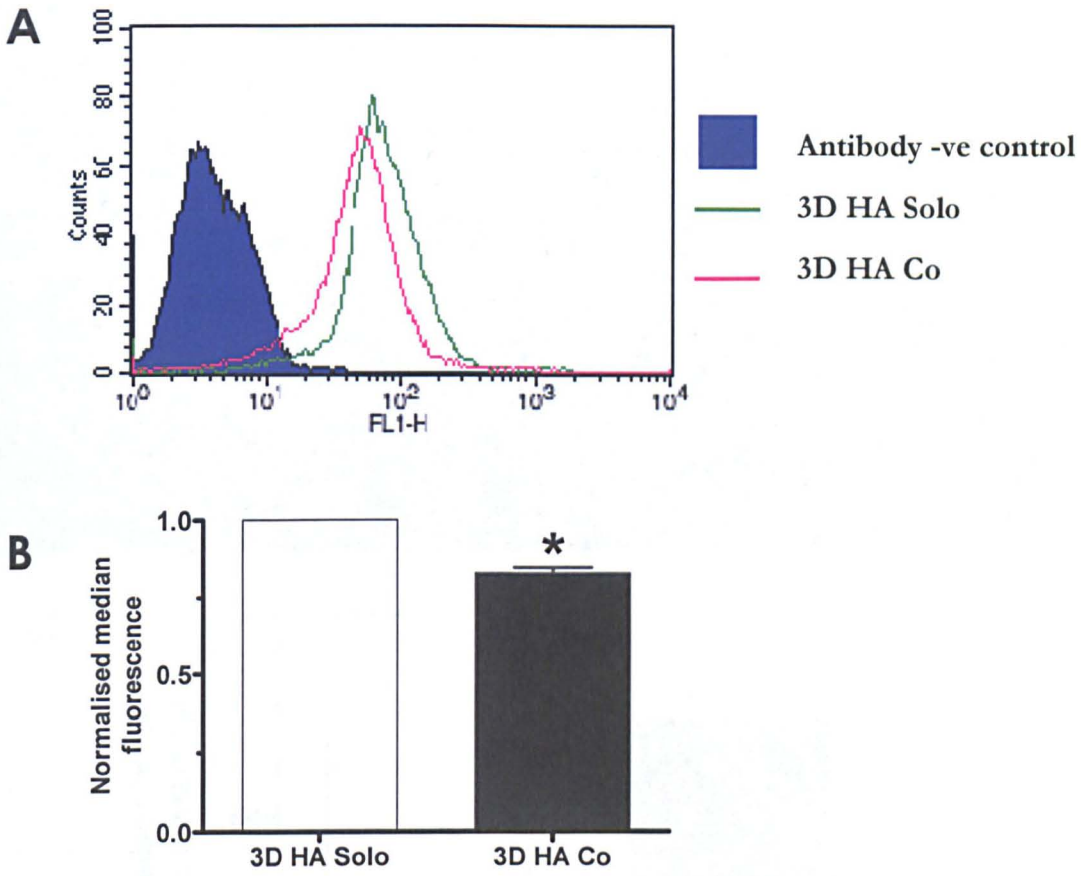

Figure 4-4 Astrocytic AQP4 expression was further decreased in 3D co-culture compared to 3D solo-culture as analysed by flow cytometry

HA were cultured in collagen gels either alone (3D HA solo) or co-cultured with hCMEC/D3 (3D HA co) for 7 days before they were isolated by two-step collagenase digestion and analysed for AQP4 expression by double immunofluorescence flow cytometry. PECAM1 was used to exclude endothelial cells. Median fluorescence values were compared between the samples. AQP4 expression was less in 3D HA co-culture compared to 3D HA solo-culture. **A:** A representative histogram plot of flow cytometry is shown. **B:** Bar diagram showing the decreased expression of AQP4 in 3D HA co-culture compared to 3D HA solo-culture. For ease of comprehension mean ± SEM of normalised data were plotted. However, a Paired *t*-test was performed on raw data. * indicates $P \leq 0.05$. N = 3.

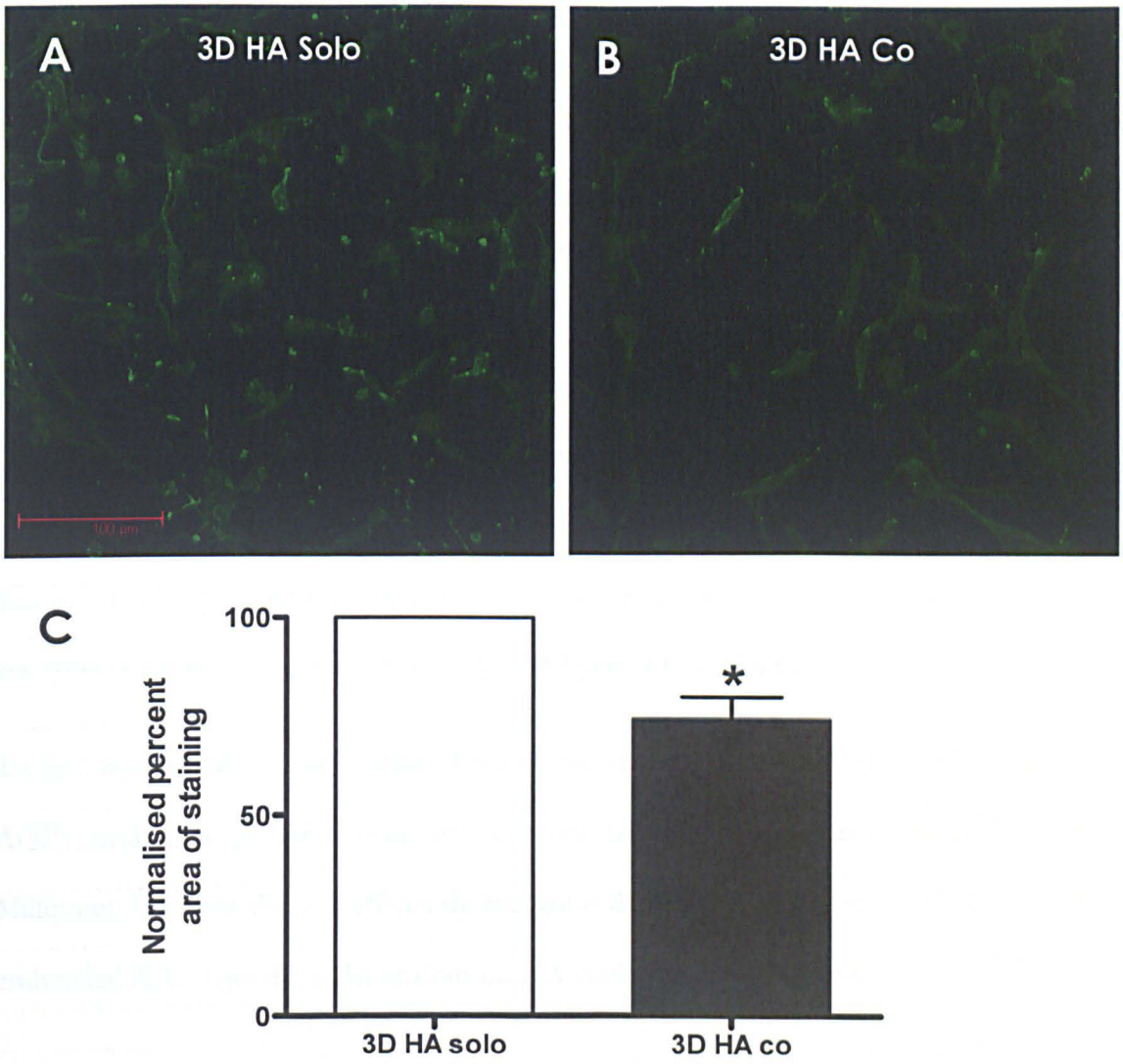

Figure 4-5 Astrocytic AQP4 was further decreased in 3D co-culture compared to 3D solo-culture as analysed by immunofluorescence microscopy

HA were cultured in collagen gels either alone (3D HA solo) or co-cultured with hCMEC/D3 cells (3D HA co) for seven days before they were fixed and analysed for AQP4 expression by immunofluorescence confocal microscopy imaging. Three random fields per sample were imaged; the percentage area of staining per cell was measured and compared between the solo and co cultures. AQP4 expression was less in 3D HA co-culture compared to 3D HA solo-culture. **A:** A representative image showing AQP4 expression in 3D HA solo-culture. **B:** A representative image showing decreased AQP4 expression in 3D HA co-culture. **C:** Bar diagram showing the statistically significant decreased expression of AQP4 in 3D HA co-culture compared to 3D HA solo-culture. * indicates $P \leq 0.05$ using a Paired *t*-test, N = 3. Scale bar represents 100 μm, and is applicable to both the images.

4.3.4 The role of endothelial-astrocyte physical contact on astrocytic AQP4 polarisation

To examine whether the astrocytic membrane in contact with endothelial cells expresses higher AQP4 compared to a non-contacting membrane, and to determine whether endothelium-released factors have any role on the expression levels or localisation of astrocytic AQP4, 3D HA solo- and co- cultures were analysed by immunogold transmission electron microscopy (TEM). 3D HA solo- and co-cultures were set up as described in section 2.2.3. HA were plated at 2×10^5 cells/400 µl and hCMEC/D3 cells were plated at 4×10^4 cells/cm^2. Visualisation by TEM revealed that there were too few physical contact points between both cell types to carry out a quantitative analysis (**Figure 4-6** and **Figure 4-7**).

To find out the role of endothelium-released factors on astrocytic AQP4 expression, anti-AQP4 antibodies procured from two commercial sources were tried (Santa Cruz and Millipore), but they did not efficiently recognise the human AQP4 epitopes on the resin embedded HA. Therefore, the analysis on HA could not be continued.

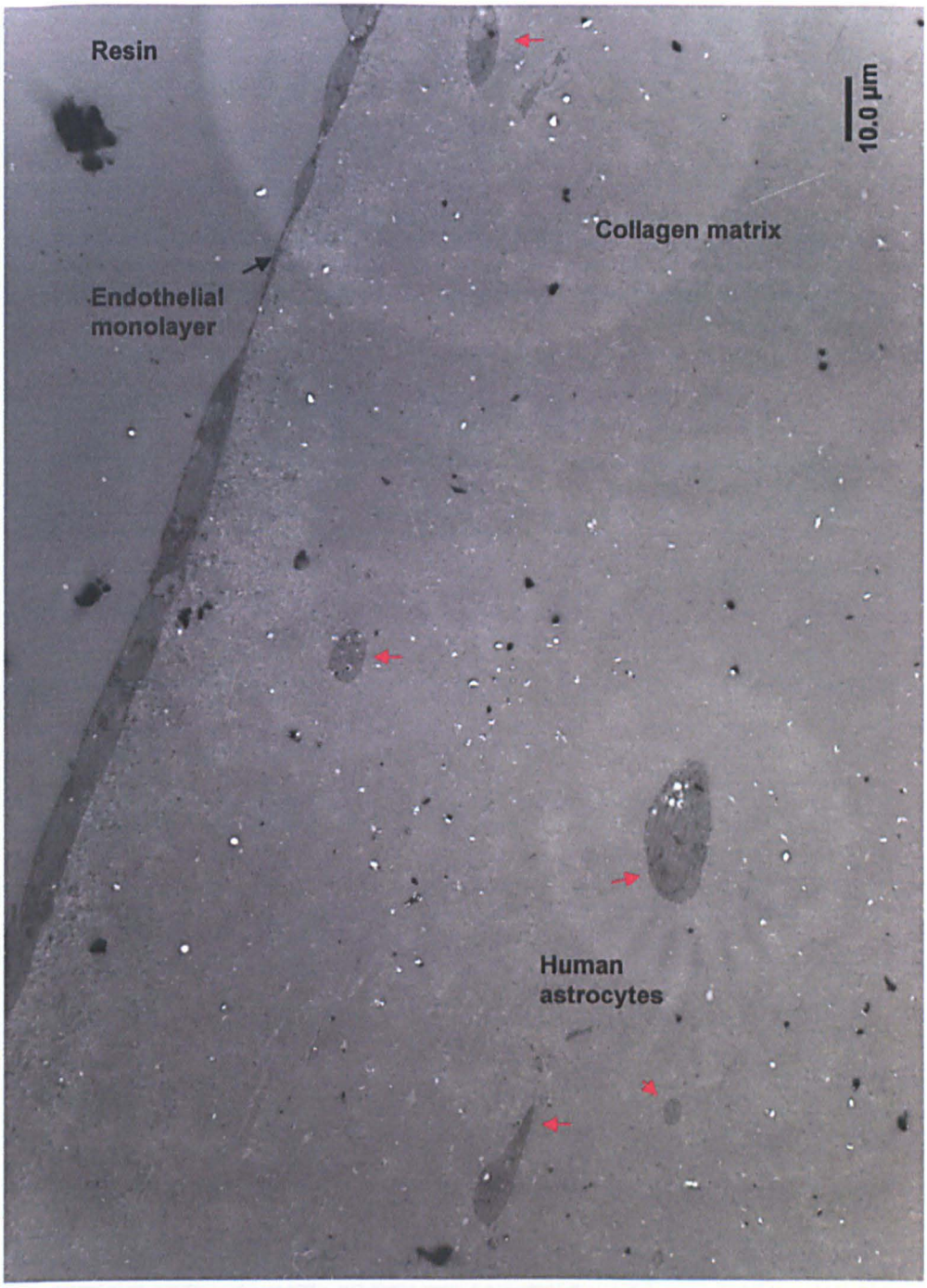

Figure 4-6 A transverse section view of a 3D HA co culture at low magnification by TEM

In a typical 3D co-culture, HA were grown inside the collagen gel matrix while hCMEC/D3 cells were grown on its surface. A transverse section of (70 nm thickness) a 3D HA co-culture in a collagen gel at low magnification is visualised using a JEOL JEM 1400 transmission electron microscope. A representative image shows sparsely distributed astrocytes (red arrows) in the gel matrix. Because of low cell density, the HA that make contact with endothelial monolayer are rare. The experiment was performed at least thrice. Scale bar represents 10 µm.

Figure 4-7 A transverse section view of a 3D HA co culture at high magnification by TEM

A representative image shows a transverse section view of a 3D HA co-culture in a collagen gel at high magnification. A 70 nm section is visualised using a JEOL JEM 1400 transmission electron microscope. In a typical 3D co-culture, HA were grown inside the collagen gel matrix while hCMEC/D3 cells were grown on its surface. An astrocyte proximal to the endothelial monolayer is shown. The experiment was performed at least thrice. Scale bar represents 2 μm.

4.3.5 3D collagen cultures are amenable to immunogold TEM

To exclude the possibility that collagen gel cultures are not suitable for immunogold TEM analysis, an experiment was carried out on primary cultures of rat astrocytes (RA). A 3D rat solo-culture was setup and analysed by immunogold TEM with the same experimental parameters that were used for HA. Millipore antibodies did recognise rat AQP4. Gold particles were predominantly present on the cell membrane while very few were present in the cytoplasm and nucleus (**Figure 4-8**). In the negative control where irrelevant rabbit IgG were used, very few randomly situated gold particles were detected. These results indicated that 3D collagen gel cultures are amenable for immunogold TEM analysis, and that the problems encountered with human astrocytes may be due to the available antibodies, being unsuitable for immunogold staining.

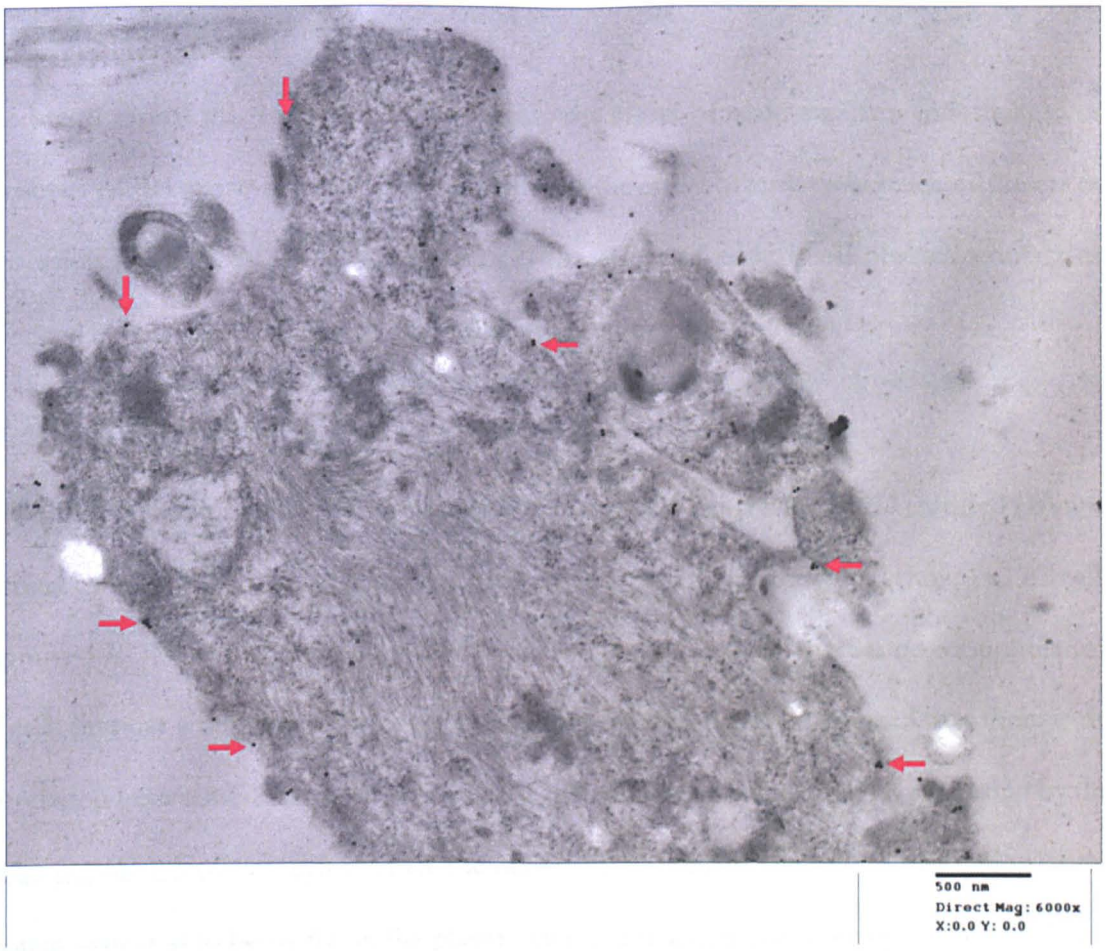

Figure 4-8 A transmission electron microscopic image showing the AQP4 expression on a rat astrocyte

A 3D RA solo-culture was set up in collagen gel matrix. After 7 days, gels were fixed, embedded into resin, and cut into 70 nm thin sections and analysed for AQP4 expression by immunogold TEM. Arrows show 10 nm gold particles conjugated to secondary antibodies that are bound to anti-AQP4 antibodies. Location of gold particles indicates that AQP4 is mainly present on the cell membrane. This demonstrates that 3D collagen gel cultures are suitable for immunogold TEM analysis. Scale bar represents 500 nm.

4.4 DISCUSSION

The broad aim of this study was to investigate the effect of brain capillary endothelium on astrocytic AQP4 expression. More specifically, (1) the effect of endothelial released factors on expression levels of AQP4 in astrocytes, (2) the effect of endothelial physical contact on polarised expression of AQP4 on astrocytic endfeet membrane.

4.4.1 HA 2D *in vitro* cultures express AQP4

In vivo astrocytes express AQP4 (Wolburg, 2009b). AQP4 expression in 2D cultured HA was verified by immunoblotting, fluorescence microscopy and flowcytometry techniques. All cells expressed AQP4 and expression levels appeared to be uniform i.e. there is no subpopulation of cells that has a different level or pattern of expression. It can be inferred that there is no correlation between GFAP expression and AQP4 expression since AQP4 is expressed by the entire population of astrocytes, which includes GFAP +ve and –ve cells. Localisation of the protein appeared to be partly on the plasma membrane and partly in cytoplasmic vesicles.

4.4.2 Role of endothelial-astrocyte physical contact on polarised expression of astrocytic AQP4 could not be studied

One of the major aims of this chapter was to analyse the effect of physical contact between endothelium and astrocytes on redistribution of astrocytic AQP4. TEM analysis revealed that there were too few physical contact points between the endothelial monolayer and astrocytes, to do a quantitative analysis. The HA cell density used in this study, 5×10^5 cells/ml, appears to be insufficient, to facilitate abundant physical contact between the two cell types. Therefore, this analysis could not be carried out further using either HA or RA.

4.4.3 3D growth environment reduces AQP4 expression in HA

After determining that 2D cultured HA express AQP4, it was examined whether a 3D growth environment alters the expression level of AQP4 in HA. Comparative expression analysis of

astrocytic AQP4 in 3D HA solo- vs. 2D HA solo-cultures by flow cytometry and fluorescence microscopy image analysis indicated that when astrocytes are transferred from a 2D growth matrix to a 3D growth matrix, their total cellular expression of AQP4 decreases without changes in the cellular localisation. This observation is consistent with East *et al.* (2009) who reported that when rat astrocytes were cultured in a 3D collagen gel matrix, their AQP4 expression was decreased. AQP4 has been shown to be overexpressed in migrating astrocytes during glial scar formation (Neal, 2007, Saadoun, 2005). In addition, AQP4 mRNA was found to be induced in reactive hypertrophic astrocytes (Vizuete, 1999). Consequently, it was used as a molecular marker to identify the reactive state of the astrocytes (East, 2009). Therefore, it may be inferred that, down-regulation of astrocytic AQP4 in 3D culture compared to 2D culture could be because the astrocytes are less reactive or less motile/mobile in a 3D collagen gel matrix.

4.4.4 Endothelial released factors reduce the astrocytic AQP4 expression

To study the role of endothelial released factors on the astrocytic AQP4 expression, HA were cultured alone (3D HA solo) or co-cultured with hCMEC/D3 cells (3D HA co) and total AQP4 expression levels were compared by two analytical techniques *viz.* flow cytometry and fluorescence microscopy. Results from these analyses indicated that total, cellular astrocytic AQP4 expression was decreased in 3D HA co-culture compared to 3D HA solo-culture.

This effect was not dependent on physical contact with hCMEC/D3 cells, as the down-regulation was homogeneous across the HA population as evidenced by a unimodal distribution of AQP4 expression in flow cytometry. Moreover, in the model used in this study, the number of HA present near the surface of collagen gel that would be in contact with hCMEC/D3 cells is small. Therefore, it was inferred that the observed down-regulation of astrocytic AQP4 in co-culture is independent of physical contact with hCMEC/D3 cells.

These observations were reproduced in a pilot study ($N=1$) of immunogold TEM analysis on RA. AQP4 expression levels on RA were decreased when co-cultured with endothelial cells (see **Appendix-C**). In co-culture, RA situated proximal to the endothelial monolayer had similar levels of AQP4 compared to those situated more distally (see **Appendix-D**). Since the aim of this project was to study HA, further study on RA was discontinued.

4.4.5 Significance of AQP4 down-regulation in CNS

Localisation of AQP4 on the perivascular endfeet of astrocytes suggests a role for AQP4 in brain water balance. It transports water to both sides i.e., into brain and out of the brain (Amiry-Moghaddam, 2003), and is involved in the water resorption of brain that occurs postnatally (Wen, 1999, Yao, 2008). In the adult, under normal physiological conditions, AQP4 seems to have a modest role as AQP4 deficient mice had normal development, survival, growth, and neuromuscular function, but had a deficit in their urinary water retention (Ma, 1997). Though Zhou *et al.* (2008) reported its beneficial role in BBB function, recent studies in AQP4 gene deletion in mice suggests its lack of role in maintenance of blood-brain barrier integrity (Saadoun, 2009, Haj-Yasein, 2011, Eilert-Olsen, 2011).

The activities of the AQP4 channel and K^+ channel are coupled on the cell membrane (Strohschein, 2011). Hence, AQP4 not only regulates water homeostasis but also indirectly regulates K^+ homeostasis of the brain. Therefore, it has a role in neuronal signal transduction as evidenced by increased seizure duration in AQP4 deficient mice (Binder, 2006). *In vitro* studies have shown that AQP4 also has a role in astrocyte migration in response to chemotatic stimuli which is required for mobilisation of astrocytes to nerve injury sites and the formation of glial scars (Saadoun, 2005).

AQP4 has a major role in pathological conditions like brain edema. In vasogenic edema, an increase of water content in the extracellular brain parenchyma occurs; whereas in cytotoxic edema, swelling of astrocytic foot processes is a prominent feature (reviewed in Francesca,

2010). Hence, AQP4 mediates opposite biological effects in cytotoxic edema and vasogenic edema.

In vasogenic edema where water enters into the brain independently of AQP4, it is cleared by AQP4 (Papadopoulos, 2004). Therefore, AQP4 seems to have a protective role in this context. In cytotoxic edema where swelling of astrocytic foot processes is the prominent feature, AQP4 seems to have a negative pathogenic role. Studies in AQP4 deficient mice have shown that AQP4 expression aggravates the edema and loss of AQP4 expression reduces the edema (Manley, 2000). Similarly, transgenic mice with overexpression of astrocytic AQP4 were shown to undergo acute cytotoxic brain swelling following acute water intoxication (Yang, 2008).

So, depending on the context, down-regulation of AQP4 could be beneficial to the CNS as in cytotoxic edema. Taken together, based on these results, it can be assumed that in pathological conditions where cytotoxic edema occurs, brain endothelial cells may have a protective function by down regulating astrocytic AQP4 through secreted factors.

4.4.6 2D cultured hCMEC/D3 cells also express AQP4

In this study, 2D cultured hCMEC/D3 cells were also found to expressAQP4, with a slightly different cellular distribution compared to HA. There are contradictory reports about the AQP4 expression in BMVEC. Sobue *et al.* (1999a) detected AQP4 mRNA in primary and immortalised bovine brain endothelial cells. Similarly, AQP4 mRNA and protein expression in rat brain microvessels was also reported (Kobayashi, 2001). Later, Amiry-Moghaddam *et al.* (2004) found low expression in mouse brain endothelial cells *in vivo* by electron microscopy. In another recent electron microscopic study, low expression was also observed in wild type mice by Haj-Yasein *et al.* (2011).

However, according to Haj-Yasein *et al.*, the few gold particles on the abluminal membrane of BMVEC actually represent the AQP4 present on the astrocytic endfoot membrane. The length of the epitope-antibody-gold particle complex is comparable to the distance between the perivascular endfoot membrane and the abluminal membrane of BMVEC. Therefore, it is possible that some of the AQP4 complexes that are actually bound to the astrocytic endfeet will appear on the BMVEC abluminal membrane. Moreover, the staining on BMVEC was observed only when they were directly apposed to astrocytic endfeet but not when pericytes were in between. Furthermore, in these mice, when AQP4 was deleted only in GFAP promoter expressing cells *i.e.*, astrocytes but not in endothelial cells, AQP4 staining was lost on the membrane of both astrocytic endfeet and BMVEC. In congruence with this study, Dolman *et al.* (2005) did not find AQP4 expression in cultured rat brain endothelial cells.

In this context, the finding that hCMEC/D3 cells do express AQP4 would add to the debate of AQP4 expression by BMVEC. In addition, this is the first study to report AQP4 expression in human BMVEC. However, this finding should be taken with a caveat that these are immortalised, *in vitro* cultured cells.

4.4.7 Limitations and future work

1. There were very few physical contact points between the hCMEC/D3 monolayer and HA. Hence, the effect of physical contact on AQP4 polarisation could not be investigated. Modification of the model is necessary to increase the physical contact between astrocytes and BMVEC and to study its effects.
2. In addition, TEM analysis of AQP4 in 2D and 3D HA needs to be carried out to complement the immunofluorescence microscopy and flowcytometry results.
3. A systematic comparison between 2D and 3D co-cultures needs to be carried out to determine whether the further down-regulation of astrocytic AQP4 in 3D co-culture is limited to 3D culture conditions.

4.5 CONCLUSIONS

1. A 3D culture environment reduces the total, cellular, astrocytic AQP4 expression.
2. In 3D co-cultures, total, cellular, astrocytic AQP4 expression decreases further.
3. The observed effect appears not to depend on the proximity between HA and hCMEC/D3 cells and hence could be mediated by a diffusible factor(s) released by hCMEC/D3 cells.
4. hCMEC/D3 cells, immortalised brain microvascular endothelial cells, also express AQP4
5. The present configuration of the model does not provide an adequate physical contact between astrocytes and the endothelial monolayer.

Chapter 5:

Role of Endothelin-1 on astrocytic AQP4 down-regulation in co-culture of HA and hCMEC/D3 cells

5.1 INTRODUCTION

Data presented in the previous chapter have shown that total, cellular, astrocytic AQP4 expression decreases when co-cultured with hCMEC/D3 cells. This effect did not seem to depend on either physical contact or proximity between HA and hCMEC/D3 cells. Hence, it appears that the effect was mediated by a diffusible factor secreted by hCMEC/D3 cells.

It has been shown that BMVEC secrete factors such as endothelin-1 (Et-1) (Bacic, 1992), leukaemia inhibitory factor (Mi, 2001) and nitric oxide (Morin, 1993) and influence the properties of perivascular cells especially astrocytes. Therefore, it was hypothesised that a soluble factor(s) released by hCMEC/D3 cells could be responsible for astrocytic AQP4 down-regulation in 3D co-cultures. We then determined whether endothelial-secreted Et-1 was a soluble factor responsible for the observed effect on AQP4.

5.1.1 Endothelin-1 (Et-1)

Endothelin-1 (Et-1), a peptide consisting of 21 aminoacid residues, is a well studied potent vasoconstrictor (Yanagisawa, 1988). Et-1 is synthesised as pre-pro-endothelin and, after a series of proteolytic cleavages by endothelin converting enzymes, the final mature peptide is secreted into the extracellular space. Endothelin-1 mediates its cellular actions through two receptors, endothelin receptor type A (EDNRA, ETA) and endothelin receptor type B (EDNRB, ETB). Both receptors are members of the G protein-coupled superfamily of receptors. Apart from these, Et-1 may bind to additional receptors that do not conform to the standard EDNRA/EDNRB classification (Warner, 1993, Shyamala, 1994, Cheng, 1993). Et-1

can act in an autocrine or a paracrine manner. Like other human vascular endothelia, BMVEC also secrete Et-1 (Bacic, 1992, Didier, 2003). BMVEC predominantly expresses EDNRA receptors (Stanimirovic, 1994) but the presence of EDNRB receptors also has been reported (Masaki, 1994). Astrocytes also secrete Et-1 (Ehrenreich, 1991) and they predominantly express EDNRB receptor (Lazarini, 1996, Hosli, 1991, Hama, 1992, Ehrenreich, 1999).

First, the secretion of Et-1 by hCMEC/D3 cells was quantitated. Then expression of EDNRB receptors on HA was analysed. Finally, the possible effects of exogenous Et-1 on AQP4 expression were investigated.

5.2 METHODS

The reagents and antibodies used in this study are listed in **appendices A** and **B** respectively.

5.2.1 Culture setup and supernatant collection

To determine whether hCMEC/D3 cells secrete Et-1 in solo and co cultures, both cultures were set up as described in section 2.2.3. 3D HA were plated in a 24 well plate at 2 x 10^5 cells/400 µl and hCMEC/D3 cells were plated at 8 x 10^4 cells/well. 2D HA culture (2 X 10^5 cells) was set up on the surface of collagen gel (400 µL) in a well of 12-well plate. Cultures were maintained in 2.5 ml of D3M media. After 3 days, culture media supernatants were harvested for assay. In all experiments, supernatants were mixed with a protease inhibitor cocktail, then stored at -70 °C until analysed by ELISA.

5.2.2 Transwell insert cultures to analyse polarised secretion of Et-1

HA and hCMEC/D3 cells were plated onto collagen coated transwell inserts in D3M (1 x 10^5 cells/insert). The insert membrane is made of polyester (PET), with an effective growth surface area of 1.12 cm^2, with a pore size of 0.4 µm, and with a pore density of 4 x 10^6 pores/cm^2. After 3 days, nutrient culture media was replaced with fresh media. After 24 h, culture media were harvested from the upper and lower compartments. To assess the collagen coating effect on Et-1 diffusion through the insert membrane, nutrient culture media collected from 2D cultures of hCMEC/D3 cells were placed onto collagen-coated, and uncoated empty transwell inserts, and collagen-coated and uncoated plastic culture dishes, and harvested after 24 h and analysed by ELISA.

5.2.3 Et-1 estimation in the culture supernatants by ELISA

Et-1 concentration in the culture supernatants was measured by Enzyme linked immuno-sorbent assay (ELISA) (Assay Designs) as per the manufacturer's instructions. If required, samples were diluted, to bring the Et-1 concentration into the linear range. Standards with

known concentration of Et-1 ranging from 0.73 pg/ml to 100 pg/ml were included in the assay. Optical density at 405 nm was measured using a BMG Optima ™ plate reader. The standard values were plotted using a 4-Parameter curve fitting algorithm and the concentration of Et-1 (pg/ml) in the test samples was derived by interpolation and the final concentration was obtained after adjusting for sample dilution.

5.2.4 Expression analysis of astrocytic EDNRB by flow cytometry

Cultures were set up as described in section 5.2.1 and maintained for 7 days before the cells were isolated from the gels by collagenase digestion (section 2.2.4). Permeabilised cells (0.05% saponin) were analysed by flow cytometry for EDNRB as described in section 2.2.9. Median fluorescence values were used to compare the samples. For each experiment the arithmetic mean of duplicate/triplicate treatments was calculated and these values were converted into ratios using 2D HA solo value as reference (denominator). Thus, normalised data were used for plotting. However, raw data were used for statistical testing.

5.2.5 AQP4 expression analysis in Et-1 treated 3D HA solo-cultures

3D HA culture (2×10^5 cells/gel/400 µL) was set up in a 24-well plate. Cultures were treated with either Et-1 peptide at 100 pM concentration or an equal volume of PBS (vehicle control). Nutrient culture medium was changed after the 3 rd and 5th day. After 7 days, the cells were isolated from the gels by collagenase digestion and analysed by flow cytometry for AQP4 (H 80). The data was analysed as explained in the above section except that the data was normalised by converting into ratios using Mock treatment/control value as reference (denominator).

5.2.6 Statistical analysis

Statistical significance of data was assessed by Paired *t*-test. $P \leq 0.05$ was considered as significant. * indicates $P \leq 0.05$, ** indicates $P \leq 0.01$, *** indicates $P \leq 0.001$.

5.3 RESULTS

5.3.1 hCMEC/D3 cells secrete Et-1 in solo- and co- cultures

Et-1 concentration in culture supernatants of hCMEC/D3 solo cultures was 87.6 ± 10.3 pM and in the co-cultures was 72.9 ± 8.2 pM (**Figure 5-1**). This indicates hCMEC/D3 solo-cultured cells secrete Et-1 into culture media and continue to do so in co-culture. The apparent decrease (~16.7%) in Et-1 concentration in co-cultures compared to hCMEC/D3 solo-cultures was statistically not significant.

5.3.2 HA secrete low levels of Et-1 compared to hCMEC/D3 cells

To determine whether 3D cultured HA secrete Et-1, culture media was analysed by ELISA. Estimated Et-1 concentration in culture supernatants 3D HA solo-cultures was 1.1 ± 0.1 pM (**Figure 5-1**). This is ~70 fold less than in the co-culture media (72.9 ± 8.2 pM). Therefore, it is likely that the predominant source of the Et-1 found in the co-culture media is hCMEC/D3 cells. The apparent decrease (~52.1%) in Et-1 release by 3D HA (1.1 ± 0.1 pM) compared to 2D HA cultures (2.3 ± 0.5 pM) was statistically not significant.

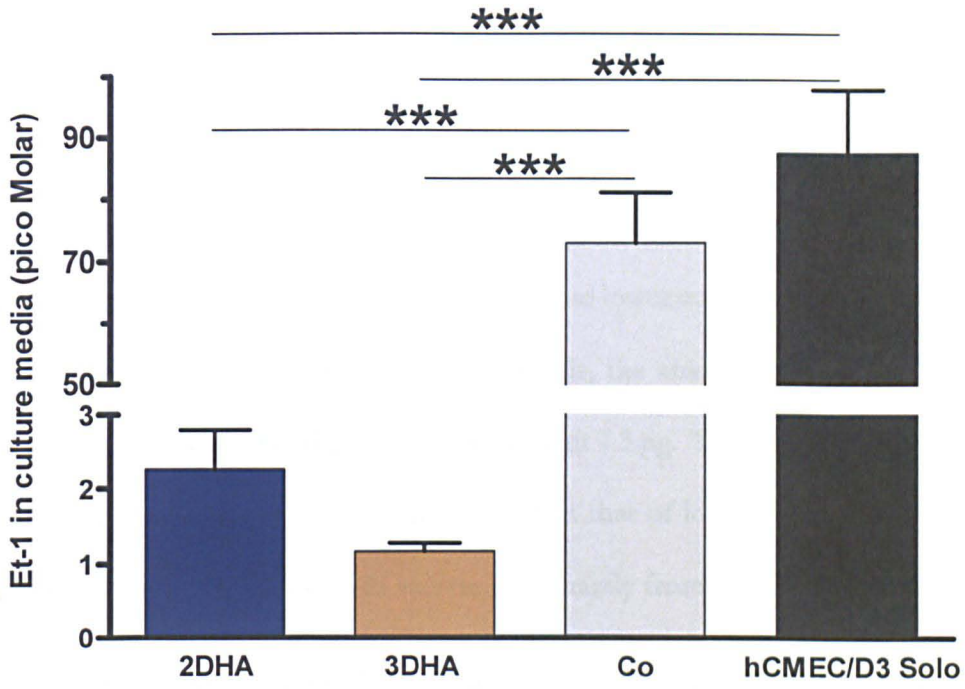

Figure 5-1 Et-1 concentration in culture media of hCMEC/D3 and HA

Et-1 concentration in culture media of 2D HA, 3D HA, hCMEC/D3 solo and co cultures was measured by ELISA. Bar diagram showing the Et-1 concentration (pico Molar units) in culture media of four different culture types. Each bar represents the mean ± SEM of data obtained from seven experiments. Both hCMEC/D3 cells and HA secrete Et-1 and continue to do so in co-cultures. The culture media of both hCMEC/D3 solo- and co- cultures have higher levels of Et-1 compared to that of 2D HA or 3D HA solo cultures. The apparent difference in the Et-1 levels between 2D HA and 3D HA and between hCMEC/D3 solo- and co- cultures is statistically not significant. *** indicates $P \leq 0.001$ using Paired *t*-test. N = 7.

5.3.3 hCMEC/D3 cells appear to secrete Et-1 predominantly from the apical surface.

To determine whether Et-1 secretion by hCMEC/D3 cells is directional, a pilot experiment (N = 1) was carried out. hCMEC/D3 cells were cultured on triplicate transwell inserts, and Et-1 secreted into nutrient culture media of the upper and lower compartments was measured by ELISA. In transwell cultures of hCMEC/D3 cells, the amount of Et 1 in the upper compartment was 88.2 pg, and in the lower compartment 7.3 pg. The amount of Et-1 present in the upper compartment was ~12.0 fold higher than that of lower compartment. These results suggested that hCMEC/D3 cells secrete Et-1 mainly from apical surface.

To examine the role of the insert membrane and collagen coating on Et-1 diffusion across the membrane, a pilot experiment was carried out (N = 1). Freshly harvested hCMEC/D3 culture media was placed in the upper compartment, after 24 h Et-1 concentration was measured in both the compartments. Concentration (pg/ml) rather than total protein (pg) was compared to determine the free diffusion across the insert membrane. The plastic culture well alone was used as the control. In both collagen-coated and uncoated inserts, Et-1 concentration (pg/ml) in the upper compartment was ~2.5 fold higher than that of the lower compartment (**Table 4**). These results suggest that although Et-1 is able to diffuse through the porous membrane, the diffusion was slow since concentrations did not reach equilibrium on both sides of the membrane until 24 h. In addition, collagen coating did not have an effect on this process. These results suggest that the insert membrane partly impedes Et-1 diffusion. As the insert-membrane's properties alone cannot explain the ~ 12-fold difference in the Et-1 levels in upper and lower compartments, it appears that these cells do indeed secrete Et-1 mostly from their apical surface.

Table 4 Diffusion of Et-1 through the transwell membrane

	Et-1 concentration (pg/ml) (Mean of triplicate measurements)	
	Collagen coated	**Uncoated**
Plastic well (500 μL)	49.6	52.7
Upper compartment: Transwell (500 μL)	19.23	18.7
Lower compartment: Transwell (1500 μL)	7.16	7.96

5.3.4 HA express EDNRB in 3D solo- and 3D co- cultures as analysed by flow cytometry

To respond to Et-1, astrocytes require EDNRB receptor. Therefore, a comparative expression analysis of EDNRB in all three culture types *viz.*, 2D HA solo-, 3D HA solo- and 3D HA co-cultures was carried out by flow cytometry (**Figure 5-2 A**). EDNRB expression in 3D HA solo-culture was slightly (~16%) decreased compared to 2D HA solo-culture (**Figure 5-2 B**). The observed down-regulation was statistically significant. There was no statistically significant difference between the EDNRB levels of 3D HA solo-culture and 3D co- culture. These results suggested that HA continued to express EDNRB in 3D co-culture and so would be able to respond to Et-1.

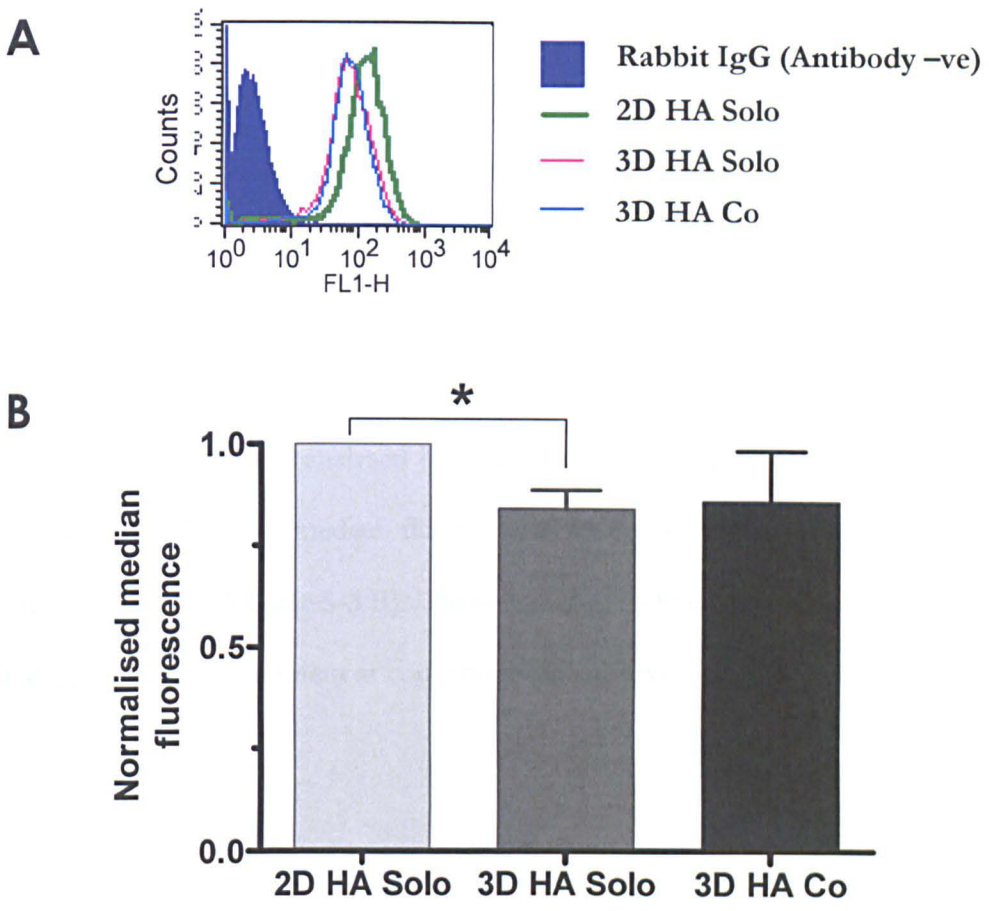

Figure 5-2 Astrocytic EDNRB expression analysis by flow cytometry

Expression analysis of EDNRB in 2D HA solo-, 3D HA solo- and 3D HA co- cultures was carried out by flow cytometry. **A:** A representative histogram of flowcytometry analysis is shown. **B:** Within each experiment, values were converted into ratios using the 2D HA solo value as reference. Each bar represents the mean ± SEM of normalised median fluorescence value. Statistical analysis was carried out on the raw data. EDNRB expression in 3D HA solo culture was ~16% decreased compared to 2D HA solo culture while there was no statistically significant difference between 3D HA solo culture and 3D co culture. These results suggest that HA retained the expression of EDNRB in 3D HA co-culture and so would be able to respond to Et 1. * indicates $P \leq 0.05$ using Paired *t*-test, N = 3.

5.3.5 Exogenous Et-1 exposure did not affect astrocytic AQP4 expression levels as analysed by flow cytometry

Having determined that hCMEC/D3 cells continue to secrete Et-1 in co-culture (72.9 ± 8.2 pM), the effect of exogenously added Et-1 peptide to culture medium on the astrocytic AQP4 expression levels was investigated. 3D HA culture was treated with 100 pM Et-1, a concentration that approximates that previously measured in 3D co-culture media, and total cellular AQP4 expression was analysed by flow cytometry (**Figure 5-3 A**). Compared to vehicle-treated 3D HA, the median fluorescence values of Et-1-treated 3D HA were statistically not different (**Figure 5-3 B**). These data suggest that astrocytic AQP4 expression was not affected by Et-1 treatment at concentrations observed in the 3D co-culture media.

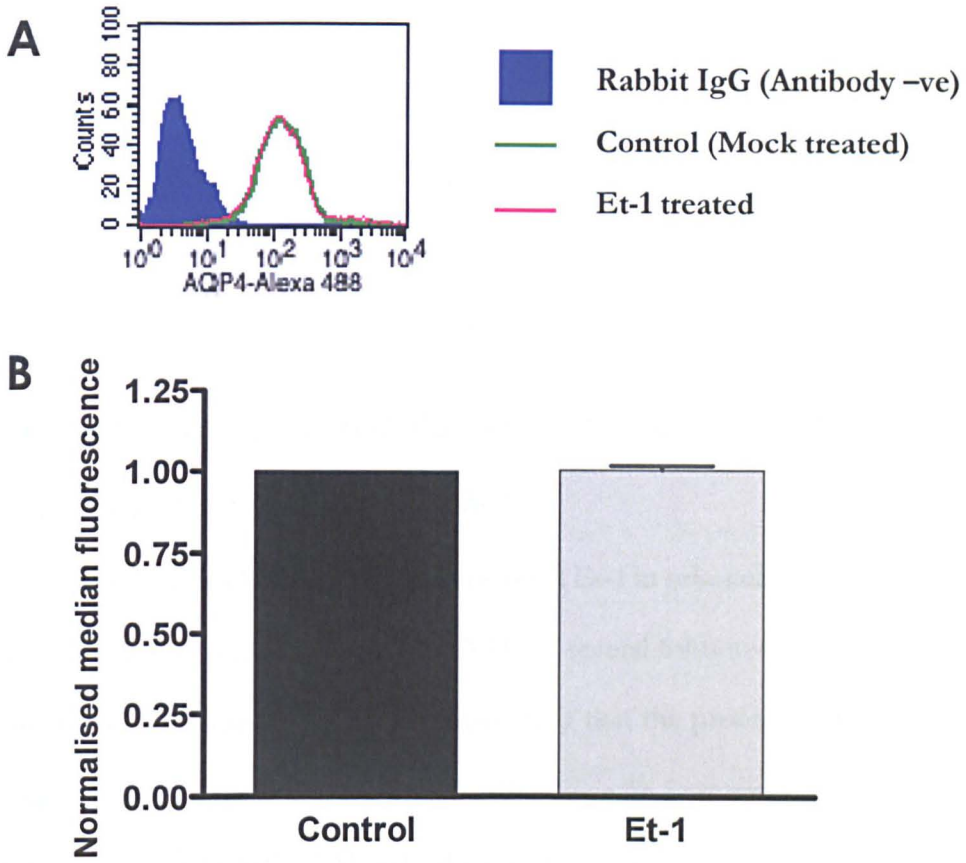

Figure 5-3 Effect of exogenous Et-1 on astrocytic AQP4 expression

3D HA culture was treated with 100 pM Et-1 for seven days, before total cellular AQP4 expression levels were analysed by flow cytometry. **A:** A representative histogram of flowcytometry analysis is shown. **B:** Within each experiment, values were converted into ratios using mock treatment (control) as reference. Each bar represents the mean ± SEM of normalised median fluorescence value. Statistical analysis was carried out on the raw data. Compared to mock treated 3D HA, the median fluorescence value of Et-1 treated 3D HA was not different. This suggests total cellular astrocytic AQP4 expression was not affected by exogenous Et-1 treatment. $P \leq 0.05$ was accepted as significant using Paired *t*-test, N = 3.

5.4 DISCUSSION

It was hypothesised, based on the results presented in chapter 4, that a diffusible factor(s) released by hCMEC/D3 cells could be responsible for the astrocytic AQP4 down-regulation in 3D co-cultures. Since BMVEC secrete Et-1, the possibility of Et-1 as a mediator of the observed effect was investigated in this chapter.

5.4.1 Et-1 secreted by hCMEC/D3 cells may act on HA through EDNRB receptor in a paracrine manner

First, it was confirmed that hCMEC/D3 cells secreted Et-1 in solo-cultures and in co-cultures with HA. The amount of Et-1 secreted by 3D HA is several folds lower than that present in culture media of co-cultures. Hence, it is most likely that the predominant source of Et-1 found in the co-cultures is from hCMEC/D3 cells. Since Et-1 secreted by HA themselves is several fold lower than hCMEC/D3 cells, the effect of astrocytic Et-1 would have a smaller role on astrocytic AQP4 down-regulation than the paracrine effect of Et-1 released by hCMEC/D3 cells.

Astrocytes mainly express EDNRB (Hosli, 1991, Hama, 1992, Ehrenreich, 1999, Wang, 2006). It also has been shown that Et-1 acts through EDNRB receptor to bring about AQP4 down-regulation in rat astrocytes (Koyama, 2010, Tanaka, 2011). Therefore, to respond to Et-1 released by hCMEC/D3 cells, HA in 3D co-culture should express EDNRB receptors on them. Flow cytometry has shown that HA express EDNRB receptor in 3D co-culture at a similar level to 3D solo-culture. Taken together, in 3D co-culture, by virtue of their EDNRB expression, HA would be able to respond in a paracrine manner to Et-1 released by hCMEC/D3 cells.

5.4.2 Directional secretion of Et-1 by hCMEC/D3 cells

Results of a pilot experiment suggested that hCMEC/D3 cells appear to secrete Et-1 from their apical surface. This observation is contradictory to previous published studies. HUVEC cells that are grown on an acellular amniotic membrane (Wagner, 1992) and bovine brain capillary cells that are grown on transwell insert membranes (Dehouck, 1997) have been shown to secrete Et-1 mostly to basolateral side. It is possible that species differences, prolonged *in vitro* culture, or the immortalised nature of the cells used in this study could have contributed to these conflicting results. If indeed, the endothelial cells secrete predominantly to the apical side, much of the released Et-1 would enter the blood circulation and act in an endocrine manner rather than on abluminally-situated astrocytes in a paracrine manner.

The directionality of Et-1 secretion is an important issue in the 2D transwell insert co-culture models, since the secreted Et-1 should be able to reach the target cells present in the basal compartment to act upon them. Unlike the insert membrane culture where the monolayer forms a tight barrier without gaps between the monolayer and the insert wall, Et-1 can freely diffuse into 3D collagen gel cultures through the side gaps into the gel containing the astrocytes. So, in the model used in this study, even if hCMEC/D3 cells secreted Et-1 exclusively to apical side, the Et-1 could still reach the HA present on the basal side by diffusing through the gap between the monolayer and the wall of the culture dish.

5.4.3 Et-1 by itself does not mediate astrocytic AQP4 down-regulation in co-culture

Having estimated the concentration of Et-1 that HA were subjected to in 3D co-cultures, and having determined that HA express EDNRB in 3D co-culture, it was examined whether exogenous addition of Et-1 into culture media of 3D HA solo-culture, would decrease AQP4 expression. Results show that exogenous addition of Et-1 did not have an effect on the total

cellular AQP4 expression levels. This indicates that Et-1 by itself cannot cause the decrease in astrocytic AQP4 in co-culture.

This result is in contradiction to the study of Tanaka and Koyama on *in vitro* cultured rat astrocytes, in which exogenous treatment of Et-1 at 100 nM concentration for 12 h decreased the expression of cell membrane and total cellular AQP4 protein (Tanaka, 2011). They have also shown that Et-1 induces down-regulation of AQP4 through EDNRB receptor activation (Koyama, 2010). The discrepancy between their work and the present study could be attributed to any of the following three factors. (1) This study used 3D human astrocyte cultures while they have used 2D rat astrocyte culture. (2) In their case, Et-1 treatment was carried out in the absence of serum while in this study it was performed in the presence of serum. (3) While they have used MEM, this study was carried out using endothelial growth medium with growth factors (EGM-2-MV®), referred to as D3M in this thesis.

Based on the results observed in this study, it can be speculated that Et-1 by itself is not responsible for the effect and therefore, either endothelial released factor(s) other than Et-1 or Et-1 in conjunction with some other factor could be responsible for the down-regulation of astrocytic AQP4 in the 3D co-culture model.

5.4.4 Decreased expression of EDNRB in 3D HA culture may indicate a less reactive state

In the present study, in 3D HA, compared 2D HA, EDNRB expression was slightly (~16%) decreased but Et-1 secretion did not change. Astrocytes are autocrine targets of Et-1 (Hasselblatt, 2003, Lazarini, 1996). Increased expression of Et-1 and EDNRB receptor after CNS injury has been reported (Rogers, 1997, Baba, 1998, Rogers, 2003). A causative role of Et-1 on the induction of reactive gliosis *in vivo* through the EDNRB receptor also has been demonstrated (Koyama, 1999, Gadea, 2008). Taken together, although Et-1 did not change,

the decreased expression of EDNRB may signal a less reactive state of HA in 3D collagen culture.

5.4.5 Limitations of the study and future work

The hypothesis of this part of investigation was that astrocytic AQP4 down-regulation in co-culture was caused by a soluble factor, Et-1, released by hCMEC/D3 cells. To test this hypothesis, the effect of exogenous addition of Et-1 was investigated, based on the available literature (Koyama, 2010, Tanaka, 2011). To reach definitive conclusions, the investigation could be continued by examining whether hCMEC/D3 cell conditioned media can produce the same effect *i.e.,* AQP4 down-regulation in 3D HA culture. After confirming the role of certain soluble factor(s) in this process, identification of the candidate factor(s) could be determined as described below.

The role of known soluble factors released by endothelial cells, such as leukaemia inhibitory factor and nitric oxide, in this phenomenon can be determined in two steps. (1) Analyse the effects by blocking the synthesis of the factor of interest (e.g., RNA interference) or by inhibiting its functional activity using a specific antibody or a specific inhibitor molecule against it or its receptor. (2) Then, confirm the effects observed in the previous step by exogenous addition of the factor to the culture media.

To find out the role of unknown soluble factors in this phenomenon, the identity of these factors can be determined by fractionation of culture supernatants e.g., by gel filtration or ion exchange chromatography (Gupta, 1995) followed by the examination of the effects of these fractions on the astrocytic AQP4. Alternatively, a high throughput approach such as mass-spectrometric analysis of culture supernatants of hCMEC/D3 cells can be performed, which enables the detection of even low abundance proteins (Finoulst, 2011, Mattow, 2003). The secretome of BMVEC has not been determined however, the secretome of human umbilical vein endothelial cells grown under static conditions, consisting of 78 proteins, has

been reported recently (Burghoff, 2011). Serum free culture and stringent washing can circumvent the problem of sample contamination with bovine serum proteins (Pellitteri-Hahn, 2006).

5.5 CONCLUSIONS

In co-culture, although hCMEC/D3 cells secrete Et-1, it is by itself not responsible for the astrocytic AQP4 down-regulation. Further work is needed to identify the factor(s) released by hCMEC/D3 cells that is/are responsible for astrocytic AQP4 down-regulation.

Chapter 6:

Summary and Final Discussion

6.1 Summary of the results

Establishment of the model

The main drawback of the current 2D co-culture models of astrocytes and endothelial cells is that astrocytes are cultured on a 2D surface. In this study, with an aim to improve upon this shortcoming, an *in vitro* human 3D co-culture model was developed using collagen type-I as 3D matrix. The basic principle of the design of the model is to mimic the *in vivo* geometric relationship between endothelium and astrocytes at the BBB. In this model, human primary astrocytes were cultured inside the collagen gel while hCMEC/D3 cells were cultured on the surface of the gel. Both cell types were of human origin. The main features of the model, as presented in section 2.1, are:

1. Culture of astrocytes in a 3D environment.
2. Interaction of 3D cultured astrocytes with the abluminal side of the endothelial monolayer, mainly through soluble factors.
3. Culture of the endothelium on a soft substrate as opposed to the hard substrate in a conventional 2D culture system.

3D HA differ from 2D HA but not in their barrier enhancing properties

To determine the effect of the 3D environment on HA, the proliferation rate and the expression of four molecules namely, GFAP, AQP4, Et-1, EDNRB were compared between 3D and 2D HA. Increased expression of GFAP (Wu, 1998), AQP4 (Vizuete, 1999), Et-1 and EDNRB (Koyama, 1999, Gadea, 2008) are considered as markers of reactive astrocytes. Although GFAP expression and Et-1 release did not suggest reduced reactivity of 3D HA, the

decreased expression of AQP4 and EDNRB did so. Most importantly, the reduced proliferation rate of 3D HA suggested their reduced reactivity and a similarity to their *in vivo* counterparts. Taken together these data suggest that 3D HA differ from 2D HA in some of their properties, and resemble more closely *in vivo* HA.

Following this, it was investigated whether they differ in their barrier induction capacities. Analysis of three expression markers (ZO-1 and CLDN5, and ABCB1) of barrier phenotype and paracellular permeability suggested that 3D HA were not different from 2D HA in their barrier phenotype induction potential. However, to come to a more definitive conclusion, more work is needed as discussed in chapter 3 (section 3.4.4).

Effect of endothelium on astrocytic AQP4 expression

The established model was used to study the effect of endothelium on AQP4 expression in HA. It was found that total, cellular astrocytic AQP4 expression decreases when co-cultured with endothelial cells. The results could not be explained by physical-contact and therefore endothelial released factors may be implicated. The role of Et-1 was investigated; however, the results showed that Et-1, at least by itself, does not induce astrocytic AQP4 down-regulation. Further work, as discussed in section 5.4.5, is necessary to identify the responsible factor(s). The role of endothelial-astrocyte physical contact on astrocytic AQP4 localisation could not be studied since there were very few contact points between the endothelial monolayer and astrocytes, as revealed by TEM analysis. Potential improvements to the current 3D model to increase physical contact between astrocytes and endothelial cells are discussed in section 6.3.1.

6.2 Critique of the model

The model developed in this study is easy to set up, monitor, and analyse by various analytical methods. The design and configuration of the model is novel and has been implemented for the first time.

6.2.1 Utilities of the model developed in this study

The model can be used to study both endothelial cells and astrocytes and the effect of each cell type on each other. The model, as demonstrated in this study, is amenable to analytical methods such as immunofluorescence microscopy, flowcytometry, ELISA, and immunogold TEM. The two-step collagenase digestion method developed in this study broadens its usability. The method can be used to isolate endothelial cells and astrocytes from the gel into two separate cell fractions with >90% purity. For experiments where 90-95% purity is not enough, it is possible to improve the purity by doing an extra wash step after detachment of endothelial monolayer. These cell suspensions can be used to prepare cell lysates or to isolate nucleic acids, which then can be analysed by even more molecular biology techniques such as western blotting, RT-PCR, transcriptome profiling, and proteome profiling. While the model is very useful to study the effect of endothelium on astrocytic biology, there are some assets and limitations to study the effect of astrocytes on endothelium. The model developed in this study has the following utilities.

1. **Role of astrocytes on barrier phenotype of endothelium.** In this model, endothelial cells are cultured as a monolayer, which makes it easy to study the expression markers of barrier phenotype such as tight junctions, and transporter molecules using fluorescence microscopy, TEM, or flowcytometry *etc.* Although not demonstrated in this study, it is possible to analyse directly the endothelium on the gel surface, or after harvesting the cells by the two-step collagenase digestion method, to

determine how its barrier markers are affected by the inductive effect of astrocytes or any other barrier enhancing or destructive agent.

2. **Nanoparticle delivery across BBB.** CNS drug delivery is a major challenge because of the protective function of BBB. Using nanoparticles as carriers to deliver drugs into CNS is currently an active area of research (reviewed in Haque, 2012). Using this model, the ability of nanoparticles to cross a BMVEC monolayer and to target brain resident cells such as astrocytes can be studied. The model has been successfully employed by our laboratory to study the transfer of glucose-coated nanoparticles across hCMEC/D3 monolayers and targeting to HA that are embedded in the gel. Gold nanoparticles were visualised by silver enhanced TEM (data not shown). The leakage of particles (27kDa, 5nm) at the edge of the gel was not a problem in this study, since there was no evidence for a higher rate of diffusion at the edge of the gel, in comparison to the centre. Therefore, the model may be used, not only for nanoparticle crossing, but also other macro substances such as DNA plasmid vectors (6 kb = ~40 nm), and infectious agents such as viruses (20-400 nm) or bacteria (0.2-5 μm). Altogether, the model mimics the *in vivo* configuration of endothelial barriers and brain parenchyma, and is suitable for investigation of crossing of macro substances ($\geq$ 5 nm) across the endothelial barrier and entry into cell types that are seeded in the collagen gel. Apart from astrocytes, other brain resident cell types such as neurons can be seeded into the collagen gel and can be studied. When fluorescent-tagged nanoparticles are used, it is possible to detect them by fluorescence microscopy.

3. **Transmigration of leukocytes across the endothelial monolayer.** During an inflammatory response, leukocytes transmigrate across the endothelium, and then move along chemotatic gradients into the site of damage or infection. The current model is suitable for studying the different stages of the transmigration process. Cell

tracker loaded leukocytes can be plated onto the endothelial monolayer, after a certain time, those that transmigrate and enter into the collagen gel can be detected by fluorescence microscopy. This analysis can be carried out in real-time or at an end-point (by fixing the gels). The role of normal and inflamed astrocytes (stimulated with cytokines such as tumor necrosis factor-alpha and interferon gamma) on the transmigration process can be studied. The suitability of the model for these experiments is currently being tested in our laboratory (data not shown). It is possible to create a gradient of astrocyte-released factors by seeding the astrocytes at varying densities within a gel, in order to study whether leukocytes are attracted towards the high cell density regions.

4. **Biology of astrocytes.** This model is very convenient for investigating astrocytic biology. As demonstrated in this study, the model can be used to study the effect of endothelial released soluble factors on astrocytes with the added advantage of studying 3D cultured HA, which makes the findings more relevant to the condition *in vivo*. Known effects of endothelium on astrocytic functions such as proliferation, differentiation, calcium signalling *etc.* were derived from studies on 2D cultured HA (section 1.7). To increase the relevance of these observations, such analyses should be carried out using the present model. In the present configuration, only soluble factor-mediated but not contact-dependent properties can be studied.

5. **Proximity dependent effect.** In this co-culture model, HA are situated all along the depth of the gel, and those at the top are nearest to endothelial cells, and those at the bottom are farthest. If a factor released by endothelial cells is not freely diffusible in the collagen matrix, a gradient of concentration can form with the highest concentration near to the endothelial cells and lowest at the bottom of the gel. In such a scenario, the response of proximal astrocytes may differ from the distal astrocytes.

The feasibility of studying differential spatial effects that are dependent on proximity is a striking advantage of the present model over existing 3D culture models and 2D culture models. The feasibility of this approach was demonstrated in this study, through a pilot experiment that compared the astrocytic AQP4 levels in proximal versus distal astrocytes in a co-culture (Appendix-D). In this study, the analysis was carried out by immunogold TEM; however, fluorescence microscopy can be also used.

6.2.2 Limitations of the model

In this model, HA were seeded in the gel at 0.5 million per ml, which is ~40 times lower than the *in vivo* cell density. Because of the low cell density, cell-cell interactions amongst HA are minimal, and between HA and endothelial monolayer are negligible. Cell density could not be increased since it causes gel contraction.

The model can be set up in a transwell insert, so that TEER can be measured. However, there are two concerns. One, low TEER (<40 $\Omega.cm^2$) of hCMEC/D3 cells make the model less than ideal for the TEER based experiments. Two, it was expected that there may be a small gap between the gel and the wall of transwell insert although the gel visually appears to be un-contracted at the current cell density. This gap cannot be sealed by the confluent endothelial monolayer on a gel, unlike in a routine 2D transwell system, where the endothelial monolayer grown directly on an insert membrane seals the gap by tightly abutting the insert wall. It was presumed that the leakage of ions, through this gap might further contribute to the decrease in the TEER value. Therefore, the model at the present configuration using hCMEC/D3 cells is not suitable for TEER measurement studies. The model substituted with different BMVEC that have better paracellular tightness may make the model suitable for TEER based studies, but it remains to be tested.

To carry out paracellular permeability and drug efflux assays, it is required to measure the concentration of substance that crossed the monolayer. There is no simple way to quantify the

substance that has entered into the gel, unlike in a transwell system where the lower chamber fluid is easily accessible to determine the concentration. Altogether,

1. The model is currently not convenient to assess the functional barrier phenotype of endothelium.
2. The model does not provide adequate physical contact between the endothelial monolayer and astrocytes, hence it is not suitable to study contact dependent properties on either endothelium or astrocytes.

6.2.3 Comparison with 2D co-culture models

To study endothelial cells

The most important feature of the model is that HA are cultured in a 3D matrix and therefore are expected to display different properties to 2D HA. The study has demonstrated that 3D HA indeed behave differently from 2D HA and resemble astrocytes *in vivo* by being quiescent. Therefore, it was investigated whether 3D HA have improved barrier-inducing potential than 2D HA and if usage of 3D HA is beneficial over 2D HA to build a tighter *in vitro* BBB model. However, the results showed that 3D HA did not differ from 2D HA in their barrier phenotype enhancing capacities. Since the present study is not comprehensive (section 3.4.4), a more thorough investigation is needed to decide upon the advantage of 3D HA over 2D HA to build a tighter *in vitro* BBB model.

Another distinct feature of the 3D model developed in this study, compared to 2D co-culture models, is its better resemblance to the *in vivo* BBB configuration. Whether this simulation has improved the barrier-phenotype of endothelium (*in situ*) that is cultured on the gel surface has not been tested in this study. A main asset of a 2D transwell model is its amenability to evaluate functional barrier phenotype directly on the endothelial monolayer (Ogunshola, 2011). The 3D model developed in this study, even if it is set up in a transwell insert, is not convenient to do functional assays such as paracellular permeability, TEER measurement, and drug permeability, directly on the endothelial monolayer (*in situ*) that is present on the gel surface. In these aspects, as an *in vitro* BBB model, the present model has limited usability compared to 2D transwell models. The present model also lacks in provision of shear stress, which is being furnished in the flow-based models developed in recent times (section 1.8.2).

To study astrocytes

A self-evident advantage of the present model over 2D co-culture models is the facility to study astrocytes in a more physiologically relevant state. Therefore, the model may be useful to reassess the existing findings of 2D models, to determine their translatability to the situation *in vivo*. However, only soluble factor mediated, but not physical contact dependent, effects can be studied. In the aspect of physical contact between endothelium and astrocytes, the model is better than non-contact transwell cultures but similar to contact transwell cultures as TEM analysis revealed few physical contact points between the cell types. Another advantage of the present model over 2D models is the facility to study proximity dependent effects. In 2D cultures, all astrocytes are in a single plane but in the present model, astrocytes are situated all along the height of the gel at different distances from the endothelial monolayer. Apart from these, setting up 3D co-cultures using collagen type-I is cost-effective compared to the 2D co-culture models that use transwell apparatus.

6.2.4 Comparison with other 3D co-culture models

The published 3D co-culture models (Al Ahmad, 2010, Chow, 2001, Ment, 1997) are mixed co-culture models in which endothelial cells and astrocytes are mixed and cultured together in a collagen gel. The model developed by Al Ahmad *et al.* (2010), though similar to the other two models in its design, differs by incorporating pericytes as well. Al Ahmad *et al.*'s model is more relevant for the present study since it was used to study the development of the BBB phenotype of endothelial cells (barriergenesis), in addition to tubulogenesis while the other two exclusively studied angiogenesis. Since the model developed in this study is different from the mixed co-culture model in its design, its utilities, strengths and limitations also are different.

A unique advantage of the mixed co-culture model of Al Ahmad *et al.* is the provision of direct physical contact between the cell types and therefore, it is particularly suitable to study physical contact dependent properties on either cell type, for example, the induction of AQP4 polarity on astrocyte membranes, and the induction of gamma-glutamyl transpeptidase on BMVEC. In contrast to their model, the present model does not facilitate sufficient physical contact between endothelium and astrocytes, and is therefore not suitable to study contact-dependent properties on either cell type.

In their model, endothelial cells are cultured inside a gel along with astrocytes and pericytes, therefore simulating a 3D architecture of microvessels and thus the developing BBB. It is therefore suitable for studying the interaction between multiple cell types and for monitoring their spatial and temporal reorganisation during vasculogenesis and angiogenesis, a feature that is not possible using the present model. In contrast, in the present model, the endothelium is cultured as a confluent monolayer, at the liquid-solid interface, and therefore simulates a mature, functional BBB at the lumen of a microvessel. Hence, the present model is convenient to study the monolayer-dependent properties of endothelium and can be used as

an *in vitro* BBB model for a few specific purposes such as transcytosis of large substances (≥5 nm) and leukocyte transmigration, as discussed in section 6.2.1.

In addition, compared to a mixed co-culture model, the present model can be analysed by a larger number of techniques because of the two-step collagenase method developed in this study (section 6.2.1). In a mixed co-culture 3D model, this is not possible without fluorescent activated cell sorting (FACS) procedure, which has limitations such as time delay (a factor that may alter the expression profile), and the requirement of equipment, and reagents. In contrast, this method is easily executable and quick, as it takes no more than 45-60 min from the start of the procedure to acquiring of the cell pellet.

In vitro cultured endothelial cells display a differentiated, mature, barrier phenotype at confluence. Therefore, to decide when to do experimental analysis of barrier phenotype, it is crucial to be able to recognise the confluence state of cells. In the present model, since endothelial cells are grown as monolayer, it is relatively easy to judge through microscopy, the confluence state of the cell monolayer; in general, confluence is uniform across the monolayer. By contrast, in a mixed co-culture model, it is difficult to identify confluence of endothelial cells (tubule formation), and the confluence may not be uniform. Quality and extensiveness of the barrier phenotype may therefore not be uniform and quantitative analysis becomes difficult. In the model developed in this study, phase contrast microscopic observation of endothelium and analysis of the expression markers of barrier phenotype through fluorescent and electron microscopy appear to be relatively easier than in mixed co-culture models.

Additional assets of their model, which make it closer to the *in vivo* BBB, are a relatively high (five times) cell density of astrocytes, than that used in this study, and the presence of pericytes. Although pericytes are not cultured in the present model, it is possible to seed them together with astrocytes to make a more realistic BBB model. Since the present model is

human, a higher astrocyte cell density was not possible. On the other hand, being a human model has advantages over their rat model.

Common limitations to both types of 3D models are the absence of shear stress on endothelium, and the difficulty of measuring the functional tightness of endothelium for paracellular tracers. An obvious common strength to both the models is that astrocytes are cultured in a 3D environment. Taken together, the two models, as discussed above, owing to different design, have different applications.

6.3 Future directions of this work

6.3.1 Modifications to make the model more realistic

The present model was designed to simulate the *in vivo* geometry. However, the present configuration has a few drawbacks. Therefore, to make the model more closely resemble the *in vivo* situation and to improve its usability, the following modifications are suggested.

1. Improvement of physical contact between endothelium and astrocytes

In vivo, at least two thirds of the endothelial surface is in direct contact with astrocytic end feet (section 1.2.2). In this model, at a cell density of 0.5 million per ml, there was very little physical contact between the endothelial cells and astrocytes. Even among astrocytes, the cell-cell contact is low compared to the cell density *in vivo*, which is ~40 times higher. Therefore, to recreate *in vivo* cell-cell physical contacts the model needs modifications that increase physical contact between the cell types and among astrocytes. Possible ways to improve the physical contact are:

1. **Real Architecture for 3D Tissues (RAFT) technology™:** The collagen gel seeded with HA may be compressed (plastic compression) using RAFT technology™ (TAP Biosystems Ltd.). This system uses an absorbent plug to remove water, while compressing the gel. Thus, the gel is reduced to 2-10% of its original volume, consequently cell density and collagen concentration is increased proportionately, and the cell density could approach the *in vivo* levels. A typical compressed gel will be ~100 micron thick, and therefore, will have more HA at the interface of the gel and hCMEC/D3 monolayer, producing more physical contacts between endothelial cells and HA. However, because of the gel compression, the collagen fibre density increases, this in turn increases the rigidity of the matrix, which may be much higher than the *in vivo* brain, and therefore physiologically unrealistic. This can cause cells to

assume the properties of 2D cultured cells, and the potential benefits of culturing the cells in the soft matrix would be lost. Another problem could be the increased collagen fibre density and the cell density may result in impaired nutrient and gas exchange, and it remains to be determined empirically whether a perfusion system is required.

2. **Bi-layer model:** HA may be plated as a monolayer on the surface of a collagen gel; a very thin layer of collagen gel is then placed to act as substratum for overlying endothelial cells, not thick enough to separate two cell layers by more than a few μm. In this configuration HA will still be in a 3D environment, since they are surrounded by the collagen gel, but are situated very near the endothelial monolayer. A potential problem is that the high local cell density of the HA may lead to gel contraction. Nevertheless, the new configuration could be tried even to determine the problem exists.

2. Multicellular Interaction

So far, astrocytes are the most frequently co-cultured cells in the BBB models. However, there is evidence for the role of other cell types in the induction of the BBB including pericytes, perivascular macrophages, and neurons (section 1.6). Therefore, addition of these cell types into this co-culture model could make the model closer to the *in vivo* barrier. The importance of other cells is evident as rat BMVEC acquired a phenotype closer to that occurring *in vivo*, at least for a few genes such as carboxypeptidase E, when co-cultured with neuronal progenitor cell derived astrocytes and neurons but not with rat astrocytes alone (Lippmann, 2011).

Most importantly, as the positive influence of pericytes on the BBB integrity is increasingly being revealed (Armulik, 2010, Daneman, 2010, Al Ahmad, 2009), researchers have also incorporated pericytes into their co-culture models of astrocytes and endothelial cells, to make better 2D (Nakagawa, 2009, Hatherell, 2011) as well as 3D (Al Ahmad, 2010) *in vitro* BBB

models. It would be effective to add pericytes to the present model and to examine the effect on each cell type. The modified model will be different from a mixed co-culture model (Al Ahmad, 2010) in that only astrocytes and pericytes will be cultured in the 3D gel matrix while endothelial cells will be cultured on the gel surface.

3. Shear stress

Shear stress is an important contributor for BBB phenotype induction (section 1.8.2) and culturing the BMVEC under flow is essential to simulate conditions *in vivo*. Therefore, addition of flow-based shear stress to this model will make it more similar to *in vivo* conditions. The flow system developed by Janigro's group (Stanness, 1996) and the parallel-plate flow chamber system (Gerszten, 1996) that is commonly used for leukocyte transmigration studies are not suitable for accommodating a 3D collagen gel culture. The flow system introduced by Siddharthan *et al.* (2007) or the cone-plate apparatus (**Figure 1-8 and Figure 1-10**) could be adapted with some modifications for the present model.

4. Matrix composition

Cellular functions are influenced by the type of extra cellular matrix molecules on/in which they are cultured (Gjorevski, 2009). For example, astrocyte proliferation and morphology are modulated by the type of matrix molecule. Compared to collagen type-I or type-IV, fibronectin (Goetschy, 1987) or laminin (Nagano, 1993) the coated 2D substrate induces proliferation and more ramification in astrocytes and astrocytoma cells (Nagano, 1996). Astrocytes grown on a Tenascin-C coated 2D substrate display a reduced reactive phenotype (Holley, 2005). In the CNS, during recovery from injury, astrocytes secrete increased levels of Tenascin-C, thus a modified ECM can induce astrocytes to revert to a normal phenotype (Gutowski, 1999). Therefore, choosing an extracellular matrix composition that is physiologically relevant is crucial.

Unlike other tissues, brain is a soft tissue and does not have much ECM, and therefore, it has very little collagen type I and type III proteins (Engelhardt, 2009). In this study, collagen type-I was chosen for ease of gel preparation, its mechanical strength, and more importantly to make the results comparable with the existing literature (section 2.4.1.1). There are several ECM proteins present in the *in vivo* bilayered basal lamina between BMVEC and astrocytes and some of them are specific to each layer (section 1.2.1.1) and probably have their role only on either cell type. Therefore, to make the model physiologically realistic, BMVEC and HA should be provided with their native ECM proteins.

Complete substitution of the collagen type-I with another ECM protein may not be feasible, but adding other ECM proteins into this matrix can be attempted. ECM proteins specific to astrocytes or glial basal lamina (e.g., laminin-211) or common to both glial and endothelial basal lamina can be added to the collagen gel mixture and ECM molecules that are specific to endothelial basal lamina can be used to coat the gel surface before seeding endothelial cells. In this way, astrocytes and endothelial cells are furnished with their specific ECM molecules. For example, a mixture of collagen type-I and fibronectin (17:1 ratio) has been used (Schechner, 2000), which combines the structural properties of type-I collagen fibres with the cell adhesive and survival enhancing properties (Fukai, 1998) of fibronectin. Thus, providing the cells with an ECM that is physiologically relevant will approximate the model to the conditions *in vivo*.

5. Rigidity of the matrix

Rigidity of the matrix influences the cell growth, motility, differentiation, and signalling mechanisms (Kaufman, 2005, reviewed in Janmey, 2009, Kshitiz, 2012). Each cell type responds to the rigidity of the matrix differently. For example, to proliferate, neurons prefer softer matrices, whereas astrocytes prefer stiffer matrixes (Georges, 2005). Tubule formation and the network of endothelial cells *in vitro* are modulated by the stiffness of the collagen matrix (Sieminski, 2004, Vernon, 1992). Moreover, it has been shown that matrix rigidity

similar to that *in vivo* will induce stem cells to differentiate into specific cell types (Engler, 2006). Therefore, the rheological property of the scaffold is an important, but often overlooked, aspect of the experimental system. *In vivo* brain (adult rat study) is a soft tissue whose shear modulus is ~125 Pa (Georges, 2006). The present model uses gels made of collagen type-I, at 1.72 mg/ml, whose expected shear modulus will be <80 Pa at maximum (Velegol, 2001), which is less than that of brain. The shear modulus of the gel matrix can be increased by increasing the collagen concentration. So, for future studies, preparation of gels with higher concentrations of collagen should be considered. Alternatively, to increase the rigidity of the gel without increasing the collagen concentration, collagen can be glycated before polymerisation (Mason, 2012).

6. All-human model

In vitro findings are not always translatable to humans because of various factors. The probability of translatability of findings increases if the *in vitro* cell model is human. With this objective both endothelial cells and astrocytes of human origin were used in this study. However, the nutrient culture media was supplemented with foetal bovine serum. Comparative analyses have shown that human serum elicits different immune responses (Brewer, 1992, Jancic, 1998), cell differentiation (Shahdadfar, 2005), and transcriptome profiles (Lindroos, 2010, Bieback, 2010) compared with bovine serum. Another reason for why human serum should be chosen is to keep the model species consistent. It is possible that certain serum factors may have a complementary role in BBB induction and these may not be conserved across species and so may require human serum instead of foetal calf serum since both interacting cell types are of human origin. Therefore, to make the present model more humanised and species-consistent, instead of bovine serum, human serum should be used. This all-human 3D model would be useful not only to address novel questions but also to evaluate the existing findings of non-human models, to assess their applicability to humans *in*

vivo. Altogether, this would be an intermediate bridge between conventional *in vitro* models and clinical research.

7. Nutrient media composition

Nutrient culture media used in this study includes vascular endothelial growth factor (VEGF, VEGFA) among other growth factors (section 2.2.2.1). VEGF is proangiogeneic, and a known inducer of vascular permeability. It is highly expressed in the embryonic brain when angiogenesis occurs, but not expressed or expressed at low levels in the adult brain under normal physiological conditions when angiogenesis is blocked and so has a role in the maintenance of differentiated endothelium (Risau, 1998). But during hypoxia and ischemia, enhanced production of VEGF causes BBB disruption (Kaur, 2008), through the down-regulation of occludin and the disruption of ZO-1 organisation (Wang, 2001). It is possible that the barrier-enhancing effect of astrocytic factors could be nullified by the presence of VEGF in the culture media. Therefore, soon after the hCMEC/D3 monolayer becomes confluent, VEGF, serum and other pro-proliferation factors should not be included or may be provided at reduced concentration in the nutrient culture media (Nitz, 2003). The presence of such factors inhibits the switch from proliferative to barrier forming phenotype in endothelial cells (Reinhardt, 1997).

6.3.2 Modification to the model to extend its utility

The current model does not allow assessment of barrier properties of the endothelial monolayer. Therefore, to measure paracellular permeability, TEER, and drug transport functions, configuration of the model can be modified as follows. hCMEC/D3 cells can be seeded on a transwell insert, which can be rested on a collagen gel culture of HA. At the time of assay, the insert can be separated and used for a TEER measurement. However, potential benefits of culturing endothelium on a soft collagen gel matrix will be lost and moreover, only

soluble factor mediated effects can be studied as direct physical contact between the cell types would be negligible.

6.3.3 Investigation of phenotypic changes of endothelium in the model

One of the presumptions of the model is that since the configuration mimics that *in vivo*, the endothelium will acquire an enhanced barrier phenotype. This assumption was not tested in this study, but should be investigated in future by analysing whether the expression of tight junctional markers, or transporter molecules are enhanced. The immune phenotype of hCMEC/D3 cells could also be studied since astrocytic released factors regulate cell adhesion molecules e.g., VCAM1 on endothelial cells (Urich, 2012).

In addition, whether the model actually induces the polarisation of endothelial cells could be investigated. *In vivo,* tight junctions are located at the apical intercellular cleft and some molecules are predominantly expressed on the luminal membrane e.g., cell adhesion molecules like ICAM1, ICAM2, and VCAM1, transporters like GLUT1, efflux transporters P-gp and MRP2 and chemokine receptors. Molecules such as β1-integrin, utrophin, OAT3/SLC22A8, hexokinase are mainly localised on the basolateral membrane (See section 1.1.2). We attempted in this study to examine, by TEM analysis, whether P-gp is localised at the apical membrane. However, this analysis could not be completed because of technical difficulties.

6.3.4 Transcriptome profiling of solo- vs. co- cultured BMVEC

Generally, to date, researchers have focused on only a handful of standard BBB markers to determine the induction potential of astrocytes. Recently, two high-throughput studies have analysed the effect of astrocytes on the whole transcriptome (Urich, 2012) and proteome (Pottiez, 2011) in BMVEC. This kind of high-throughput expression analysis can help to identify specific pathways, signalling mechanisms and transcription factors involved in the induction of BBB phenotype. Similarly, 3D HA solo vs. 3D HA co, 2D HA solo vs. 3D HA solo, and 2D hCMEC/D3 co vs. 3D hCMEC/D3 co comparisons would be desirable. In

addition, microRNA profiling could also reveal new information about the regulation of the BBB phenotype in HBMVEC since ever-growing evidence has shown that microRNAs are important post-transcriptional regulators of gene expression and can potentially modulate all aspects of cellular functions.

6.4 Concluding statement

The *in vitro* human co-culture model developed in this study is easy to set up and analyse by various techniques. The configuration of the model is novel and has a few unique features, some of which need further validation. Although the model does not supersede existing models of either 2D or 3D, it has some exclusive advantages and utilities, which will help to advance the field of research. With the suggested modifications, the proposed 3D endothelial-astrocyte co-culture model approximate their *in vivo* counterparts and its utility can be extended.

References

ABBOTT, A. (2003) Cell culture: biology's new dimension. *Nature,* 424, 870-2.

ABBOTT, N. J. (2002) Astrocyte-endothelial interactions and blood-brain barrier permeability. *J Anat,* 200, 629-38.

ABBOTT, N. J. (2005) Dynamics of CNS barriers: evolution, differentiation, and modulation. *Cell Mol Neurobiol,* 25, 5-23.

ABBOTT, N. J., PATABENDIGE, A. A., DOLMAN, D. E., YUSOF, S. R. & BEGLEY, D. J. (2010) Structure and function of the blood-brain barrier. *Neurobiol Dis,* 37, 13-25.

ABBOTT, N. J., RONNBACK, L. & HANSSON, E. (2006) Astrocyte-endothelial interactions at the blood-brain barrier. *Nat Rev Neurosci,* 7, 41-53.

ADELOW, C. A. & FREY, P. (2007) Synthetic hydrogel matrices for guided bladder tissue regeneration. *Methods Mol Med,* 140, 125-40.

AIRD, W. C. (2007) Phenotypic heterogeneity of the endothelium: I. Structure, function, and mechanisms. *Circ Res,* 100, 158-73.

AKIMOTO, S., MITSUMATA, M., SASAGURI, T. & YOSHIDA, Y. (2000) Laminar shear stress inhibits vascular endothelial cell proliferation by inducing cyclin-dependent kinase inhibitor p21(Sdi1/Cip1/Waf1). *Circ Res,* 86, 185-90.

AL AHMAD, A., GASSMANN, M. & OGUNSHOLA, O. O. (2009) Maintaining blood-brain barrier integrity: pericytes perform better than astrocytes during prolonged oxygen deprivation. *J Cell Physiol,* 218, 612-22.

AL AHMAD, A., TABOADA, C. B., GASSMANN, M. & OGUNSHOLA, O. O. (2010) Astrocytes and pericytes differentially modulate blood-brain barrier characteristics during development and hypoxic insult. *J Cereb Blood Flow Metab,* 31, 693-705.

ALLT, G. & LAWRENSON, J. G. (1997) Is the pial microvessel a good model for blood-brain barrier studies? *Brain Res Brain Res Rev,* 24, 67-76.

ALVAREZ, J. I., DODELET-DEVILLERS, A., KEBIR, H., IFERGAN, I., FABRE, P. J., TEROUZ, S., SABBAGH, M., WOSIK, K., BOURBONNIERE, L., BERNARD, M., VAN HORSSEN, J., DE VRIES, H. E., CHARRON, F. & PRAT, A. (2011) The Hedgehog pathway promotes blood-brain barrier integrity and CNS immune quiescence. *Science,* 334, 1727-31.

AMIRY-MOGHADDAM, M. & OTTERSEN, O. P. (2003) The molecular basis of water transport in the brain. *Nat Rev Neurosci,* 4, 991-1001.

AMIRY-MOGHADDAM, M., XUE, R., HAUG, F. M., NEELY, J. D., BHARDWAJ, A., AGRE, P., ADAMS, M. E., FROEHNER, S. C., MORI, S. & OTTERSEN, O. P. (2004) Alpha-syntrophin deletion removes the perivascular but not endothelial pool of aquaporin-4 at the blood-brain barrier and delays the development of brain edema in an experimental model of acute hyponatremia. *Faseb J,* 18, 542-4.

ANDO, J. & KAMIYA, A. (1996) Flow-dependent regulation of gene expression in vascular endothelial cells. *Jpn Heart J,* 37, 19-32.

ANTONETTI, D. A., BARBER, A. J., HOLLINGER, L. A., WOLPERT, E. B. & GARDNER, T. W. (1999) Vascular endothelial growth factor induces rapid phosphorylation of tight junction proteins occludin and zonula occluden 1. A potential mechanism for vascular permeability in diabetic retinopathy and tumors. *J Biol Chem,* 274, 23463-7.

APPAIX, F., GIROD, S., BOISSEAU, S., ROMER, J., VIAL, J. C., ALBRIEUX, M., MAURIN, M., DEPAULIS, A., GUILLEMAIN, I. & VAN DER SANDEN, B. (2012) Specific in vivo staining of astrocytes in the whole brain after intravenous injection of sulforhodamine dyes. *PLoS One,* 7, e35169.

ARMSTRONG, R., FRIEDRICH, V. L., JR., HOLMES, K. V. & DUBOIS-DALCQ, M. (1990) In vitro analysis of the oligodendrocyte lineage in mice during demyelination and remyelination. *J Cell Biol,* 111, 1183-95.

ARMULIK, A., GENOVE, G. & BETSHOLTZ, C. (2011) Pericytes: developmental, physiological, and pathological perspectives, problems, and promises. *Dev Cell,* 21, 193-215.

ARMULIK, A., GENOVE, G., MAE, M., NISANCIOGLU, M. H., WALLGARD, E., NIAUDET, C., HE, L., NORLIN, J., LINDBLOM, P., STRITTMATTER, K., JOHANSSON, B. R. & BETSHOLTZ, C. (2010) Pericytes regulate the blood-brain barrier. *Nature,* 468, 557-61.

ARTHUR, F. E., SHIVERS, R. R. & BOWMAN, P. D. (1987) Astrocyte-mediated induction of tight junctions in brain capillary endothelium: an efficient in vitro model. *Brain Res,* 433, 155-9.

ASABA, H., HOSOYA, K., TAKANAGA, H., OHTSUKI, S., TAMURA, E., TAKIZAWA, T. & TERASAKI, T. (2000) Blood-brain barrier is involved in the efflux transport of a neuroactive steroid, dehydroepiandrosterone sulfate, via organic anion transporting polypeptide 2. *J Neurochem,* 75, 1907-16.

BABA, A. (1998) Role of endothelin B receptor signals in reactive astrocytes. *Life Sci,* 62, 1711-5.

BACIC, F., UEMATSU, S., MCCARRON, R. M. & SPATZ, M. (1992) Secretion of immunoreactive endothelin-1 by capillary and microvascular endothelium of human brain. *Neurochem Res,* 17, 699-702.

BAKER, S. E., HOPKINSON, S. B., FITCHMUN, M., ANDREASON, G. L., FRASIER, F., PLOPPER, G., QUARANTA, V. & JONES, J. C. (1996) Laminin-5 and hemidesmosomes: role of the alpha 3 chain subunit in hemidesmosome stability and assembly. *J Cell Sci,* 109 (Pt 10), 2509-20.

BALDA, M. S. & MATTER, K. (2000) The tight junction protein ZO-1 and an interacting transcription factor regulate ErbB-2 expression. *Embo J,* 19, 2024-33.

BALLABH, P., BRAUN, A. & NEDERGAARD, M. (2004) The blood-brain barrier: an overview: structure, regulation, and clinical implications. *Neurobiol Dis,* 16, 1-13.

BALLERMANN, B. J. & OTT, M. J. (1995) Adhesion and differentiation of endothelial cells by exposure to chronic shear stress: a vascular graft model. *Blood Purif,* 13, 125-34.

BALTES, S., GASTENS, A. M., FEDROWITZ, M., POTSCHKA, H., KAEVER, V. & LOSCHER, W. (2007) Differences in the transport of the antiepileptic drugs phenytoin, levetiracetam and carbamazepine by human and mouse P-glycoprotein. *Neuropharmacology,* 52, 333-46.

BASU, S. & YANG, S. T. (2005) Astrocyte growth and glial cell line-derived neurotrophic factor secretion in three-dimensional polyethylene terephthalate fibrous matrices. *Tissue Eng,* 11, 940-52.

BAUER, H. C. & BAUER, H. (2000) Neural induction of the blood-brain barrier: still an enigma. *Cell Mol Neurobiol,* 20, 13-28.

BAUER, H. C., TONTSCH, U., AMBERGER, A. & BAUER, H. (1990) Gamma-glutamyl-transpeptidase (GGTP) and NA+K(+)-ATPase activities in different subpopulations of cloned cerebral endothelial cells: responses to glial stimulation. *Biochem Biophys Res Commun,* 168, 358-63.

BECK, D. W., ROBERTS, R. L. & OLSON, J. J. (1986) Glial cells influence membrane-associated enzyme activity at the blood-brain barrier. *Brain Res,* 381, 131-7.

BECK, D. W., VINTERS, H. V., HART, M. N. & CANCILLA, P. A. (1984) Glial cells influence polarity of the blood-brain barrier. *J Neuropathol Exp Neurol,* 43, 219-24.

BECK, L. H., JR., GOODWIN, A. M. & D'AMORE, P. A. (2004) Culture of large vessel endothelial cells on floating collagen gels promotes a phenotype characteristic of endothelium in vivo. *Differentiation,* 72, 162-70.

BEGLEY, D. J. (2004) ABC transporters and the blood-brain barrier. *Curr Pharm Des,* 10, 1295-312.

BERNACKI, J., DOBROWOLSKA, A., NIERWINSKA, K. & MALECKI, A. (2008) Physiology and pharmacological role of the blood-brain barrier. *Pharmacol Rep,* 60, 600-22.

BETZ, A. L., FIRTH, J. A. & GOLDSTEIN, G. W. (1980) Polarity of the blood-brain barrier: distribution of enzymes between the luminal and antiluminal membranes of brain capillary endothelial cells. *Brain Res,* 192, 17-28.

BEVAN, J. A. (1979) Sites of transition between functional systemic and cerebral arteries of rabbits occur at embryological junctional sites. *Science,* 204, 635-7.

BIEBACK, K., HA, V. A., HECKER, A., GRASSL, M., KINZEBACH, S., SOLZ, H., STICHT, C., KLUTER, H. & BUGERT, P. (2010) Altered gene expression in human adipose stem cells cultured with fetal bovine serum compared to human supplements. *Tissue Eng Part A,* 16, 3467-84.

BINDER, D. K., YAO, X., ZADOR, Z., SICK, T. J., VERKMAN, A. S. & MANLEY, G. T. (2006) Increased seizure duration and slowed potassium kinetics in mice lacking aquaporin-4 water channels. *Glia,* 53, 631-6.

BLASIG, I. E., GIESE, H., SCHROETER, M. L., SPORBERT, A., UTEPBERGENOV, D. I., BUCHWALOW, I. B., NEUBERT, K., SCHONFELDER, G., FREYER, D., SCHIMKE, I.,

SIEMS, W. E., PAUL, M., HASELOFF, R. F. & BLASIG, R. (2001) *NO and oxyradical metabolism in new cell lines of rat brain capillary endothelial cells forming the blood-brain barrier. *Microvasc Res,* 62, 114-27.

BOUCHAUD, C., LE BERT, M. & DUPOUEY, P. (1989) Are close contacts between astrocytes and endothelial cells a prerequisite condition of a blood-brain barrier? The rat subfornical organ as an example. *Biol Cell,* 67, 159-65.

BOVERI, M., BEREZOWSKI, V., PRICE, A., SLUPEK, S., LENFANT, A. M., BENAUD, C., HARTUNG, T., CECCHELLI, R., PRIETO, P. & DEHOUCK, M. P. (2005) Induction of blood-brain barrier properties in cultured brain capillary endothelial cells: comparison between primary glial cells and C6 cell line. *Glia,* 51, 187-98.

BRAET, K., PAEMELEIRE, K., D'HERDE, K., SANDERSON, M. J. & LEYBAERT, L. (2001) Astrocyte-endothelial cell calcium signals conveyed by two signalling pathways. *Eur J Neurosci,* 13, 79-91.

BREWER, G. J. & ASHFORD, J. W. (1992) Human serum stimulates Alzheimer markers in cultured hippocampal neurons. *J Neurosci Res,* 33, 355-69.

BRIGHTMAN, M. W. & REESE, T. S. (1969) Junctions between intimately apposed cell membranes in the vertebrate brain. *J Cell Biol,* 40, 648-77.

BROWN, J., READING, S. J., JONES, S., FITCHETT, C. J., HOWL, J., MARTIN, A., LONGLAND, C. L., MICHELANGELI, F., DUBROVA, Y. E. & BROWN, C. A. (2000) Critical evaluation of ECV304 as a human endothelial cell model defined by genetic analysis and functional responses: a comparison with the human bladder cancer derived epithelial cell line T24/83. *Lab Invest,* 80, 37-45.

BROWN, R. C. & DAVIS, T. P. (2002) Calcium modulation of adherens and tight junction function: a potential mechanism for blood-brain barrier disruption after stroke. *Stroke,* 33, 1706-11.

BURGHOFF, S. & SCHRADER, J. (2011) Secretome of human endothelial cells under shear stress. *J Proteome Res,* 10, 1160-9.

BUSHONG, E. A., MARTONE, M. E. & ELLISMAN, M. H. (2004) Maturation of astrocyte morphology and the establishment of astrocyte domains during postnatal hippocampal development. *Int J Dev Neurosci,* 22, 73-86.

BUSSOLARI, S. R., DEWEY, C. F., JR. & GIMBRONE, M. A., JR. (1982) Apparatus for subjecting living cells to fluid shear stress. *Rev Sci Instrum,* 53, 1851-4.

BUTT, A. M., JONES, H. C. & ABBOTT, N. J. (1990) Electrical resistance across the blood-brain barrier in anaesthetized rats: a developmental study. *J Physiol,* 429, 47-62.

CANFIELD, A. E., BOOT-HANDFORD, R. P. & SCHOR, A. M. (1990) Thrombospondin gene expression by endothelial cells in culture is modulated by cell proliferation, cell shape and the substratum. *Biochem J,* 268, 225-30.

CECCHELLI, R., DEHOUCK, B., DESCAMPS, L., FENART, L., BUEE-SCHERRER, V. V., DUHEM, C., LUNDQUIST, S., RENTFEL, M., TORPIER, G. & DEHOUCK, M. P. (1999) In vitro model for evaluating drug transport across the blood-brain barrier. *Adv Drug Deliv Rev,* 36, 165-178.

CHAT, M., BAYOL-DENIZOT, C., SULEMAN, G., ROUX, F. & MINN, A. (1998) Drug metabolizing enzyme activities and superoxide formation in primary and immortalized rat brain endothelial cells. *Life Sci,* 62, 151-63.

CHENG, H. F., SU, Y. M., YEH, J. R. & CHANG, K. J. (1993) Alternative transcript of the nonselective-type endothelin receptor from rat brain. *Mol Pharmacol,* 44, 533-8.

CHIQUET, M., GELMAN, L., LUTZ, R. & MAIER, S. (2009) From mechanotransduction to extracellular matrix gene expression in fibroblasts. *Biochim Biophys Acta,* 1793, 911-20.

CHOW, J., OGUNSHOLA, O., FAN, S. Y., LI, Y., MENT, L. R. & MADRI, J. A. (2001) Astrocyte-derived VEGF mediates survival and tube stabilization of hypoxic brain microvascular endothelial cells in vitro. *Brain Res Dev Brain Res,* 130, 123-32.

COISNE, C., DEHOUCK, L., FAVEEUW, C., DELPLACE, Y., MILLER, F., LANDRY, C., MORISSETTE, C., FENART, L., CECCHELLI, R., TREMBLAY, P. & DEHOUCK, B. (2005) Mouse syngenic in vitro blood-brain barrier model: a new tool to examine inflammatory events in cerebral endothelium. *Lab Invest,* 85, 734-46.

COLODNER, K. J., MONTANA, R. A., ANTHONY, D. C., FOLKERTH, R. D., DE GIROLAMI, U. & FEANY, M. B. (2005) Proliferative potential of human astrocytes. *J Neuropathol Exp Neurol,* 64, 163-9.

CONNOLLY, D. T. (1991) Vascular permeability factor: a unique regulator of blood vessel function. *J Cell Biochem,* 47, 219-23.

CORNFORD, E. M. & HYMAN, S. (2005) Localization of brain endothelial luminal and abluminal transporters with immunogold electron microscopy. *NeuroRx,* 2, 27-43.

COURAUD, P. O., GREENWOOD, J., ROUX, F. & ADAMSON, P. (2003) Development and characterization of immortalized cerebral endothelial cell lines. *Methods Mol Med,* 89, 349-64.

CRIVELLATO, E., NICO, B. & RIBATTI, D. (2007) Contribution of endothelial cells to organogenesis: a modern reappraisal of an old Aristotelian concept. *J Anat,* 211, 415-27.

CRONE, C. & OLESEN, S. P. (1982) Electrical resistance of brain microvascular endothelium. *Brain Res,* 241, 49-55.

CUCULLO, L., COURAUD, P. O., WEKSLER, B., ROMERO, I. A., HOSSAIN, M., RAPP, E. & JANIGRO, D. (2008) Immortalized human brain endothelial cells and flow-based vascular modeling: a marriage of convenience for rational neurovascular studies. *J Cereb Blood Flow Metab,* 28, 312-28.

CUCULLO, L., HOSSAIN, M., PUVENNA, V., MARCHI, N. & JANIGRO, D. (2011) The role of shear stress in Blood-Brain Barrier endothelial physiology. *BMC Neurosci,* 12, 40.

CUCULLO, L., HOSSAIN, M., RAPP, E., MANDERS, T., MARCHI, N. & JANIGRO, D. (2007) Development of a humanized in vitro blood-brain barrier model to screen for brain penetration of antiepileptic drugs. *Epilepsia,* 48, 505-16.

CUCULLO, L., MCALLISTER, M. S., KIGHT, K., KRIZANAC-BENGEZ, L., MARRONI, M., MAYBERG, M. R., STANNESS, K. A. & JANIGRO, D. (2002) A new dynamic in vitro model for the multidimensional study of astrocyte-endothelial cell interactions at the blood-brain barrier. *Brain Res,* 951, 243-54.

CUKIERMAN, E., PANKOV, R., STEVENS, D. R. & YAMADA, K. M. (2001) Taking cell-matrix adhesions to the third dimension. *Science,* 294, 1708-12.

CULLEN, D. K., VUKASINOVIC, J., GLEZER, A. & LAPLACA, M. C. (2007) Microfluidic engineered high cell density three-dimensional neural cultures. *J Neural Eng,* 4, 159-72.

CULOT, M., LUNDQUIST, S., VANUXEEM, D., NION, S., LANDRY, C., DELPLACE, Y., DEHOUCK, M. P., BEREZOWSKI, V., FENART, L. & CECCHELLI, R. (2008) An in vitro blood-brain barrier model for high throughput (HTS) toxicological screening. *Toxicol In Vitro,* 22, 799-811.

DANEMAN, R., ZHOU, L., KEBEDE, A. A. & BARRES, B. A. (2010) Pericytes are required for blood-brain barrier integrity during embryogenesis. *Nature,* 468, 562-6.

DANIELS, B. P., CRUZ-ORENGO, L., PASIEKA, T. J., COURAUD, P. O., ROMERO, I. A., WEKSLER, B., COOPER, J. A., DOERING, T. L. & KLEIN, R. S. (2013) Immortalized human cerebral microvascular endothelial cells maintain the properties of primary cells in an in vitro model of immune migration across the blood brain barrier. *J Neurosci Methods,* 212, 173-179.

DAVIS, G. E., KOH, W. & STRATMAN, A. N. (2007) Mechanisms controlling human endothelial lumen formation and tube assembly in three-dimensional extracellular matrices. *Birth Defects Res C Embryo Today,* 81, 270-85.

DAVIS, G. E., STRATMAN, A. N., SACHARIDOU, A. & KOH, W. (2012) Molecular basis for endothelial lumen formation and tubulogenesis during vasculogenesis and angiogenic sprouting. *Int Rev Cell Mol Biol,* 288, 101-65.

DAVSON, H. & OLDENDORF, W. H. (1967) Symposium on membrane transport. Transport in the central nervous system. *Proc R Soc Med,* 60, 326-9.

DEBAULT, L. E. (1981) gamma-Glutamyltranspeptidase induction mediated by glial foot process-to endothelium contact in co-culture. *Brain Res,* 220, 432-5.

DEBAULT, L. E. & CANCILLA, P. A. (1980) gamma-Glutamyl transpeptidase in isolated brain endothelial cells: induction by glial cells in vitro. *Science,* 207, 653-5.

DECLEVES, X., JACOB, A., YOUSIF, S., SHAWAHNA, R., POTIN, S. & SCHERRMANN, J. M. (2011) Interplay of drug metabolizing CYP450 enzymes and ABC transporters in the blood-brain barrier. *Curr Drug Metab,* 12, 732-41.

DEHOUCK, B., DEHOUCK, M. P., FRUCHART, J. C. & CECCHELLI, R. (1994) Upregulation of the low density lipoprotein receptor at the blood-brain barrier: intercommunications between brain capillary endothelial cells and astrocytes. *J Cell Biol,* 126, 465-73.

DEHOUCK, M. P., JOLLIET-RIANT, P., BREE, F., FRUCHART, J. C., CECCHELLI, R. & TILLEMENT, J. P. (1992) Drug transfer across the blood-brain barrier: correlation between in vitro and in vivo models. *J Neurochem,* 58, 1790-7.

DEHOUCK, M. P., MERESSE, S., DELORME, P., FRUCHART, J. C. & CECCHELLI, R. (1990) An easier, reproducible, and mass-production method to study the blood-brain barrier in vitro. *J Neurochem,* 54, 1798-801.

DEHOUCK, M. P., VIGNE, P., TORPIER, G., BREITTMAYER, J. P., CECCHELLI, R. & FRELIN, C. (1997) Endothelin-1 as a mediator of endothelial cell-pericyte interactions in bovine brain capillaries. *J Cereb Blood Flow Metab,* 17, 464-9.

DEMEUSE, P., KERKHOFS, A., STRUYS-PONSAR, C., KNOOPS, B., REMACLE, C. & VAN DEN BOSCH DE AGUILAR, P. (2002) Compartmentalized coculture of rat brain endothelial cells and astrocytes: a syngenic model to study the blood-brain barrier. *J Neurosci Methods,* 121, 21-31.

DERMIETZEL, R. & KRAUSE, D. (1991) Molecular anatomy of the blood-brain barrier as defined by immunocytochemistry. *Int Rev Cytol,* 127, 57-109.

DESCAMPS, L., COISNE, C., DEHOUCK, B., CECCHELLI, R. & TORPIER, G. (2003) Protective effect of glial cells against lipopolysaccharide-mediated blood-brain barrier injury. *Glia,* 42, 46-58.

DEWEY, C. F., JR., BUSSOLARI, S. R., GIMBRONE, M. A., JR. & DAVIES, P. F. (1981) The dynamic response of vascular endothelial cells to fluid shear stress. *J Biomech Eng,* 103, 177-85.

DIDIER, N., ROMERO, I. A., CREMINON, C., WIJKHUISEN, A., GRASSI, J. & MABONDZO, A. (2003) Secretion of interleukin-1beta by astrocytes mediates endothelin-1 and tumour necrosis factor-alpha effects on human brain microvascular endothelial cell permeability. *J Neurochem,* 86, 246-54.

DOHGU, S., TAKATA, F., YAMAUCHI, A., NAKAGAWA, S., EGAWA, T., NAITO, M., TSURUO, T., SAWADA, Y., NIWA, M. & KATAOKA, Y. (2005) Brain pericytes contribute to the induction and up-regulation of blood-brain barrier functions through transforming growth factor-beta production. *Brain Res,* 1038, 208-15.

DOLMAN, D., DRNDARSKI, S., ABBOTT, N. J. & RATTRAY, M. (2005) Induction of aquaporin 1 but not aquaporin 4 messenger RNA in rat primary brain microvessel endothelial cells in culture. *J Neurochem,* 93, 825-33.

DURIEU-TRAUTMANN, O., FOIGNANT-CHAVEROT, N., PERDOMO, J., GOUNON, P., STROSBERG, A. D. & COURAUD, P. O. (1991) Immortalization of brain capillary endothelial cells with maintenance of structural characteristics of the blood-brain barrier endothelium. *In Vitro Cell Dev Biol,* 27A, 771-8.

EAST, E., GOLDING, J. P. & PHILLIPS, J. B. (2009) A versatile 3D culture model facilitates monitoring of astrocytes undergoing reactive gliosis. *J Tissue Eng Regen Med,* 3, 634-46.

EHRENREICH, H., ANDERSON, R. W., OGINO, Y., RIECKMANN, P., COSTA, T., WOOD, G. P., COLIGAN, J. E., KEHRL, J. H. & FAUCI, A. S. (1991) Selective autoregulation of endothelins in primary astrocyte cultures: endothelin receptor-mediated potentiation of endothelin-1 secretion. *New Biol,* 3, 135-41.

EHRENREICH, H., LOFFLER, B. M., HASSELBLATT, M., LANGEN, H., OLDENBURG, J., SUBKOWSKI, T., SCHILLING, L. & SIREN, A. L. (1999) Endothelin converting enzyme activity in primary rat astrocytes is modulated by endothelin B receptors. *Biochem Biophys Res Commun,* 261, 149-55.

EILERT-OLSEN, M., HAJ-YASEIN, N. N., VINDEDAL, G. F., ENGER, R., GUNDERSEN, G. A., HODDEVIK, E. H., PETERSEN, P. H., HAUG, F. M., SKARE, O., ADAMS, M. E., FROEHNER, S. C., BURKHARDT, J. M., THOREN, A. E. & NAGELHUS, E. A. (2011) Deletion of aquaporin-4 changes the perivascular glial protein scaffold without disrupting the brain endothelial barrier. *Glia.*

EL-BACHA, R. S. & MINN, A. (1999) Drug metabolizing enzymes in cerebrovascular endothelial cells afford a metabolic protection to the brain. *Cell Mol Biol (Noisy-le-grand),* 45, 15-23.

EL HAFNY, B., CHAPPEY, O., PICIOTTI, M., DEBRAY, M., BOVAL, B. & ROUX, F. (1997) Modulation of P-glycoprotein activity by glial factors and retinoic acid in an immortalized rat brain microvessel endothelial cell line. *Neurosci Lett,* 236, 107-11.

ENGELHARDT, B. (2003) Development of the blood-brain barrier. *Cell Tissue Res,* 314, 119-29.

ENGELHARDT, B. & SOROKIN, L. (2009) The blood-brain and the blood-cerebrospinal fluid barriers: function and dysfunction. *Semin Immunopathol,* 31, 497-511.

ENGLER, A. J., SEN, S., SWEENEY, H. L. & DISCHER, D. E. (2006) Matrix elasticity directs stem cell lineage specification. *Cell,* 126, 677-89.

ESTRADA, C., BREADY, J. V., BERLINER, J. A., PARDRIDGE, W. M. & CANCILLA, P. A. (1990) Astrocyte growth stimulation by a soluble factor produced by cerebral endothelial cells in vitro. *J Neuropathol Exp Neurol,* 49, 539-49.

FALLIER-BECKER, P., SPERVESLAGE, J., WOLBURG, H. & NOELL, S. (2011) The impact of agrin on the formation of orthogonal arrays of particles in cultured astrocytes from wild-type and agrin-null mice. *Brain Res,* 1367, 2-12.

FIACCO, T. A. & MCCARTHY, K. D. (2006) Astrocyte calcium elevations: properties, propagation, and effects on brain signaling. *Glia,* 54, 676-90.

FINOULST, I., VINK, P., ROVERS, E., PIETERSE, M., PINKSE, M., BOS, E. & VERHAERT, P. (2011) Identification of low abundant secreted proteins and peptides from primary culture supernatants of human T-cells. *J Proteomics,* 75, 23-33.

FLYNN, G., MARU, S., LOUGHLIN, J., ROMERO, I. A. & MALE, D. (2003) Regulation of chemokine receptor expression in human microglia and astrocytes. *J Neuroimmunol,* 136, 84-93.

FRAMPTON, J. P., HYND, M. R., SHULER, M. L. & SHAIN, W. (2011) Fabrication and optimization of alginate hydrogel constructs for use in 3D neural cell culture. *Biomed Mater,* 6, 015002.

FRANCESCA, B. & REZZANI, R. (2010) Aquaporin and blood brain barrier. *Curr Neuropharmacol,* 8, 92-6.

FRANKE, H., GALLA, H. & BEUCKMANN, C. T. (2000) Primary cultures of brain microvessel endothelial cells: a valid and flexible model to study drug transport through the blood-brain barrier in vitro. *Brain Res Brain Res Protoc,* 5, 248-56.

FRANKE, H., GALLA, H. J. & BEUCKMANN, C. T. (1999) An improved low-permeability in vitro-model of the blood-brain barrier: transport studies on retinoids, sucrose, haloperidol, caffeine and mannitol. *Brain Res,* 818, 65-71.

FUKAI, F., MASHIMO, M., AKIYAMA, K., GOTO, T., TANUMA, S. & KATAYAMA, T. (1998) Modulation of apoptotic cell death by extracellular matrix proteins and a fibronectin-derived antiadhesive peptide. *Exp Cell Res,* 242, 92-9.

FURUSE, M., HIRASE, T., ITOH, M., NAGAFUCHI, A., YONEMURA, S., TSUKITA, S. & TSUKITA, S. (1993) Occludin: a novel integral membrane protein localizing at tight junctions. *J Cell Biol,* 123, 1777-88.

GADEA, A., SCHINELLI, S. & GALLO, V. (2008) Endothelin-1 regulates astrocyte proliferation and reactive gliosis via a JNK/c-Jun signaling pathway. *J Neurosci,* 28, 2394-408.

GAILLARD, P. J., VAN DER SANDT, I. C., VOORWINDEN, L. H., VU, D., NIELSEN, J. L., DE BOER, A. G. & BREIMER, D. D. (2000) Astrocytes increase the functional expression of P-glycoprotein in an in vitro model of the blood-brain barrier. *Pharm Res,* 17, 1198-205.

GAILLARD, P. J., VOORWINDEN, L. H., NIELSEN, J. L., IVANOV, A., ATSUMI, R., ENGMAN, H., RINGBOM, C., DE BOER, A. G. & BREIMER, D. D. (2001) Establishment and functional characterization of an in vitro model of the blood-brain barrier, comprising a co-culture of brain capillary endothelial cells and astrocytes. *Eur J Pharm Sci,* 12, 215-22.

GARDNER, T. W., LIETH, E., KHIN, S. A., BARBER, A. J., BONSALL, D. J., LESHER, T., RICE, K. & BRENNAN, W. A., JR. (1997) Astrocytes increase barrier properties and ZO-1 expression in retinal vascular endothelial cells. *Invest Ophthalmol Vis Sci,* 38, 2423-7.

GEORGES, P. C. & JANMEY, P. A. (2005) Cell type-specific response to growth on soft materials. *J Appl Physiol,* 98, 1547-53.

GEORGES, P. C., MILLER, W. J., MEANEY, D. F., SAWYER, E. S. & JANMEY, P. A. (2006) Matrices with compliance comparable to that of brain tissue select neuronal over glial growth in mixed cortical cultures. *Biophys J,* 90, 3012-8.

GERHARDT, H. & BETSHOLTZ, C. (2003) Endothelial-pericyte interactions in angiogenesis. *Cell Tissue Res,* 314, 15-23.

GERHARDT, H., LIEBNER, S., REDIES, C. & WOLBURG, H. (1999) N-cadherin expression in endothelial cells during early angiogenesis in the eye and brain of the chicken: relation to blood-retina and blood-brain barrier development. *Eur J Neurosci,* 11, 1191-201.

GERHARDT, H., WOLBURG, H. & REDIES, C. (2000) N-cadherin mediates pericytic-endothelial interaction during brain angiogenesis in the chicken. *Dev Dyn,* 218, 472-9.

GERSZTEN, R. E., LUSCINSKAS, F. W., DING, H. T., DICHEK, D. A., STOOLMAN, L. M., GIMBRONE, M. A., JR. & ROSENZWEIG, A. (1996) Adhesion of memory lymphocytes to vascular cell adhesion molecule-1-transduced human vascular endothelial cells under simulated physiological flow conditions in vitro. *Circ Res,* 79, 1205-15.

GIRANDON, L., KREGAR-VELIKONJA, N., BOZIKOV, K. & BARLIC, A. (2011) In vitro models for adipose tissue engineering with adipose-derived stem cells using different scaffolds of natural origin. *Folia Biol (Praha),* 57, 47-56.

GJOREVSKI, N. & NELSON, C. M. (2009) Bidirectional extracellular matrix signaling during tissue morphogenesis. *Cytokine Growth Factor Rev,* 20, 459-65.

GOETSCHY, J. F., ULRICH, G., AUNIS, D. & CIESIELSKI-TRESKA, J. (1987) Fibronectin and collagens modulate the proliferation and morphology of astroglial cells in culture. *Int J Dev Neurosci,* 5, 63-70.

GOMI, H., YOKOYAMA, T., FUJIMOTO, K., IKEDA, T., KATOH, A., ITOH, T. & ITOHARA, S. (1995) Mice devoid of the glial fibrillary acidic protein develop normally and are susceptible to scrapie prions. *Neuron,* 14, 29-41.

GOODPASTER, T., LEGESSE-MILLER, A., HAMEED, M. R., AISNER, S. C., RANDOLPH-HABECKER, J. & COLLER, H. A. (2008) An immunohistochemical method for identifying fibroblasts in formalin-fixed, paraffin-embedded tissue. *J Histochem Cytochem,* 56, 347-58.

GREEN, J. A. & YAMADA, K. M. (2007) Three-dimensional microenvironments modulate fibroblast signaling responses. *Adv Drug Deliv Rev,* 59, 1293-8.

GREENWOOD, J., PRYCE, G., DEVINE, L., MALE, D. K., DOS SANTOS, W. L., CALDER, V. L. & ADAMSON, P. (1996) SV40 large T immortalised cell lines of the rat blood-brain and blood-retinal barriers retain their phenotypic and immunological characteristics. *J Neuroimmunol,* 71, 51-63.

GUIDRY, C. (1992a) Extracellular matrix contraction by fibroblasts: peptide promoters and second messengers. *Cancer Metastasis Rev,* 11, 45-54.

GUIDRY, C., MCFARLAND, R. J., MORRIS, R., WITHERSPOON, C. D. & HOOK, M. (1992b) Collagen gel contraction by cells associated with proliferative vitreoretinopathy. *Invest Ophthalmol Vis Sci,* 33, 2429-35.

GUILLEMIN, G. J. & BREW, B. J. (2004) Microglia, macrophages, perivascular macrophages, and pericytes: a review of function and identification. *J Leukoc Biol,* 75, 388-97.

GUMBLETON, M. & AUDUS, K. L. (2001) Progress and limitations in the use of in vitro cell cultures to serve as a permeability screen for the blood-brain barrier. *J Pharm Sci,* 90, 1681-98.

GUPTA, S. K., HASSEL, T. & SINGH, J. P. (1995) A potent inhibitor of endothelial cell proliferation is generated by proteolytic cleavage of the chemokine platelet factor 4. *Proc Natl Acad Sci U S A,* 92, 7799-803.

GUTOWSKI, N. J., NEWCOMBE, J. & CUZNER, M. L. (1999) Tenascin-R and C in multiple sclerosis lesions: relevance to extracellular matrix remodelling. *Neuropathol Appl Neurobiol,* 25, 207-14.

HAJ-YASEIN, N. N., VINDEDAL, G. F., EILERT-OLSEN, M., GUNDERSEN, G. A., SKARE, O., LAAKE, P., KLUNGLAND, A., THOREN, A. E., BURKHARDT, J. M., OTTERSEN, O. P. & NAGELHUS, E. A. (2011) Glial-conditional deletion of aquaporin-4 (Aqp4) reduces blood-brain water uptake and confers barrier function on perivascular astrocyte endfeet. *Proc Natl Acad Sci U S A,* 108, 17815-20.

HAMA, H., SAKURAI, T., KASUYA, Y., FUJIKI, M., MASAKI, T. & GOTO, K. (1992) Action of endothelin-1 on rat astrocytes through the ETB receptor. *Biochem Biophys Res Commun,* 186, 355-62.

HAQUE, S., MD, S., ALAM, M. I., SAHNI, J. K., ALI, J. & BABOOTA, S. (2012) Nanostructure-based drug delivery systems for brain targeting. *Drug Dev Ind Pharm,* 38, 387-411.

HARTMANN, C., ZOZULYA, A., WEGENER, J. & GALLA, H. J. (2007) The impact of glia-derived extracellular matrices on the barrier function of cerebral endothelial cells: an in vitro study. *Exp Cell Res,* 313, 1318-25.

HASELOFF, R. F., BLASIG, I. E., BAUER, H. C. & BAUER, H. (2005) In search of the astrocytic factor(s) modulating blood-brain barrier functions in brain capillary endothelial cells in vitro. *Cell Mol Neurobiol,* 25, 25-39.

HASSELBLATT, M., BUNTE, M., DRINGEN, R., TABERNERO, A., MEDINA, J. M., GIAUME, C., SIREN, A. L. & EHRENREICH, H. (2003) Effect of endothelin-1 on astrocytic protein content. *Glia,* 42, 390-7.

HATHERELL, K., COURAUD, P. O., ROMERO, I. A., WEKSLER, B. & PILKINGTON, G. J. (2011) Development of a three-dimensional, all-human in vitro model of the blood-brain barrier using mono-, co-, and tri-cultivation Transwell models. *J Neurosci Methods.*

HAWKINS, R. A., O'KANE, R. L., SIMPSON, I. A. & VINA, J. R. (2006) Structure of the blood-brain barrier and its role in the transport of amino acids. *J Nutr,* 136, 218S-26S.

HAYASHI, K., NAKAO, S., NAKAOKE, R., NAKAGAWA, S., KITAGAWA, N. & NIWA, M. (2004) Effects of hypoxia on endothelial/pericytic co-culture model of the blood-brain barrier. *Regul Pept,* 123, 77-83.

HAYASHI, Y., NOMURA, M., YAMAGISHI, S., HARADA, S., YAMASHITA, J. & YAMAMOTO, H. (1997) Induction of various blood-brain barrier properties in non-neural endothelial cells by close apposition to co-cultured astrocytes. *Glia,* 19, 13-26.

HAYNES, B. F., SCEARCE, R. M., LOBACH, D. F. & HENSLEY, L. L. (1984) Phenotypic characterization and ontogeny of mesodermal-derived and endocrine epithelial components of the human thymic microenvironment. *J Exp Med,* 159, 1149-68.

HOHEISEL, D., NITZ, T., FRANKE, H., WEGENER, J., HAKVOORT, A., TILLING, T. & GALLA, H. J. (1998) Hydrocortisone reinforces the blood-brain barrier properties in a serum free cell culture system. *Biochem Biophys Res Commun,* 244, 312-6.

HOLASH, J. A., NODEN, D. M. & STEWART, P. A. (1993) Re-evaluating the role of astrocytes in blood-brain barrier induction. *Dev Dyn,* 197, 14-25.

HOLLEY, J. E., GVERIC, D., WHATMORE, J. L. & GUTOWSKI, N. J. (2005) Tenascin C induces a quiescent phenotype in cultured adult human astrocytes. *Glia,* 52, 53-8.

HORI, S., OHTSUKI, S., HOSOYA, K., NAKASHIMA, E. & TERASAKI, T. (2004) A pericyte-derived angiopoietin-1 multimeric complex induces occludin gene expression in brain capillary endothelial cells through Tie-2 activation in vitro. *J Neurochem,* 89, 503-13.

HORNING, J. L., SAHOO, S. K., VIJAYARAGHAVALU, S., DIMITRIJEVIC, S., VASIR, J. K., JAIN, T. K., PANDA, A. K. & LABHASETWAR, V. (2008) 3-D tumor model for in vitro evaluation of anticancer drugs. *Mol Pharm,* 5, 849-62.

HOSLI, E. & HOSLI, L. (1991) Autoradiographic evidence for endothelin receptors on astrocytes in cultures of rat cerebellum, brainstem and spinal cord. *Neurosci Lett,* 129, 55-8.

HSUCHOU, H., KASTIN, A. J., TU, H., JOAN ABBOTT, N., COURAUD, P. O. & PAN, W. (2010) Role of astrocytic leptin receptor subtypes on leptin permeation across hCMEC/D3 human brain endothelial cells. *J Neurochem,* 115, 1288-98.

HUBER, J. D., EGLETON, R. D. & DAVIS, T. P. (2001) Molecular physiology and pathophysiology of tight junctions in the blood-brain barrier. *Trends Neurosci,* 24, 719-25.

HURST, R. D. & FRITZ, I. B. (1996) Properties of an immortalised vascular endothelial/glioma cell co-culture model of the blood-brain barrier. *J Cell Physiol,* 167, 81-8.

HURWITZ, A. A., BERMAN, J. W., RASHBAUM, W. K. & LYMAN, W. D. (1993) Human fetal astrocytes induce the expression of blood-brain barrier specific proteins by autologous endothelial cells. *Brain Res,* 625, 238-43.

IGARASHI, Y., UTSUMI, H., CHIBA, H., YAMADA-SASAMORI, Y., TOBIOKA, H., KAMIMURA, Y., FURUUCHI, K., KOKAI, Y., NAKAGAWA, T., MORI, M. & SAWADA, N. (1999) Glial cell line-derived neurotrophic factor induces barrier function of endothelial cells forming the blood-brain barrier. *Biochem Biophys Res Commun,* 261, 108-12.

ISOBE, I., WATANABE, T., YOTSUYANAGI, T., HAZEMOTO, N., YAMAGATA, K., UEKI, T., NAKANISHI, K., ASAI, K. & KATO, T. (1996) Astrocytic contributions to blood-brain barrier (BBB) formation by endothelial cells: a possible use of aortic endothelial cell for in vitro BBB model. *Neurochem Int,* 28, 523-33.

ITOH, K. (2002) Culture of oligodendrocyte precursor cells (NG2(+)/O1(-)) and oligodendrocytes (NG2(-)/O1(+)) from embryonic rat cerebrum. *Brain Res Brain Res Protoc,* 10, 23-30.

JANCIC, C., CHULUYAN, H. E., MORELLI, A., LARREGINA, A., KOLKOWSKI, E., SARACCO, M., BARBOZA, M., LEIVA, W. S. & FAINBOIM, L. (1998) Interactions of dendritic cells with fibronectin and endothelial cells. *Immunology,* 95, 283-90.

JANICKE, R. U., SOHN, D., ESSMANN, F. & SCHULZE-OSTHOFF, K. (2007) The multiple battles fought by anti-apoptotic p21. *Cell Cycle,* 6, 407-13.

JANIN, A., KONTTINEN, Y. T., GRONBLAD, M., KARHUNEN, P., GOSSET, D. & MALMSTROM, M. (1990) Fibroblast markers in labial salivary gland biopsies in progressive systemic sclerosis. *Clin Exp Rheumatol,* 8, 237-42.

JANMEY, P. A., WINER, J. P., MURRAY, M. E. & WEN, Q. (2009) The hard life of soft cells. *Cell Motil Cytoskeleton,* 66, 597-605.

JANZER, R. C. & RAFF, M. C. (1987) Astrocytes induce blood-brain barrier properties in endothelial cells. *Nature,* 325, 253-7.

JELIAZKOVA-MECHEVA, V. V. & BOBILYA, D. J. (2003) A porcine astrocyte/endothelial cell co-culture model of the blood-brain barrier. *Brain Res Brain Res Protoc,* 12, 91-8.

JIN, B. J., ROSSI, A. & VERKMAN, A. S. (2011) Model of aquaporin-4 supramolecular assembly in orthogonal arrays based on heterotetrameric association of M1-M23 isoforms. *Biophys J,* 100, 2936-45.

JUNG, J. S., BHAT, R. V., PRESTON, G. M., GUGGINO, W. B., BARABAN, J. M. & AGRE, P. (1994) Molecular characterization of an aquaporin cDNA from brain: candidate osmoreceptor and regulator of water balance. *Proc Natl Acad Sci U S A,* 91, 13052-6.

KAKINUMA, Y., HAMA, H., SUGIYAMA, F., YAGAMI, K., GOTO, K., MURAKAMI, K. & FUKAMIZU, A. (1998) Impaired blood-brain barrier function in angiotensinogen-deficient mice. *Nat Med,* 4, 1078-80.

KALIMO, H., VINTERS, H. V. & INTERNATIONAL SOCIETY OF NEUROPATHOLOGY. (2005) *Cerebrovascular diseases,* Basel, Switzerland, ISN.

KANG, W. & HEBERT, J. M. (2011) Signaling pathways in reactive astrocytes, a genetic perspective. *Mol Neurobiol,* 43, 147-54.

KAUFMAN, L. J., BRANGWYNNE, C. P., KASZA, K. E., FILIPPIDI, E., GORDON, V. D., DEISBOECK, T. S. & WEITZ, D. A. (2005) Glioma expansion in collagen I matrices: analyzing collagen concentration-dependent growth and motility patterns. *Biophys J,* 89, 635-50.

KAUR, C. & LING, E. A. (2008) Blood brain barrier in hypoxic-ischemic conditions. *Curr Neurovasc Res,* 5, 71-81.

KEEP, R. F. (2011) Neural progenitor cells and blood-brain barrier modeling. *J Neurochem,* 119, 417-8.

KIDO, Y., TAMAI, I., OKAMOTO, M., SUZUKI, F. & TSUJI, A. (2000) Functional clarification of MCT1-mediated transport of monocarboxylic acids at the blood-brain barrier using in vitro cultured cells and in vivo BUI studies. *Pharm Res,* 17, 55-62.

KIM, J. W., HO, W. J. & WU, B. M. (2011) The role of the 3D environment in hypoxia-induced drug and apoptosis resistance. *Anticancer Res,* 31, 3237-45.

KOBAYASHI, H., MINAMI, S., ITOH, S., SHIRAISHI, S., YOKOO, H., YANAGITA, T., UEZONO, Y., MOHRI, M. & WADA, A. (2001) Aquaporin subtypes in rat cerebral microvessels. *Neurosci Lett,* 297, 163-6.

KOFRON, C. M., FONG, V. J. & HOFFMAN-KIM, D. (2009) Neurite outgrowth at the interface of 2D and 3D growth environments. *J Neural Eng,* 6, 016002.

KOH, W., STRATMAN, A. N., SACHARIDOU, A. & DAVIS, G. E. (2008) In vitro three dimensional collagen matrix models of endothelial lumen formation during vasculogenesis and angiogenesis. *Methods Enzymol,* 443, 83-101.

KOYAMA, Y., TAKEMURA, M., FUJIKI, K., ISHIKAWA, N., SHIGENAGA, Y. & BABA, A. (1999) BQ788, an endothelin ET(B) receptor antagonist, attenuates stab wound injury-induced reactive astrocytes in rat brain. *Glia,* 26, 268-71.

KOYAMA, Y. & TANAKA, K. (2010) Decreases in rat brain aquaporin-4 expression following intracerebroventricular administration of an endothelin ET B receptor agonist. *Neurosci Lett,* 469, 343-7.

KRUEGER, M. & BECHMANN, I. (2010) CNS pericytes: concepts, misconceptions, and a way out. *Glia,* 58, 1-10.

KSHITIZ, HUBBI, M. E., AHN, E. H., DOWNEY, J., AFZAL, J., KIM, D. H., REY, S., CHANG, C., KUNDU, A., SEMENZA, G. L., ABRAHAM, R. M. & LEVCHENKO, A. (2012) Matrix rigidity controls endothelial differentiation and morphogenesis of cardiac precursors. *Sci Signal,* 5, ra41.

KUO, Y. C. & LU, C. H. (2011) Effect of human astrocytes on the characteristics of human brain-microvascular endothelial cells in the blood-brain barrier. *Colloids Surf B Biointerfaces.*

LARSEN, M., ARTYM, V. V., GREEN, J. A. & YAMADA, K. M. (2006) The matrix reorganized: extracellular matrix remodeling and integrin signaling. *Curr Opin Cell Biol,* 18, 463-71.

LAZARINI, F., STROSBERG, A. D., COURAUD, P. O. & CAZAUBON, S. M. (1996) Coupling of ETB endothelin receptor to mitogen-activated protein kinase stimulation and DNA synthesis in primary cultures of rat astrocytes. *J Neurochem,* 66, 459-65.

LECHARDEUR, D., SCHWARTZ, B., PAULIN, D. & SCHERMAN, D. (1995) Induction of blood-brain barrier differentiation in a rat brain-derived endothelial cell line. *Exp Cell Res,* 220, 161-70.

LEE, J., CUDDIHY, M. J. & KOTOV, N. A. (2008) Three-dimensional cell culture matrices: state of the art. *Tissue Eng Part B Rev,* 14, 61-86.

LEE, S. W., KIM, W. J., CHOI, Y. K., SONG, H. S., SON, M. J., GELMAN, I. H., KIM, Y. J. & KIM, K. W. (2003) SSeCKS regulates angiogenesis and tight junction formation in blood-brain barrier. *Nat Med,* 9, 900-6.

LEYBAERT, L., CABOOTER, L. & BRAET, K. (2004) Calcium signal communication between glial and vascular brain cells. *Acta Neurol Belg,* 104, 51-6.

LI, G. N., LIVI, L. L., GOURD, C. M., DEWEERD, E. S. & HOFFMAN-KIM, D. (2007) Genomic and morphological changes of neuroblastoma cells in response to three-dimensional matrices. *Tissue Eng,* 13, 1035-47.

LI, L., LUNDKVIST, A., ANDERSSON, D., WILHELMSSON, U., NAGAI, N., PARDO, A. C., NODIN, C., STAHLBERG, A., APRICO, K., LARSSON, K., YABE, T., MOONS, L., FOTHERINGHAM, A., DAVIES, I., CARMELIET, P., SCHWARTZ, J. P., PEKNA, M., KUBISTA, M., BLOMSTRAND, F., MARAGAKIS, N., NILSSON, M. & PEKNY, M. (2008) Protective role of reactive astrocytes in brain ischemia. *J Cereb Blood Flow Metab,* 28, 468-81.

LI, S., LAO, J., CHEN, B. P., LI, Y. S., ZHAO, Y., CHU, J., CHEN, K. D., TSOU, T. C., PECK, K. & CHIEN, S. (2003) Genomic analysis of smooth muscle cells in 3-dimensional collagen matrix. *Faseb J,* 17, 97-9.

LIEBNER, S., CORADA, M., BANGSOW, T., BABBAGE, J., TADDEI, A., CZUPALLA, C. J., REIS, M., FELICI, A., WOLBURG, H., FRUTTIGER, M., TAKETO, M. M., VON MELCHNER, H., PLATE, K. H., GERHARDT, H. & DEJANA, E. (2008) Wnt/beta-catenin signaling controls development of the blood-brain barrier. *J Cell Biol,* 183, 409-17.

LIEBNER, S., FISCHMANN, A., RASCHER, G., DUFFNER, F., GROTE, E. H., KALBACHER, H. & WOLBURG, H. (2000) Claudin-1 and claudin-5 expression and tight junction morphology are altered in blood vessels of human glioblastoma multiforme. *Acta Neuropathol,* 100, 323-31.

LIEDTKE, W., EDELMANN, W., BIERI, P. L., CHIU, F. C., COWAN, N. J., KUCHERLAPATI, R. & RAINE, C. S. (1996) GFAP is necessary for the integrity of CNS white matter architecture and long-term maintenance of myelination. *Neuron,* 17, 607-15.

LINDROOS, B., AHO, K. L., KUOKKANEN, H., RATY, S., HUHTALA, H., LEMPONEN, R., YLI-HARJA, O., SUURONEN, R. & MIETTINEN, S. (2010) Differential gene expression in adipose stem cells cultured in allogeneic human serum versus fetal bovine serum. *Tissue Eng Part A,* 16, 2281-94.

LIPPMANN, E. S., WEIDENFELLER, C., SVENDSEN, C. N. & SHUSTA, E. V. (2011) Blood-brain barrier modeling with co-cultured neural progenitor cell-derived astrocytes and neurons. *J Neurochem,* 119, 507-20.

LU, J. (2012) A novel hypothesis of blood-brain barrier (BBB) development and in vitro BBB model: neural stem cell is the driver of BBB formation and maintenance. *J Exp Integr Med,* 2, 39-43.

LYCK, R., RUDERISCH, N., MOLL, A. G., STEINER, O., COHEN, C. D., ENGELHARDT, B., MAKRIDES, V. & VERREY, F. (2009) Culture-induced changes in blood-brain barrier

transcriptome: implications for amino-acid transporters in vivo. *J Cereb Blood Flow Metab,* 29, 1491-502.

MA, S. H., LEPAK, L. A., HUSSAIN, R. J., SHAIN, W. & SHULER, M. L. (2005) An endothelial and astrocyte co-culture model of the blood-brain barrier utilizing an ultra-thin, nanofabricated silicon nitride membrane. *Lab Chip,* 5, 74-85.

MA, T., YANG, B., GILLESPIE, A., CARLSON, E. J., EPSTEIN, C. J. & VERKMAN, A. S. (1997) Generation and phenotype of a transgenic knockout mouse lacking the mercurial-insensitive water channel aquaporin-4. *J Clin Invest,* 100, 957-62.

MACHEIN, M. R., KULLMER, J., FIEBICH, B. L., PLATE, K. H. & WARNKE, P. C. (1999) Vascular endothelial growth factor expression, vascular volume, and, capillary permeability in human brain tumors. *Neurosurgery,* 44, 732-40; discussion 740-1.

MACIKOVA, I., PERZELOVA, A., MRAZ, P., BIZIK, I. & STENO, J. (2009) GFAP-positive astrocytes are rare or absent in primary adult human brain tissue cultures. *Biologia,* 64, 833-839.

MADARA, J. L. (1998) Regulation of the movement of solutes across tight junctions. *Annu Rev Physiol,* 60, 143-59.

MALINA, K. C., COOPER, I. & TEICHBERG, V. I. (2009) Closing the gap between the in-vivo and in-vitro blood-brain barrier tightness. *Brain Res,* 1284, 12-21.

MALTMAN, D. J. & PRZYBORSKI, S. A. (2010) Developments in three-dimensional cell culture technology aimed at improving the accuracy of in vitro analyses. *Biochem Soc Trans,* 38, 1072-5.

MANLEY, G. T., FUJIMURA, M., MA, T., NOSHITA, N., FILIZ, F., BOLLEN, A. W., CHAN, P. & VERKMAN, A. S. (2000) Aquaporin-4 deletion in mice reduces brain edema after acute water intoxication and ischemic stroke. *Nat Med,* 6, 159-63.

MARCHESI, V. T. (1965) The role of pinocytic vesicles in the transport of materials across the walls of small blood vessels. *Invest Ophthalmol,* 4, 1111-21.

MASAKI, T. (1994) Endothelin in vascular biology. *Ann N Y Acad Sci,* 714, 101-8.

MASON, B. N., STARCHENKO, A., WILLIAMS, R. M., BONASSAR, L. J. & REINHART-KING, C. A. (2012) Tuning three-dimensional collagen matrix stiffness independently of collagen concentration modulates endothelial cell behavior. *Acta Biomater.*

MATHIISEN, T. M., LEHRE, K. P., DANBOLT, N. C. & OTTERSEN, O. P. (2010) The perivascular astroglial sheath provides a complete covering of the brain microvessels: an electron microscopic 3D reconstruction. *Glia,* 58, 1094-103.

MATTER, K. & BALDA, M. S. (2003) Signalling to and from tight junctions. *Nat Rev Mol Cell Biol,* 4, 225-36.

MATTOW, J., SCHAIBLE, U. E., SCHMIDT, F., HAGENS, K., SIEJAK, F., BRESTRICH, G., HAESELBARTH, G., MULLER, E. C., JUNGBLUT, P. R. & KAUFMANN, S. H. (2003) Comparative proteome analysis of culture supernatant proteins from virulent Mycobacterium tuberculosis H37Rv and attenuated M. bovis BCG Copenhagen. *Electrophoresis,* 24, 3405-20.

MAXWELL, K., BERLINER, J. A. & CANCILLA, P. A. (1989) Stimulation of glucose analogue uptake by cerebral microvessel endothelial cells by a product released by astrocytes. *J Neuropathol Exp Neurol,* 48, 69-80.

MCALLISTER, M. S., KRIZANAC-BENGEZ, L., MACCHIA, F., NAFTALIN, R. J., PEDLEY, K. C., MAYBERG, M. R., MARRONI, M., LEAMAN, S., STANNESS, K. A. & JANIGRO, D. (2001) Mechanisms of glucose transport at the blood-brain barrier: an in vitro study. *Brain Res,* 904, 20-30.

MCCASLIN, A. F., CHEN, B. R., RADOSEVICH, A. J., CAULI, B. & HILLMAN, E. M. (2011) In vivo 3D morphology of astrocyte-vasculature interactions in the somatosensory cortex: implications for neurovascular coupling. *J Cereb Blood Flow Metab,* 31, 795-806.

MEGARD, I., GARRIGUES, A., ORLOWSKI, S., JORAJURIA, S., CLAYETTE, P., EZAN, E. & MABONDZO, A. (2002) A co-culture-based model of human blood-brain barrier: application to active transport of indinavir and in vivo-in vitro correlation. *Brain Res,* 927, 153-67.

MENT, L. R., STEWART, W. B., SCARAMUZZINO, D. & MADRI, J. A. (1997) An in vitro three-dimensional coculture model of cerebral microvascular angiogenesis and differentiation. *In Vitro Cell Dev Biol Anim,* 33, 684-91.

METEA, M. R. & NEWMAN, E. A. (2006) Glial cells dilate and constrict blood vessels: a mechanism of neurovascular coupling. *J Neurosci,* 26, 2862-70.

MEYER, J., RAUH, J. & GALLA, H. J. (1991) The susceptibility of cerebral endothelial cells to astroglial induction of blood-brain barrier enzymes depends on their proliferative state. *J Neurochem,* 57, 1971-7.

MI, H. & BARRES, B. A. (1999) Purification and characterization of astrocyte precursor cells in the developing rat optic nerve. *J Neurosci,* 19, 1049-61.

MI, H., HAEBERLE, H. & BARRES, B. A. (2001) Induction of astrocyte differentiation by endothelial cells. *J Neurosci,* 21, 1538-47.

MITRA, M., MOHANTY, C., HARILAL, A., MAHESWARI, U. K., SAHOO, S. K. & KRISHNAKUMAR, S. (2012) A novel in vitro three-dimensional retinoblastoma model for evaluating chemotherapeutic drugs. *Mol Vis,* 18, 1361-78.

MIZUGUCHI, H., HASHIOKA, Y., FUJII, A., UTOGUCHI, N., KUBO, K., NAKAGAWA, S., BABA, A. & MAYUMI, T. (1994) Glial extracellular matrix modulates gamma-glutamyl transpeptidase activity in cultured bovine brain capillary and bovine aortic endothelial cells. *Brain Res,* 651, 155-9.

MOORADIAN, D. L. & DIGLIO, C. A. (1991) Production of a transforming growth factor-beta-like growth factor by RSV-transformed rat cerebral microvascular endothelial cells. *Tumour Biol,* 12, 171-83.

MORIN, A. M. & STANBOLI, A. (1993) Nitric oxide synthase in cultured endothelial cells of cerebrovascular origin: cytochemistry. *J Neurosci Res,* 36, 272-9.

MURUGANANDAM, A., HERX, L. M., MONETTE, R., DURKIN, J. P. & STANIMIROVIC, D. B. (1997) Development of immortalized human cerebromicrovascular endothelial cell line as an in vitro model of the human blood-brain barrier. *Faseb J,* 11, 1187-97.

NAG, S. & BEGLEY, D. J. (2005) Blood-brain barrier, exchange of metabolites and gases. IN KALIMO, H., VINTERS, H. V. & INTERNATIONAL SOCIETY OF NEUROPATHOLOGY. (Eds.) *Pathology of genetics. Cerebrovascular diseases.* Basel, Switzerland, ISN Neropath. Press.

NAGANO, N., AOYAGI, M. & HIRAKAWA, K. (1993) Extracellular matrix modulates the proliferation of rat astrocytes in serum-free culture. *Glia,* 8, 71-6.

NAGANO, N., AOYAGI, M., HIRAKAWA, K., YAMAMOTO, M. & YAMAMOTO, K. (1996) Organization of F-actin filaments in human glioma cell lines cultured on extracellular matrix proteins. *J Neurooncol,* 27, 215-24.

NAIK, P. & CUCULLO, L. (2012) In vitro blood-brain barrier models: current and perspective technologies. *J Pharm Sci,* 101, 1337-54.

NAKAGAWA, S., DELI, M. A., KAWAGUCHI, H., SHIMIZUDANI, T., SHIMONO, T., KITTEL, A., TANAKA, K. & NIWA, M. (2009) A new blood-brain barrier model using primary rat brain endothelial cells, pericytes and astrocytes. *Neurochem Int,* 54, 253-63.

NAKANO, I., KATO, S., YAZAWA, I. & HIRANO, A. (1992) Anchorage densities associated with hemidesmosome-like structures in perivascular reactive astrocytes. *Acta Neuropathol,* 84, 85-8.

NEAL, C. J., LEE, E. Y., GYORGY, A., ECKLUND, J. M., AGOSTON, D. V. & LING, G. S. (2007) Effect of penetrating brain injury on aquaporin-4 expression using a rat model. *J Neurotrauma,* 24, 1609-17.

NEUWELT, E., ABBOTT, N. J., ABREY, L., BANKS, W. A., BLAKLEY, B., DAVIS, T., ENGELHARDT, B., GRAMMAS, P., NEDERGAARD, M., NUTT, J., PARDRIDGE, W., ROSENBERG, G. A., SMITH, Q. & DREWES, L. R. (2008) Strategies to advance translational research into brain barriers. *Lancet Neurol,* 7, 84-96.

NICCHIA, G. P., FRIGERI, A., LIUZZI, G. M., SANTACROCE, M. P., NICO, B., PROCINO, G., QUONDAMATTEO, F., HERKEN, R., RONCALI, L. & SVELTO, M. (2000) Aquaporin-4-containing astrocytes sustain a temperature- and mercury-insensitive swelling in vitro. *Glia,* 31, 29-38.

NICCHIA, G. P., NICO, B., CAMASSA, L. M., MOLA, M. G., LOH, N., DERMIETZEL, R., SPRAY, D. C., SVELTO, M. & FRIGERI, A. (2004) The role of aquaporin-4 in the blood-brain barrier development and integrity: studies in animal and cell culture models. *Neuroscience,* 129, 935-45.

NIELSEN, S., NAGELHUS, E. A., AMIRY-MOGHADDAM, M., BOURQUE, C., AGRE, P. & OTTERSEN, O. P. (1997) Specialized membrane domains for water transport in glial cells: high-resolution immunogold cytochemistry of aquaporin-4 in rat brain. *J Neurosci,* 17, 171-80.

NISHIYAMA, T., TOMINAGA, N., NAKAJIMA, K. & HAYASHI, T. (1988) Quantitative evaluation of the factors affecting the process of fibroblast-mediated collagen gel contraction by separating the process into three phases. *Coll Relat Res,* 8, 259-73.

NITTA, T., HATA, M., GOTOH, S., SEO, Y., SASAKI, H., HASHIMOTO, N., FURUSE, M. & TSUKITA, S. (2003) Size-selective loosening of the blood-brain barrier in claudin-5-deficient mice. *J Cell Biol,* 161, 653-60.

NITZ, T., EISENBLATTER, T., PSATHAKI, K. & GALLA, H. J. (2003) Serum-derived factors weaken the barrier properties of cultured porcine brain capillary endothelial cells in vitro. *Brain Res,* 981, 30-40.

NOELL, S., FALLIER-BECKER, P., DEUTSCH, U., MACK, A. F. & WOLBURG, H. (2009) Agrin defines polarized distribution of orthogonal arrays of particles in astrocytes. *Cell Tissue Res,* 337, 185-95.

O'BRIEN, L. E., ZEGERS, M. M. & MOSTOV, K. E. (2002) Opinion: Building epithelial architecture: insights from three-dimensional culture models. *Nat Rev Mol Cell Biol,* 3, 531-7.

OGUNSHOLA, O. O. (2011) In vitro modeling of the blood-brain barrier: simplicity versus complexity. *Curr Pharm Des,* 17, 2755-61.

OLDENDORF, W. H., CORNFORD, M. E. & BROWN, W. J. (1977) The large apparent work capability of the blood-brain barrier: a study of the mitochondrial content of capillary endothelial cells in brain and other tissues of the rat. *Ann Neurol,* 1, 409-17.

OMIDI, Y., BARAR, J., AHMADIAN, S., HEIDARI, H. R. & GUMBLETON, M. (2008) Characterization and astrocytic modulation of system L transporters in brain microvasculature endothelial cells. *Cell Biochem Funct,* 26, 381-91.

OTT, M. J. & BALLERMANN, B. J. (1995) Shear stress-conditioned, endothelial cell-seeded vascular grafts: improved cell adherence in response to in vitro shear stress. *Surgery,* 117, 334-9.

OZEKI, M., KURODA, S., KON, K. & KASUGAI, S. (2011) Differentiation of bone marrow stromal cells into osteoblasts in a self-assembling peptide hydrogel: in vitro and in vivo studies. *J Biomater Appl,* 25, 663-84.

PAPADOPOULOS, M. C., MANLEY, G. T., KRISHNA, S. & VERKMAN, A. S. (2004) Aquaporin-4 facilitates reabsorption of excess fluid in vasogenic brain edema. *Faseb J,* 18, 1291-3.

PAPADOPOULOS, M. C., SAADOUN, S., WOODROW, C. J., DAVIES, D. C., COSTA-MARTINS, P., MOSS, R. F., KRISHNA, S. & BELL, B. A. (2001) Occludin expression in microvessels of neoplastic and non-neoplastic human brain. *Neuropathol Appl Neurobiol,* 27, 384-95.

PARDRIDGE, W. M. (1998) *Introduction to the blood-brain barrier : methodology, biology, and pathology,* Cambridge, Cambridge University Press.

PEKNY, M., LEVEEN, P., PEKNA, M., ELIASSON, C., BERTHOLD, C. H., WESTERMARK, B. & BETSHOLTZ, C. (1995) Mice lacking glial fibrillary acidic protein display astrocytes devoid of intermediate filaments but develop and reproduce normally. *Embo J,* 14, 1590-8.

PEKNY, M., STANNESS, K. A., ELIASSON, C., BETSHOLTZ, C. & JANIGRO, D. (1998) Impaired induction of blood-brain barrier properties in aortic endothelial cells by astrocytes from GFAP-deficient mice. *Glia,* 22, 390-400.

PELLITTERI-HAHN, M. C., WARREN, M. C., DIDIER, D. N., WINKLER, E. L., MIRZA, S. P., GREENE, A. S. & OLIVIER, M. (2006) Improved mass spectrometric proteomic profiling of the secretome of rat vascular endothelial cells. *J Proteome Res,* 5, 2861-4.

PERRIERE, N., YOUSIF, S., CAZAUBON, S., CHAVEROT, N., BOURASSET, F., CISTERNINO, S., DECLEVES, X., HORI, S., TERASAKI, T., DELI, M., SCHERRMANN, J. M., TEMSAMANI, J., ROUX, F. & COURAUD, P. O. (2007) A functional in vitro model of rat blood-brain barrier for molecular analysis of efflux transporters. *Brain Res,* 1150, 1-13.

POST, G. R. & DAWSON, G. (1992) Characterization of a cell line derived from a human oligodendroglioma. *Mol Chem Neuropathol,* 16, 303-17.

POTTIEZ, G., DUBAN-DEWEER, S., DERACINOIS, B., GOSSELET, F., CAMOIN, L., HACHANI, J., COURAUD, P. O., CECCHELLI, R., DEHOUCK, M. P., FENART, L., KARAMANOS, Y. & FLAHAUT, C. (2011) A differential proteomic approach identifies structural and functional components that contribute to the differentiation of brain capillary endothelial cells. *J Proteomics,* 75, 628-41.

PRAT, A., BIERNACKI, K., WOSIK, K. & ANTEL, J. P. (2001) Glial cell influence on the human blood-brain barrier. *Glia,* 36, 145-55.

PRUDHOMME, J. G., SHERMAN, I. W., LAND, K. M., MOSES, A. V., STENGLEIN, S. & NELSON, J. A. (1996) Studies of Plasmodium falciparum cytoadherence using immortalized human brain capillary endothelial cells. *Int J Parasitol,* 26, 647-55.

PULFORD, K. A., RIGNEY, E. M., MICKLEM, K. J., JONES, M., STROSS, W. P., GATTER, K. C. & MASON, D. Y. (1989) KP1: a new monoclonal antibody that detects a monocyte/macrophage associated antigen in routinely processed tissue sections. *J Clin Pathol,* 42, 414-21.

RANSOM, B. R. & RANSOM, C. B. (2012) Astrocytes: multitalented stars of the central nervous system. *Methods Mol Biol,* 814, 3-7.

RASH, J. E., YASUMURA, T., HUDSON, C. S., AGRE, P. & NIELSEN, S. (1998) Direct immunogold labeling of aquaporin-4 in square arrays of astrocyte and ependymocyte plasma membranes in rat brain and spinal cord. *Proc Natl Acad Sci U S A,* 95, 11981-6.

REDDEN, R. A. & DOOLIN, E. J. (2003) Collagen crosslinking and cell density have distinct effects on fibroblast-mediated contraction of collagen gels. *Skin Res Technol,* 9, 290-3.

REGINA, A., ROMERO, I. A., GREENWOOD, J., ADAMSON, P., BOURRE, J. M., COURAUD, P. O. & ROUX, F. (1999) Dexamethasone regulation of P-glycoprotein activity in an immortalized rat brain endothelial cell line, GPNT. *J Neurochem,* 73, 1954-63.

REICHENBACH, A. & WOLBURG, H. (2004) Neuroglia. IN KETTEMANN, H. & RANSOM, B. R. (Eds.) *Neuroglia.* 2 ed. New York, Oxford Univ. Press,.

REINHARDT, C. A. & GLOOR, S. M. (1997) Co-culture blood-brain barrier models and their use for pharmatoxicological screening. *Toxicol In Vitro,* 11, 513-8.

REZAIE, P., ULFIG, N. & MALE, D. (2003) Distribution and Morphology of GFAP-Positive Astrocytes in the Human Fetal Brain at Second Trimester. *Neuroembryology and Aging,* 2.

RICHARDS, L. J., KILPATRICK, T. J., DUTTON, R., TAN, S. S., GEARING, D. P., BARTLETT, P. F. & MURPHY, M. (1996) Leukaemia inhibitory factor or related factors promote the differentiation of neuronal and astrocytic precursors within the developing murine spinal cord. *Eur J Neurosci,* 8, 291-9.

RICHTER-LANDSBERG, C. & HEINRICH, M. (1995) S-100 immunoreactivity in rat brain glial cultures is associated with both astrocytes and oligodendrocytes. *J Neurosci Res,* 42, 657-65.

RISAU, W., ESSER, S. & ENGELHARDT, B. (1998) Differentiation of blood-brain barrier endothelial cells. *Pathol Biol (Paris),* 46, 171-5.

RIST, R. J., ROMERO, I. A., CHAN, M. W., COURAUD, P. O., ROUX, F. & ABBOTT, N. J. (1997) F-actin cytoskeleton and sucrose permeability of immortalised rat brain microvascular endothelial cell monolayers: effects of cyclic AMP and astrocytic factors. *Brain Res,* 768, 10-8.

RIVKIN, M. J., FLAX, J., MOZELL, R., OSATHANONDH, R., VOLPE, J. J. & VILLA-KOMAROFF, L. (1995) Oligodendroglial development in human fetal cerebrum. *Ann Neurol,* 38, 92-101.

ROGERS, S. D., DEMASTER, E., CATTON, M., GHILARDI, J. R., LEVIN, L. A., MAGGIO, J. E. & MANTYH, P. W. (1997) Expression of endothelin-B receptors by glia in vivo is increased after CNS injury in rats, rabbits, and humans. *Exp Neurol,* 145, 180-95.

ROGERS, S. D., PETERS, C. M., POMONIS, J. D., HAGIWARA, H., GHILARDI, J. R. & MANTYH, P. W. (2003) Endothelin B receptors are expressed by astrocytes and regulate astrocyte hypertrophy in the normal and injured CNS. *Glia,* 41, 180-90.

ROUX, F. & COURAUD, P. O. (2005) Rat brain endothelial cell lines for the study of blood-brain barrier permeability and transport functions. *Cell Mol Neurobiol,* 25, 41-58.

RUBIN, L. L. (1991a) The blood-brain barrier in and out of cell culture. *Curr Opin Neurobiol,* 1, 360-3.

RUBIN, L. L., HALL, D. E., PORTER, S., BARBU, K., CANNON, C., HORNER, H. C., JANATPOUR, M., LIAW, C. W., MANNING, K., MORALES, J. & ET AL. (1991b) A cell culture model of the blood-brain barrier. *J Cell Biol,* 115, 1725-35.

RUTKA, J. T., GIBLIN, J. R., BALKISSOON, R., WEN, D., MYATT, C. A., MCCULLOCH, J. R. & ROSENBLUM, M. L. (1987) Characterization of fetal human brain cultures. Development of a potential model for selectively purifying human glial cells in culture. *Dev Neurosci,* 9, 154-73.

SAADOUN, S., PAPADOPOULOS, M. C., WATANABE, H., YAN, D., MANLEY, G. T. & VERKMAN, A. S. (2005) Involvement of aquaporin-4 in astroglial cell migration and glial scar formation. *J Cell Sci,* 118, 5691-8.

SAADOUN, S., TAIT, M. J., REZA, A., DAVIES, D. C., BELL, B. A., VERKMAN, A. S. & PAPADOPOULOS, M. C. (2009) AQP4 gene deletion in mice does not alter blood-brain barrier integrity or brain morphology. *Neuroscience,* 161, 764-72.

SAITOU, M., FURUSE, M., SASAKI, H., SCHULZKE, J. D., FROMM, M., TAKANO, H., NODA, T. & TSUKITA, S. (2000) Complex phenotype of mice lacking occludin, a component of tight junction strands. *Mol Biol Cell,* 11, 4131-42.

SAKAKIBARA, A., FURUSE, M., SAITOU, M., ANDO-AKATSUKA, Y. & TSUKITA, S. (1997) Possible involvement of phosphorylation of occludin in tight junction formation. *J Cell Biol,* 137, 1393-401.

SANO, Y., SHIMIZU, F., ABE, M., MAEDA, T., KASHIWAMURA, Y., OHTSUKI, S., TERASAKI, T., OBINATA, M., KAJIWARA, K., FUJII, M., SUZUKI, M. & KANDA, T. (2010) Establishment of a new conditionally immortalized human brain microvascular endothelial cell line retaining an in vivo blood-brain barrier function. *J Cell Physiol,* 225, 519-28.

SANTAGUIDA, S., JANIGRO, D., HOSSAIN, M., OBY, E., RAPP, E. & CUCULLO, L. (2006) Side by side comparison between dynamic versus static models of blood-brain barrier in vitro: a permeability study. *Brain Res,* 1109, 1-13.

SAUNDERS, N. R., KNOTT, G. W. & DZIEGIELEWSKA, K. M. (2000) Barriers in the immature brain. *Cell Mol Neurobiol,* 20, 29-40.

SAVETTIERI, G., DI LIEGRO, I., CATANIA, C., LICATA, L., PITARRESI, G. L., D'AGOSTINO, S., SCHIERA, G., DE CARO, V., GIANDALIA, G., GIANNOLA, L. I. & CESTELLI, A. (2000) Neurons and ECM regulate occludin localization in brain endothelial cells. *Neuroreport,* 11, 1081-4.

SCHECHNER, J. S., NATH, A. K., ZHENG, L., KLUGER, M. S., HUGHES, C. C., SIERRA-HONIGMANN, M. R., LORBER, M. I., TELLIDES, G., KASHGARIAN, M., BOTHWELL, A. L. & POBER, J. S. (2000) In vivo formation of complex microvessels lined by human endothelial cells in an immunodeficient mouse. *Proc Natl Acad Sci U S A,* 97, 9191-6.

SCHIERA, G., BONO, E., RAFFA, M. P., GALLO, A., PITARRESI, G. L., DI LIEGRO, I. & SAVETTIERI, G. (2003) Synergistic effects of neurons and astrocytes on the differentiation of brain capillary endothelial cells in culture. *J Cell Mol Med,* 7, 165-70.

SCHROETER, M. L., MERTSCH, K., GIESE, H., MULLER, S., SPORBERT, A., HICKEL, B. & BLASIG, I. E. (1999) Astrocytes enhance radical defence in capillary endothelial cells constituting the blood-brain barrier. *FEBS Lett,* 449, 241-4.

SERGENT-TANGUY, S., MICHEL, D. C., NEVEU, I. & NAVEILHAN, P. (2006) Long-lasting coexpression of nestin and glial fibrillary acidic protein in primary cultures of astroglial cells with a major participation of nestin(+)/GFAP(-) cells in cell proliferation. *J Neurosci Res,* 83, 1515-24.

SHAHDADFAR, A., FRONSDAL, K., HAUG, T., REINHOLT, F. P. & BRINCHMANN, J. E. (2005) In vitro expansion of human mesenchymal stem cells: choice of serum is a determinant of cell proliferation, differentiation, gene expression, and transcriptome stability. *Stem Cells,* 23, 1357-66.

SHYAMALA, V., MOULTHROP, T. H., STRATTON-THOMAS, J. & TEKAMP-OLSON, P. (1994) Two distinct human endothelin B receptors generated by alternative splicing from a single gene. *Cell Mol Biol Res,* 40, 285-96.

SIDDHARTHAN, V., KIM, Y. V., LIU, S. & KIM, K. S. (2007) Human astrocytes/astrocyte-conditioned medium and shear stress enhance the barrier properties of human brain microvascular endothelial cells. *Brain Res,* 1147, 39-50.

SIEMINSKI, A. L., HEBBEL, R. P. & GOOCH, K. J. (2004) The relative magnitudes of endothelial force generation and matrix stiffness modulate capillary morphogenesis in vitro. *Exp Cell Res,* 297, 574-84.

SIMARD, M., ARCUINO, G., TAKANO, T., LIU, Q. S. & NEDERGAARD, M. (2003) Signaling at the gliovascular interface. *J Neurosci,* 23, 9254-62.

SMALL, R. K., WATKINS, B. A., MUNRO, P. M. & LIU, D. (1993) Functional properties of retinal Muller cells following transplantation to the anterior eye chamber. *Glia,* 7, 158-69.
SOBUE, K., YAMAMOTO, N., YONEDA, K., FUJITA, K., MIURA, Y., ASAI, K., TSUDA, T., KATSUYA, H. & KATO, T. (1999a) Molecular cloning of two bovine aquaporin-4 cDNA isoforms and their expression in brain endothelial cells. *Biochim Biophys Acta,* 1489, 393-8.
SOBUE, K., YAMAMOTO, N., YONEDA, K., HODGSON, M. E., YAMASHIRO, K., TSURUOKA, N., TSUDA, T., KATSUYA, H., MIURA, Y., ASAI, K. & KATO, T. (1999b) Induction of blood-brain barrier properties in immortalized bovine brain endothelial cells by astrocytic factors. *Neurosci Res,* 35, 155-64.
SOFRONIEW, M. V. (2009) Molecular dissection of reactive astrogliosis and glial scar formation. *Trends Neurosci,* 32, 638-47.
SOFRONIEW, M. V. & VINTERS, H. V. (2010) Astrocytes: biology and pathology. *Acta Neuropathol,* 119, 7-35.
SOMMER, I. & SCHACHNER, M. (1982) Cell that are O4 antigen-positive and O1 antigen-negative differentiate into O1 antigen-positive oligodendrocytes. *Neurosci Lett,* 29, 183-8.
SPOERRI, P. E., GRANT, M. B., GOMEZ, J. & VERNADAKIS, A. (1997) Endothelial cell conditioned media mediated regulation of glutamine synthetase activity in glial cells. *Brain Res Dev Brain Res,* 104, 205-8.
STANIMIROVIC, D. B., YAMAMOTO, T., UEMATSU, S. & SPATZ, M. (1994) Endothelin-1 receptor binding and cellular signal transduction in cultured human brain endothelial cells. *J Neurochem,* 62, 592-601.
STANNESS, K. A., GUATTEO, E. & JANIGRO, D. (1996) A dynamic model of the blood-brain barrier "in vitro". *Neurotoxicology,* 17, 481-96.
STANNESS, K. A., WESTRUM, L. E., FORNACIARI, E., MASCAGNI, P., NELSON, J. A., STENGLEIN, S. G., MYERS, T. & JANIGRO, D. (1997) Morphological and functional characterization of an in vitro blood-brain barrier model. *Brain Res,* 771, 329-42.
STEGEMANN, J. P., HONG, H. & NEREM, R. M. (2005) Mechanical, biochemical, and extracellular matrix effects on vascular smooth muscle cell phenotype. *J Appl Physiol,* 98, 2321-7.
STEVENSON, B. R., SILICIANO, J. D., MOOSEKER, M. S. & GOODENOUGH, D. A. (1986) Identification of ZO-1: a high molecular weight polypeptide associated with the tight junction (zonula occludens) in a variety of epithelia. *J Cell Biol,* 103, 755-66.
STEWART, P. A. & WILEY, M. J. (1981) Developing nervous tissue induces formation of blood-brain barrier characteristics in invading endothelial cells: a study using quail--chick transplantation chimeras. *Dev Biol,* 84, 183-92.
STINS, M. F., PRASADARAO, N. V., ZHOU, J., ARDITI, M. & KIM, K. S. (1997) Bovine brain microvascular endothelial cells transfected with SV40-large T antigen: development of an immortalized cell line to study pathophysiology of CNS disease. *In Vitro Cell Dev Biol Anim,* 33, 243-7.
STONE, D. M. & NIKOLICS, K. (1995) Tissue- and age-specific expression patterns of alternatively spliced agrin mRNA transcripts in embryonic rat suggest novel developmental roles. *J Neurosci,* 15, 6767-78.
STRATMAN, A. N., MALOTTE, K. M., MAHAN, R. D., DAVIS, M. J. & DAVIS, G. E. (2009) Pericyte recruitment during vasculogenic tube assembly stimulates endothelial basement membrane matrix formation. *Blood,* 114, 5091-101.
STROHSCHEIN, S., HUTTMANN, K., GABRIEL, S., BINDER, D. K., HEINEMANN, U. & STEINHAUSER, C. (2011) Impact of aquaporin-4 channels on K+ buffering and gap junction coupling in the hippocampus. *Glia,* 59, 973-80.
SUN, T., JACKSON, S., HAYCOCK, J. W. & MACNEIL, S. (2006) Culture of skin cells in 3D rather than 2D improves their ability to survive exposure to cytotoxic agents. *J Biotechnol,* 122, 372-81.
TADDEI, A., GIAMPIETRO, C., CONTI, A., ORSENIGO, F., BREVIARIO, F., PIRAZZOLI, V., POTENTE, M., DALY, C., DIMMELER, S. & DEJANA, E. (2008) Endothelial adherens junctions control tight junctions by VE-cadherin-mediated upregulation of claudin-5. *Nat Cell Biol,* 10, 923-34.
TAI, L. M., REDDY, P. S., LOPEZ-RAMIREZ, M. A., DAVIES, H. A., MALE, D. K., LOUGHLIN, A. J. & ROMERO, I. A. (2009) Polarized P-glycoprotein expression by the immortalised

human brain endothelial cell line, hCMEC/D3, restricts apical-to-basolateral permeability to rhodamine 123. *Brain Res,* 1292, 14-24.
TAKENAGA, K. & KOZLOVA, E. N. (2006) Role of intracellular S100A4 for migration of rat astrocytes. *Glia,* 53, 313-21.
TALIANA, L., EVANS, M. D., DIMITRIJEVICH, S. D. & STEELE, J. G. (2000) Vitronectin or fibronectin is required for corneal fibroblast-seeded collagen gel contraction. *Invest Ophthalmol Vis Sci,* 41, 103-9.
TANAKA, K. & KOYAMA, Y. (2011) Endothelins decrease the expression of aquaporins and plasma membrane water permeability in cultured rat astrocytes. *J Neurosci Res,* 89, 320-8.
TAO-CHENG, J. H., NAGY, Z. & BRIGHTMAN, M. W. (1987) Tight junctions of brain endothelium in vitro are enhanced by astroglia. *J Neurosci,* 7, 3293-9.
TAO-CHENG, J. H., NAGY, Z. & BRIGHTMAN, M. W. (1990) Astrocytic orthogonal arrays of intramembranous particle assemblies are modulated by brain endothelial cells in vitro. *J Neurocytol,* 19, 143-53.
TATSUTA, T., NAITO, M., OH-HARA, T., SUGAWARA, I. & TSURUO, T. (1992) Functional involvement of P-glycoprotein in blood-brain barrier. *J Biol Chem,* 267, 20383-91.
TEIFEL, M. & FRIEDL, P. (1996) Establishment of the permanent microvascular endothelial cell line PBMEC/C1-2 from porcine brains. *Exp Cell Res,* 228, 50-7.
THANABALASUNDARAM, G., PIEPER, C., LISCHPER, M. & GALLA, H. J. (2010) Regulation of the blood-brain barrier integrity by pericytes via matrix metalloproteinases mediated activation of vascular endothelial growth factor in vitro. *Brain Res,* 1347, 1-10.
THANABALASUNDARAM, G., SCHNEIDEWIND, J., PIEPER, C. & GALLA, H. J. (2011) The impact of pericytes on the blood-brain barrier integrity depends critically on the pericyte differentiation stage. *Int J Biochem Cell Biol,* 43, 1284-93.
TILLING, T., ENGELBERTZ, C., DECKER, S., KORTE, D., HUWEL, S. & GALLA, H. J. (2002) Expression and adhesive properties of basement membrane proteins in cerebral capillary endothelial cell cultures. *Cell Tissue Res,* 310, 19-29.
TILLING, T., KORTE, D., HOHEISEL, D. & GALLA, H. J. (1998) Basement membrane proteins influence brain capillary endothelial barrier function in vitro. *J Neurochem,* 71, 1151-7.
TIRUPPATHI, C., MINSHALL, R. D., PARIA, B. C., VOGEL, S. M. & MALIK, A. B. (2002) Role of Ca2+ signaling in the regulation of endothelial permeability. *Vascul Pharmacol,* 39, 173-85.
TONTSCH, U. & BAUER, H. C. (1991) Glial cells and neurons induce blood-brain barrier related enzymes in cultured cerebral endothelial cells. *Brain Res,* 539, 247-53.
TRAN, N. D., CORREALE, J., SCHREIBER, S. S. & FISHER, M. (1999) Transforming growth factor-beta mediates astrocyte-specific regulation of brain endothelial anticoagulant factors. *Stroke,* 30, 1671-8.
TRAWEGER, A., LEHNER, C., FARKAS, A., KRIZBAI, I. A., TEMPFER, H., KLEMENT, E., GUENTHER, B., BAUER, H. C. & BAUER, H. (2008) Nuclear Zonula occludens-2 alters gene expression and junctional stability in epithelial and endothelial cells. *Differentiation,* 76, 99-106.
URICH, E., LAZIC, S. E., MOLNOS, J., WELLS, I. & FRESKGARD, P. O. (2012) Transcriptional profiling of human brain endothelial cells reveals key properties crucial for predictive in vitro blood-brain barrier models. *PLoS One,* 7, e38149.
UTSUMI, H., CHIBA, H., KAMIMURA, Y., OSANAI, M., IGARASHI, Y., TOBIOKA, H., MORI, M. & SAWADA, N. (2000) Expression of GFRalpha-1, receptor for GDNF, in rat brain capillary during postnatal development of the BBB. *Am J Physiol Cell Physiol,* 279, C361-8.
VALCU, M. & VALCU, C. M. (2011) Data transformation practices in biomedical sciences. *Nat Methods,* 8, 104-5.
VELEGOL, D. & LANNI, F. (2001) Cell traction forces on soft biomaterials. I. Microrheology of type I collagen gels. *Biophys J,* 81, 1786-92.
VERNON, R. B., ANGELLO, J. C., IRUELA-ARISPE, M. L., LANE, T. F. & SAGE, E. H. (1992) Reorganization of basement membrane matrices by cellular traction promotes the formation of cellular networks in vitro. *Lab Invest,* 66, 536-47.
VIZUETE, M. L., VENERO, J. L., VARGAS, C., ILUNDAIN, A. A., ECHEVARRIA, M., MACHADO, A. & CANO, J. (1999) Differential upregulation of aquaporin-4 mRNA

expression in reactive astrocytes after brain injury: potential role in brain edema. *Neurobiol Dis,* 6, 245-58.

VORBRODT, A. W., LOSSINSKY, A. S. & WISNIEWSKI, H. M. (1986) Localization of alkaline phosphatase activity in endothelia of developing and mature mouse blood-brain barrier. *Dev Neurosci,* 8, 1-13.

WAGNER, O. F., CHRIST, G., WOJTA, J., VIERHAPPER, H., PARZER, S., NOWOTNY, P. J., SCHNEIDER, B., WALDHAUSL, W. & BINDER, B. R. (1992) Polar secretion of endothelin-1 by cultured endothelial cells. *J Biol Chem,* 267, 16066-8.

WAGNER, S. & GARDNER, H. (2000) Modes of regulation of laminin-5 production by rat astrocytes. *Neurosci Lett,* 284, 105-8.

WAGNER, S., TAGAYA, M., KOZIOL, J. A., QUARANTA, V. & DEL ZOPPO, G. J. (1997) Rapid disruption of an astrocyte interaction with the extracellular matrix mediated by integrin alpha 6 beta 4 during focal cerebral ischemia/reperfusion. *Stroke,* 28, 858-65.

WANG, D. D. & BORDEY, A. (2008) The astrocyte odyssey. *Prog Neurobiol,* 86, 342-67.

WANG, L., FORTUNE, B., CULL, G., DONG, J. & CIOFFI, G. A. (2006) Endothelin B receptor in human glaucoma and experimentally induced optic nerve damage. *Arch Ophthalmol,* 124, 717-24.

WANG, W., DENTLER, W. L. & BORCHARDT, R. T. (2001) VEGF increases BMEC monolayer permeability by affecting occludin expression and tight junction assembly. *Am J Physiol Heart Circ Physiol,* 280, H434-40.

WARNER, T. D., ALLCOCK, G. H., CORDER, R. & VANE, J. R. (1993) Use of the endothelin antagonists BQ-123 and PD 142893 to reveal three endothelin receptors mediating smooth muscle contraction and the release of EDRF. *Br J Pharmacol,* 110, 777-82.

WEIDENFELLER, C., SCHROT, S., ZOZULYA, A. & GALLA, H. J. (2005) Murine brain capillary endothelial cells exhibit improved barrier properties under the influence of hydrocortisone. *Brain Res,* 1053, 162-74.

WEIDENFELLER, C., SVENDSEN, C. N. & SHUSTA, E. V. (2007) Differentiating embryonic neural progenitor cells induce blood-brain barrier properties. *J Neurochem,* 101, 555-65.

WEKSLER, B. B., SUBILEAU, E. A., PERRIERE, N., CHARNEAU, P., HOLLOWAY, K., LEVEQUE, M., TRICOIRE-LEIGNEL, H., NICOTRA, A., BOURDOULOUS, S., TUROWSKI, P., MALE, D. K., ROUX, F., GREENWOOD, J., ROMERO, I. A. & COURAUD, P. O. (2005) Blood-brain barrier-specific properties of a human adult brain endothelial cell line. *Faseb J,* 19, 1872-4.

WEN, H., NAGELHUS, E. A., AMIRY-MOGHADDAM, M., AGRE, P., OTTERSEN, O. P. & NIELSEN, S. (1999) Ontogeny of water transport in rat brain: postnatal expression of the aquaporin-4 water channel. *Eur J Neurosci,* 11, 935-45.

WIJSMAN, J. A. & SHIVERS, R. R. (1998) Immortalized mouse brain endothelial cells are ultrastructurally similar to endothelial cells and respond to astrocyte-conditioned medium. *In Vitro Cell Dev Biol Anim,* 34, 777-84.

WILLIAMS, M. J., LOWRIE, M. B., BENNETT, J. P., FIRTH, J. A. & CLARK, P. (2005) Cadherin-10 is a novel blood-brain barrier adhesion molecule in human and mouse. *Brain Res,* 1058, 62-72.

WILLIS, C. L., NOLAN, C. C., REITH, S. N., LISTER, T., PRIOR, M. J., GUERIN, C. J., MAVROUDIS, G. & RAY, D. E. (2004) Focal astrocyte loss is followed by microvascular damage, with subsequent repair of the blood-brain barrier in the apparent absence of direct astrocytic contact. *Glia,* 45, 325-37.

WOLBURG-BUCHHOLZ, K., MACK, A. F., STEINER, E., PFEIFFER, F., ENGELHARDT, B. & WOLBURG, H. (2009) Loss of astrocyte polarity marks blood-brain barrier impairment during experimental autoimmune encephalomyelitis. *Acta Neuropathol,* 118, 219-33.

WOLBURG, H. & LIPPOLDT, A. (2002) Tight junctions of the blood-brain barrier: development, composition and regulation. *Vascul Pharmacol,* 38, 323-37.

WOLBURG, H., NOELL, S., MACK, A., WOLBURG-BUCHHOLZ, K. & FALLIER-BECKER, P. (2009a) Brain endothelial cells and the glio-vascular complex. *Cell Tissue Res,* 335, 75-96.

WOLBURG, H., NOELL, S., WOLBURG-BUCHHOLZ, K., MACK, A. & FALLIER-BECKER, P. (2009b) Agrin, aquaporin-4, and astrocyte polarity as an important feature of the blood-brain barrier. *Neuroscientist,* 15, 180-93.

WOLBURG, H., WOLBURG-BUCHHOLZ, K., KRAUS, J., RASCHER-EGGSTEIN, G., LIEBNER, S., HAMM, S., DUFFNER, F., GROTE, E. H., RISAU, W. & ENGELHARDT, B. (2003) Localization of claudin-3 in tight junctions of the blood-brain barrier is selectively lost during experimental autoimmune encephalomyelitis and human glioblastoma multiforme. *Acta Neuropathol,* 105, 586-92.

WU, V. W. & SCHWARTZ, J. P. (1998) Cell culture models for reactive gliosis: new perspectives. *J Neurosci Res,* 51, 675-81.

WUEST, D. M. & LEE, K. H. (2012) Optimization of endothelial cell growth in a murine in vitro blood-brain barrier model. *Biotechnol J,* 7, 409-17.

XIAO, L., YANG, C., DOROVINI-ZIS, K., TANDON, N. N., ADES, E. W., LAL, A. A. & UDHAYAKUMAR, V. (1996) Plasmodium falciparum: involvement of additional receptors in the cytoadherence of infected erythrocytes to microvascular endothelial cells. *Exp Parasitol,* 84, 42-55.

YAMADA, K. M., PANKOV, R. & CUKIERMAN, E. (2003) Dimensions and dynamics in integrin function. *Braz J Med Biol Res,* 36, 959-66.

YANAGISAWA, M., KURIHARA, H., KIMURA, S., GOTO, K. & MASAKI, T. (1988) A novel peptide vasoconstrictor, endothelin, is produced by vascular endothelium and modulates smooth muscle Ca2+ channels. *J Hypertens Suppl,* 6, S188-91.

YANG, B., ZADOR, Z. & VERKMAN, A. S. (2008) Glial cell aquaporin-4 overexpression in transgenic mice accelerates cytotoxic brain swelling. *J Biol Chem,* 283, 15280-6.

YAO, X., HRABETOVA, S., NICHOLSON, C. & MANLEY, G. T. (2008) Aquaporin-4-deficient mice have increased extracellular space without tortuosity change. *J Neurosci,* 28, 5460-4.

YODER, E. J. (2002) Modifications in astrocyte morphology and calcium signaling induced by a brain capillary endothelial cell line. *Glia,* 38, 137-45.

ZENKER, D., BEGLEY, D., BRATZKE, H., RUBSAMEN-WAIGMANN, H. & VON BRIESEN, H. (2003) Human blood-derived macrophages enhance barrier function of cultured primary bovine and human brain capillary endothelial cells. *J Physiol,* 551, 1023-32.

ZHOU, J., KONG, H., HUA, X., XIAO, M., DING, J. & HU, G. (2008) Altered blood-brain barrier integrity in adult aquaporin-4 knockout mice. *Neuroreport,* 19, 1-5.

ZIEGLER, T. & NEREM, R. M. (1994) Effect of flow on the process of endothelial cell division. *Arterioscler Thromb,* 14, 636-43.

ZONTA, M., ANGULO, M. C., GOBBO, S., ROSENGARTEN, B., HOSSMANN, K. A., POZZAN, T. & CARMIGNOTO, G. (2003) Neuron-to-astrocyte signaling is central to the dynamic control of brain microcirculation. *Nat Neurosci,* 6, 43-50.

ZOZULYA, A., WEIDENFELLER, C. & GALLA, H. J. (2008) Pericyte-endothelial cell interaction increases MMP-9 secretion at the blood-brain barrier in vitro. *Brain Res,* 1189, 1-11.

Appendix-A: List of reagents used in this study

Table 5 List of reagents used in this study

Reagent/material	Catalogue ID	Supplier/manufacturer
Cell tracker™ Green CMFDA	#C2925	Molecular probes, inc.
Collagen type 1, from calf skin	#C-8919	Sigma-Aldrich inc.
Collagen type-I rat tail (2.15 mg/ml in 0.6% acetic acid), for gel formation	#60-30-810	First link (UK) ltd.
Collagenase from Clostridium histolyticum	#C9697	Sigma-Aldrich inc.
Cover glass, 19 mm diameter, 0.16 mm thickness	#631-0156	VWR International Ltd
CoverWell™ imaging chambers, diam. × D 20 mm × 2.5 mm	#Z365882	Sigma-Aldrich inc.
DAPI-fluoromount-G™	#0100-20	Southern biotech
Detergent compatible protein assay kit II	#500-0112	Biorad
DMEM, Dulbecco's modified Eagle's medium	#D5921	Sigma-Aldrich inc.
DNase 1, from bovine pancreas	#1284932001	Roche applied science
ECL Hyper films	#28906836	Amersham™ , GE health care
ECL Western blotting detection reagents	#RPN2106	Amersham™ , GE health care
EGM-2 MV Bullet kit	#CC-3202	Clonetics®, Lonza inc.
Endothelin-1 ELISA kit	#ADI-900-020A	Enzo Life Sciences (UK) LTD.
Et-1 peptide	#E7764	Sigma-Aldrich inc.
Fibronectin	#F1141	Sigma-Aldrich inc.
Fluorescein isothiocyanate-dextran	#FD70	Sigma-Aldrich inc.
Goat serum, normal	#G9023	Sigma-Aldrich inc.
Hank's balanced salts solution (HBSS)	#H8264	Sigma-Aldrich inc.
Hank's balanced salts solution (HBSS) without Ca^{2+} and Mg^{2+}	#H6648	Sigma-Aldrich inc.

Reagent/material	Catalogue ID	Supplier/manufacturer
Hoechst 33258	#861405	Sigma-Aldrich inc.
Human astrocyte medium (HAM)	#1801	Sciencell research laboratories
Human astrocytes (HA)	#1800-HA	Sciencell research laboratories
Minimum essential medium (MEM) with Phenol Red, 10×	#M0275	Sigma-Aldrich inc.
Nitrocellulose membranes, Hybond ECL, 0.45 μm	#RPN303D	Amersham™ , GE health care
Protease inhibitor cocktail	#P8340	Sigma-Aldrich inc.
RIPA buffer	#R0278	Sigma-Aldrich inc.
Saponin, for molecular biology	#47036	Sigma-Aldrich inc.
Transwell® Corning® PET membrane inserts,0.4 μm, 12 mm	#CLS3460	Sigma-Aldrich inc.
Trypsin (0.25%)-EDTA (20 mM)	#59430C	Sigma-Aldrich inc.

Appendix-B: List of antibodies used in this study

Table 6 List of antibodies used in this study

Antibody	Clonality	Immunogen	Concentration used	Company
Anti-mouse IgG antibodies, Alexa Fluor® 488 conjugated, raised in Goat	Goat IgG (H+L)	Mouse IgG	10 μg/ml	#A11001, Invitrogen, Ltd.
Anti-mouse IgG antibodies, Alexa Fluor® 555 conjugated, raised in Goat	Goat IgG (H+L)	Mouse IgG	10 μg/ml	#A21422, Invitrogen Ltd.
Anti-mouse IgM heavy chain antibodies, conjugated to FITC	Rat IgG2a, monoclonal, LOMM9	Polyclonal and monoclonal mouse IgM	5 μg/ml	#MCA199F, AbD Serotec
Anti-rabbit IgG antibodies, Alexa Fluor® 488 conjugated, raised in Goat	Goat IgG (H+L)	Rabbit IgG	10 μg/ml	#A11008, Invitrogen Ltd.
Anti-rabbit IgG antibodies conjugated to DyLight® 549	Goat IgG (H+L)	Rabbit IgG	5 μg/ml	#DI-1549, Vector laboratories
Actin β (ACTB)	Mouse IgG1, AC-15	slightly modified synthetic β-cytoplasmic actin N-terminal peptide	1μg/ml for Immunoblotting	#A1978, Sigma-Aldrich, Inc.
AQP4	Rabbit polyclonal	Synthetic linear peptide corresponding to C-terminus of Rat AQP4	20 μg/ml, for immunogold electron microscopy; at 1 μg/ml for western blotting	#AB2218, Millipore (U.K.) Ltd.

Antibody	Clonality	Immunogen	Concentration used	Company
AQP4 (H-80)	Rabbit polyclonal	Amino acids 244-323 mapping at the cytoplasmic C-terminus of AQP4 of human origin	2 μg/ml for flow cytometry, and immuno-fluorescence microscopy	#sc-20812, Santa Cruz Biotechnology, Inc
CD68, KP1, anti-human, conjugated to FITC	Mouse, IgG1 kappa, clone KP1	Lysosomal granules from human lung macrophages.	2 μg/ml	#F7135, Dako UK Ltd.
Claudin-5 (CLDN5)	Mouse IgG1, 4C3C2	Synthetic peptide derived from the mouse Claudin-5 protein	2.5 μg/ml for immuno-fluorescence	#35-2500, Invitrogen Ltd.
Claudin-5 (CLDN5)	Rabbit polyclonal	Synthetic peptide derived from the C-terminal sequence of mouse Claudin-5.	at 1.7 μg/ml for western blotting	#34-1600, Invitrogen Ltd
EDNRB	Rabbit polyclonal	Amino acid residues 298-313 of rat ET-B	8 μg/ml	#AER-002, Alomone labs
GFAP G-A-5	Mouse IgG1, #G-A-5	Purified GFAP from pig spinal cord	2.4 μg/ml	#G3893, Sigma-Aldrich, Inc.
GFAP	Rabbit, IgG	Purified bovines GFAP	1/2000	#AB5804, Millipore (U.K.) Ltd.
Horse-radish peroxidase (HRP)-conjugated secondary antibodies	Goat IgG (H+L)	Rabbit IgG	1/4000	#65-6120, Invitrogen Ltd.
Horse-radish peroxidase (HRP)-conjugated secondary antibodies	Goat IgG (H+L)	Mouse IgG	1/10000	#32230, Pierce Biotechnology

Antibody	Clonality	Immunogen	Concentration used	Company
ICAM2	Mouse IgG1, B-T1	Human-ICAM2 transfected CHO cells	10 μg/ml	#MCA1140, AbD serotec
Mouse IgG1	Mouse IgG1,κ (MOPC-21)		Equal to the corresponding primary antibody concentration	# M 5284, Sigma-Aldrich, Inc.
Mouse IgG2a	Clone UPC-10		Equal to the corresponding primary antibody concentration	#M5409, Sigma-Aldrich Inc
O1 marker for oligodendrocytes	Mouse IgM Clone # O1	Bovine brain corpus callosum white matter	1 μg/ml	#MAB1327, R & D Systems
PECAM1	Mouse IgG1, Clone # 9G11	Activated human umbilical vein endothelial cells	10 μg/ml for flowcytometry	#BBA7, R&D Systems Europe Ltd.
PECAM1 anti-bodies conjugated PerCP-eFluor® 710	Mouse IgG1, K; WM-59	Human PECAM1	1.25 μg/ml for flow cytometry	#46-0319-42, eBioscience, Ltd.,
P-glycoprotein-1	Mouse IgG2a, MRK16	Surface epitope of human P-glyco-protein.	5 μg/ml	#MC012, Kamiya biomedical company
S100B antibody [EP1576Y]	Rabbit monoclonal, IgG, EP1576Y	Synthetic peptide corresponding to residues on the C-terminus of human S100 beta	1:200	#ab52642, abcam
TE-7 clone, anti-fibroblasts	Mouse, IgG1, TE-7	Whole human thymic stroma cells	0.67 μg/ml	#CBL271, Millipore (U.K.) Ltd
ZO-1	Rabbit polyclonal antibodies	amino acids corresponding to 463-1109 of human ZO-1 cDNA	2.5 μg/ml for Immuno-fluorescence; 1.7 μg/ml for immunoblotting	#61-7300, Zymed

Appendix-C: Rat astrocytic AQP4 expression was decreased in 3D co-culture compared to 3D solo-culture as analysed by immunogold TEM

3D rat astrocyte (RA) solo- and co-cultures were set up as described in section 2.2.3 except that instead of HA, RA were used. AQP4 localisation and expression were compared by immunogold TEM as described in section 4.2.7. In both culture conditions, gold particles were predominantly present on the cell membrane while very few were present in the cytoplasm and nucleus. Hence, the cell membrane expression levels were compared between the culture conditions. In comparison to 3D RA solo-culture, 3D RA co-cultures expressed statistically significantly less AQP4 on their cell membrane (**Figure A-C**).

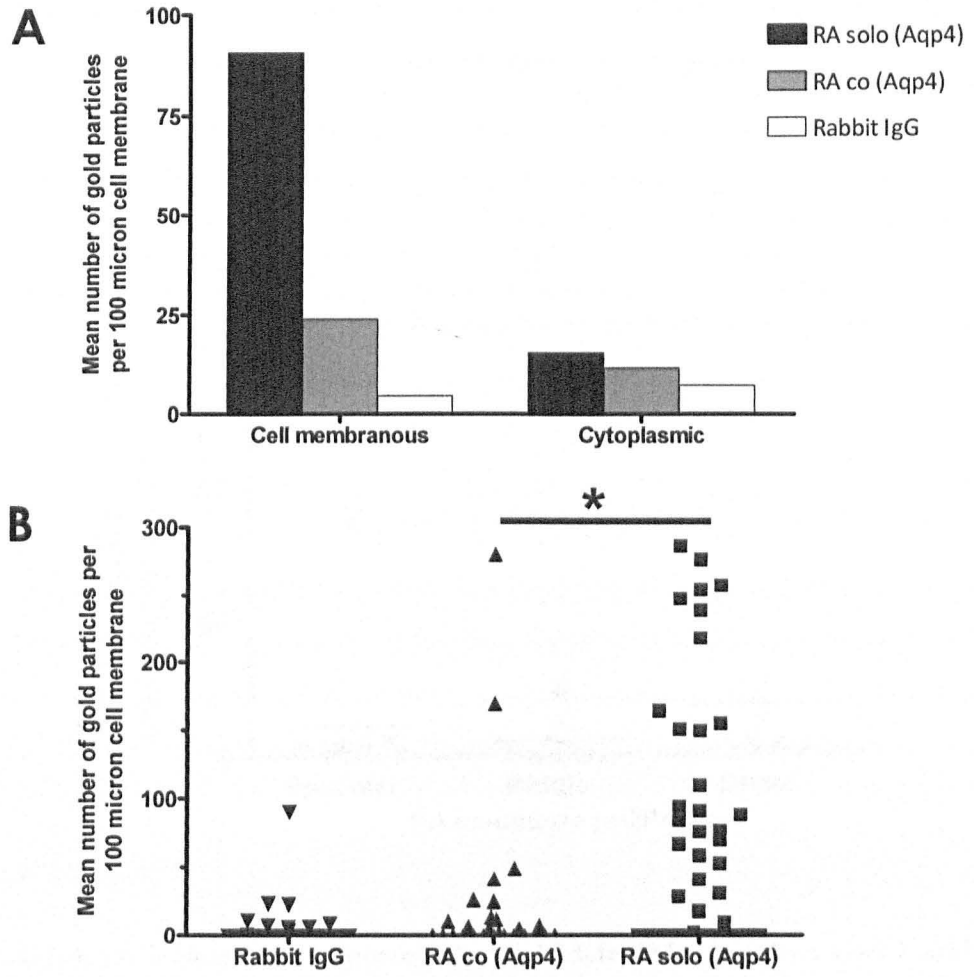

Figure A-C: Relative levels of AQP4 in 3D RA cultures measured by TEM analysis

AQP4 expression in 3D RA solo- and co-cultures were analysed by immunogold TEM. For rabbit IgG, 40 cells; RA co-culture, 27 cells; and RA solo-cultures, 42 cells were analysed. For each condition, at least 690 μm of membrane was analysed. The number of gold particles present per unit length of the cell membrane and cytoplasmic particles were counted and compared between the solo- and co-cultures. The gold particles present within 100 nm distance from the cell membrane were considered as cell membrane localised. **A:** In both culture conditions, gold particles were predominantly present on the cell membrane while very few were present in the cytoplasm and nucleus. **B:** Scatter plot showing the cell membranous expression. Each dot represents the data of a single cell. AQP4 expression was significantly decreased in RA co-culture compared to RA solo-culture as seen by fewer gold particles in RA solo-culture. $^{*}P \leq 0.05$ using Mann-Whitney test, N = 1

Appendix-D: AQP4 expression levels in proximal vs. distal astrocytes in 3D RA co-culture

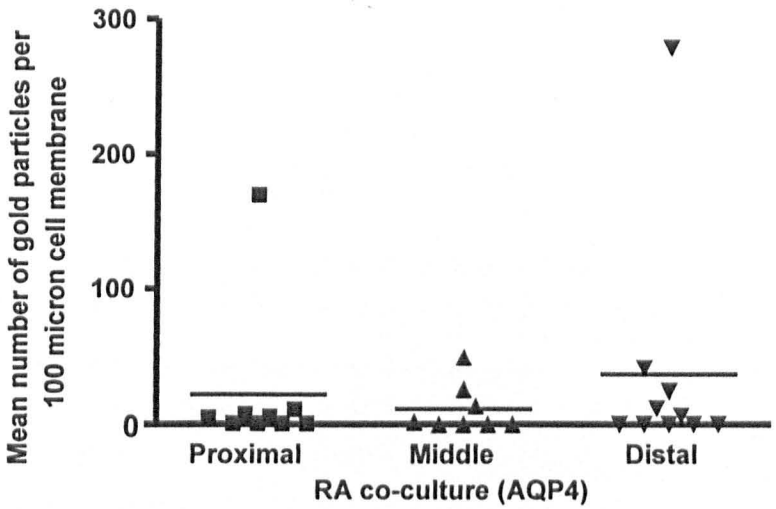

Figure A-D Relative levels of AQP4 in proximal vs. distal RA, in 3D RA co-culture as analysed by TEM

To determine whether the observed down-regulation of AQP4 in RA co-cultures was dependent on their proximity to endothelial cells the following analysis was carried out. The 3D RA co-culture section (Appendix-C) was divided into three regions along its depth. The region within 250 μm distance from the hCMEC/D3 monolayer was considered as proximal, 250-500μm was considered middle, and 500-750 μm was considered distal. Cell membranous gold particles per unit length were compared across the three regions. Results are shown in the scatter plot. Each dot represents the data of a single cell. The horizontal bar represents the mean of the population. AQP4 expression levels of any region were statistically not different from any other region. These results suggest that down-regulation of astrocytic AQP4 expression did not depend on the proximity between astrocytes and endothelial cells or depth of the gel. It also suggests that the endothelial released factor that is responsible for the down-regulation is diffusible in the 3D matrix and there is no concentration gradient of this factor. Statistical significance was tested by Mann-Whitney test, $P \geq 0.05$ was considered as non-significant. $N = 1$.

-The End of the Document-